Imperial College
London

EVALUATING SORBENTS PRODUCED FROM WASTE TO REMOVE MERCURY IN SIMULATED FLUE GASES FROM COAL COMBUSTION

Hemantha Revata Seneviratne

Department of Chemical Engineering

Imperial College London

University of London

A thesis submitted for the degree of Doctor of Philosophy of the University of London and the Diploma of Imperial College

2008

Abstract

Coal-fired utility plants are the largest anthropogenic source of mercury emissions. Mercury abatement legislation for these plants is in place in Canada and U.S.A. Several facilities are achieving mercury emission reductions by injecting commercial activated carbons into the flue gas stream and capturing spent sorbents with the plant's particulate control system. However, these carbons are expensive and add to the unit cost of generated power. The present project aimed to determine mercury capture efficiencies of some coal fly ashes and sorbents produced from waste materials (scrap tyre rubber and sewage sludge), compared to the effectiveness of commercial active carbons. E.U. legislation limits the methods available for disposing of waste materials and using these wastes to manufacture sorbents provides a cost-effective disposal solution whilst producing a re-usable by product.

A novel bench scale fixed-bed sorbent test system was designed and built for evaluating mercury capture efficiencies of sorbents by exposing the samples to different gaseous atmospheres, simulating flue gas compositions from bituminous coal combustion. Additional information on the effect of acid gases was obtained by pre-treating selected sorbents with a gas stream containing either NO_x or HCl. Thermal desorption experiments completed on spent sorbents provided indications regarding the adsorption process whilst suggesting which constituent in the flue gas stream was most important for mercury capture. A thermodynamic equilibrium study was also completed, for estimating mercury speciation that occurs whilst flue gases cool to the operating temperatures of particulate collection systems in U.K. coal-fired power plants.

When the samples were evaluated in the absence of acid gases, the bromide-impregnated activated carbons made from waste material matched the performance of Norit Darco Hg-LH™ and were significantly superior to other sorbents tested. Tests with the more realistic simulated flue gas stream, containing N_2, NO, NO_2, SO_2, HCl, CO_2, O_2 , water vapour and mercury, indicated that charcoal and steam activated carbons made from waste were as effective as Norit Darco Hg™. Coal fly ashes proved to be inferior to carbons when evaluated with this gas stream. Very little mercury was removed during leaching tests on spent sorbents indicating that they can be processed using the current practice employed for disposing fly ash from coal-fired power plants.

The results of the bench-scale tests suggest that steam activated tyre rubber carbon may be a useful substitute to Norit Darco Hg™, whilst bromide-impregnated carbon produced from tyre rubber appears to be suitable as an alternative to Norit Darco Hg-LH™.

Acknowledgements

I am greatly indebted to my supervisors Prof. Rafael Kandiyoti and Prof. Denis Dugwell for their guidance to perform this work. The financial support for this study by the British Coal Utilisation Research Association (BCURA) under contract No. B73 is gratefully acknowledged. I would like to thank my BCURA industrial supervisor Dr. David Fitzgerald of Doosan Babcock Energy Limited, BCURA industrial partners Dr. Will Quick and Dr Susan Weatherstone of E.ON U.K. for their helpful advice. I would like to express my gratitude for the help given by Dr. Graham Reed in designing the bench-scale sorbent test system. I am grateful to P.S. Analytical U.K. for providing the Cavkit mercury generator used during the course of this study. The help and advice provided by Dr. Warren Corns and Jasmina Allen at P.S. Analytical U.K. regarding mercury analysis of the spent impregnated sorbents evaluated during this research is much appreciated. Thanks are also due to Dr Geoffrey Fowler of the Environmental & Water Resource Engineering Section, Imperial College London for use of the carbon activation rig and to Dr. Fraser Wigley from the Department of Materials, Imperial College London for advice on XRD and SEM analyses. My thanks are also extended to Cedric Charpenteau, my other colleagues in the Energy Engineering group and my brothers for all the help, encouragement and friendship during this research.

Dedicated to my parents

Contents

1. Introduction **1**
1.1. Motivation for the present research 2
1.1.1. Benefits of using scrap tyre rubber to manufacture sorbents 3
1.1.2. Benefits of using sewage sludge to manufacture sorbents 3
1.1.3. Benefits of using zinc bromide activated carbons 4
1.1.4. An insight into the method of mercury captured on some selected PACs 4
1.1.5. The leachability of the mercury retained on the sorbents 4
1.2. Structure of the thesis 5
2. Background **7**
2.1. Mercury emissions from coal-fired power plants 7
2.1.1. Mercury in coal 9
2.1.2. Effect of current pollution control technologies 11
2.1.2.1. Low NOx burners 11
2.1.2.2. Particulate control devices 12
2.1.2.3. Wet flue gas desulphurisation 13
2.1.2.4. Spray dryer absorbers and selective catalytic reduction 14
2.2. Chemistry of formation 14
2.2.1. Homogeneous mercury chlorination reactions 16
2.2.2. Heterogeneous mercury reactions and capture 17
2.2.2.1. Surface properties of fly ash and carbon 17
2.2.2.2. Effects of acid gases on mercury sorption 18
2.3. Mercury emission limits for coal-fired power plants 20
2.4. Experimental results to-date on low cost sorbents 22
2.4.1. Activated carbon sorbents 22
2.4.2. Fly ash sorbents 26
2.4.3. Bromide impregnated PAC – effect during full-scale tests 27
3. Thermodynamic equilibrium modelling **30**
3.1. Application of MTDATA 30
3.2. Predicted thermodynamic equilibrium composition 34
3.2.1. Effect of chlorine on mercury speciation 34
3.2.2. Mercury speciation when combusting different coals 36

3.3. Conclusions from the MTDATA modelling 39
4. Sorbents evaluated in this study 41
4.1. Norit Darco Hg™ and Norit Darco Hg-LH™ 42
4.2. The coal fly ashes evaluated in this study 42
4.3. Producing charcoal from scrap tyre rubber 43
4.4. Producing steam activated carbons from tyre rubber 44
4.5. Producing bromide-impregnated PACs from scrap tyre rubber 46
4.6. Producing charcoal from sewage sludge 46
4.7. Producing bromide-impregnated PACs from sewage sludge 47
5. Characterisation of the sorbents 49
5.1. The sorbent surface area and microporosity 49
5.2. Investigating specific elements in the sorbents 54
5.3. X-ray diffraction analysis 57
5.4. Scanning electron microscopy and energy dispersive X-ray analysis 59
5.5. Conclusions from sorbent characterisation 72
6. Experimental procedures 75
6.1. Analytical techniques for mercury quantification 75
6.1.1. LECO AMA 254 Mercury Analyser 75
6.1.2. PSA 10.025 Millennium Merlin System 76
6.1.2.1. Aqua Regia digestion procedure 77
6.1.2.2. Preparation of the reductant 77
6.1.2.3. Preparation of reagent for calibration standards and for blank solution 77
6.1.2.4. Preparation of the calibration standards 78
6.1.2.5. Mercury determination using the PSA 10.025 analyser 78
6.2. Experimental scheme to test the sorbents at low temperatures 80
6.2.1. Reactor for testing sorbents at low temperatures 80
6.2.2. Experimental schemes to obtain information on mercury capture 84
6.2.2.1. Experimental setup used during tests with gas schemes Exp. 1 to Exp. 5 94
6.2.2.2. Experimental system used for tests with the most complete simulated flue gas scheme (Exp. 6). 94
6.2.2.3. Experimental procedure to test effect of initial exposure to NO_x or HCl 96
6.2.2.4. Thermal desorption tests on spent sorbents 97
6.2.2.5. Test to determine if $HgCl_2$ is preset in the simulated flue gas streams 98
6.2.3. Leachability of mercury captured by the sorbents 100

7. Mercury capture tests – Results and discussion 102
7.1. Mercury adsorption on selected sorbents in relation to different exposure times 102
7.2. Effect of varying the sorbent mass and the associated change in residence time 103
7.3. Effect of test temperature on sorbent performance 105
7.4. Effect of gas composition 107
7.4.1. Tests with a sample mass of 100 mg 107
7.4.2. Tests with a sample mass of 20 mg 110
7.5. Effect of initial exposure to NO_x and HCl 112
7.6. Desorption of retained mercury 115
7.7. Studying the presence of $HgCl_2$ in the simulated flue gas streams 118
7.8. Bromide impregnated activated carbons 120
7.9. A closer analysis of mercury capture by fly ash 123
7.10. Leachability of mercury retained on the sorbents 129
7.11. Comparing sorbents made under the same process conditions 131
7.12. Discussion on sorbent performance and stability of captured mercury 133
7.12.1. Transfer of mercury from the gas stream to the sorbent surface and into the particle's pores 134
7.12.2. Mercury capture by physical adsorption and by active sites on the sorbents 137
7.12.3. Long term stability of the adsorbed mercury 140
8. Selecting alternative sorbents for capturing mercury 142
8.1. Comparing the laboratory-scale results against full-scale tests 142
8.2. Alternative sorbents for Norit Darco Hg™ and Norit Darco Hg-LH™ 145
8.2.1. Substitute sorbent for Norit Darco Hg™ 146
8.2.2. Substitute sorbent for Norit Darco Hg-LH™ 149
8.2.3. Proposed large scale manufacturing process for making the sorbents 151
9. Summary, conclusions and recommendations for future work 154
9.1. Summary 154
9.2. Conclusions 156
9.2.1. Experimental scheme used during the study 156
9.2.2. Thermodynamic equilibrium modelling 157
9.2.3. Sorbents evaluated during this study 157
9.2.4. Mercury capture by the sorbents 159
9.3. Recommendations for future work 163

9.3.1. Formulating models to predict the effectiveness of activated carbons injected into coal combustion flue gases 163
9.3.2. Inclusion of SO_3 in the simulate flue gas stream 164
9.3.3. Entrained flow reactor 165
9.3.4. Foam index tests on fly ash/sorbent mixtures 165
References 168
Appendix -A 177
Appendix -B 178
Appendix -C 179
Appendix -D 181
Appendix -E 182
Appendix -F 183
Appendix -G 185

List of tables

Table 1-1 Fate of fly ash from coal combustion in the United States in 1999.[17] 5
Table 1-2 Solubility of some mercury compounds.[19] 5
Table 2-1 Comparison of Appalachian (Bituminous) and Western Subbituminous coal compositions – analysed on a dry basis[29] 10
Table 2-2 Average mercury capture by coal rank and APCD configuration in US coal-fired utility plants.[15] 11
Table 2-3 Mercury capture in particulate control devices.[4] 12
Table 2-4 Mercury capture when WFGD follows a particulate control device.[4] 13
Table 2-5 Equilibrium reactions between mercury and flue gas constituents.[31] 16
Table 2-6 Mercury emission limits for US coal fired utility plants – based on gross energy output.[37] 21
Table 2-7 Mercury emission limits established by some US states.[38] 22
Table 2-8 Average annual mercury emission limits for Canadian coal-fired utility plants.[23] 22
Table 2-9 Elemental mercury capacity of different PACs – results from bench scale tests with simulated flue gases that did not contain NO_x.[4] 25
Table 3-1 The different gaseous atmospheres that were modelled with MTDATA during the present study 31
Table 3-2 Composition of the flue gases evaluated by the MTDATA thermodynamic equilibrium modelling 33
Table 3-3 Individual components of the flue gases that were input to MTDATA thermodynamic equilibrium modelling 33
Table 4-1 The different sorbents evaluated in this study 41
Table 4-2 Specifications of Norit Darco Hg™ and Darco Hg-LH™ published by Norit Americas Inc.[51] 42
Table 4-3 Particle size distribution of the fly ashes D and F 43
Table 5-1 Surface area, micropore volume and micropore area of the sorbents 53
Table 5-2 Moisture, ash and elemental analysis of the sorbents 56
Table 5-3 Chemical composition of the crystalline phases found using XRD 56
Table 6-1 Instrumental conditions for Millennium Merlin (PSA 10.025) 79

Table 6-2 Individual gas/vapour concentrations and flow rates for the more complete simulated flue gas schemes used during this study. 85
Table 6-3 Coefficient of variability of the results from three different experimental schemes 90
Table 6-4 The different gas schemes used in this study to evaluate the sorbents' mercury capture efficiencies 91
Table 6-5 Flow controller setting used for the different gas conditions 94
Table 7-1 Sorbent bed height and gas stream residence time for different sample masses 135
Table 8-1 Mercury capture efficiencies and carbon/mercury ratios achieved during full-scale tests with Norit Darco Hg™ at U.S. coal-fired utility plants 147

List of figures

Figure 2-1 Mercury speciation in the flue gases from different coal ranks.[29] 10
Figure 2-2 Potential mercury transformations during coal combustion and subsequently in the resulting flue gas.[28] 15
Figure 2-3 Suggested heterogeneous model for mercury capture showing potential impact of acid gases.[34] 18
Figure 2-4 Binding site model for activated carbon.[35] 19
Figure 2-5 Oxidation site model for activated carbon—the role of hydrochlorination in generating carbenium oxidant.[35] 20
Figure 2-6 Mercury removal efficiencies of PAC during full-scale field tests 28
Figure 3-1 MTDATA results when the effect of chlorine on mercury speciation in a flue gas stream was evaluated 35
Figure 3-2 MTDATA results for major mercury species present in flue gas from the combustion of lignite 36
Figure 3-3 MTDATA results for major mercury species present in flue gas from the combustion of Harworth coal (U.K. bituminous coal) 37
Figure 3-4 MTDATA results for major mercury species present in flue gas from the combustion of a U.S. bituminous coal 38
Figure 3-5 MTDATA results for major mercury species present in flue gas from the combustion of Eastern bituminous coal 38
Figure 3-6 MTDATA results for major mercury species present in flue gas from the combustion of low sulphur Eastern bituminous coal 39
Figure 3-7 MTDATA results for major mercury species present in flue gas from the combustion of Western bituminous coal 39
Figure 4-1 Schematic diagram of the rig for pyrolysis of scrap tyre rubber (Modified from the figure published by Miguel et al.[45]) 44
Figure 4-2 Schematic diagram of the rig for the activation of scrap tyre rubber.[58] 45
Figure 5-1 Micropore surface area in each fly ash sample versus LOI content. 54
Figure 5-2 XRD scan results of some selected activated carbons, fly ashes and sorbents from scrap tyre rubber 60
Figure 5-3 XRD scan results of char from sewage sludge and some selected bromide impregnated activated carbons 61

Figure 5-4 SEM & EDX analysis of Norit Darco Hg™ (at x1000 magnification). 62
Figure 5-5 SEM & EDX analysis of Norit Darco HG-LH™ (at x1000 magnification) ... 62
Figure 5-6 SEM & EDX analysis of fly ash D (at x1000 magnification). 63
Figure 5-7 SEM & EDX analysis of fly ash E (at x1000 magnification) 63
Figure 5-8 SEM & EDX analysis of fly ash F (at x100 magnification). 64
Figure 5-9 SEM & EDX analysis of fly ash G (at x100 magnification). 65
Figure 5-10 SEM & EDX analysis of tyre char R1 (at x450 magnification). 66
Figure 5-11 SEM & EDX analysis of tyre char R1 (at x1000 magnification). 66
Figure 5-12 SEM & EDX analysis of tyre char R3 (at x1000 magnification). 67
Figure 5-13 SEM & EDX analysis of tyre AC R1 (at x1000 magnification). 68
Figure 5-14 SEM & EDX analysis of tyre AC R3 (at x1000 magnification). 69
Figure 5-15 SEM & EDX analysis of sewage sludge char (at x1000 magnification) 70
Figure 5-16 SEM & EDX analysis of sewage sludge char (at x1000 magnification) 70
Figure 5-17 SEM & EDX analysis of sewage sludge AC R3 (at x1000 magnification). . 71
Figure 5-18 SEM & EDX analysis of sewage sludge AC R3 (at x1000 magnification). . 72
Figure 6-1 Schematic diagram of the continuous flow vapour generator (PSA 10.025).[69] 79
Figure 6-2 Sectional view of the low temperature sorbent test reactor 82
Figure 6-3 Individual borosilicate components of the low temperature sorbent test reactor 83
Figure 6-4 Low temperature sorbent test reactor with borosilicate components are assembled 83
Figure 6-5 2mm thick Kaowool support used to hold the sorbent sample. 84
Figure 6-6 Bench scale system for testing sorbent's mercury capture efficiencies in a gas stream of Hg^0 vapour mixed with only N_2. 86
Figure 6-7 Norit Darco Hg™ based backup capture unit 88
Figure 6-8 Experimental setup when the sorbents were tested with the most complete simulated flue gas stream – Exp. 6 91
Figure 6-9 Experimental protocol used during the present study 93
Figure 6-10 Bench-scale sorbent test system that was used with gas scheme Exp. 6 95
Figure 6-11 The Dreschel bottle that is used as a water vapour generator 95
Figure 6-12 Experimental scheme to initially expose sorbents to NO_x and HCl gases. ... 97
Figure 6-13 The experimental set-up used for the thermal decomposition test. 98

Figure 7-1 Mercury capture efficiencies at different hold times with a gas stream of only mercury vapour and nitrogen gas 103
Figure 7-2 Mercury capture efficiencies when sorbent mass of 20 and 100 mg were used on tests with a gas scheme of only mercury vapour and nitrogen gas. 104
Figure 7-3 Mercury capture efficiencies at different test temperatures with a gas scheme of only mercury vapour and nitrogen gas (Exp. 1)..... 106
Figure 7-4 Mercury capture efficiencies at different test temperatures with gas stream of mercury vapour, nitrogen, nitrogen oxide and nitrogen dioxide gas (Exp. 2)..... 107
Figure 7-5 Mercury capture efficiencies of the sorbents when tested with gas schemes Exp. 1 to Exp. 5 108
Figure 7-6 Mercury capture efficiencies for the sorbents when tested with different gas schemes..... 111
Figure 7-7 Comparing sorbent performance after initially being exposed to a gas stream with NO and NO_2. 114
Figure 7-8 Comparing sorbent performance after initially being exposed to a gas stream with HCl. 114
Figure 7-9 Results from mercury desorption tests with Norit Darco Hg, tyre char R2 and tyre AC R1..... 116
Figure 7-10 Experimental results obtained from the tests with Dowex 1X8® 119
Figure 7-11 Comparing the effectiveness of bromide impregnated PAC against PAC with no bromide impregnation (Gas scheme Exp. 1) 121
Figure 7-12 Comparing the effectiveness of bromide impregnated PAC against PAC with no bromide impregnation (Gas scheme Exp. 6) 121
Figure 7-13 Mercury capture efficiencies of some selected sorbents when their mass was reduced to less than 20 mg. 123
Figure 7-14 Mercury capture efficiencies of fly ashes (from coal-fired power plants in the UK) when tested with mercury vapour mixed with pure nitrogen gas..... 124
Figure 7-15 Mercury capture efficiency and initial mercury concentration versus LOI content in the fly ashes. 125
Figure 7-16 Mercury capture efficiency versus micropore surface area in the ash samples. 125
Figure 7-17 Initial mercury concentration on the different particle sizes in fly ash D ... 127
Figure 7-18 Initial mercury concentration on the different particle sizes of fly ash F.... 127

Figure 7-19 Mercury capture efficiencies of different particle sizes of fly ash D when tested with gas scheme Exp. 1. 128
Figure 7-20 Mercury capture efficiency of the different particle sizes of fly ash F when tested with gas scheme Exp. 1. 128
Figure 7-21 Mercury leaching results for bromide impregnated PACs that were exposed to gas scheme Exp. 1. 130
Figure 7-22 Mercury leaching results for selected sorbents that were exposed to gas scheme Exp. 5 130
Figure 7-23 Mercury capture efficiencies of sorbents made from the same process conditions (Gas scheme Exp. 1). 132
Figure 7-24 Mercury capture efficiencies of sorbents made from the same process conditions (Gas scheme Exp. 5 and Exp. 6). 133

List of symbols and abbreviations

AEA	Air-entraining agents
APCD	Air pollution control device
BET	Brunauer, Emmett and Teller
CAIR	Clean Air Interstate Rule
CAMR	Clean Air Mercury Rule
CS-ESP	Cold-side electrostatic precipitators
EDX	Energy dispersive X-ray
EPA	U.S. Environmental Protection Agency
FF	Fabric filter
HS-ESP	Hot-side electrostatic precipitators
ICDD	International Centre for Diffraction Data
ICR	Information Collection Request
LOI	Loss on ignition
MFC	Mass flow controller
MMacf	Million actual cubic feet
NTP	Normal temperature and pressure
PAC	Powdered activated carbon
PFA	Per Fluor Alkoxy
ppm	Parts per million
PRB	Powder River Basin
PS	Particle scrubber
PTFE	Poly Tetra Fluoro Ethylene
PVDF	Poly Vinylidene Difluoride
SCR	Selective catalytic reduction
SDA	Spray dry adsorber
SEM	Scanning electron microscopy
TCLP	Toxicity Characteristic Leaching Procedure
TDAC	Tyre derived activated carbons
tpy	tons per year
WFGD	Wet flue gas desulphurisation
XRD	X-ray diffraction

1. Introduction

Coal combustion is used to generate a significant proportion of the world's electric power. One major problem associated with this process is the emission of mercury to the environment; in fact coal-fired utility boilers are the largest anthropogenic sources of mercury emission. Since mercury is highly volatile, it is not effectively captured by the particulate matter control devices presently used in coal-fired power plants.[1] The mercury that is emitted eventually settles either directly into water or onto land, from whence it can be washed into water.[2] Micro-organisms present in water are believed to change metallic mercury into methyl-mercury, a highly toxic form that accumulates in fish and shellfish, and also in animals that eat those fish. Fish and shellfish are the main sources of methyl-mercury exposure to humans.[2] High levels of methyl-mercury in the bloodstream of unborn babies and young children may harm the development of the nervous system, adversely affecting the child's mental functions such as ability to think and learn.[2] In response to this health threat, both Canada and the U.S.A. have recently introduced legislation which limits mercury emissions from coal-fired power plants. Legislators in the European Union are considering the need for mercury emission legislation at the present time.

Mercury present in flue gas can be classified as particle-bound mercury and gaseous mercury. The latter form of mercury may exist as either elemental or oxidised mercury.[3] Particle-bound mercury is effectively captured by ash collection devices, such as electrostatic precipitators and fabric filters. Thus it is mainly the gaseous form of mercury that is emitted to the atmosphere by coal-fired power plants. The lifespan of elemental mercury (Hg^0) in the atmosphere is estimated to be up to a year[4]; on the other hand, oxidized forms of mercury have a short life of only a few days because of particulate settling and solubility.[4] As a result, Hg^0 can be transported over transcontinental distances, whilst oxidized gaseous and particulate forms of mercury tend to be deposited near their emission source.

Various control technologies to reduce mercury emissions from coal-fired utilities are being developed in order to find the most appropriate method of combination with

existing air pollution control devices.[5] Direct injection of powdered activated carbon (PAC) upstream of a particulate control system has been intensively studied to remove vapour-phase mercury from the flue gas streams of coal-fired utilities. At the present time, injection of PAC looks like being the most promising technology for the control of mercury emissions in the near term. However, a high ratio of carbon-to-mercury must be used in order to achieve a mercury removal efficiency of 90%. This is due to the short residence time of PAC from the injection point to the particulate control device, the existence of competing species in the flue gas that adsorb onto the active sites of the carbon, and the low concentrations of mercury in the flue gases.[4] Thus there is still scope for improving this technology further in order to reduce the associated operating costs, by reducing the level of carbon injection and also by developing cheaper carbons than those used in current U.S. tests. This situation has lead to the formulation of the current research project, sponsored by the British Coal Utilisation Research Association with the active participation of the coal-fired boiler manufacturer, Doosan Babcock Energy Limited, and the power generator, E.ON (UK) Limited.

1.1. Motivation for the present research

Legislation that restricts the amount of mercury which a coal-fired utility plant is allowed to emit has already been implemented in Canada and the U.S.A. (refer § 2.3). Injection of PAC in to the flue gas stream is currently believed to be the most favourable option for limiting these emissions. Bench-scale and full-scale tests have already been conducted in North America to evaluate the different types of PACs currently available.[4, 6-8]

In parallel, a growing research interest has developed to evaluate the production of cost-effective carbon-based adsorbents from a range of residues which are mainly industrial or agricultural by-products.[9] In the current study, sorbents produced from two such waste materials, i.e. scrap tyre rubber and sewage sludge, have been evaluated against commercially available Norit Darco Hg™, using a novel bench-scale fixed bed reactor. Coal-fly ashes from three different U.K. coal-fired power plants have also been included for evaluation in the present research, since earlier studies have shown that coal fly ashes may adsorb some of the mercury in the flue gas stream (refer § 2.4.2). The re-use of fly

ash to capture more mercury would seem to offer a particularly cheap solution to the mercury emission problem.

1.1.1. Benefits of using scrap tyre rubber to manufacture sorbents

Around 70% of the 450,000 tonnes of tyres annually disposed in the U.K. are mainly recycled or used as fuel for cement kilns.[10] However, from 2006, the new EU Landfill Directive has banned land-filling of both whole and shredded tyres.[10] Using scrap tyre rubber to produce activated carbons would provide a two-fold environmental and economic benefit: A recycling path has been developed for waste tyres and new adsorbents are produced from this waste material for use in environmental operations.[11] Tyre-derived activated carbons (TDAC) have been tested before for their ability to store natural gas and separate O_2. Previous studies have shown that sulphur-impregnation improves the activated carbon effectiveness for mercury removal (refer § 2.4.1).[11, 12] This has relevance to the use of TDACs, since sulphur is utilised in the rubber vulcanisation process and is organically bound to the carbon matrix. It is reported that approximately 78% of the original sulphur content in tyre rubber is maintained during the tyre pyrolysis process.[11] During the present study, charcoal and steam activated carbons prepared from scrap tyre rubber have therefore been evaluated for their suitability as sorbents for mercury capture.

1.1.2. Benefits of using sewage sludge to manufacture sorbents

Sewage sludge has traditionally been disposed of by incineration and by use in farmland applications and landfill.[9] Some of these methods are now under pressure from environmental regulations and so an alternative, cost-effective disposal solution for sewage sludge is urgently needed. Activated carbon preparation from sewage sludge can be considered as a possible method of reducing sludge volume and, at the same time, produce reusable by-products.[9] Recent studies have shown that it is possible to produce materials of high surface area from sewage sludge.[13, 14] The acceptability of using charcoal produced from the pyrolysis of sewage sludge for adsorbing mercury has therefore been evaluated during the present study.

1.1.3. Benefits of using zinc bromide activated carbons

Commercially available PACs without halogen impregnation (e.g. Norit Darco Hg™) had only a limited success in removing mercury from coal-fired power plants equipped with CS-ESPs and using either low rank coals, or bituminous coals with high sulphur contents (refer § 2.4.3). In contrast, full-scale test have shown that bromine impregnated PACs (e.g. Norit Darco Hg-LH™ and B-PAC™) are very effective in performing this task. In the present study, bromide impregnated activated carbons have been prepared from waste material (i.e. scrap tyre rubber and sewage sludge) to determine whether they would perform better than the PACs without bromide impregnation. Furthermore, these bromide impregnated PACs have also been compared against Norit Darco Hg-LH™ to establish their suitability as an alternative for the latter, chemically treated, activated carbon.

1.1.4. An insight into the method of mercury captured on some selected PACs

Recent studies have shown that the mercury capture performance of a sorbent depends on both the sorbent characteristics and the composition of the flue gas stream (refer § 2.2 and 2.4). The sorbents evaluated during the present research project have thus been extensively characterised using a range of analytical techniques. Furthermore, mercury adsorption and desorption tests have been conducted, using different gas mixtures, in order to obtain an insight into how the mercury is retained on each sorbent.

1.1.5. The leachability of the mercury retained on the sorbents

During any future commercial application, the sorbents used to capture mercury in the flue gas stream would probably be collected, along with the fly ash, by the APCD. At present, a majority of coal fly ash is either sold as an additive for cement replacement or is disposed of in landfills.[15-17] Table 1-1 lists the fate of fly ash from U.S. coal-fired power plants in 1999. Most of the spent sorbent would be exposed to rain water over a long time-scale and it is known that whilst Hg^0 is not soluble in water, the Hg^{2+} ions in ash are.[18] Table 1-2 list the solubility of some mercury compounds. During the current project, the leachability of mercury captured on the test sorbents was studied to ascertain the stability of the contained mercury, in order to identify any adverse issues with regard to subsequent ash disposal or use.

Table 1-1 Fate of fly ash from coal combustion in the United States in 1999.[17]

	Millions of tons	Percentage
Land disposal	42.2	67%
Concrete/grout	10.0	16%
Structural fills	3.2	5%
Waste stabilisation	1.9	3%
Mining applications	1.5	2%
Raw feed for cement kilns	1.3	2%
Road base/subbase	1.2	2%
Flowable fill	0.8	1%
Other	0.8	1%

Table 1-2 Solubility of some mercury compounds.[19]

	Elemental mercury	Mercuric chloride	Mercurous chloride	Methyl mercuric chloride	Dimethyl mercury
Molecular formula	Hg^0	$HgCl_2$	Hg_2Cl_2	CH_3HgCl	C_2H_6Hg
Oxidation state	0	+2	+1	+2	+2
Solubility	5.6×10^{-5} g/L at 25°C	69 g/L at 20°C	2.0×10^{-3} g/L at 25°C	0.1 g/L at 21°C	1 g/L at 21°C

1.2. Structure of the thesis

The thesis is divided into 9 chapters. Chapter 1 and Chapter 2 cover the introduction, the objectives this study and a literature review on the background to the work described in this thesis. The background includes a description on mercury emissions from coal fired power plants and what effects pollution control systems currently installed in these facilities have on the plant's mercury emissions. The chemistry of formation of mercury species in the flue gas and how these different forms of mercury may be adsorbed by sorbents particles and coal fly ash is also discussed. The final section in Chapter 2 outlines the experimental results that have been obtained to-date by other studies on capturing mercury from flue gas streams.

Chapter 3 discusses the results obtained from thermodynamic equilibrium modelling completed during the present study that has been used to identify the different species of

mercury present in the flue gas. In addition, the effect of chlorine on the outcome of combusting different types of coal has also been investigated.

Chapter 4 describes the sorbents evaluated in this study, i.e. charcoal, activated carbons and coal fly ash. It includes a brief introduction on two commercially available activated carbons, Norit Darco Hg™ and Norit Darco Hg-LH™ which were the reference sorbents for the present research. This chapter also contains the procedures used to produce sorbents from scrap tyre rubber and sewage sludge.

The characteristics of the sorbents, measured by a range of analytical techniques, are presented in Chapter 5. Clearly many of the sorbent properties discussed in this chapter have a direct bearing on their mercury capture performance.

Chapter 6 describes the novel reactor developed for this study and the bench-scale experimental scheme that has been used to evaluate the effectiveness of each sorbent for mercury capture. The two analytical techniques used to quantify the amount of mercury adsorbed on the test samples are also presented in this chapter.

The tests performed to evaluate sorbents for mercury capture, and the results obtained, are presented and discussed in Chapter 7. The results of the thermal desorption and leaching tests are also presented in this chapter.

Chapter 8 examines the sorbents produced from waste that would be the most suitable alternatives for commercially available Norit Darco Hg™ and Norit Darco Hg-LH™, and suggests methods for large scale production of these sorbents.

The final chapter (Chapter 9) presents a summary, the main conclusions arising from this study. The aspects that should be studied during a subsequent programme on capturing mercury in flue gas from combustion of coal is also included in this chapter.

2. Background

This chapter discusses the background to the research that has been described in this thesis. It deals with why mercury discharges from coal-fired power plants are becoming important, how these emissions vary depending on the type of coal being combusted and on the systems for particulate matter control. It also presents, the current views on the mechanisms by which mercury released during coal combustion interacts with the other flue gas constituents. The final sections of the chapter has a description of the mercury emission legislations that have recently been introduced in North America, along with a summary of the different sorbents that have been evaluated during the many studies performed by other researchers to assess mercury capture in bench-scale and full-scale plant tests.

2.1. Mercury emissions from coal-fired power plants

Coal contains many elements in trace amounts of parts per million (ppm). Mercury is one such trace element and is found in concentrations between 0.02 - 1.0 ppm[20] and is readily volatilised during coal combustion. It is estimated that coal-fired power plants emit mercury in the range of 1-10 $\mu g/m^3_{STP}$.[4, 21]

Due to the large quantity of coal being combusted at coal-fired plants, they are currently the largest single-known source of mercury emissions in the United States, Canada and the United Kingdom.[22-24] In the U.S.A. they account for about one-third of the total anthropogenic mercury emissions.[4] Data collected by the U.S. Environmental Protection Agency (EPA) indicated that during 1999, the 900 million tons of coal used in U.S. power plants contained about 75 tons of mercury. It is estimated that on average, about 40% of mercury entering the plants is captured, whilst 60% is emitted. Thus, during 1999, coal-fired power plants in the U.S. would have emitted ca. 45 tons of mercury to the atmosphere.

In Canada it has been estimated that 2.7 tones of mercury was emitted to the atmosphere in 2003 by Canadian coal-fired power plants.[23] This represents about 72% of the mercury initially present in the coal used by coal-fired power plants in Canada.

Total annual mercury emissions in the United Kingdom have been much less than either Canada or U.S.A. and for 1999 were estimated to be 8.55 tonnes.[24] However, during that year, 1.56 tonnes of mercury came from coal and coke, i.e. a contribution of 18% to the total UK mercury emissions. The UK National Atmospheric Emissions Inventory also records similar values for 1999 mercury emissions by the "public electricity and heat production" sector.[25] Coal-fired power plants would undoubtedly make the most significant contribution to this category. Furthermore, data for 2005 suggest that this sector emitted 2.34 tonnes of mercury, accounting for 31% of the total annual mercury emissions in the United Kingdom.[25]

Recent estimates of global annual mercury emissions from all sources - both natural and human-generated - range from roughly 4,400 to 7,500 tons per year. Human-caused U.S. mercury emissions was estimated to account for roughly 3% of the total global mercury emissions, while U.S. coal-fired power plants are estimated to account for about 1%.[22]

When the problem of mercury emission control is considered, coal-fired utility power generation plants have several disadvantages compared to waste incinerators, where mercury capture is mandatory.[7, 21] Zevenhoven and Kilpinen have quoted mercury concentrations in the range of 5 – 50 $\mu g/m^3_{STP}$ leaving the boiler furnace and entering the flue gas ducts in coal-fired power plants,[21] whereas municipal solid waste incinerators have mercury concentrations in the range of 200 – 1000 $\mu g/m^3$.[7] Thus coal-fired facilities have significantly lower mercury concentrations in their flue gas streams, but have far greater volumetric flow rates. Furthermore, the power station gas streams have a lower Cl/Hg ratio and a smaller fraction of oxidised mercury. All these factors combine to enhance the problem of reducing mercury emissions from power station flue gases. Mercury capture is improved in the presence of chlorine where it may be converted to an oxidised form; reasons for this are discussed in sub-sections 2.2.1 and 2.2.2.

2.1.1. Mercury in coal

In any combustion system, the fuel itself is the main source of trace elements.[26] When comparing the mercury concentration in a range of imported coal samples, it was found that the lowest mercury concentrations were in coals from Australia, Colombia, Indonesia, New Zealand and Russia (average 0.04-0.08 mg/kg).[26] High average mercury concentrations were present in some coals from Eastern USA, China and Germany, whilst the highest concentration was found in coal from Poland which had a value of approximately 0.35 mg/kg.[26]

Mercury in most coals is associated with sulphide minerals which include pyrite (FeS_2) and cinnabar (HgS), where occasional Fe atoms within the pyrite lattice are replaced by Hg atoms.[4] Mercury can also occur as metallic mercury or be incorporated into organometallic compounds in coal.[27] At combustion temperatures greater than 1400°C the above mentioned forms decompose and elemental mercury is released. In contrast to the most non-volatile or semi-volatile trace elements in coal, the mode in which mercury occurs in the coal does not affect its initial combustion transformation mechanism.[28]

Tests by other researchers have shown that the mercury concentration in the combusted flue gas is directly related to the amount of mercury in the parent coal. As an example, Pavlish et al.[29] tested two different coals during a pilot scale study, namely a lignite from Poplar River station which had twice the mercury concentration of the second lignite from the Freedom mine. As expected, they found that the flue gas produced by combusting Poplar River lignite had twice the mercury concentration of the flue gas produced from the Freedom lignite.

The oxidation state of mercury depends on combustion conditions and the presence of other flue gas components, which are related to the characteristics of the coal. As illustrated in Figure 2-1, combustion of lignite seems to produce flue gases with the greatest proportion of elemental mercury.[29] Bituminous coal flue gas, on the other hand, had the lowest percentage of Hg^0. Appalachian bituminous coal and western subbituminous coal together accounted for 81% of the mercury entering coal-fired plants in the U.S.[4] The very different compositions of these two coals has a significant impact on their mercury emissions (Table 2-1).[29] Appalachian coals had high mercury, chlorine

and sulphur contents; however, the calcium content in this coal was low. The flue gases produced thus had a high percentage of Hg^{2+}. Western sub-bituminous coals on the other hand had low concentrations of mercury, chlorine and sulphur, with high calcium content. Consequently, the combustion of this coal resulted in flue gases with a high percentage of Hg^0. A similar finding has been reported in Figure 2-1, where about 65% of the mercury in flue gases from a sub-bituminous coal was present as Hg^0, whereas the figure for a bituminous coal was low, at 20%.

Tests conducted by the EPA in 1999 have shown that, in general, plants burning sub-bituminous coal and lignite have demonstrated significantly lower mercury capture than similarly equipped bituminous-fired plants (Table 2-2).[6] It has been suggested that the poorer performance associated with the lower rank coals was the result of the presence of higher levels of elemental mercury, due to the low chlorine content of these particular coals. In conclusion, plants firing bituminous coals should be preferred targets for mercury control,[26] since bituminous coals tend to produce more mercury in the oxidised form, which is easiest to capture. Coal switching or blending could thus be a simple option to effect some reduction in emissions from some plants.

Table 2-1 Comparison of Appalachian (Bituminous) and Western Subbituminous coal compositions – analysed on a dry basis[29]

	Appalachian (Bituminous)	Western Subbituminous
Hg [ppm]	0.126	0.068
Cl [ppm]	948	124
S [ppm]	1.67	0.48
Ca [ppm]	2700	14000

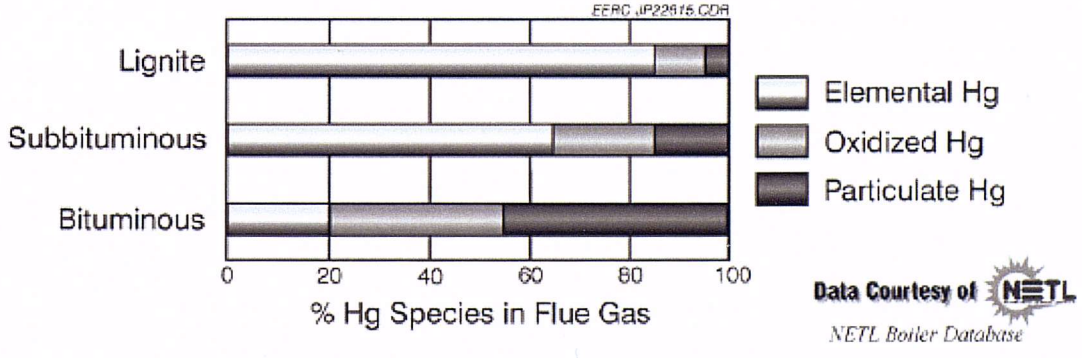


Figure 2-1 Mercury speciation in the flue gases from different coal ranks.[29]

2.1.2. Effect of current pollution control technologies

Mercury is a metal which is liquid at ambient conditions. Its control is difficult due to its high volatility, with a boiling point of only 357°C.[21] Coal rank plays a major role in the chemical transformations of mercury within boilers and pollution control devices. However each technology used in the boiler or the particulate control device, or a combination thereof, also influences the form and quantity of mercury that is captured. Most coal-fired power-plants are fitted with some form of control technology to reduce emissions of harmful pollutants. Data from the U.S. EPA Information Collection Request (ICR) indicated that very little mercury was removed in a boiler using pulverised coal, but the level of mercury oxidation at the exit of the boiler was increased when burning coal with higher chlorine content and when the exit gas temperature was lowered.[4] Table 2-2 gives a summary of average co-benefit mercury capture for various air pollution control device (APCD) configurations, for a range of coal ranks, from pulverised coal-fired utility plants in the U.S.A. The following sub-sections give an account of the effectiveness of pollution control systems on mercury capture.

Table 2-2 Average mercury capture by coal rank and APCD configuration in US coal-fired utility plants.[15]

APCD configuration	Average percentage of mercury capture		
	Bituminous	Subbituminous	Lignite
CS-ESP	36	9	1
HS-ESP	14	7	Not tested
FF	90	72	Not tested
PS	Not tested	9	Not tested
SDA + ESP	Not tested	43	Not tested
SDA + FF	98	25	2
SDA + FF + SCR	98	Not tested	Not tested
PS + WFGD	12	10	Not tested
CS-ESP + WFGD	81	29	48
HS-ESP + WFGD	46	20	Not tested
FF + WFGD	98	Not tested	Not tested

2.1.2.1. Low NOx burners

Primary measures for NO_x control usually comprise low NO_x burners with over-fire air. Low NO_x burners operate at lower combustion temperatures than conventional burners. Theoretically, low NO_x burners may affect mercury emissions by reducing the ratio of oxidised to elemental mercury, however some low NO_x burners caused an increase in

unburnt carbon-in-ash which may increase the mercury capture efficiency.[26] Due to the limited quantity of data available at present however these theories cannot be proven.[4]

2.1.2.2. Particulate control devices

Particulate control systems are employed in 75% of the coal-fired plants in the U.S., and 80% of these are cold-side electrostatic precipitators (CS-ESP).[4] Two-thirds of the coal combusted by the power generation industry was utilised by plants having either a cold side or hot-side ESP or a fabric filter (FF). Average mercury capture efficiencies for these types of particulate control devices are tabulated in Table 2-3. Fabric filters remove a significant percentage of both elemental and gaseous mercury^{2+}, due to the oxidation and capture that occurs by the excellent gas-solid contact across the dust cake on the filter.

Table 2-3 Mercury capture in particulate control devices.[4]

Tyre of particulate control	Mercury captured	Mercury exiting in elemental form
FF	58%	23%
CS-ESP	27%	47%
HS-ESP	4%	66%

A significant proportion of the particulate bound mercury that enters a cold-side electrostatic precipitator or a fabric filter is removed by the device.[4] No particulate bound mercury however is present at the inlet of the hot-side electrostatic precipitators (HS-ESP) owing to its higher operating temperature. HS-EPSs therefore had lower mercury capture efficiencies.

The speciation of mercury depends on the chlorine content in coal. At chlorine levels less than 200 ppm, it was found that although Hg^0 was oxidised, it was not removed by ESPs. Furthermore, the total gaseous mercury emissions from CS-ESPs were not significantly affected by the chlorine content. On the other hand the mercury capture effectiveness of fabric filters was found to be very sensitive to the chlorine concentration. Although FFs were practically ineffective at chlorine contents below 200 ppm, their performance increased significantly with higher chlorine concentrations leading to an average efficiency of 73% for chlorine levels in the range of 200-1400 ppm. It has also been

found that high coal sulphur contents lead to reduced mercury capture on cold-side ESPs.[4]

Although fabric filters give good mercury removal ranging from 70 – 80% for bituminous and subbituminous coals, this method of particulate control had a negligible impact on mercury removal from the flue gas from lignite coal combustion.[26]

2.1.2.3. Wet flue gas desulphurisation

In the USA, about 25% of the coal-fired power plants use wet flue gas desulphurisation (WFGD) systems.[4] In most of these units the flue gas passed through a CS-ESP, a HS-ESP or a FF, before entering the scrubber. Since Hg^{2+} is water soluble while Hg^{0} is insoluble in water, the scrubber itself removed ca. 90% of the oxidised mercury that entered the unit, but failed to remove any elemental mercury.[18]

Coal chlorine content influences the mercury removal effectiveness of systems that combine a particulate control device ahead of the scrubber. This was due to the mercury speciation (elemental mercury being converted to mercury chloride which is soluble in water) during passage through the particulate control device prior to entering the scrubber. The level of mercury removal by a flue gas desulfurisation unit placed after a CS-ESP doubled from 30% to 60% when the coal chlorine content was increased from 50 to 1000 ppm[4]. A scrubber installed after a HS-ESP had its mercury capture efficiency increase from 20% to 50% when the coal chlorine content was increased from 200 to 1000 ppm. The average mercury capture efficiencies for the combined system of a particulate control device followed by a scrubber are tabulated in Table 2-4.

Table 2-4 Mercury capture when WFGD follows a particulate control device.[4]

	Combined mercury capture	Contribution by WFGD only	Oxidised mercury entering WFGD
WFGD+FF	88%	30%	77%
WFGD+CS-ESP	49%	22%	53%
WFGD+HS-ESP	26%	22%	34%

2.1.2.4. Spray dryer absorbers and selective catalytic reduction

Spray dry absorbers that use an alkaline slurry to absorb SO_2 have also been observed to absorb ca. 90% of the oxidised gaseous mercury, so that the residue mercury escaping through the spray dryer must have been primarily in the elemental form.[4] The particulate control device that followed the spray dryer captured the generated dry sorbent and the fly ash particulates. The combined efficiency of a spray dryer with a fabric filter was very dependent on coal chlorine content and had an average combined mercury removal efficiency of 38%. This was however significantly less that the average efficiency of a WFGD system combined with fabric filters (refer Table 2-4).

The Selective Catalytic Reduction (SCR) systems, as well as the Selective Non-Catalytic Reduction (SNCR) systems, that are being installed to reduce NOx emissions are also believed to reduce mercury emissions. However, the lack of good data plus possible masking effects of other variables meant that no conclusive answers could be obtained from the full-scale tests conducted in the U.S.A.[4]

2.2. Chemistry of formation

The chemistry of mercury during combustion is of particular importance for the development of mercury control technologies.[26] Coal contains mercury in numerous forms (refer § 2.1.1), which decompose in the combustion flame to form elemental mercury. Galbreath and Zygarlicke[28] have suggested the possible physical and chemical transformations that mercury may undergo during coal combustion and, subsequently, in the resulting flue gas (Figure 2-2). In the chemically complex post-combustion environment, and with decreasing temperature, gaseous elemental mercury may remain as a monatomic species or react to form inorganic mercurous (Hg_2^{2+}) and mercuric (Hg^{2+}) compounds.[28] The principal oxidized forms of mercury in coal combustion flue gas are Hg^{2+} compounds however, because of the instability of Hg_2^{2+} compounds at low concentrations.[28]

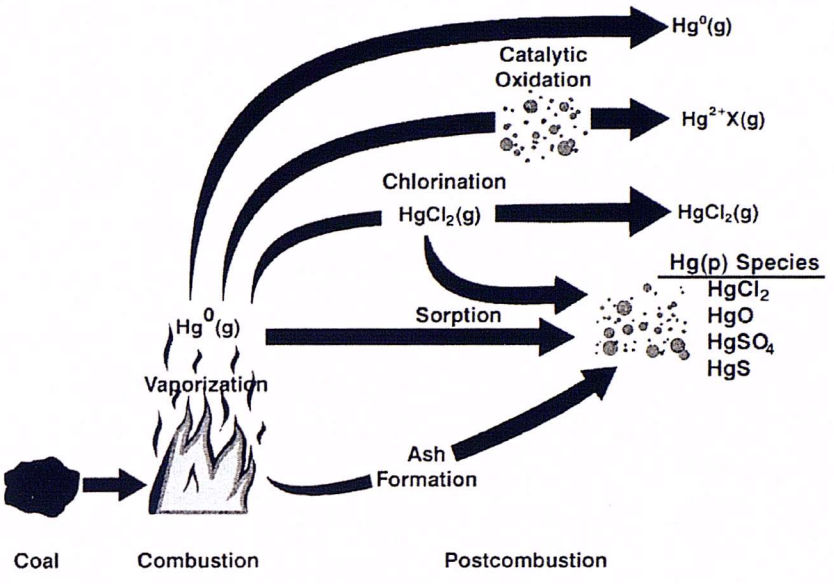


Figure 2-2 Potential mercury transformations during coal combustion and subsequently in the resulting flue gas.[28]

Miller[30] has reported that within the temperature range from 650 to 1100°C, thermodynamic equilibrium models predict that mercury is completely gaseous as Hg^0 (>98%) and HgO (<2%). Table 2-5 lists the known equilibrium reactions from one of the several thermodynamic models which have been used by other researchers to predict the speciation of mercury, as a function of temperature, in various flue gas compositions representative of coal combustion systems.[31] The model used a "the total Gibbs free energy minimization" program called MINGTSYS to obtain information on mercury speciation. It proposes that at low temperatures, and in the absence of chlorine, $HgSO_4(s)$ was the most stable form of mercury. However if $HgSO_4(s)$ was also excluded from the model then the stable product at low temperatures was HgO(s). Due to the effects of chlorine in the system, these solid phases are stable only below the temperature range 110 – 320°C. Since CS-ESPs operate within this temperature range the sorbents evaluated during the present study were also examined for mercury capture at test temperatures within this range. The results obtained by Frandsen et al.[31] suggests that if the simulated flue gas (containing chlorine, oxygen, sulphur dioxide and mercury vapour) had adequate time reach thermodynamic equilibrium conditions then the mercury in the gas stream would have condensed on to the sorbent.

Table 2-5 Equilibrium reactions between mercury and flue gas constituents.[31]

Reaction no.	Reaction[a]	Equilibrium temperature, °C
1	$HgO(g) \Leftrightarrow Hg^0(g) + 1/2\ O_2(g)$	320[b], 680[c]
2	$HgCl_2(g) + H_2O \Leftrightarrow HgO(g) + 2HCl$	430[c]
3	$HgSO_4(s) \Leftrightarrow HgO(g) + SO2(g) + 1/2\ O_2(g)$	320
4	$HgO(s) \Leftrightarrow HgO(g)$	170[d]
5	$HgSO_4(s) + Cl_2(g) \Leftrightarrow HgCl_2(g) + SO_2(g) + O_2(g)$	110[c]

Note –
a - Reaction proceed to the right at temperatures greater than, but to the left at temperatures less than, the stated temperature.
b - In the absence of chlorine.
c - In the presence of chlorine.
d - When $HgSO_4(s)$ is excluded for the model.

Equilibrium calculations by other researchers have predicted that Hg^0 should be almost completely converted to oxidized forms of volatile $Hg^{2+}X$ and Hg_p upon cooling to 400°C.[4] However measurements on boilers burning different types of coal have typically showed only 35% to 95% oxidation. This suggested that the conversion was probably kinetically controlled.

2.2.1. Homogeneous mercury chlorination reactions

Laboratory and field studies by other researchers have indicated that the conversion of elemental mercury to Hg^{2+} and Hg_p is mainly influenced by the coal chlorine content.[4] The chlorine in coal is released primarily as HCl in the high-temperature zone of the boiler.[4] As the combustion gases cool, HCl is partially oxidised to Cl_2 by the Deacon Process reaction in the presence of O_2 and H_2O.[4]

Hutson et al.[32] have suggested that elemental mercury vapour is the dominant mercury form in the coal combustor. The elemental mercury vapour then interacts with acid species by homogenous (gas-phase) and heterogeneous (gas-solid, surface catalysed) reactions to form oxidised mercury vapour, Hg^{2+}. However, gas-phase mercury oxidation is characterised as being a slow reaction, highly dependent upon the amount of chlorine present in the coal.

2.2.2. Heterogeneous mercury reactions and capture

Heterogeneous mercury oxidation is a complex mechanism and depends upon the availability of surfaces having electrophilic groups that attract the electron-rich Hg^0 atom.[32] These reactions of mercury in coal combustion gases are influenced by the properties of solid surfaces and the composition of the flue gases. [4]

Results of tests on full-scale boilers combusting coal from U.K. and U.S.A. have shown that between 0% to 90% mercury removal was possible on fly ash alone without any sorbent injection.[4] The capture depended on temperature, the level of unburned carbon in ash and the catalytic effects of as-yet-unidentified inorganic ash constituents.

2.2.2.1. Surface properties of fly ash and carbon

A study by Hassett and Eylands[33] found distinct differences in the morphology of the unburnt carbon in fly ash from different coal ranks, and this could have influenced the mercury capture efficiency recorded during that investigation. The fly ash produced during the combustion of highly reactive non-caking lignite had relatively few carbon particles. These carbon particles are comparatively large and amorphous. Bituminous coal on the other hand produced a larger amount of carbon particles that were smaller and were agglomerated and flaked. Mercury was normally concentrated on the finer fly ash fractions of both low- and high-rank coals. However, Hassett and Eylands[33] also noted that carbon in the fly ash particles had a smaller surface area than activated carbon particles and may not have the same active sites for mercury capture.

Studies by other researchers have shown that during laboratory experiments on bituminous and sub-bituminous coals, mercury capture was dependent on coal rank.[4] Removal of $HgCl_2(g)$ was higher for bituminous coal chars while sub-bituminous coal chars had higher removal of elemental mercury. The concentration of organic sulphur in the char had a bearing on the capture of elemental mercury only and not on the capture of $HgCl_2$. Analysis using X-ray absorption fine structure spectroscopy seemed to suggest that the $HgCl_2(g)$ was captured as an Hg-Cl compound and that elemental mercury was removed as a mixture of Hg^0 and mercury chloride.[4]

2.2.2.2. Effects of acid gases on mercury sorption

Other investigators have found that tests conducted using a synthetic flue gas containing SO_2, HCl, NO and NO_2 showed that the interaction between SO_2 and NO_2 greatly impaired the capture of elemental mercury by activated carbon.[4] However, HCl, NO and NO_2 individually or in combination enhanced the mercury capture.[4]

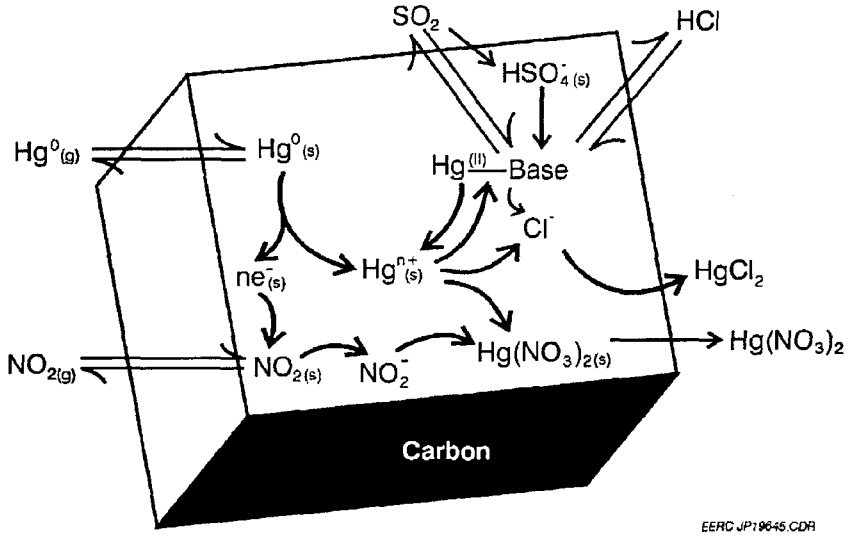


Figure 2-3 Suggested heterogeneous model for mercury capture showing potential impact of acid gases.[34]

Dunham et al. have suggested a mechanism that may explain the effects of NO_2 and SO_2 (refer Figure 2-3).[34] According to this scheme, in the presence of NO_2, elemental mercury was catalytically oxidised on the surface to form a non-volatile nitrate $Hg(NO_3)_2$, that was bound to the basic sites on the carbon. Mercury capture then continued until the binding sites were used up and a breakthrough occurred. However in the presence of SO_2, some of the catalytic sites were converted to a sulphate form where $Hg(NO_3)_2$ was no longer formed. Although mercury was still oxidised on the surface with NO_2 acting as the oxidising agent (electron sink), in this case the product that was formed was a labile sulphur compound, mercury bisulphate $[Hg(SO_4H)_2]$. The bisulphate in turn reacted with NO_3^- to form a stable volatile acidic form of mercuric nitrate $[Hg(NO_3)_2]$. Dunham et al.[34] suggested that this was the reason for the slow release of previously captured mercury over time, in the presence of NO_2 and SO_2.

The mercury capture mechanism illustrated in Figure 2-3 has been recently refined by Crocker et al.[35] This new experimentally based model of the chemical mechanism of mercury oxidation and binding offers more detail on the nature of the bonding site and its interaction with flue gases and mercury. As illustrated in Figure 2-4, the model uses the concept of zigzag carbene structures.[35] It is hypothesized that the mechanism involves the reaction with HCl to form stable carbenium ion intermediates. These intermediate species can then promote oxidation of elemental mercury and create sites for bonding.

A zigzag-edge carbene site comprises of the basic binding site for which the various acid–gas components and Hg^{2+} compete.[35] Figure 2-5 provides more details of the role of chlorine. The conversion of carbene to carbenium ion by HCl and other acids generates an oxidation site and is consistent with the promotion effect of acids on mercury oxidation. The mechanistic model shows Hg^0 oxidation by the carbenium ion to the organo-mercury intermediate and subsequent oxidation by NO_2 to the bound Hg^{2+} species.

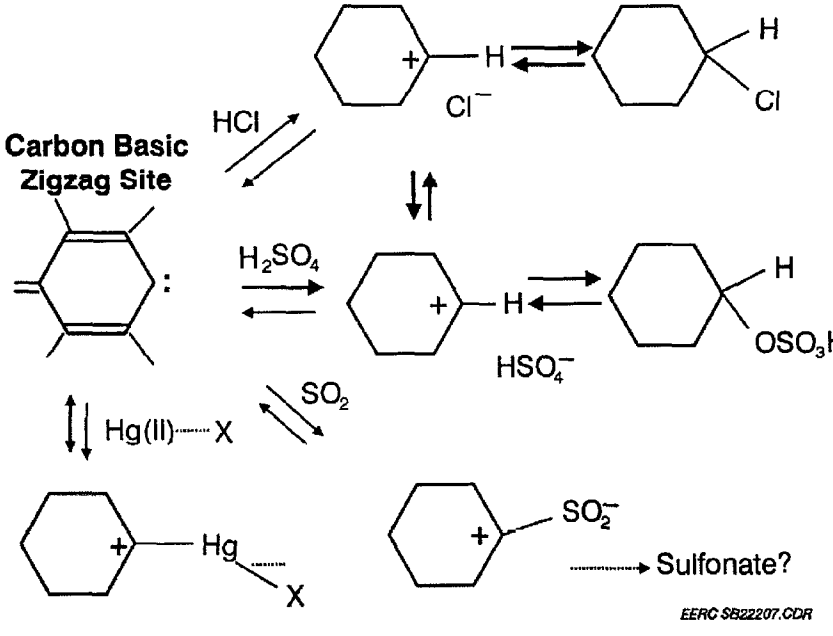


Figure 2-4 Binding site model for activated carbon.[35]

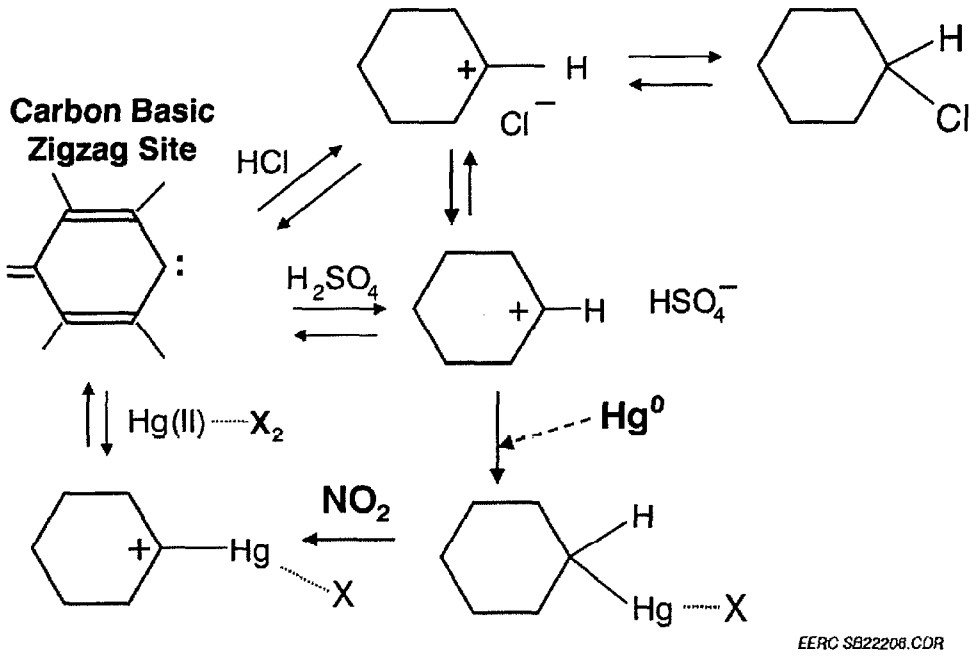


Figure 2-5 Oxidation site model for activated carbon—the role of hydrochlorination in generating carbenium oxidant.[35]

According to Laumb et al.[36] chlorine and sulphur compete at the activated carbon sites that bond these species. With continued exposure to the flue gas, Cl was displaced by S. This was believed to be due to the higher volatility of HCl when compared to H_2SO_4. Although HCl completed effectively with SO_2 for the active sites, as time progressed the formation of sulphate changed the relative volatility of the acids which resulted in HCl escaping in the gas phase.

2.3. Mercury emission limits for coal-fired power plants

In the past, emission standards for mercury which could theoretically apply to coal-fired power plants as a group, have been higher than actual emissions.[26] However on March 15, 2005, the U.S. Environmental Protection Agency (EPA) issued the first-ever Federal rule to permanently cap and reduce mercury emissions from coal-fired power plants.[5, 22] A first phase cap of 38 tons per year (tpy) would become effective in 2010, while 2018 was set as the date for the second phase cap of 15 tpy. The EPA believed that the targets for the first phase cap could be met by taking advantage of "co-benefit" reductions.

According to this scheme, the systems in place for limiting sulphur dioxide (SO_2) and nitrogen oxides (NO_x) emissions under the EPA's Clean Air Interstate Rule (CAIR) would also achieve, in-parallel, the required reductions in mercury emissions. Mercury emissions limited by using a cap-and-trade approach, where allowances could be readily transferred among all regulated facilities, was believed to be the most cost effective way of reducing these emissions from the power sector.

The mercury emission limits for the new "Clean Air Mercury Rule"(CAMR), based on gross energy output, applicable to coal-fired utility plants that were constructed, modified or reconstructed after January 30, 2004 are listed in Table 2-6.[37] Under this scheme, plants combusting bituminous coal have one of the lowest emission limits, at approximately 9.5 kg/TWh.

In setting the limit so far into the future, the EPA recognised that mercury control technologies were not commercially available, and would not be generally available until after 2010.[38] Many observers disagreed with that conclusion, including a growing number of states in the U.S.A. As of February 2007, 18 U.S. states have established more stringent emission limits, which take effect sooner than the EPA limits, and four other U.S. states are developing regulations that would do so. Table 2-7 lists mercury emission limits that have been established by some of these U.S. states.

In 2006, the Canadian Council of Ministers for the Environment endorsed a Canada-wide standard (CWS) that will provide a gold standard to limit mercury emissions from their coal-fired power generation sector (Table 2-8).[23] These emission limits are more stringent than the EPA limits in the U.S.A, Canadian coal-fired utility plants using bituminous coal will have to operate with an average annual mercury emission as low as 3 kg/TWh.

Table 2-6 Mercury emission limits for US coal fired utility plants – based on gross energy output.[37]

Coal rank/plant type	Emission limit
Bituminous units	9.5 kg/TWh
Subbituminous units	
Wet FGD	19.1 kg/TWh
Dry FGD	35.5 kg/TWh
IGCC units	9.1 kg/TWh

Table 2-7 Mercury emission limits established by some US states.[38]

	Effective date	Reduction / emission limit
Arizona	2013	90% or 3.9 kg/TWh
Delaware	Jan 1, 2009	80% or 1.5 kg/TWh
	Jan 1, 2013	90% or 0.9 kg/TWh
Massachusetts	Jan 1, 2008	85% or 3.4 kg/TWh
	Jan 1, 2012	95% or 1.1 kg/TWh

Table 2-8 Average annual mercury emission limits for Canadian coal-fired utility plants.[23]

Coal rank	Emission limit
Bituminous units	3 kg/TWh
Sub-bituminous units	8 kg/TWh
Lignite units	15 kg/TWh
Blends	3 kg/TWh

2.4. Experimental results to-date on low cost sorbents

The injection of sorbents upstream of existing particulate control devices such as electrostatic precipitators or bag-houses is one of the most favourable options for mercury control.[26] This mercury capture technology depended on many variables that include[26]:

- mass transfer to the sorbent surface
- sorbent average particle size and size distribution
- sorbent capacity as a function of mercury speciation and flue gas temperature
- residence time in the flue gas
- type of particulate control device
- inlet mercury concentration

2.4.1. Activated carbon sorbents

Although commercially available activated carbons[†] have been successful in capturing mercury from waste incinerators, powered activated carbons (PAC) have had only a limited success in coal-fired utility plants. A pilot-scale study using two commercially

[†] Activated carbons are carbon based solid materials with exceptionally high surfaces area per unit mass. They can be produced from a wide variety carbon based raw material including coal and biomass. Since the properties of activated carbons vary widely, the characteristics of the PACs used in this study and relevant for capturing mercury are described in Chapter 5 of this thesis.

available activated carbons (Norit Darco Hg™ [formally Norit Darco FGD™ [6]] and Calgon FluePac™) to limit mercury emissions in the flue gas from low-sulphur bituminous coal, suggested that the capture efficiency depended on the sorbent injection rates and bag-house temperature.[26] For the operational conditions in the pilot-plant, lignite-derived Norit Darco Hg™ was found to be the more effective sorbent. The findings from extensive laboratory studies on Norit Darco Hg™ could be summarised as follows.[4, 7]

- Although, chemisorption of oxidised species such as $HgCl_2$ or $Hg_2O(NO_3)_2$ may be ultimately responsible for binding mercury to Norit Darco Hg™ (refer § 2.2.2), mercury was initially adsorbed on to the carbon by a physical sorption mechanism. An eventual capacity of 200 μg Hg/g C was measured when the flue gas had a mercury concentration of 10 $\mu g/Nm^3$. However, due to kinetic limitations relating to surface reactions, this capacity would not be attainable in the residence time available, ranging from seconds to minutes for particulate control devices. Mercuric chloride was removed at a faster rate than elemental mercury. Activated carbon thus captured mercury more effectively after the mercury had been converted into an oxidised form.
- The sorbent particle size was the parameter that determined the minimum sorbent requirement needed to effect mass transfer from the bulk gas to the sorbent particles. The results from theoretical studies suggests that since Norit Darco Hg™ has mainly 9 to 15μm sized particles, mercury capture on this carbon may be limited by mass transfer from the bulk gas to the particle's surface.
- The equilibrium adsorption capacity for $HgCl_2$ was considerably enhanced if water vapour was completely absent in the flue gas. In addition, the deficiency of moisture also increased the adsorption capacity for elemental mercury by a small degree. However, both these capacities are only minimally affected by flue gas moisture variations between 1 - 10%, so that the fluctuations in flue gas moisture content caused by burning a different rank coal, or by varying coal moisture content, would not significantly affect the capture of mercury by the sorbent.
- The concentration of HCl significantly affected the equilibrium adsorption capacity for elemental mercury; its effect on mercuric chloride capacity was on the other hand found to be more moderate. When HCl was not present in the flue gas, Norit Darco Hg™ was ineffective in capturing any elemental mercury.

- The sorbent capacity for elemental and oxidised mercury was reduced by the presence of SO_2 in the flue gas. This reduction in elemental mercury capacity was further amplified when NO_2 was also present.
- Simulated flue gas that lacked HCl and NO_x had a zero equilibrium adsorption capacity for elemental mercury. Although the Hg^0 capture on Norit Darco Hg™ improved to ca. 640 μg Hg/g C when NO_x alone was increased to 100 ppm, it decreased with any further increase in NO_x concentration. Furthermore the significant capacity for retention of elemental mercury due to the presence of 50 ppm of HCl was also greatly reduced if the flue gas contained any NO_x.

According to Pavlish et al.[29] bench-scale tests have shown that when the carbon based sorbents (including Norit Darco Hg™) were exposed to low-chlorine (1 ppm) simulated flue gas (similar to flue gas from lignite coal), an initial conditioning period of 30 – 40 minutes was required. After this period, mercury in the flue gas was captured for about three hours. In contrast, no initial breakthrough was observed when Luscar-activated carbon (produced from a Canadian coal [Luscar]) and Norit Darco Hg™ were tested on simulated flue gas with higher concentrations of HCl, SO_2, NO and NO_2.[29]

Zeng et al. and Hsi et al. have tested activated carbons impregnated with chloride and sulphur respectively.[12, 39] They found that these impregnations do improve the elemental mercury adsorption capacity. In the case of chloride-impregnated activated carbon, the elemental mercury capacity increased to over eight times the capacity of the parent activated carbon.

Table 2-9 lists the elemental mercury adsorption capacity of different activated carbons that have been studied in several investigations.[4] No conclusive evidence has been found to support the hypothesis that the precursor coal affects the activated carbon's mercury capture capacity. According to Pavlish et al.[4], diffusion control models showed that if sorbents with a uniform particle size of ca. 5 μm were injected into a coal-fired plant that had an inlet mercury concentration of 10 $\mu g/Nm^3$, and an in-flight time of 1 to 2 seconds, then C/Hg ratios in the range of 4000 – 9000 would be needed to achieve 90% mercury capture. The differences in equilibrium capacities of the activated carbons in Table 2-9

thus do not appear to be critical, since most of the capacity values are adequate at C/Hg ratios well below 9,000.

Table 2-9 Elemental mercury capacity of different PACs – results from bench scale tests with simulated flue gases that did not contain NO_x.[4]

	Surface area (m^2/g)	Mass mean particle size (μm)	Hg^0 capacity (μg/g)
Lignite activated carbon			
Norit Darco Hg™	500 – 700	9 – 15	2460 [163°C] – 3627 [135°C]
Bituminous activated carbon			
Norit PC-100™	900	<30	1780 [100°C]
Iodine impregnated PAC			
Barneby & Sutcliffe	750	3.5	507 [163°C] – 8530 [107°C]

Previous studies have mainly concentrated on the possibility of using coal based activated carbons to capture mercury from coal combustion flue gases. The initial fixed bed mercury adsorption tests on activated carbons produced from coal used a gas stream of mercury vapour mixed in pure nitrogen.[40] When it became clear that mercury capture was affected by acid gases present in coal combustion flue gas, subsequent studies included HCl, NO_x and SO_2 and water vapour to the simulated flue gas streams.[41-44] Although Carey et al.[42], Miller et al.[41], Stuart[43] and Sjostrom et al.[44] investigated the effect of acid gases on the activated carbons' equilibrium capacity for mercury, none of these studies seem to have used thermal desorption of the spent sorbents to obtain information on which of the acid gases was ultimately responsible for mercury adsorption. Thermal desorption tests would also have indicated the thermal stability of the adsorbed mercury.

A number of earlier studies have shown that it is possible to produce activated carbons for waste material like scrap tyre rubber and sewage sludge.[11, 13, 44, 45] However only Lehmann[11] and Sjostrom et al.[44] have looked into the possibility of using these sorbents to capture mercury in gas streams that simulate coal combustion flue gas. On the other hand these researchers did not examine how mercury adsorption was affected by each of the acid gases (i.e. HCl, NO_x or SO_2) in the simulated flue gas stream. Furthermore since no thermal desorption experiments were completed they were not able to indicate which of the acid gases was most influential in mercury capture. The leachability of the mercury captured on these sorbents made from waste material has also not been assessed during

the previous investigations. The present study on evaluating waste material to produce sorbents capable of adsorbing mercury has therefore addressed these points.

2.4.2. Fly ash sorbents

Fly ashes are the major combustion residues (normally 60% – 88%) produced during the combustion of pulverised coal in coal-fired power plants.[46] A significant proportion of the oxidised mercury in flue gas can be captured on the fly ash in particulate control devices such as bag-houses.[26] Dunham et al.[47] found that fly ash plays a role in both the adsorption of mercury and the oxidation of elemental mercury in the flue gas. They found that during bench-scale tests on coal fly ashes with Hg^0 and $HgCl_2$ injection, many of the ash samples oxidised elemental mercury. However, not all the samples that oxidised mercury were able to retain elemental mercury.

According to Sloss[26] previous investigations have shown that mercury oxidation increases with increasing loss on ignition (LOI; a value used to approximate the level of carbon-in-ash). However the findings relating to the possibility of a correlation between LOI and mercury capture seem inconsistent. Some studies have observed no such relationship while others seem to have found a positive relationship between LOI and mercury capture on coal fly ash.[26, 33, 48, 49]

Unlike most of the previous investigations which have looked at chiefly fly ash from U.S. coal-fired power plants, the present study evaluated fly ash from U.K. coal-fired power plants for the possibility of re-using the ash to capture more mercury. [33, 47-49] The likelihood of mercury adsorption on the U.K. fly ashes being related to LOI content has also been examined. Although Dunham et al.[47] included acid gases in the fixed bed tests on mercury capture by coal fly ashes they did not compare the results against that of commercially available activated carbons. During the present study the mercury adsorption on U.K. coal fly ashes and sorbents produced from waste material have been compared against the mercury capture by Norit Darco Hg™ by using the same experimental conditions. It has therefore been possible to suggest which sorbent would be most suitable for capturing mercury in coal-fired power plant flue gases.

2.4.3. Bromide impregnated PAC – effect during full-scale tests

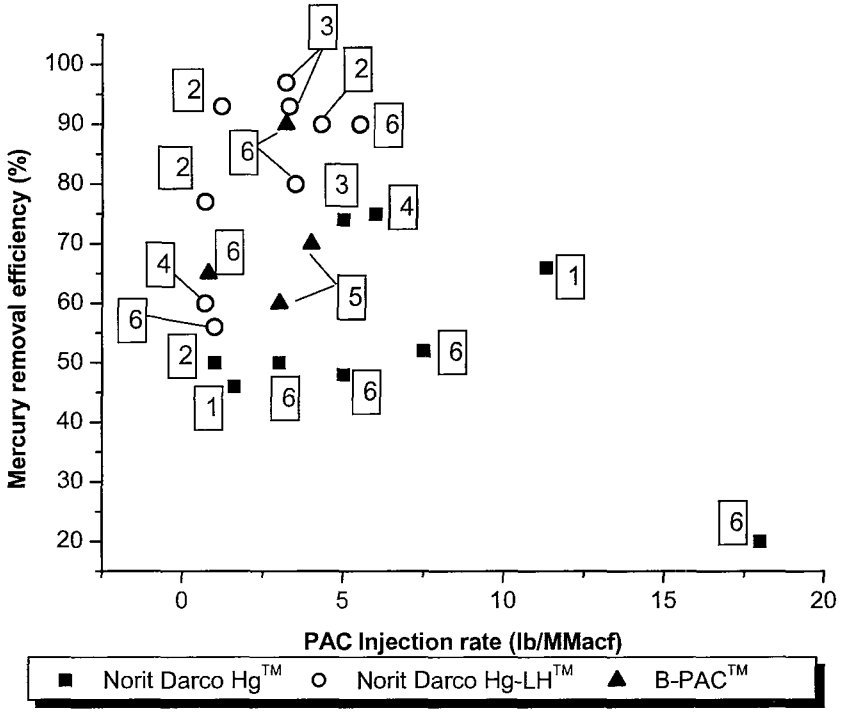
A number of full-scale tests with Norit Darco Hg ™, Norit Darco Hg-LH™ or B-PAC™ injection were recently completed at several coal-fired utility plants in the U.S.A.[6, 8, 50] Norit Darco Hg-LH™ and B-PAC™ are bromine impregnated PACs manufactured by Norit Americas Inc. and Sorbent Technologies Corporation, respectively, for coal-fired utility plants that use low halogen coals.[50, 51] Figure 2-6 is a summary of the mercury capture efficiencies that were obtained with different sorbent injection rates. The results show that although Norit Darco Hg™ was found to be very efficient in bench-scale experiments, its performance on full-scale tests varied, depending on coal type and the APCD that was employed on the particular plant.

At the Pleasant Prairie plant, which combusted sub-bituminous coal and uses a CS-ESP, a mercury reduction of only 46% was achieved when Norit Darco Hg™ was injected at 1.6 lb/MMacf.[6] Even when the injection rate was increased to 11.3 lb/MMacf[‡], only about 66% of the mercury was captured. Tests at the Stanton Station's Unit 1, which is also equipped with CS-ESPs and combusted PRB (Powder River Basin) sub-bituminous coal, showed that the mercury capture performance of Norit Darco Hg™ was constant at ca. 50%, across the injection rate range tested, from 1 lb/MMacf to 5.5 lb/MMacf.[50] The mercury removal at the latter plant was significantly improved when bromine impregnated PACs (Norit Darco Hg-LH™ and B-PAC™) were used. In this case, injection rates between 3.2 – 5.5 lb/MMacf achieved ca. 90% mercury reduction. Similar results were also obtained at the Meramec Station which also combusted PRB sub-bituminous coal and had CS-ESPs.

Full-scale tests results at the Lausche coal-fired utility plant showed that Norit Darco Hg™ was not a suitable sorbent for mercury capture when high sulphur bituminous coal is combusted in a plant fitted with SDA/FF.[8] Norit Darco Hg™ injected at 18 lb/MMacf only achieved 20% mercury reduction, while a 70% reduction was obtain with B-PAC™ injected at 4 lb/MMacf.

[‡] lb/MMacf = Pounds per million actual cubic feet is a measure of the mass of sorbent injected per unit volume of flue gas determined at the actual conditions maintained at the sorbent injection location in the flue gas duct.

Field tests have thus shown that bromine impregnated PACs are more suitable for plants using sub-bituminous coals or lignite, which typically contain less chlorine than bituminous coal. Furthermore, these impregnated sorbents were more effective when high sulphur bituminous coals are combusted. In this case, the effectiveness of Norit Darco Hg™ may have been reduced by the SO_3 produced from the high sulphur coal.[8]



Note:
1 – Pleasant Prairie plant test with sub-bituminous coal & CS-ESP APCD [6]
2 – Holcomb plant with PRB sub-bituminous coal & SDA/FF APCD [6]
3 – Meramec plant with PRB sub-bituminous coal & CS-ESP APCD [6]
4 – Stanton plant unit 10 with lignite & SDA/FF APCD [6]
5 – Lausche plant with high sulphur bituminous coal & CS-ESP APCD [8]
6 – Stanton plant unit 1 with PRB sub-bituminous coal & CS-ESP APCD[50]

Figure 2-6 Mercury removal efficiencies of PAC during full-scale field tests

Although Sjostrom et al.[44] have investigated sulphur impregnated bituminous coal fly ash, the literature survey completed during the present study did not find any previous research that had looked into the possibility of using waste material to produce bromide impregnated activated carbons capable of adsorbing mercury in flue gases from coal-fired power plants with low halogen coals. The leachability of mercury adsorbed by bromide

impregnated sorbents made from scrap tyre rubber or sewage sludge has therefore not been published previously. During the present study mercury adsorption ability bromide impregnated sorbents produced from these waste materials have been compared against the effectiveness of Norit Darco Hg-LH™ by using the same experimental method. Leachabilty tests were also completed on spent sorbents by following a modified TCLP leaching procedure.[52]

3. Thermodynamic equilibrium modelling

This chapter describes the thermodynamic equilibrium modelling work that was carried out during the present study by using a commercially available free energy minimisation software package called "Multiphase module of the Metallurgical and Themochemical Databank" (MTDATA). The programme was applied to calculate the state of mercury species present in coal combustion flue gas systems under thermodynamic equilibrium conditions. Since oxidised mercury is more easily captured by sorbents, this approach for predicting the mercury species has the potential for providing information on removing mercury in flue gas from coal combustion.[4, 7] The effects of kinetic and mass transfer limitations are however not considered in the MTDATA calculations.

The following sections introduce the method and means by which the modelling was done, and the results obtained when the flue gases produced by combustion of different coals were simulated.

3.1. Application of MTDATA

The thermodynamic equilibrium composition for different flue gas conditions was modelled by using the Multiphase module of MTDATA (Version 4.74), a Gibbs free energy minimisation software package supplied by the National Physical Laboratory, U.K.[53] In order to run the models, the Substance Database (SUB_SGTE Version 10.0 – 9 May 2001) containing the thermodynamic data from the Scientific Group Thermodata Europe (SGTE) was employed with the assumptions listed below.

- The gas phases were considered to be ideal gases
- The condensed phases were assumed to be pure substances
- Global equilibrium was assumed to be maintained

In order to gain a better understanding of mercury speciation occurring in flue gases from the combustion of different coals, thermodynamic equilibrium modelling has been carried out on a number of gaseous environments and these are listed in Table 3-1. Frandsen et al.[31] have suggested that mercury will react with chlorine in preference to the other flue gas constituents. The effect of chlorine on mercury speciation was therefore assessed during the present study by removing chlorine from one of the gaseous environments (refer MTDATA atmosphere 1 in Table 3-1 and Table 3-2). The flue gas streams MTDATA atmosphere 3 to MTDATA atmosphere 8 listed in Table 3-1 were used to provide an indication of the mercury speciation at thermodynamic equilibrium conditions when different coals are combusted.

Table 3-1 The different gaseous atmospheres that were modelled with MTDATA during the present study

Gas atmosphere	Description
MTDATA atmosphere 1	Used to test the effect of Cl on Hg speciation – Chlorine **absent** in this gaseous atmosphere
MTDATA atmosphere 2	Used to test the effect of Cl on Hg speciation – Chlorine **present** in this gaseous atmosphere
MTDATA atmosphere 3	Flue gas atmosphere produced from the combustion of a U.S. lignite coal
MTDATA atmosphere 4	Flue gas atmosphere produced from the combustion of a U.K. bituminous coal (Harworth)[54]
MTDATA atmosphere 5	Flue gas atmosphere produced from the combustion of a U.S. bituminous coal
MTDATA atmosphere 6	Flue gas atmosphere produced from the combustion of a U.S. Eastern bituminous coal
MTDATA atmosphere 7	Flue gas atmosphere produced from the combustion of a U.S. low sulphur Eastern bituminous coal
MTDATA atmosphere 8	Flue gas atmosphere produced from the combustion of a U.S. Western bituminous coal

The compositions of the flue gas atmospheres that were modelled are tabulated in Table 3-2. The number of moles of each constituent was initially normalized so that the total number of moles in the flue gas was equal to 1 mole. To enter the flue gas composition into MTDATA the number of moles of each individual atomic species was needed. It was found that if too low a value was used in the model, e.g. for Hg, numerical errors occurred during the computation. The number of moles of each atomic species were therefore normalised so that the total number of atomic species in the flue gas was equal to 100,000 moles (refer Table 3-3). A temperature range of 40 – 400°C was examined for all thermodynamic equilibrium models, always at atmospheric pressure. These conditions more than cover the likely range of stack temperatures in any coal fired utility boiler. In a typical UK power plant, the flue gases from a 500 MW boiler will be cooled to around 130°C by the point of entry to the ESP. The speciation of mercury in the flue gas in the region of the APCD is of critical concern with regard to the possibility of emission to the atmosphere.

Table 3-2 Composition of the flue gases evaluated by the MTDATA thermodynamic equilibrium modelling

	H_2O (moles)	Hg^0 (moles)	$HgCl_2$ (moles)	O_2 (moles)	CO_2 (moles)	SO_2 (moles)	HCl (moles)	NO (moles)	NO_2 (moles)	N_2 (moles)
MTDATA atmosphere 1[a]	0.050	$3.0x10^{-6}$		0.070	0.100	$1.7x10^{-4}$				0.780
MTDATA atmosphere 2[b]	0.050		$3.0x10^{-6}$	0.070	0.100	$1.7x10^{-4}$				0.780
MTDATA atmosphere 3[c]	0.150	$1.2x10^{-9}$		0.060	0.120	$5.8x10^{-4}$	$9.9x10^{-7}$	$1.2x10^{-4}$	$6.0x10^{-6}$	0.669
MTDATA atmosphere 4[d]	0.068	$4.7x10^{-9}$		0.056	0.123	$1.8x10^{-3}$	$2.0x10^{-4}$	$4.9x10^{-4}$	$1.7x10^{-4}$	0.751
MTDATA atmosphere 5[e]	0.060	$7.5x10^{-9}$		0.040	0.140	$1.7x10^{-3}$	$5.0x10^{-5}$	$5.5x10^{-4}$	$2.7x10^{-5}$	0.758
MTDATA atmosphere 6[f]	0.070	$6.0x10^{-9}$		0.060	0.120	$1.6x10^{-3}$	$5.0x10^{-5}$	$3.8x10^{-4}$	$2.0x10^{-5}$	0.748
MTDATA atmosphere 7[f]	0.070	$6.0x10^{-9}$		0.060	0.120	$4.0x10^{-4}$	$5.0x10^{-5}$	$3.8x10^{-4}$	$2.0x10^{-5}$	0.749
MTDATA atmosphere 8[e]	0.080	$6.5x10^{-10}$		0.060	0.120	$1.6x10^{-3}$	$5.0x10^{-5}$	$3.0x10^{-4}$	$2.0x10^{-5}$	0.738

Note -

a – Study conducted to investigate the effect of chlorine on Hg speciation – Chlorine **absent** in the gas[1]

b – Study conducted to investigate the effect of chlorine on Hg speciation – Chlorine **present** in the gas[1]

c – Data for the U.S. lignite coal flue gas composition obtained from literature[29]

d – Data for the UK bituminous coal (Harworth) flue gas composition obtained from E.ON UK

e – Data for the US bituminous coal flue gas and US Western bituminous coal flue gas compositions obtained from literature[47]

f – Data for the US Eastern bituminous coal flue gas and US low sulphur Eastern bituminous coal flue gas compositions obtained from literature[12]

Table 3-3 Individual components of the flue gases that were input to MTDATA thermodynamic equilibrium modelling

	H (moles)	O (moles)	Hg (moles)	C (moles)	S (moles)	Cl (moles)	N (moles)
MTDATA atmosphere 1	4651	18154	$1.4x10^{-1}$	4651	8.05		72536
MTDATA atmosphere 2	4651	18154	$1.4x10^{-1}$	4651	8.05	0.28	72536
MTDATA atmosphere 3	13212	22518	$5.3x10^{-5}$	5285	25.54	0.04	58959
MTDATA atmosphere 4	6173	19612	$2.1x10^{-4}$	5595	82.07	9.12	68528
MTDATA atmosphere 5	5452	19258	$3.4x10^{-5}$	6359	77.21	2.27	68851
MTDATA atmosphere 6	6390	19785	$2.7x10^{-4}$	5475	73.01	2.28	68274
MTDATA atmosphere 7	6394	19787	$2.7x10^{-4}$	5478	18.26	2.28	68421
MTDATA atmosphere 8	7269	20146	$3.0x10^{-5}$	5450	72.67	2.27	67059

3.2. Predicted thermodynamic equilibrium composition

3.2.1. Effect of chlorine on mercury speciation

The MTDATA results on the mercury species that would exist in thermodynamic equilibrium when chlorine is absent in the flue gas are shown in Figure 3-1. At 400°C, mercury was predicted to exist mainly as elemental mercury in the gaseous phase, with a very small fraction in the form of gaseous mercury oxide. As the flue gas cooled to below 350°C the mercury speciation in the flue gas changed to a condensed form of $HgSO_4$. However, if chlorine was also included in the gas stream, then the main mercury species that was predicted to exist while the flue gas cooled from 400°C to 50°C was gaseous $HgCl_2$ (refer Figure 3-1). As the temperature reduced from 50°C to 40°C, condensed $HgCl_2$ became the major mercury species. MTDATA results with chlorine present also show that while the gas cools to 325°C a very small fraction of the mercury would exists as gaseous Hg^0 and that minute concentrations of $HgSO_4$ would be present as the flue gas cools from 350°C to ca. 100°C.

The results therefore suggests that $HgCl_2$ will be the dominant mercury species in the flue gas when coals with high chlorine contents are combusted and the flue gas constituents have adequate time to reach thermodynamic equilibrium. On the other hand if high sulphur content coals that have no chlorine present are used and thermodynamic equilibrium is attained, then condensed $HgSO_4$ will probably be the dominant form of mercury in the flue gas as it cools to the operating temperature of CS-ESPs.

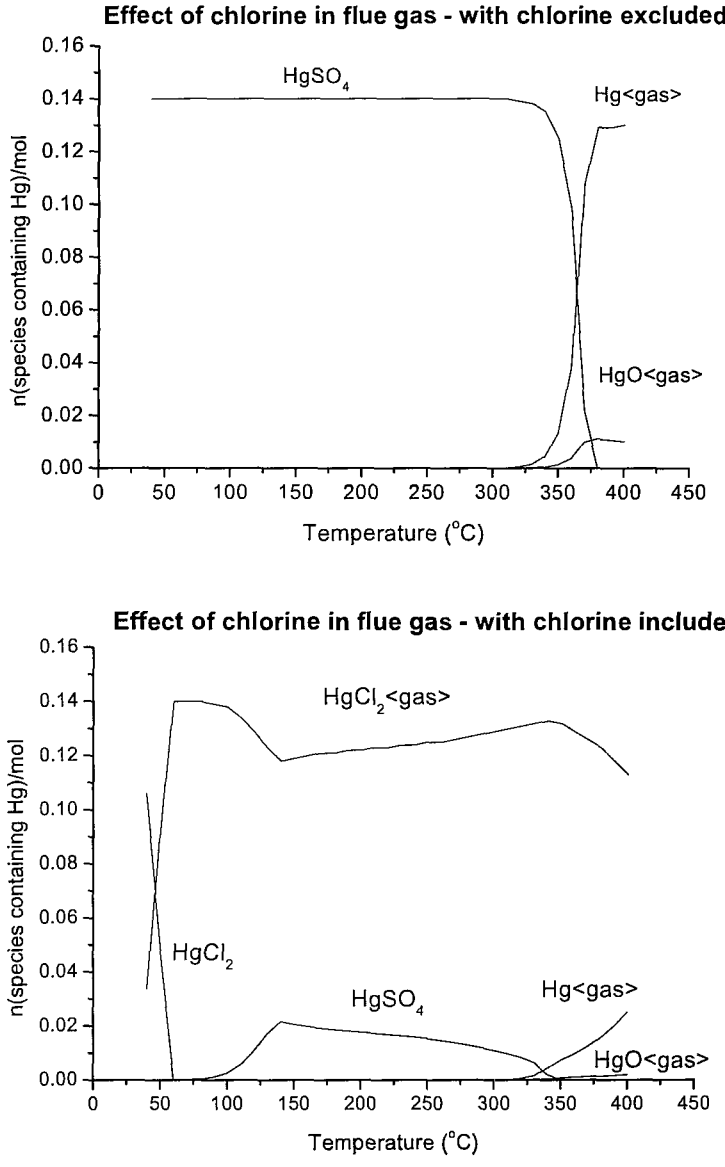


Figure 3-1 MTDATA results when the effect of chlorine on mercury speciation in a flue gas stream was evaluated

3.2.2. Mercury speciation when combusting different coals

The MTDATA results for the predicted mercury species (at thermodynamic equilibrium) in flue gases from the combustion of different coals are shown in Figure 3-2 to Figure 3-7. At a temperature of 400°C lignite is expected to produce mainly gaseous forms of $HgCl_2$, Hg and HgO; a small amount of gaseous HgCl is also predicted to exist at this temperature (refer Figure 3-2). As the gas is cooled to below 175°C, the main mercury species is predicted to be gaseous $HgCl_2$.

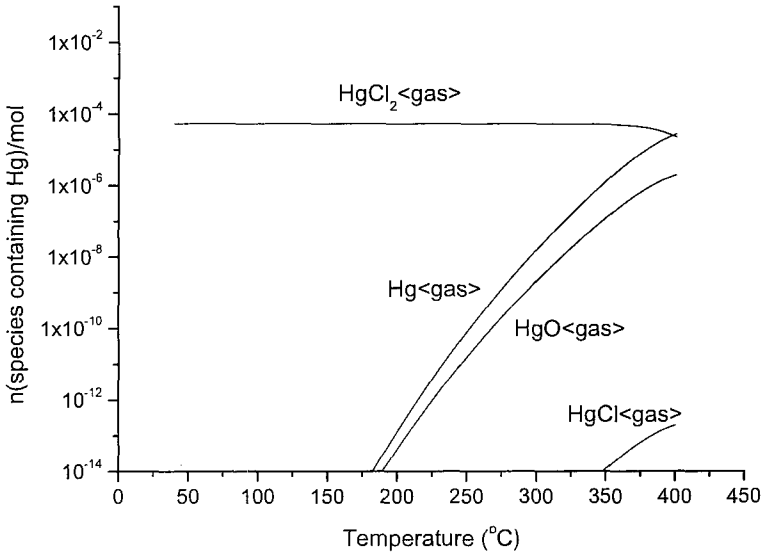


Figure 3-2 MTDATA results for major mercury species present in flue gas from the combustion of lignite

The thermodynamic equilibrium modelling results for mercury speciation in the flue gas from the combustion of the five bituminous coals listed in Table 3-1 were very similar (refer Figure 3-3 to Figure 3-7), indicating that mercury would exist mainly as gaseous $HgCl_2$. The fact that some of these coals contain a substantial concentration of sulphur e.g. Harworth coal from the U.K., does not seem to affect the mercury speciation over the temperature range that was studied. The models also predicted that the flue gases from all five bituminous coals would initially contain small concentrations of gaseous Hg^0 and HgO. These mercury species would however gradually diminish in concentration and become negligible as the gases cooled to ca. 250°C. The calculations suggested that mercury which was initially in the form of Hg^0 and HgO was converted to $HgCl_2$.

However this effect cannot be seen on Figure 3-3 to Figure 3-7. This was because the initial $HgCl_2$ concentrations in the flue gases from the different bituminous coals were much larger than the amount of Hg^0 and HgO, therefore the resulting increase in $HgCl_2$ concentrations were very small.

When compared to the mercury speciation for bituminous coals, the MTDATA results for the flue gas from the combustion of lignite indicated that there would be much larger concentrations of gaseous Hg^0 and HgO in this flue gas stream, as the gas cooled from 400°C to 175°C. On the other hand when the flue gas temperature reached 150°C (the operating temperature of CS-ESPs), the mercury species from the combustion of lignite or the bituminous coals were predicted to be similar and to be only in the form of gaseous $HgCl_2$.

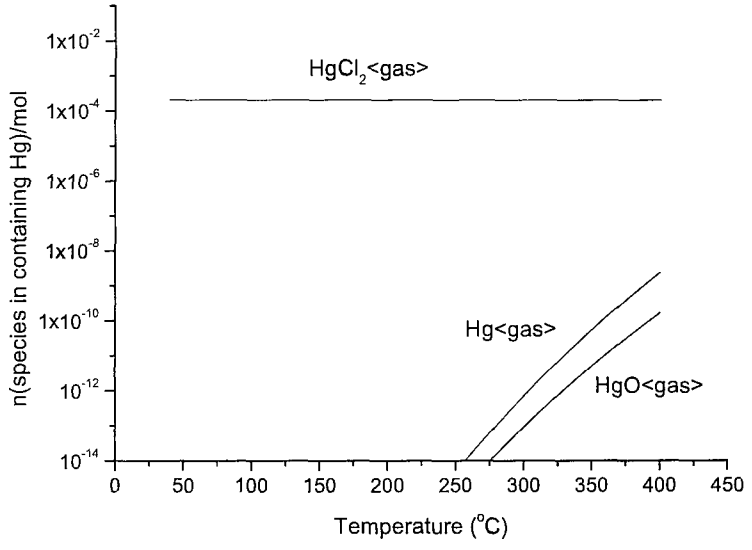


Figure 3-3 MTDATA results for major mercury species present in flue gas from the combustion of Harworth coal (U.K. bituminous coal)

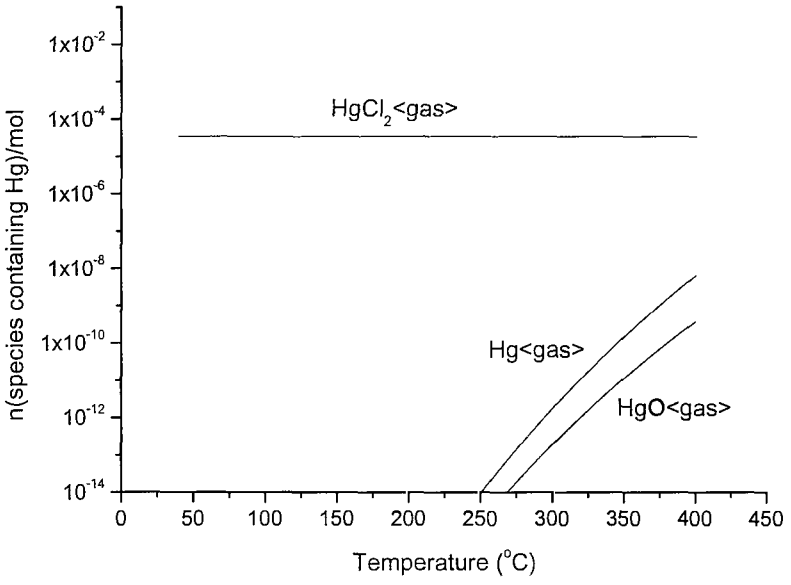


Figure 3-4 MTDATA results for major mercury species present in flue gas from the combustion of a U.S. bituminous coal

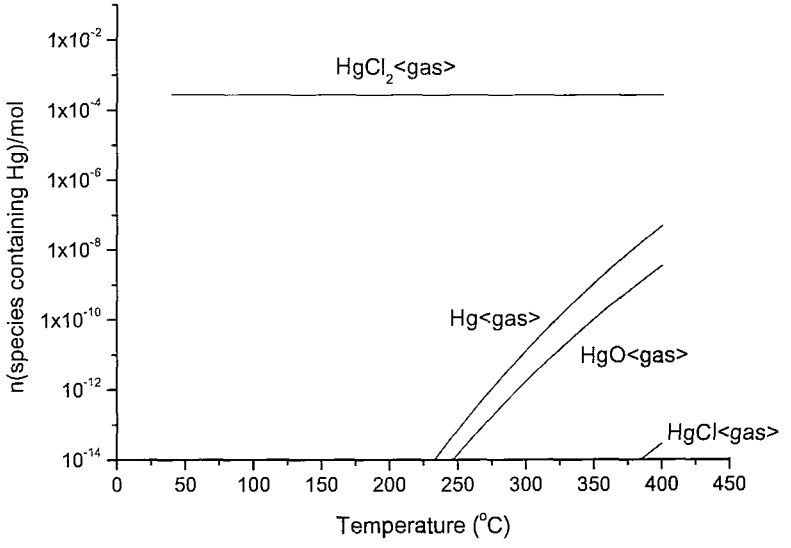


Figure 3-5 MTDATA results for major mercury species present in flue gas from the combustion of Eastern bituminous coal

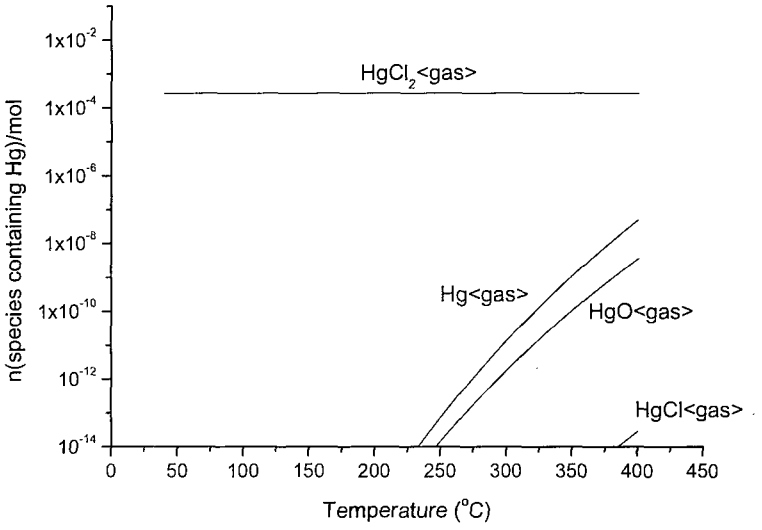


Figure 3-6 MTDATA results for major mercury species present in flue gas from the combustion of low sulphur Eastern bituminous coal

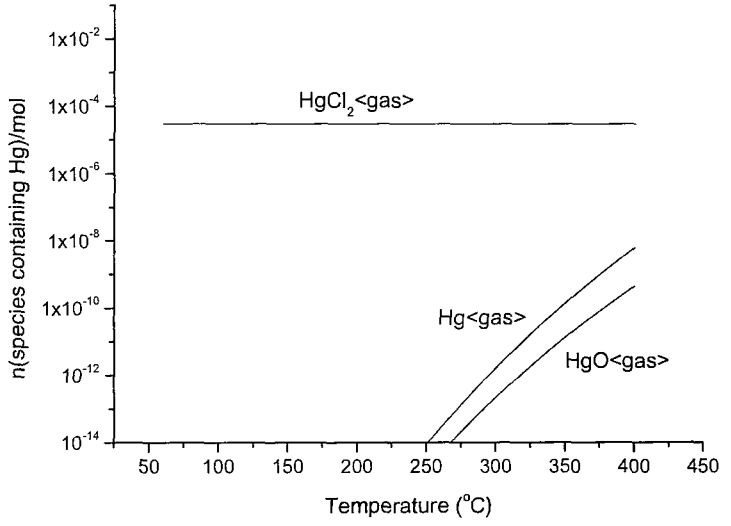


Figure 3-7 MTDATA results for major mercury species present in flue gas from the combustion of Western bituminous coal

3.3. Conclusions from the MTDATA modelling

The thermodynamic modelling results obtained during the present study show that mercury would mainly react with chlorine in the flue gas in preference to the other flue gas constituents. It is predicted that the flue gases generated by the combustion of lignite differ from those generated from bituminous coals in regard to the mercury compounds

present, at temperatures of 400°C. However, as the flue gas is cooled down to 150°C, i.e. to the maximum operating temperature of ESPs in the UK, the flue gases of both lignite and bituminous coals are predicted to contain one mercury species only (gaseous $HgCl_2$). The results obtained from the MTDATA thermodynamic modelling carried out during the present study are consistent with information that has been published by other researchers.[31]

However, as with the predictions of other thermodynamic equilibrium models, the results from MTDATA should be considered with caution, since they represent a prediction of the species that would exist at true thermodynamic equilibrium. The effects of kinetic and mass transfer limitations are not considered. Furthermore, the database used for the modelling completed during this study did not contain the species that may form if mercury reacts with NO_x in the gas stream, or the heterogeneous mercury reactions that could occur at the active sites on sorbents for mercury capture. Other researchers have suggested the gas-phase mercury oxidation reactions are characterised as being slow reactions.[32] For example, according to Ghorishi et al., gas-phase studies indicated that oxidation of Hg^0 in the presence of hydrogen chloride (HCl) is rather slow, and proceeds at measurable rates only at temperatures >700 °C and HCl concentrations in the range of 100–200 ppm.[55] Full scale studies on the other hand have shown that for plants equipped with CS-ESPs, mercury capture on fly ash and PAC sorbents occurs mainly during the in-flight period between the sorbent injection point (i.e. after the air preheater) and the APCD.[56] The residence time for reactions with mercury in the flue gas is therefore of the order of seconds.[56, 57] Consequently, the results obtained from the MTDATA modelling should be considered only as an indication of the mercury species that could form at thermodynamic equilibrium conditions.

4. Sorbents evaluated in this study

During this study sorbents produced from waste material (scrap tyre rubber and sewage sludge) and fly ashes from coal-fired power plants have been ranked against Norit Darco Hg™ and Norit Darco Hg-LH™ which are marketed by Norit Americans Inc. The different sorbents that were evaluated are listed in below in Table 4-1.

Table 4-1 The different sorbents evaluated in this study

• Norit Darco Hg™	• Norit Darco Hg-LH™
• Fly ash A	• Fly ash B
• Fly ash C	• Fly ash D
• Fly ash E	• Fly ash F
• Fly ash G	• Fly ash H
• Tyre char R1	• Tyre char R2
• Tyre char R3	• Tyre AC R1
• Tyre AC R2	• Tyre AC R3
• Sewage sludge char	• Sewage sludge AC R1
• Sewage sludge AC R2	• Sewage sludge AC R3

Scrap tyre rubber obtained from Blue Circle Limited (Derbyshire)[58] was the raw material that was used to make the sorbents tyre char R1 – R3 and tyre AC R1 – R3. Tyre char R1 – R3 are charcoal samples produced from the pyrolysis of scrap tyre rubber, while tyre AC R1 and R2 are activated carbons made from steam activation. Tyre AC R3 is a zinc bromide impregnated activated carbon.

Dewatered mesophilic, anaerobically digested (DEMAD) sewage sludge obtained from Ashford Sewage Works, UK was used to produce the charcoal from pyrolysis of sewage sludge and the zinc bromide impregnated activated carbons (sewage sludge AC R1 – R3).

Subsections 4.3 to 4.7 describe how these sorbents were produced at the Centre for Environmental Control & Waste Management, Imperial College London.

4.1. Norit Darco Hg™ and Norit Darco Hg-LH™

Norit Darco Hg™ and Norit Darco Hg-LH™ are lignite-based, commercially available, activated carbon marketed by Norit Americas Inc. specifically produced for the removal of mercury from flue gases.[51] Both these carbons have been processed at temperatures in excess of 870°C.[51] The mean particle size of Norit Darco Hg™ has been reported to be between ca. 9 to 15 μm.[4] Norit Americas Inc. have manufactured Norit Darco Hg-LH™ which is a brominated carbon[16] specifically for capturing mercury when coals with low halogen contents are used in coal-fired power plants.[51] The specifications of these two PAC that have been published by Norit Americas Inc. are listed in Table 4-2.

Table 4-2 Specifications of Norit Darco Hg™ and Darco Hg-LH™ published by Norit Americas Inc.[51]

	Darco Hg™	Darco Hg-LH™
Less than 45 μm	95%	95%
Total Sulfur	1.2%	1.2%
Bulk desity, tamped (g/ml)	0.51	0.6
Surface area (m^2/g)	600	550

4.2. The coal fly ashes evaluated in this study

The mercury capture effectiveness of eight different fly ash samples from three U.K. coal-fired power plants was evaluated in this study. Since these samples had been in contact with flue gases from the combustion of coal, they already contained some mercury. The present research was therefore done to determine if the samples were able to retain more mercury if exposed to a simulated flue gas stream.

The fly ash samples A – D are from the same UK coal-fired power plant. These samples were produced during a test which investigated the effect of LOI content on the mercury retained on the fly ash samples when combusting UK coal. The fly ash samples E and F were produced from another UK coal-fired power plant combusting Russian coal, while fly ash samples G and H are from a third UK coal-fired power plant combusting a different Russian coal.

If in the future, fly ash is re-injected into the flue gas duct as a sorbent for mercury capture, it might be done without any screening to remove the larger sized ash particles. The study was therefore conducted using the as-received fly ash samples directly, i.e. without any bias towards a particular particle size. However, in order to study the effect of fly ash particle size on mercury capture, two fly ash samples (fly ash D and F) were also sieved to segregate the ash samples according to their particle size. Both fly ash D and F had a similar particle size distribution, with a majority of the particles being smaller that 38 μm (Table 4-3).

Table 4-3 Particle size distribution of the fly ashes D and F.

	fly ash D	fly ash F
Particles larger than 150 μm	1%	5%
Particles between 106 – 150 μm	3%	4%
Particles between 75 – 106 μm	14%	5%
Particles between 38 – 75 μm	21%	25%
Particles less than 38 μm	61%	61%

4.3. Producing charcoal from scrap tyre rubber

The tyre rubber charcoal samples were made using the same scheme published by Miguel (ref. Figure 4-1).[58] A Carbolite HTR 11/150 laboratory scale rotary furnace (diameter ca. 150 mm) with an internal volume of approximately 4.5 L was therefore used in the present study. The quartz reaction vessel was rotated at ca.10 rpm. For tyre pyrolysis run R1, approximately 340 g of cut scrap tyre rubber pieces (less than 15 mm in size) were heated in an inert atmosphere at a rate of 10°C/min. This inert atmosphere was maintained by having a nitrogen sweep gas flow of 500 mL/min. A holding time of half an hour at 700°C was used for the pyrolysis runs; resulting in a char yield of 34%.

Tyre char R2 was produced by using the same process conditions as the first tyre rubber pyrolysis run. In this case, a tyre rubber mass of 291 g was used which produced ca. 99 g of charcoal. The char yield from these two pyrolysis runs was therefore similar (34%).

A third tyre pyrolysis run (Tyre char R3) was performed to identify the effect of steam activation. The pyrolysis was therefore completed by using the same temperature programme employed for the steam activation (§ 4.4). However, since the rubber was to be pyrolysed, instead of a steam/nitrogen gas mix, a constant 500 mL/min nitrogen sweep gas flow was maintained throughout the carbonisation process. The charcoal yield from the third pyrolysis run was ca. 33%.

The aim of this study is to rank low cost sorbents against Norit Darco Hg™; this sorbent has a mean particle size between 9 – 15 μm.[4] Since Rostam-Abadi et al. found that particle size contributed to the mercury capture on some fly ashes,[59] the pyrolysis chars from scrap tyre rubber were crushed and only the smallest recoverable size fraction (38–75 μm) was tested for mercury retention efficiency.

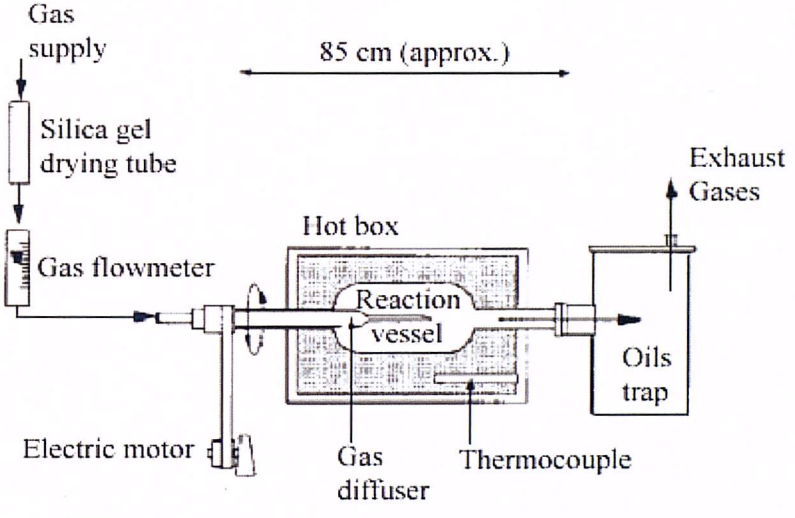


Figure 4-1 Schematic diagram of the rig for pyrolysis of scrap tyre rubber (Modified from the figure published by Miguel et al.[45]).

4.4. Producing steam activated carbons from tyre rubber

During physical activation, steam or CO_2 gas is injected to the activation kiln.[60] However in general, steam activation is preferred to CO_2 as an activation gas because the water molecule has a smaller van der Waals radius than CO_2 (~3.8 Å vs. ~4.8 Å).[11] This leads to a faster diffusion of steam in the porous matrix of the carbon and a faster reaction rate.

The steam activated carbons were produced from scrap tyre rubber by using the scheme published by Miguel et al. which results in carbons with a high surface area.[45] The Carbolite HTR 11/150 laboratory scale rotary furnace that pyrolysed the scrap tyre rubber (§ 4.3) was therefore employed for the steam activation; the complete system is illustrated in Figure 4-2. During activation runs R1 and R2, approximately 200 g of cut scrap tyre rubber pieces (less than 15 mm in size) was heated at 5°C/min in an inert atmosphere maintained by a nitrogen gas flow of 500 ml/min. Once the temperature had reached 700°C, this atmosphere was rapidly substituted by a flow of 500 ml/min of steam/nitrogen (80:20, v/v). This was generated by having a water flow of 0.3 ml/min and a nitrogen gas flow of 100 ml/min. As prescribed by Miguel et al.[45], the same heating rate of 5°C/min was maintained until the activation temperature of 925°C was reached. Active carbon with a yield of 29% for tyre AC R1 and 27% for tyre AC R2 were obtained by using these conditions with a holding time of 80 minutes at the activation temperature.

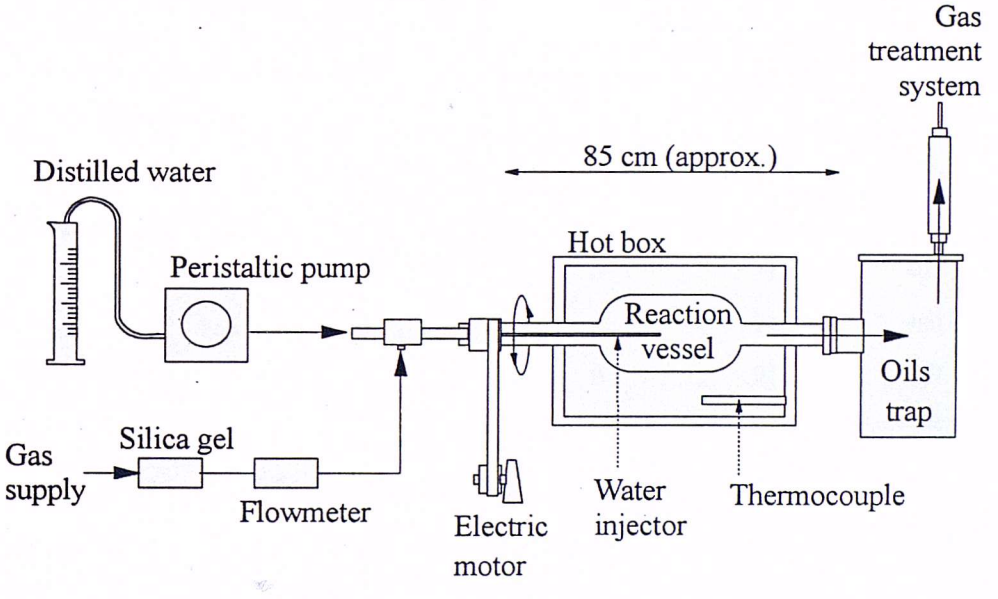


Figure 4-2 Schematic diagram of the rig for the activation of scrap tyre rubber.[58]

The steam activated carbons made from scrap tyre rubber also followed the same crushing and sieving process used to obtain the tyre rubber pyrolysis chars evaluated in this study (§ 4.3). This meant that only the activated carbon particles that passed though a 75 μm sieve, but remained on a 38 μm sieve, were tested for mercury capture.

4.5. Producing bromide-impregnated PACs from scrap tyre rubber

The bromide-impregnated activated carbon, tyre AC R3, was produced by using the experience gained from the pyrolysis of scrap tyre rubber (§ 4.3) and from producing bromide-impregnated activated carbon from sewage sludge (§ 4.7). In order to make the activation more effective it was decided to first pyrolyse the tyre rubber and then mix the charcoal that was produced with zinc bromide solution. 50 g of charcoal from the tyre pyrolysis run R2 (§ 4.3) was therefore treated as the raw material and it followed the same process steps that were used to make sewage sludge AC R3. As a result the charcoal was first mixed with a zinc bromide solution (containing 50 g of $ZnBr_2$), then dried over night and crushed to less than 2 mm seized particles. As with zinc bromide activation of sewage sludge, the tyre rubber charcoal activation with $ZnBr_2$ was also performed at 600°C for one hour. However unlike sewage sludge, the tyre rubber charcoal had already been carbonised. Therefore, the activation was done by using a single thermal treatment step, i.e. heating the charcoal to the activation temperature at a rate of 5°C/min. The solid particles that were collected after the reactor had cooled went through the same post activation treatment that was used to make sewage sludge AC-R3 (§ 4.7). The final activated carbon yield based on the mass of tyre pyrolysis charcoal was 78%, while that based on the initial mass of scrap tyre rubber was 26%.

4.6. Producing charcoal from sewage sludge

The charcoal and activated carbons made from DEMAD sewage sludge that were evaluated during this study were obtained by using the same process that Gee[13] had used to produce activated carbons from waste material. The heating sequence employed for making both the charcoal and the bromide-impregnated activated carbon from sewage sludge was the same and is described in sub-section 4.7. Direct comparison could therefore be made between the sorbents and any effect of bromine impregnation on the mercury capture performance could be investigated.

The charcoal from the pyrolysis of sewage sludge was obtained by first drying the DEMAD sludge overnight at 110°C in a circulating oven until a constant sludge mass was obtained. The mass of dry sludge was 33% the mass of the initial sludge that was

placed in the oven. The dried sludge was crushed and subsequently carbonised in the bench scale rotary kiln that Miguel [58] had previously used to make low cost sorbents from scrap tyre rubber. Figure 4-1 therefore illustrates the system that was used to pyrolyse the dried sewage sludge. The charcoal particles obtained from the carbonisation were later reduced in size and the particles between 38 μm and 75 μm were recovered for mercury capture testing. The charcoal yield based on the mass of dry DEMAD sewage sludge used for the pyrolysis process was 48% and 16% when based on the initial mass of wet DEMAD sewage sludge.

4.7. Producing bromide-impregnated PACs from sewage sludge

In this study, a modified version of the procedure Gee[13] found effective to produce activated carbons using $ZnCl_2$ was employed to make the bromide-impregnated activated carbon. Wet DEMAD sludge was first mixed with a 25% saturated solution of $ZnBr_2$. The mass of $ZnBr_2$ that was mixed with the wet sewage sludge was equal to the calculated mass of dry DEMAD sewage sludge. Hence for making Sewage sludge AC R1 and R2, 150 g of $ZnBr_2$ was mixed with 500 g of wet DEMAD sludge that contained 70% water (w/w basis). The slurry was then dried overnight at 110°C in a circulating oven until a constant sludge mass was obtained. The dry solid was subsequently crushed to less than 2 mm sized particles and later activated using the same bench-scale rotary kiln that was employed to prepare the charcoal from sewage sludge (§ 4.6). During the activation process, the solid was first carbonised at 450°C for two hours and then activated at 600°C for one hour. The same heating rate of 5°C/min was used to raise the temperature to each holding stage. During both runs a 500 mL/min nitrogen sweep gas flow was maintained to ensure that the volatile products were removed from the activation area.

Acid washing is often used by activated carbon manufacturers for certain activated carbons that have a high ash content.[60] Washing with hydrochloric or other acids removes minerals and ash resulting in a product with higher purity.[60] Furthermore, according to Pollard, acid washing removes traces of uncarbonised oil and any zinc that is not bound to the carbon.[61] The activated carbon that was produced from the activation runs "sewage sludge AC R1 and R2" were later washed using a standard post-treatment procedure that was previously used by Pollard.[61] This consisted of first washing with a 2M HCl solution

and subsequent vacuum filtering with Whatman® No1 filter paper (Grade 1, Cat. No. 1001 110). After the solid residue was washed with de-ionised water it was dried overnight in a circulating oven. The dried solids were finally crushed and particles between 38 μm and 75 μm were recovered for the mercury capture tests.

When the sewage sludge AC R1 and R2 samples were subsequently analysed for their chemical content, they were found to contain significantly more chlorine than the charcoal from sewage sludge pyrolysis (refer § 5.2). This is believed to be due to the HCl washing of these activated carbons. A third sewage sludge activation run was therefore performed, with the activated carbon being washed with 2M HBr solution instead. The solid residue was later washed several times with de-ionised water until the filtered liquid had a constant pH value (ca. 5.3). The pH readings after each de-ionised water wash are illustrated in Appendix -A. The solids that remained from this third run went through the same final stages of the post-treatment process that was used for the first two activated carbons, namely it was also dried, crushed and later sieved. 500 g of wet DEMAD sludge was used for the last run, and since this sludge had a water content of 71%, the initial mass of dry sludge was 144 g. Based on this initial mass of dry sludge the final activated carbon yield of sewage sludge AC R3 after the de-ionised washing was 39% and 11% when based on the mass of wet DEMAD sewage sludge. .

5. Characterisation of the sorbents

The sorbents that were evaluated during this study were characterised using a number of techniques. Information was gained on the factors which enable some sorbents to be more effective than others in capturing mercury. This chapter describes the results obtained from the different analyses that were conducted, and the characteristics of some sorbents which affect their mercury adsorption capability.

5.1. The sorbent surface area and microporosity

Activated carbons have pores with sizes ranging from less than a nanometer to several thousand nanometers.[62] The International Union of Pure and Applied Chemistry (IUPAC) has adopted a classification based on the pore width, which represents the distance between the walls of a slit-shaped pore or the radius of a cylindrical pore.[62] The pores are divided into three groups: micropores, mesopores (transitional pores), and macropores.

Each of these groups is specifically related to the adsorption process. Micropores have molecular dimensions, the effective radii being less than 2 nm (20 Å).[62] The micropore surface area and micropore volume in an activated carbon determine its adsorption capacity to a considerable extent.[62] The adsorption in these pores occurs through volume filling, and the adsorption energy is large compared to the bigger mesopores because of the overlap of adsorption forces from opposite walls of the micropores.[62] Micropores are therefore filled at relatively low vapour pressures before the commencement of capillary condensation.[62] Mesopores, also called transitional pores, have effective dimensions in the range of 2 to 50 nm.[62] These pores are filled at relatively high pressures along with capillary condensation. Such pores also act as conduits leading the adsorbate molecules to the micropore cavity. Macropores (pores larger than 50 nm) are not of much importance in the process of adsorption in active carbons; they mainly act as transport channels to enable adsorbate molecules to pass rapidly to smaller meso- and micropores situated deeper in the particles of active carbon.

The atomic radius of mercury is 1.6 Å[63] thus these atoms would be expected to diffuse into the micropores (pores less than 20Å)[62] of the sorbents tested in this study. Brunauer, Emmett and Teller (BET) surface area and thickness plot (T-plot) analysis was performed to obtain information about the surface area and micropore distribution of each sorbent by using a Micromeritics® ASAP 2000 Surface Area Analyzer. A typical sample mass of approximately 150 mg was used to study the activated carbons. Since fly ash has a smaller surface area than activated carbon, a larger sample mass of approximately 500 mg was needed to obtain accurate results. Each analysis was carried out by first degassing the samples at 105°C, then infusing with nitrogen gas at 77 K, and evaluating the volume adsorbed onto the tests samples. The results obtained are tabulated in Table 5-1. The percentage deviation of the BET surface area for each sample was within ±5%, while the regression analysis for the T-plots used to obtain the information on the micropores in each sample had very high correlation coefficients, ca. 0.997.

The activated carbons (except tyre AC R3) seem to have a significantly larger surface area and micropore volume than the other sorbents. The BET surface area for Norit Darco Hg™ listed in Table 5-1 was comparable to the value reported by Norit Americas Inc. and Pavlish et al.[4, 51] Most of the surface area in this activated carbon seems to be due to its micropores, while its macropores contributed very little towards the total surface area. The BET surface area of Norit Darco Hg-LH™ is almost half the surface area of Norit Darco Hg™. This reduction seems to be due to the smaller micropore surface area in the brominated PAC, as both activated carbons had similar mesopore and macropore surface areas. Although the Norit Americas Inc. data sheet also showed a reduction in the surface area of its impregnated activated carbon, the BET surface area measured in this study is ca. 33% less than the value published by the activated carbon manufacturer (ref. Table 4-2 & Table 5-1). The fact that the surface area of the Norit impregnated PAC was less than its non-brominated version, suggests that the bromination process may have been done after activation, thereby consuming of some of microporosity of the initial activated carbon. This hypothesis cannot be confirmed, however, since Norit Americas Inc. has not released any information pertaining to the manufacturing process for Norit Darco Hg-LH™.

Compared to the other sorbents tested in this study, the fly ash samples had the smallest BET surface areas. Except for fly ash E and F, the other fly ash samples had total surface

areas which were approximately 100 times less than Norit Darco Hg™. The micropores and mesopores in the fly ashes contributed most towards the surface area, while the pore volumes in the fly ashes were mainly due to their mesopores and macropores. The surface area due to micropores in the ash samples does seem to correlate with the LOI content in the fly ashes (Figure 5-1). This is probably because it is the carbon content in the fly ashes that contributes most towards their surface area, rather than the inorganic constituents.

The sorbents produced from scrap tyre rubber have a very different distribution of surface area and pore volumes compared to Norit Darco Hg™ and Norit Darco Hg-LH™. Although the scrap tyre based sorbents had smaller BET surface area than the PACs from Norit Americas Inc., the surface area and pore volumes due to their macropores were considerably larger than the two commercial PACs evaluated in this study.

The BET surface area and T-plot analysis of the scrap tyre based sorbents showed that steam activation increased the surface area of the sorbent by producing more micropores. Miguel reported comparable BET surface area values for pyrolysis charcoal (82 m^2/g).[58] He also obtained a similar result for steam activated carbon (283 m^2/g) produced from scrap tyre rubber, when using the same process conditions as followed in the present study.[58] Although steam activation did increase the surface area, it was still less than half that of Norit Darco Hg™. On the other hand, zinc bromide activation of charcoal from scrap tyre rubber increased the BET surface area by only ca. 27% compared to the 225% increase for steam activation. This could be because an activation temperature higher than 600°C may be needed to make a more porous bromide impregnated activated carbon from scrap tyre rubber. However, this might not be possible with $ZnBr_2$ due to practical difficulties (boiling point of $ZnBr_2$ is 650°C).[64]

Tyre char R3 and the steam activated carbons were processed at the same temperature of 925°C (refer § 4.3 and § 4.4). However, Tyre char R3 had a surface area similar to that of charcoal produced at 700°C. The results therefore indicate that temperature and the steam activation agent were together responsible for producing a more porous activated carbon from scrap tyre rubber.

Although charcoal from scrap tyre pyrolysis and sewage sludge pyrolysis had similar BET surface areas, these sorbents had radically different distributions of surface area, when considering the three classes of pores defined by the IUPAC. The surface area in sewage sludge charcoal was mainly due to its micropores and mesopores, while charcoal from tyre pryolysis had mainly mesopores and macropores. The bromide impregnated activated carbons produced from sewage sludge had surface areas and pore volumes for micropores, mesopores and macropores that were very similar to Norit Darco Hg™ (except for the macropore volumes). This suggests that the ZnB_2 activation is very effective in producing a porous sorbent from sewage sludge.

Since the bromide impregnated carbons from sewage sludge and Norit Darco Hg™ had the largest micropore volumes, they may have a greater capacity to adsorb mercury. Furthermore, since fly ash had the least micropore surface area these samples would be expected to have the least mercury capacity. However, it should also be noted that Ghorishi et al. have suggested that removal of mercury from flue gas by activated carbon may take place via reactions with surface functional groups.[65] Therefore other factors may also play a role in the capture of mercury from flue gas.

Table 5-1 Surface area, micropore volume and micropore area of the sorbents

	BET Surface area (m^2/g)	Micropore area (m^2/g)[a]	Mesopore area (m^2/g)[b]	Macropore area (m^2/g)[b]	Micropore volume (mm^3/g)[a]	Mesopore volume (mm^3/g)[c]	Macropore volume (mm^3/g)[c]
Norit Darco Hg™	660 ± 11.5	367	195	2	169	244	110
Norit Darco Hg-LH™	335 ± 4.0	133	168	4	61	308	117
Fly ash A	1 ± 0.01	0.5	0.6	0.1	0.21	1	1
Fly ash B	2 ± 0.01	0.6	1.1	0.1	0.25	2	2
Fly ash C	3 ± 0.02	0.9	1.8	0.1	0.40	3	2
Fly ash D	5 ± 0.03	1.1	3.0	0.2	0.47	5	5
Fly ash E	8 ± 0.1	2.6	3.9	0.1	1.16	6	6
Fly ash F	15 ± 0.17	5.1	7.6	0.1	2	9	4
Fly ash G	3 ± 0.02	1.1	1.5	0.1	0.48	3	3
Fly ash H	3 ± 0.02	0.9	1.8	0.1	0.37	2	2
Tyre char R1	72 ± 0.2	5	50	22	1	436	437
Tyre char R2	80 ± 0.08	5	67	20	1	445	358
Tyre char R3	73 ± 0.1	7	61	10	3	244	404
Tyre AC R1	219 ± 3.7	128	71	22	60	397	580
Tyre AC R2	279 ± 4.8	158	85	28	74	413	643
Tyre AC R3	97 ± 0.09	9	80	19	3	419	343
Sewage sludge char	53 ± 0.6	21	26	2	10	90	80
Sewage sludge AC R1	670 ± 13.3	332	187	1	151	278	37
Sewage sludge AC R2	678 ± 14.3	351	176	1	161	268	27
Sewage sludge AC R3	729 ± 8.6	298	253	3	133	311	24

Note
a – analysed by t-plot
b – analysed by BJH adsorption
c – analysed by BJH desorption

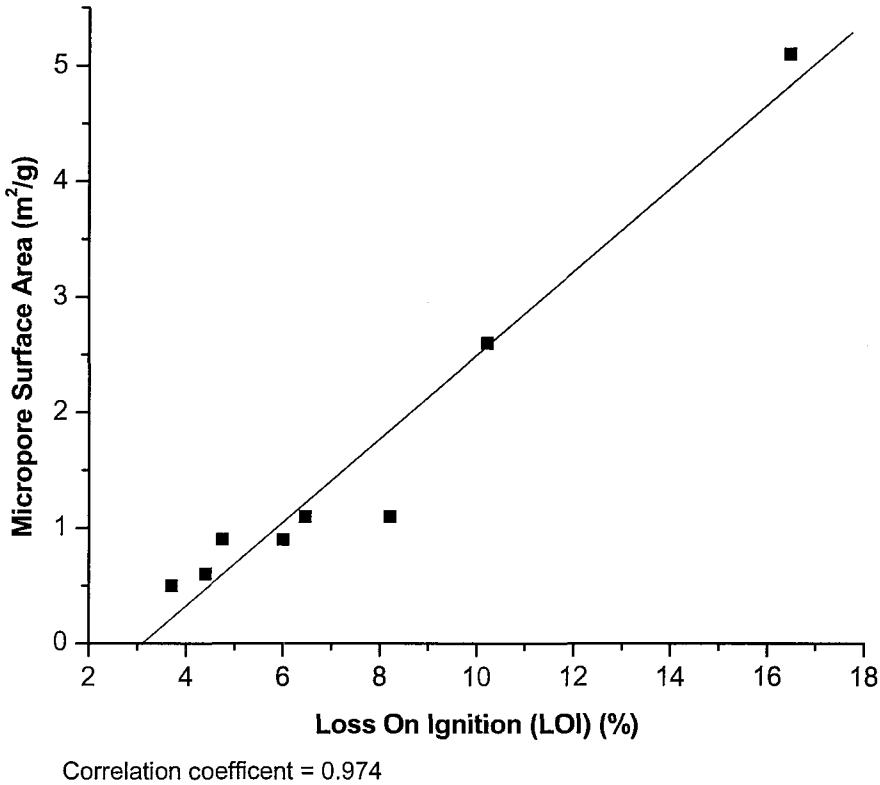


Figure 5-1 Micropore surface area in each fly ash sample versus LOI content.

5.2. Investigating specific elements in the sorbents

It has been suggested that the presence of bromine, chlorine and sulphur in sorbents may enhance mercury capture.[50, 65] Some selected sorbents were analysed at TES Bretby Limited (UK) to determine their elemental composition; the results are presented in Table 5-2. Appendix -B has a brief description of the different standard analytical techniques that were used on each sample. The concentration of bromine in Norit Darco Hg-LH™ and the bromide-impregnated activated carbons prepared during this study were only a few percent greater than the amount found in the other sorbents produced from the same raw materials. During the initial pre-activation process (i.e. mixing), the mass of $ZnBr_2$ added was similar to the mass of the dry sludge or the charcoal from scrap tyre pyrolysis (refer § 4.7 and 4.5). The low concentration of bromine that remains in the activated carbon suggests that it was either removed with the volatile compounds (during the activation process) or it was dissolved in the acid wash (during the post-activation treatment).

The chlorine concentrations in the sewage sludge AC R1 and R2 were only marginally less than the mass percentage of bromine in the sorbents. However, charcoal from the same sludge only contained a minute quantity of chlorine; this suggests that some of the chlorine from the HCl solution used to wash the carbon may have remained on the solid. Since the presence of chlorine in sewage sludge AC R1 and R2 may contribute to improvement in the sorbent performance, the post-activation step was changed to an HBr wash for the third activated carbon run with sewage sludge (refer § 4.7). This seems to have significantly reduced the amount of chlorine present in the bromide impregnated activated carbon from sewage sludge (sewage sludge AC R3).

Laboratory studies by other investigators have shown that sulphur impregnation of activated carbon significantly improves the elemental mercury adsorption capacity.[12] According to Lehmann[11], the sulphur which is utilised in the rubber vulcanisation process is organically bound with the carbon matrix of TDACs and may therefore contribute towards its mercury adsorption efficiency. Although Table 5-2 shows that the sorbents produced from scrap tyre rubber contains sulphur, it also shows that ca. 47% and 49%, respectively, of the sulphur present in the scrap tyre rubber was removed during the pyrolysis runs that produced tyre char R1 and R2. Even though the steam activation was performed at a higher temperature than the pyrolysis process, the percentage of the sulphur that was removed increased only to 54% for tyre AC R1. The results suggest that the sulphur remaining on this TDAC was more strongly bonded to the solid component and therefore was not significantly removed when activated at 925°C (refer § 4.4). On the other hand, ca. 88% of the sulphur in scrap tyre rubber was removed when tyre AC R3 was made, which indicates that the acid washing procedure was very effective in removing any sulphur that was soluble in the HBr and DI water wash.

Table 5-2 Moisture, ash and elemental analysis of the sorbents

	Moisture, ash and elemental analysis in percentages unless stated otherwise								
Sorbent	**Moisture**	**Ash**	**Carbon**	**Nitrogen**	**Oxygen**	**Hydrogen**	**Sulphur**	**Chlorine**	**Bromine**
Norit Darco Hg™	7.5	10.0	77.4	0.6	3.8	0.2	0.4	0.03	<100 ppm
Norit Darco Hg-LH™	7.0	27.5	57.8	0.4	5.8	0.3	1.1	0.03	**3.05**
Fly ash D	0.5	92.3	6.9	0.2	<0.1	<0.05	0.3	0.02	<100 ppm
Scrap tyre rubber	1.1	5.9	79.1	0.5	4.6	7.0	1.9	0.04	Not analysed
Tyre char R1	1.1	13.1	83.2	0.3	<0.1	0.3	2.9	0.03	510 ppm
Tyre char R2	0.7	12.4	84.2	0.4	<0.1	0.2	2.8	0.03	374 ppm
Tyre AC R1	2.6	12.7	82.7	0.4	<0.1	0.1	3.0	0.01	Not analysed
Tyre AC R3	1.1	4.5	90.1	0.3	3.0	0.2	0.8	0.01	**1.08**
Sewage sludge char	1.8	71.2	23.0	2.5	<0.1	0.7	1.0	0.06	0.01
Sewage sludge AC R1	5.0	31.5	47.1	4.4	8.7	1.0	1.8	**0.57**	**1.74**
Sewage sludge AC R2	2.6	33.7	48.6	4.6	7.3	1.0	1.3	**1.01**	**1.76**
Sewage sludge AC R3	6.3	32.0	46.6	4.6	7.8	0.9	1.9	0.01	**2.09**

Table 5-3 Chemical composition of the crystalline phases found using XRD

Crystalline phase	Chemical compound
Calcite	$CaCO_3$
Iron Sulphide	FeS
Lime	CaO
Magnetite	Fe_3O_4
Mullite	$3Al_2O_3.2SiO_2$
Quartz	SiO_2
Wurtzite	ZnS
Zincite	ZnO

The results in Table 5-2 indicate that sewage sludge based charcoal and activated carbons (even after acid washing) have much higher ash contents than the other activated carbon and pyrolysis sorbents evaluated in this study. However even though the sorbents produced from sewage sludge had a reduced fraction of carbon, they had BET surface areas that were comparable, if not greater, than the other charcoal and activated carbon sorbents (refer Table 5-1). This suggests that the pyrolysis and activation process of sewage sludge was effective in creating a greater micropore surface area for a given mass of carbon.

The zinc bromide activation of charcoal from scrap tyre rubber, coupled with the HBr wash, produced the sorbent with the largest proportion of carbon. However this activated carbon had ca. 16 times less micropore surface area compared to the carbons made by steam activation of scrap tyre rubber. The steam activation therefore seems to be more effective in producing a more microporous sorbent from scrap tyre rubber.

5.3. X-ray diffraction analysis

Studies using the Information Collection Request (ICR) lead Pavlish et al. to suggest that certain coal fly ashes may exercise a catalytic effect on the oxidation of elemental mercury.[4] Laboratory tests by Ghorishi et al.[66] and Lee et al.[67] using model fly ashes showed that CuO promoted mercury oxidation. Furthermore in the presence of NO_x inert components of the model fly ashes such as Al_2O_3 and SiO_2 became active in the oxidation of Hg^0.[67] Ghorishi et al. also found that CaO in ash reduces the oxidation of elemental mercury,[55] probably due to partial removal of HCl by reaction with the CaO, leaving less HCl available to react with mercury. Other studies have indicated that some forms of iron oxide (e.g. maghemite) have a catalytic effect on mercury oxidation whereas other forms of iron oxide (e.g. magnetite) showed no activity.[4]

In order to obtain a better understanding of the crystalline phases in the sorbents evaluated during the present investigation, some selected sorbents were studied using the X-ray diffraction (XRD) analyser at the Department of Materials, Imperial College London. The analysis was conducted with a Philips PW1700 series Automated Powder Diffractometer, which used Cu K-α radiation at 40 KV/40 mA with a secondary graphite

crystal monochromater. Each sample was placed in a zero background substrate (single silicon crystal) and the data were obtained over a $2\theta = 5^{\circ}$ to 80° range (steps of 0.04°), with a time per step of 2 seconds. A search match was later performed on the results by using "Philips X'Pert Graphics and Identify" software in conjunction with the International Centre for Diffraction Data (ICDD) database to identify each crystalline phase present in the sorbents.

The analysis of nine selected sorbents revealed that they contained mainly amorphous phases (Figure 5-2 and Figure 5-3). The chemical formulae for each of the crystalline compounds found in the sorbents are listed in Table 5-3. Mullite, quartz and magnetite were the main crystalline phases in the coal fly ashes. The major crystalline phases in Norit Darco Hg™ were quartz and calcite, while the charcoal and steam activated carbon produced from scrap tyre rubber had wurtzite and iron sulphide as the main crystalline phases. The scrap tyre rubber charcoal also had some zincite present

When compared to charcoal produced from tyre rubber, the steam activated carbon from the same raw material had more XRD distinct peaks for wurtzite and iron sulphide. This suggests that the latter sorbent may have a larger concentration of these crystalline phases, further suggesting that the high activation temperature employed had promoted the reaction between sulphur and metals present in the scrap tyre rubber. Zinc oxide is added during the tyre manufacture.[11] The zinc and sulphur are not initially combined in the original composition of tyre rubber, as zinc is in the form of ZnO as an additive.[11] During the activation process, a chemical reaction may be occurring to convert ZnO to ZnS.[11] However since this reaction is endothermic, the activation process may be providing sufficient energy for the reaction to proceed.[11] When compared to steam activation that tyre charcoal was made at a lower temperature. This may explain why there was still some zincite (ZnO) present in the tyre charcoal and why there was more wurtzite in the steam activated carbon produced from scrap tyre rubber. As a consequence, the steam activated carbons made from scrap tyre rubber may have less organically bound sulphur that is capable of contributing to capturing mercury. No detectable crystalline phases were found in the bromide impregnated PAC made from the same raw material. The acid washing process was thus very effective in removing the inorganic fraction in this PAC, which confirms the elemental analyses of these sorbents (refer § 5.2).

XRD analysis showed that quartz and calcite were the main crystalline phases in charcoal made from pyrolysis of sewage sludge, while the bromide impregnated activated carbon produced from the same raw material had only quartz. The HBr washing process seems to have also removed the calcite that was initially present in this bromide-impregnated activated carbon, which confirms the previous finding that a proportion of the ash in this sorbent was removed by the acid washing (refer § 5.2).

5.4. Scanning electron microscopy and energy dispersive X-ray analysis

Some selected sorbents were analysed using scanning electron microscopy (SEM) [coupled with EDX] at the Department of Materials, Imperial College London. The instrument used was an Oxford Instruments JEOL model JSM-840A with an accelerating voltage of 20 kV. The results obtained are shown in Figure 5-4 to Figure 5-18. The outcome from the elemental analysis and XRD analysis of the sorbents reported in the previous sub-sections (refer § 5.2 and § 5.3) was confirmed by the EDX scans. Since the fly ash samples had been exposed to coal combustion temperatures (>1500°C) they were distinctly different to the other sorbents. The inorganic species in the ash had agglomerated into spherical globules, as observed previously by Hassett and Eylands[33]. The results for fly ash D and F show clearly that the smaller particles are mainly inorganic while the larger particles are predominantly carbon.

SEM images of the sorbents derived from scrap tyre rubber show that some of the wurtzite (ZnS) present was not part of the carbon matrix and appeared in separate particles. EDX analysis of the impregnated sorbents (Norit Darco Hg-LH, tyre AC R3, sewage sludge AC R3) confirmed the presence of bromine in each sample.

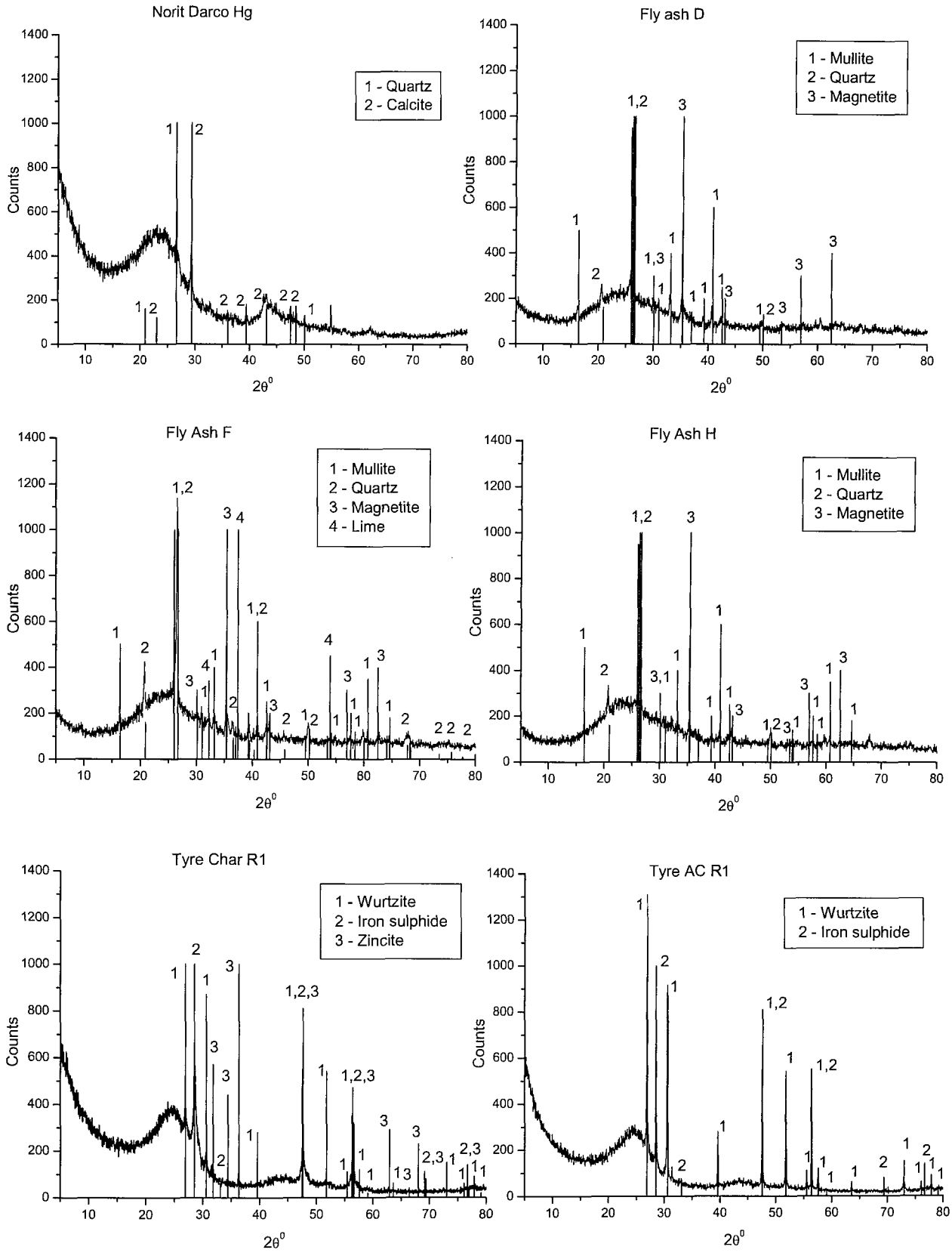


Figure 5-2 XRD scan results of some selected activated carbons, fly ashes and sorbents from scrap tyre rubber

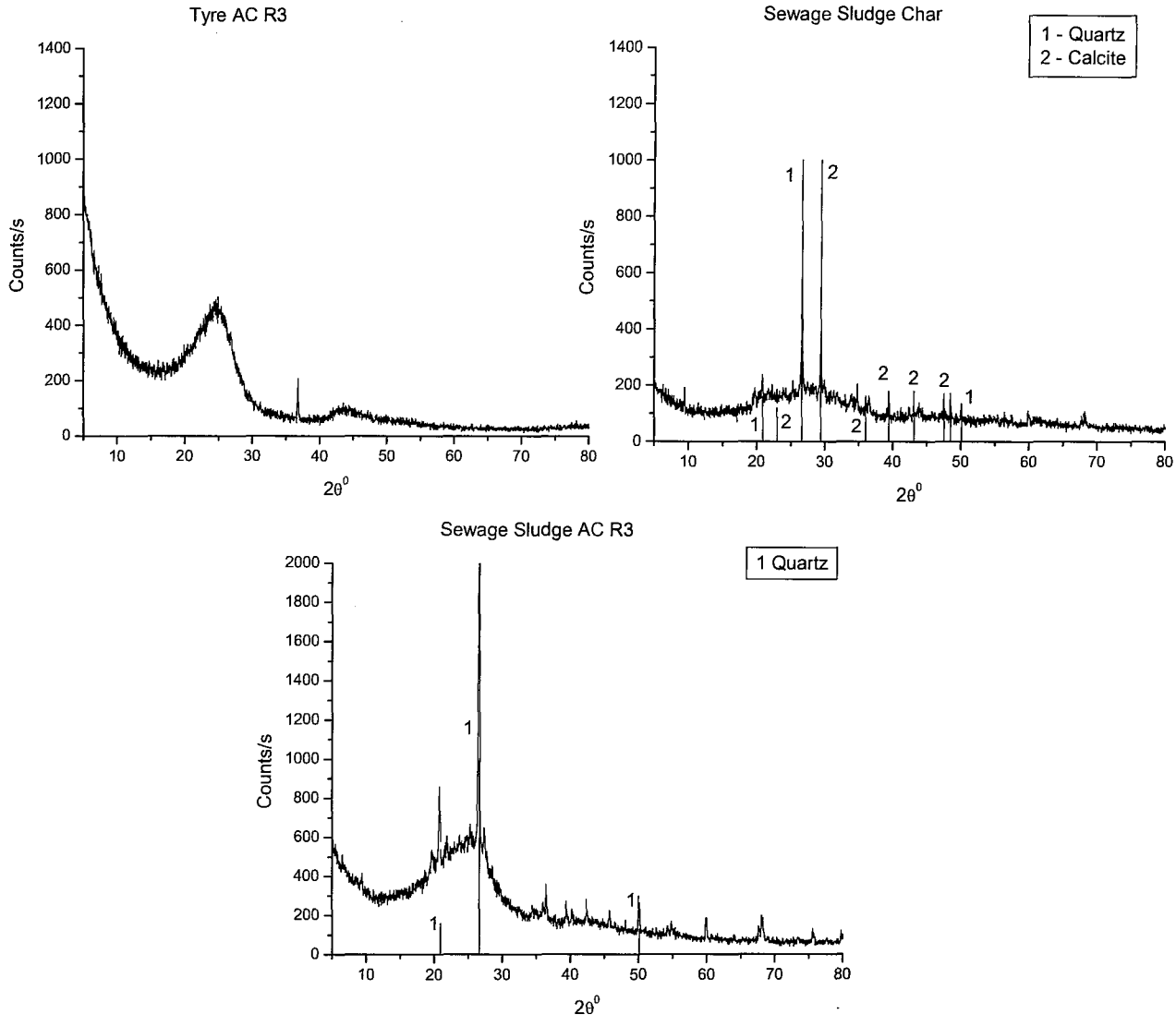


Figure 5-3 XRD scan results of char from sewage sludge and some selected bromide impregnated activated carbons

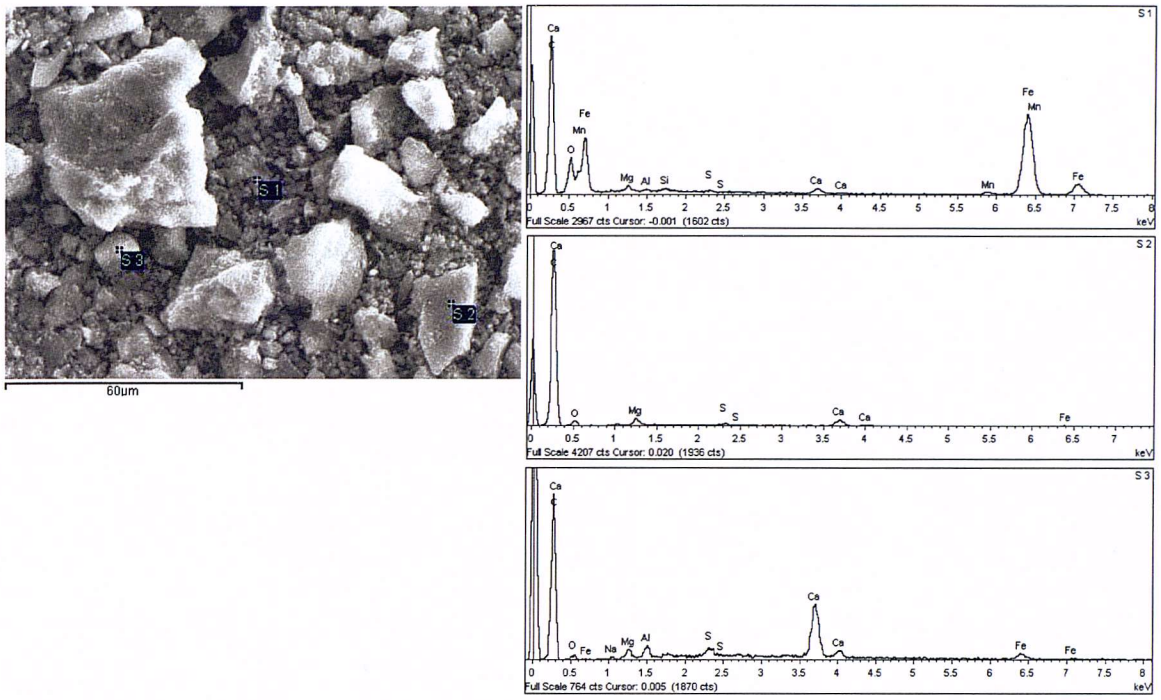


Figure 5-4 SEM & EDX analysis of Norit Darco Hg™ (at x1000 magnification).

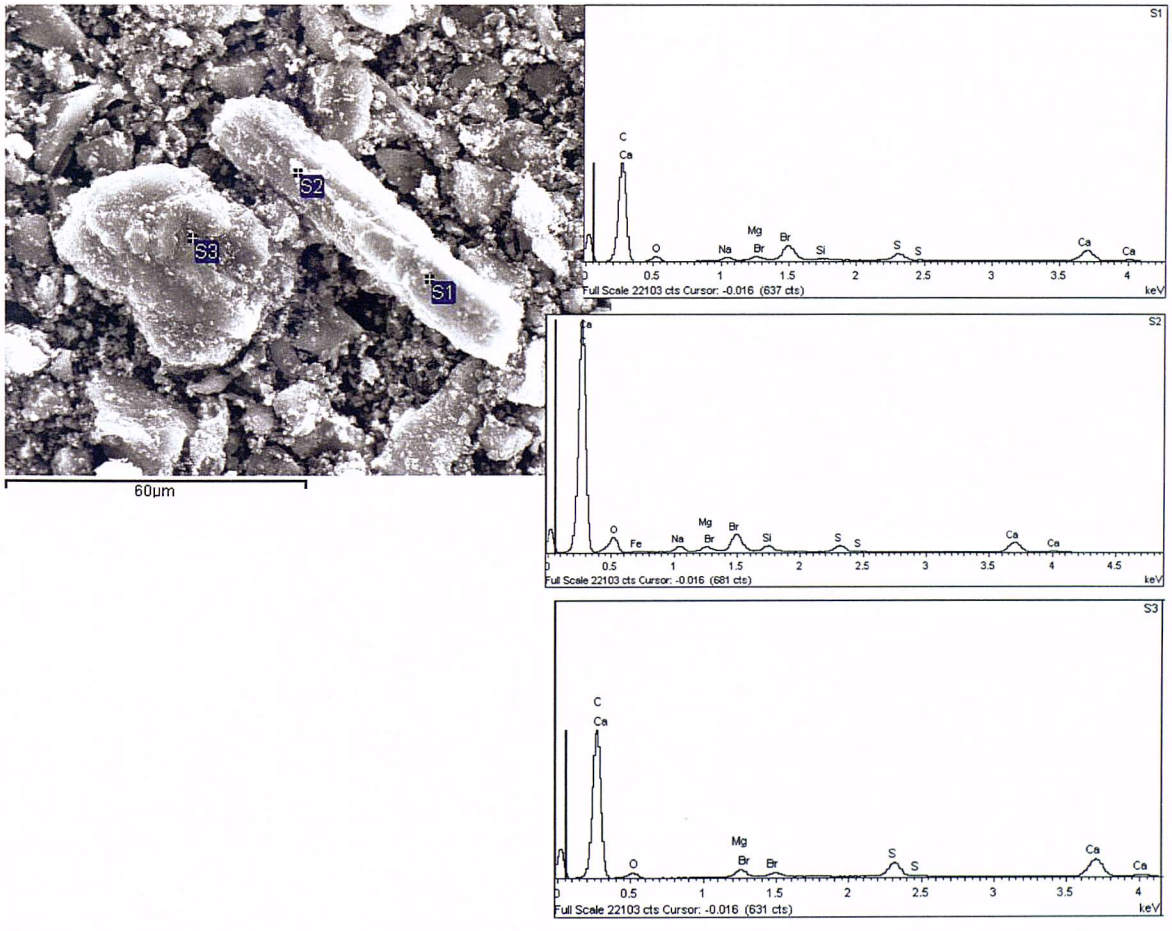


Figure 5-5 SEM & EDX analysis of Norit Darco HG-LH™ (at x1000 magnification)

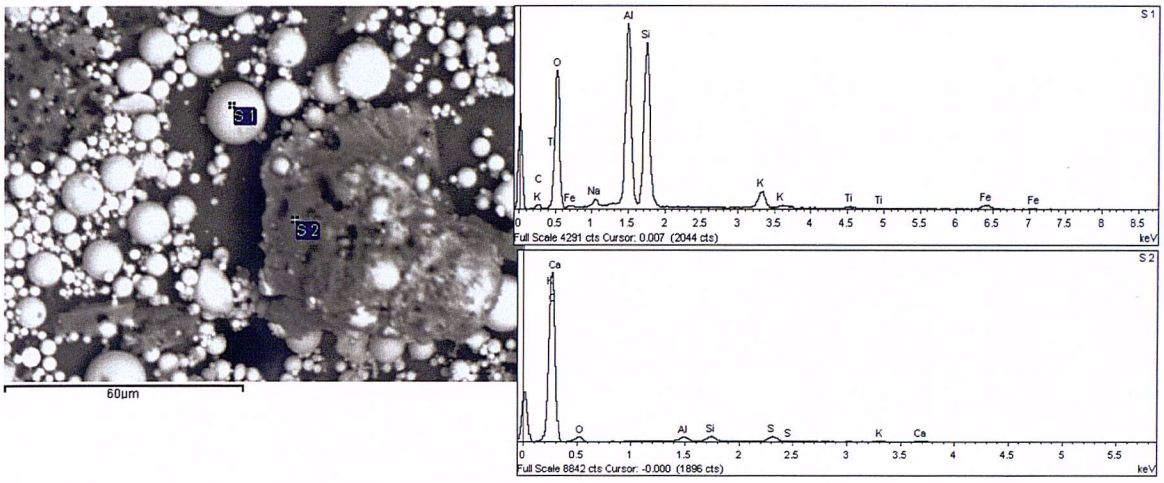


Figure 5-6 SEM & EDX analysis of fly ash D (at x1000 magnification).

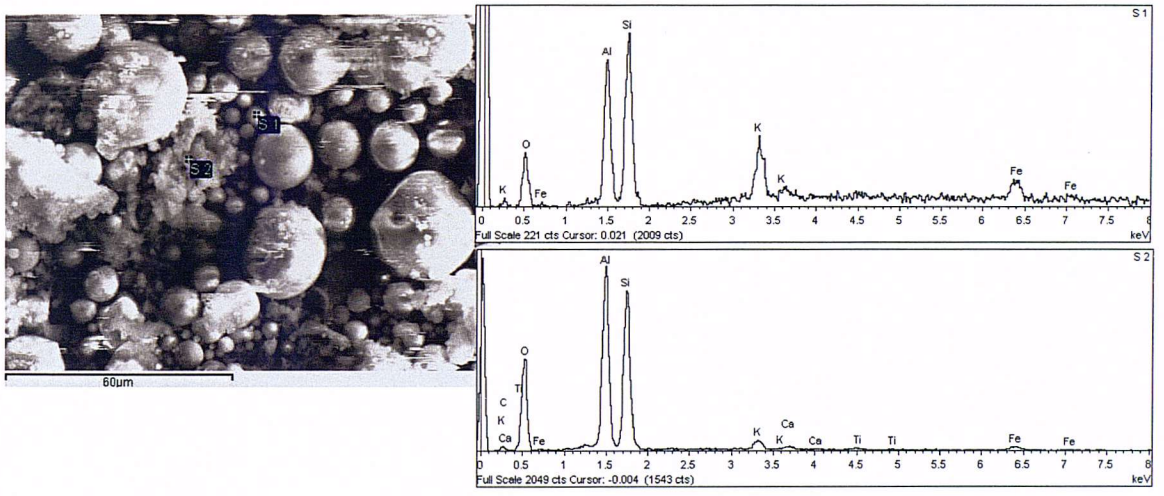


Figure 5-7 SEM & EDX analysis of fly ash E (at x1000 magnification).

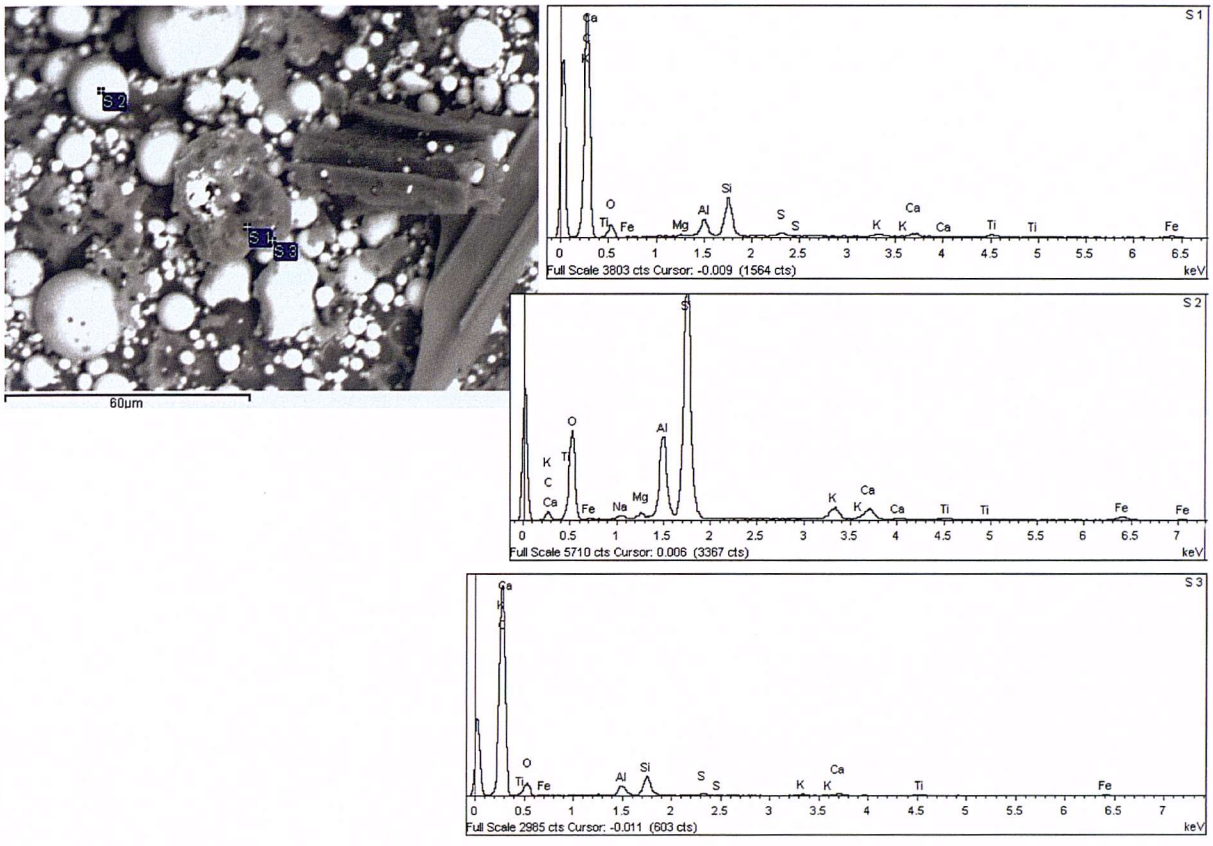


Figure 5-8 SEM & EDX analysis of fly ash F (at x100 magnification).

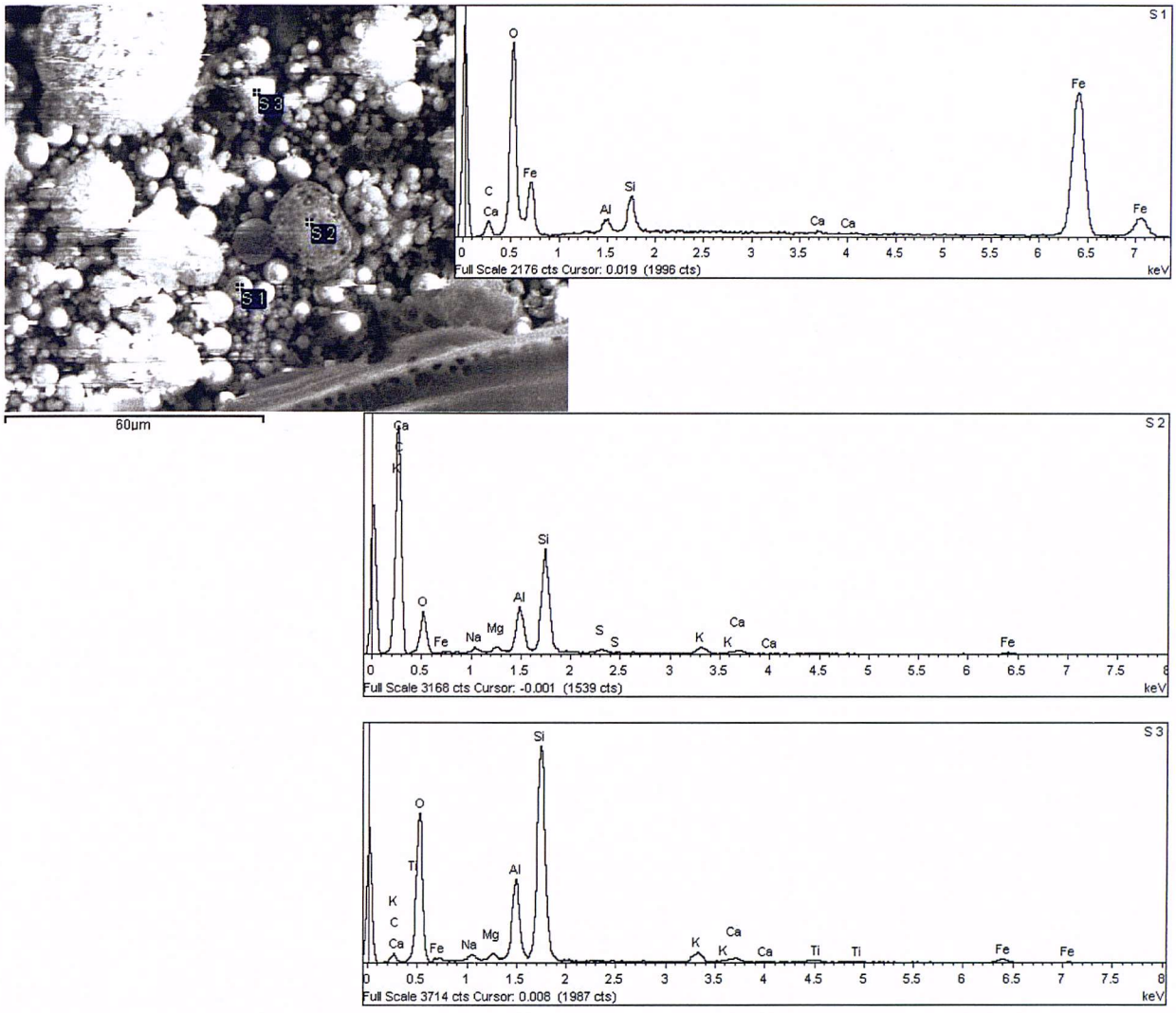


Figure 5-9 SEM & EDX analysis of fly ash G (at x100 magnification).

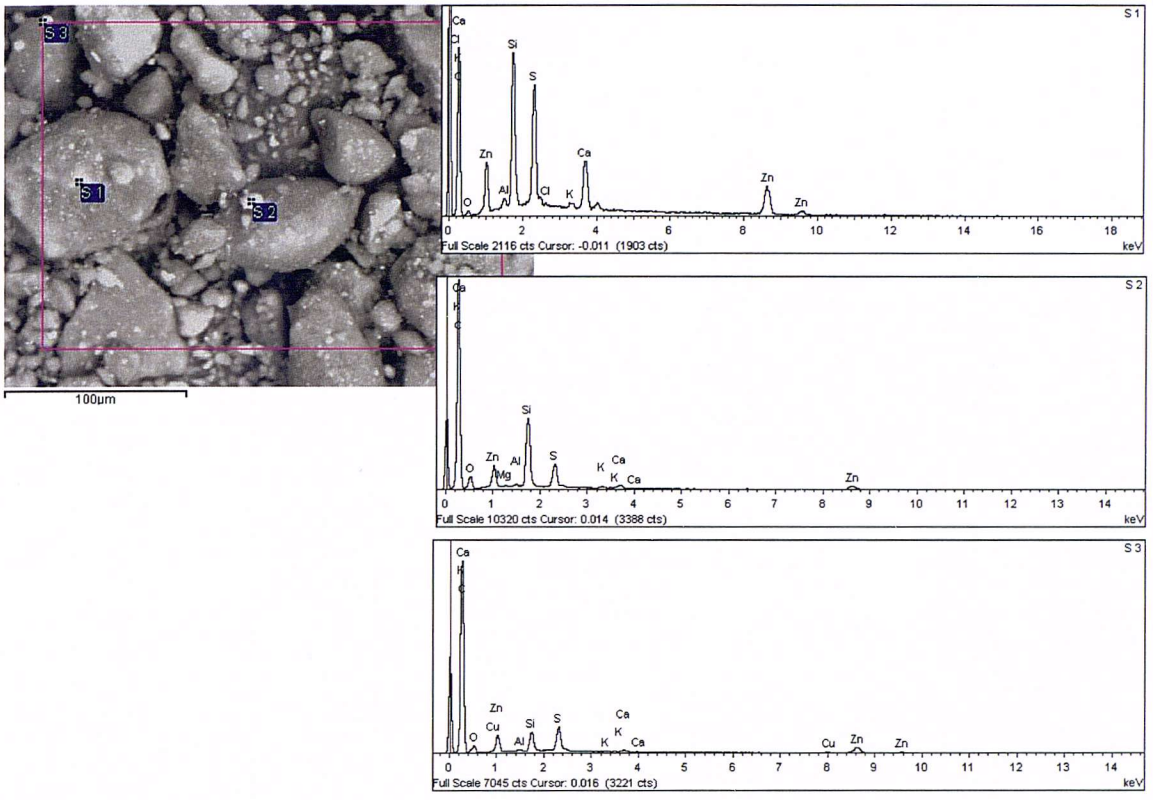


Figure 5-10 SEM & EDX analysis of tyre char R1 (at x450 magnification).

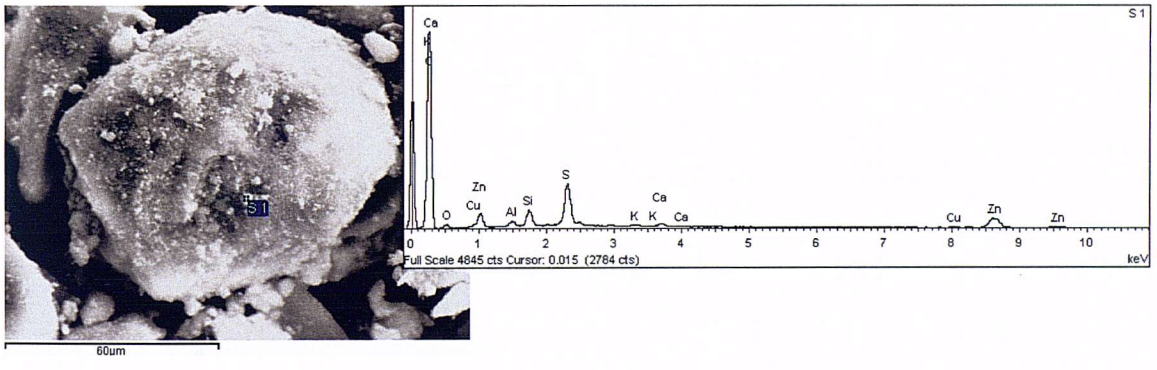


Figure 5-11 SEM & EDX analysis of tyre char R1 (at x1000 magnification).

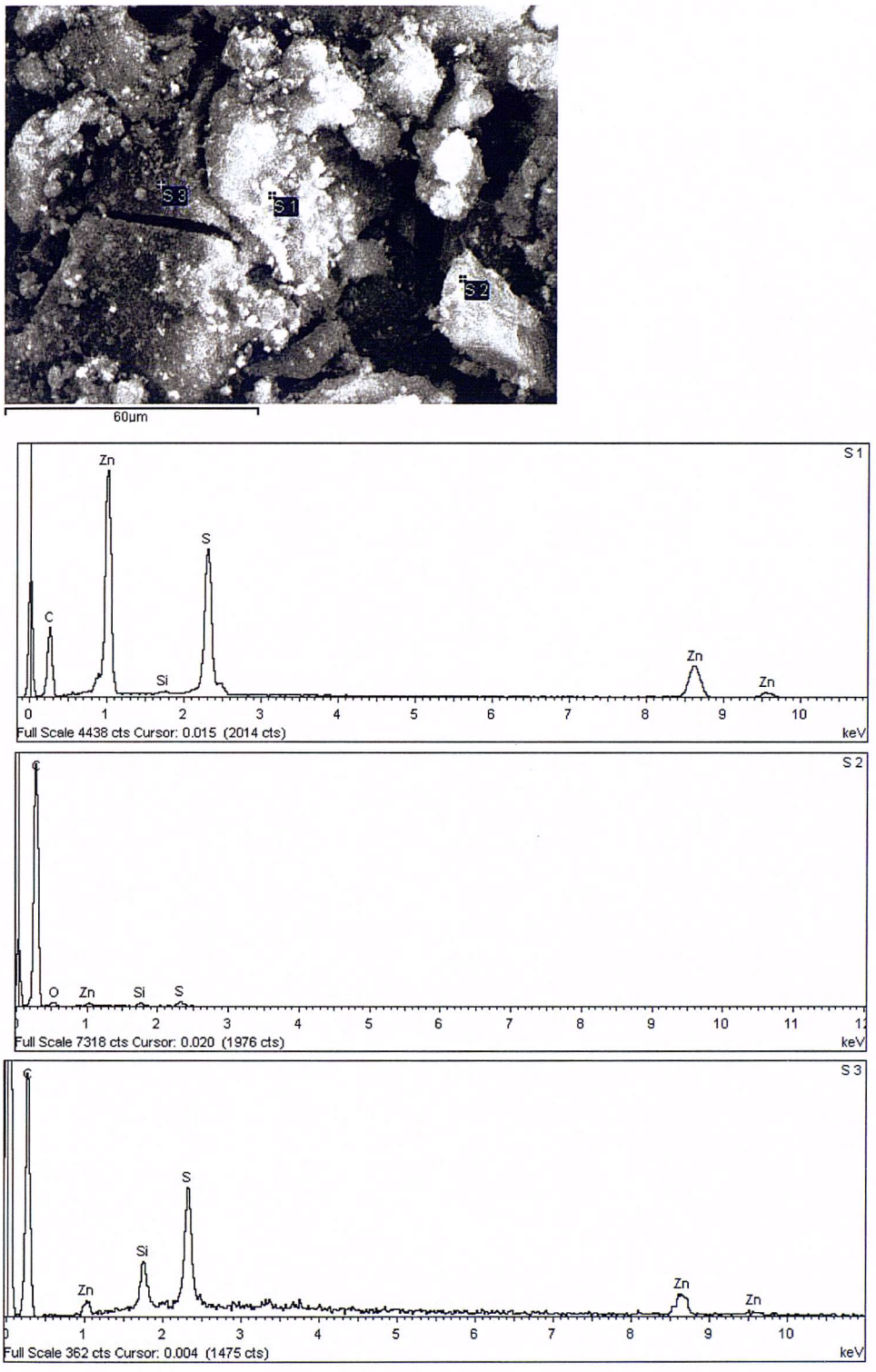


Figure 5-12 SEM & EDX analysis of tyre char R3 (at x1000 magnification).

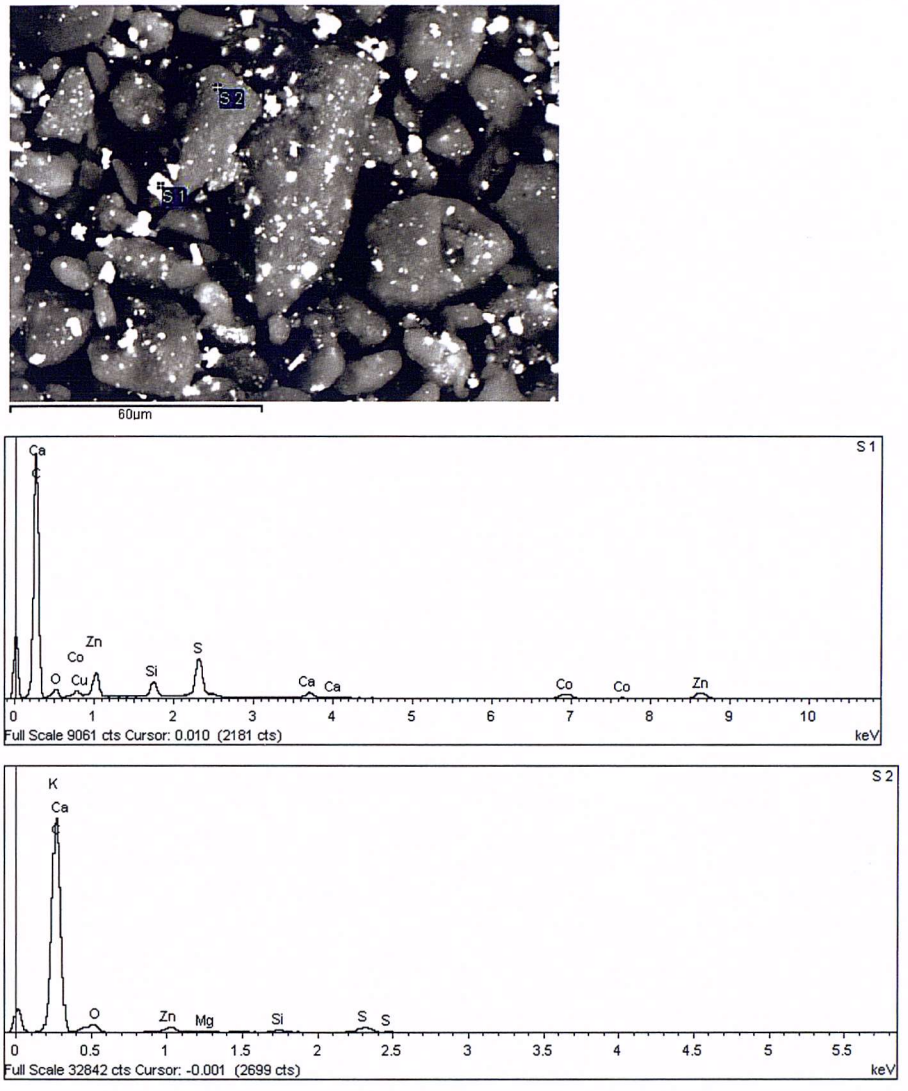


Figure 5-13 SEM & EDX analysis of tyre AC R1 (at x1000 magnification).

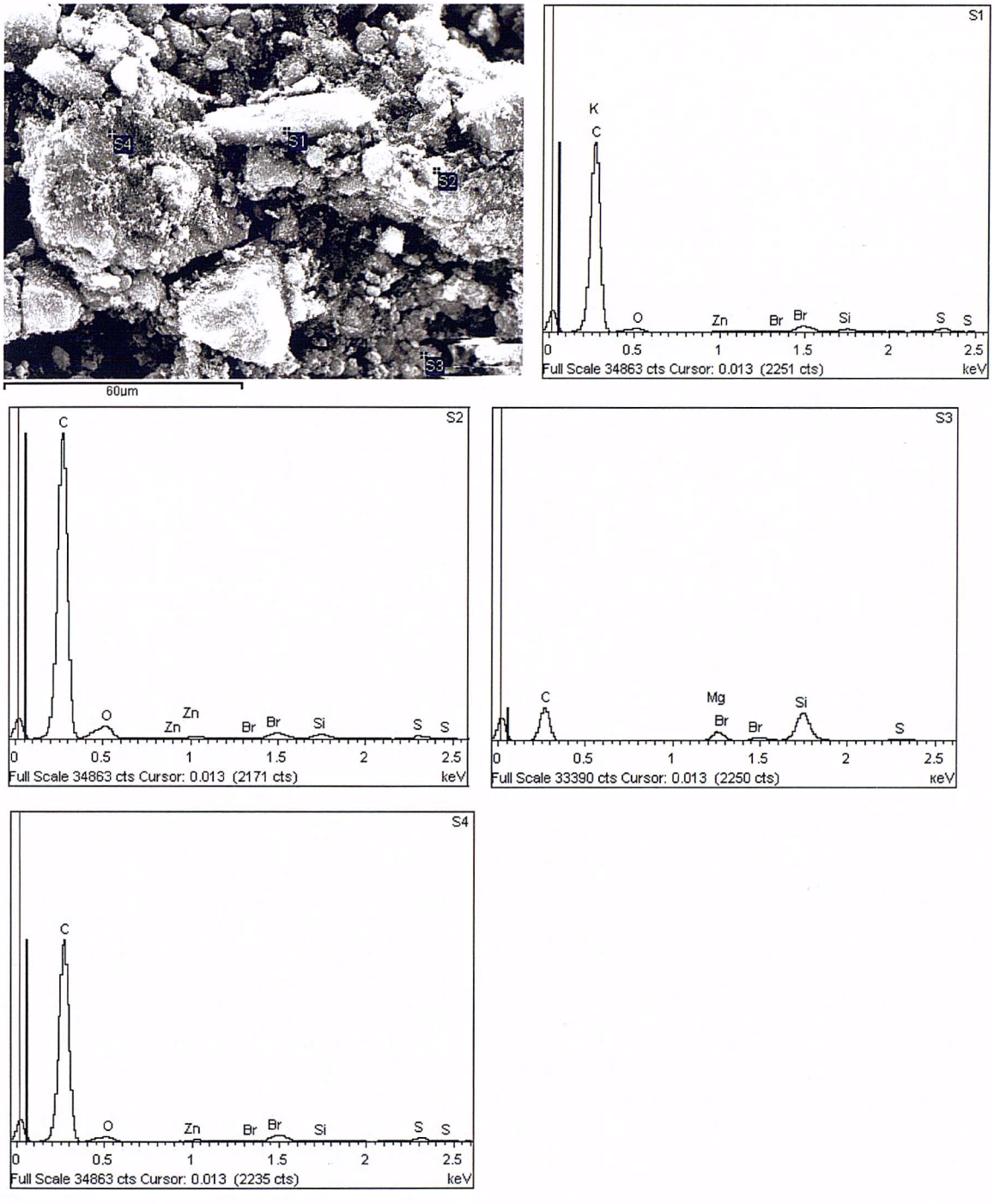


Figure 5-14 SEM & EDX analysis of tyre AC R3 (at x1000 magnification).

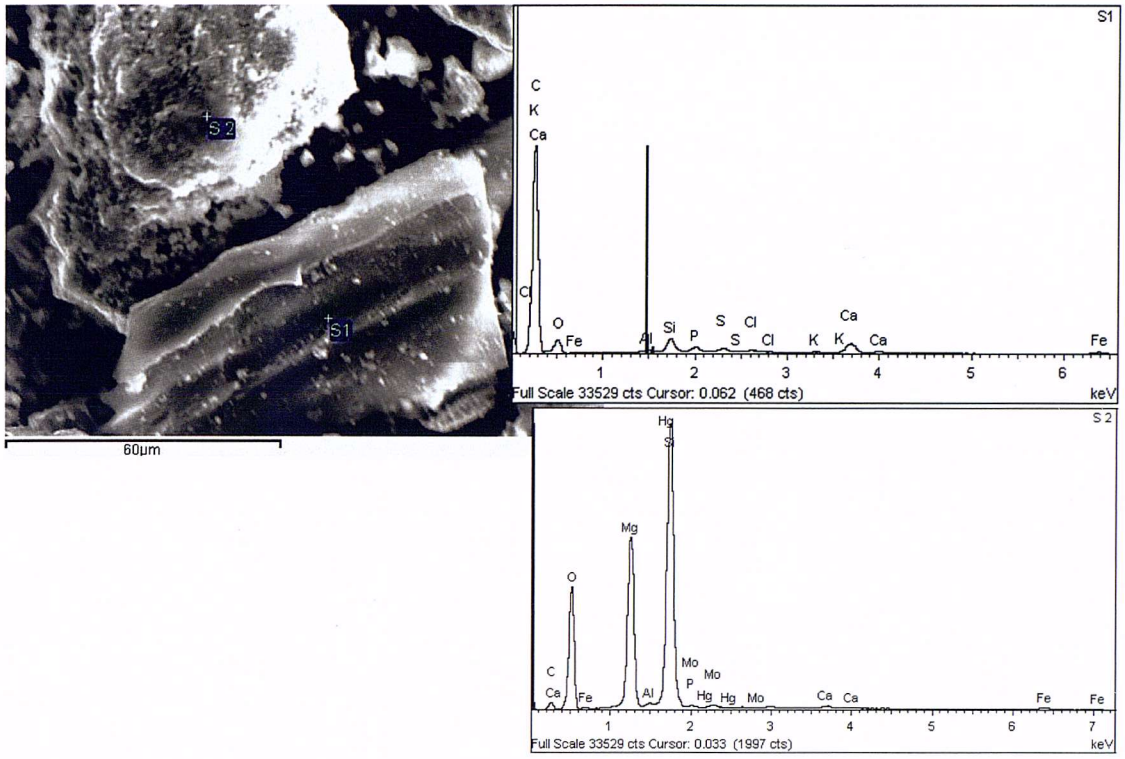


Figure 5-15 SEM & EDX analysis of sewage sludge char (at x1000 magnification).

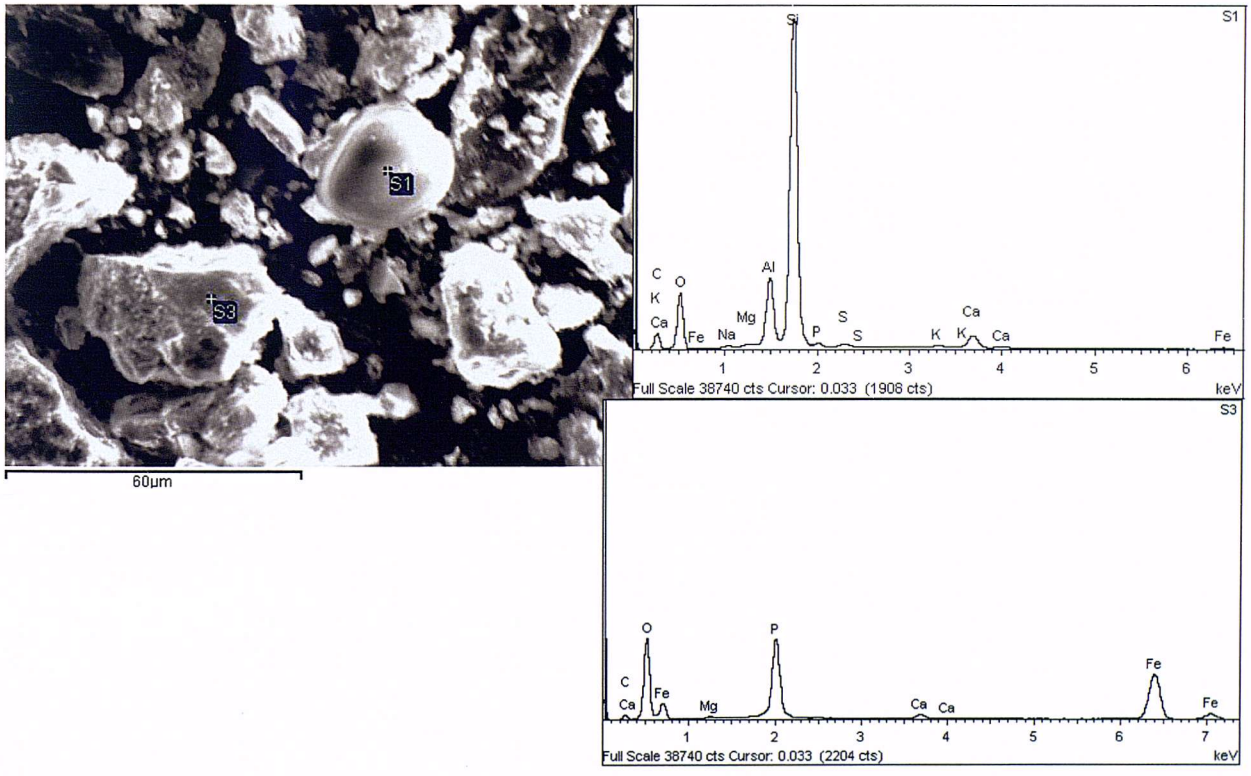


Figure 5-16 SEM & EDX analysis of sewage sludge char (at x1000 magnification).

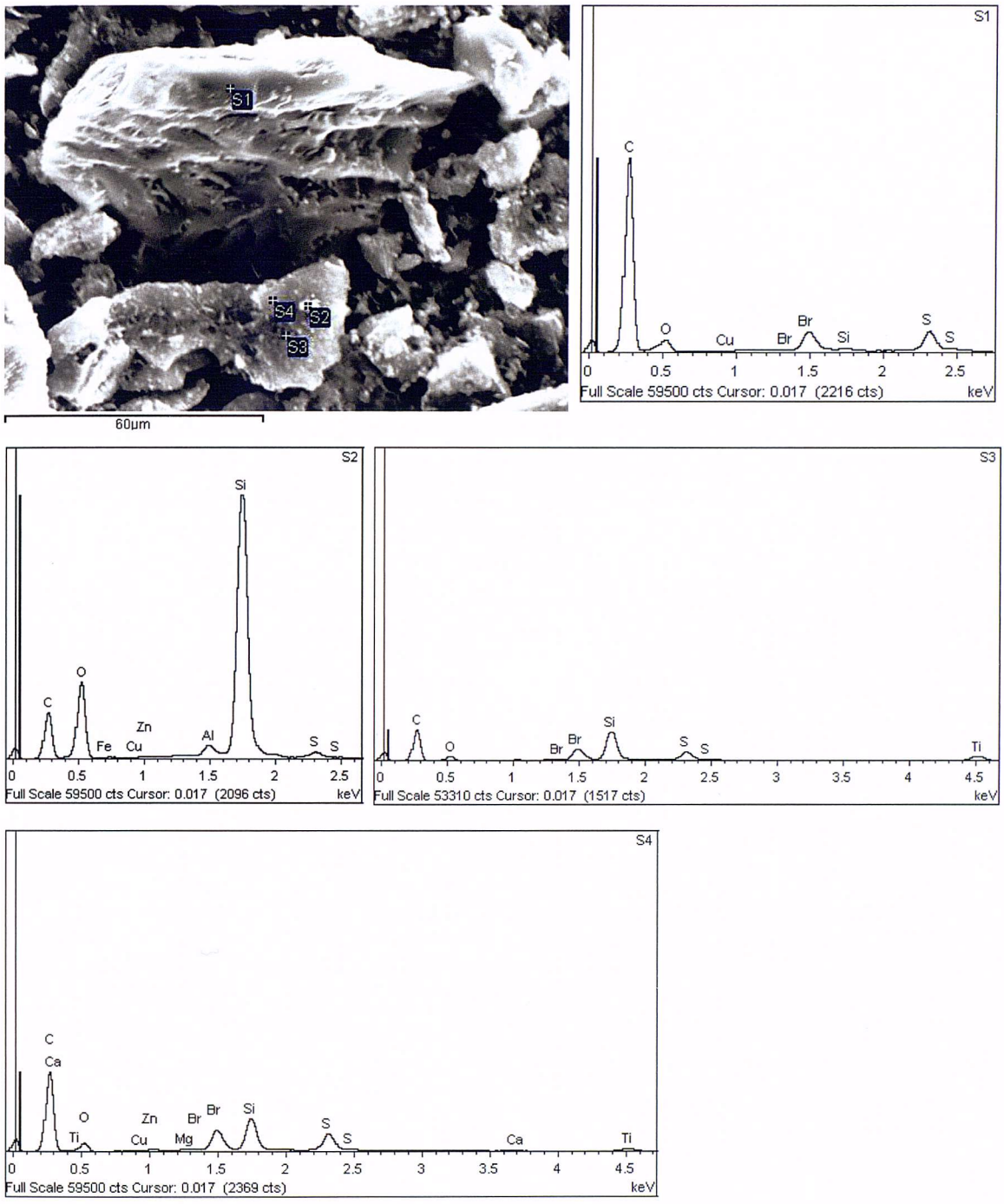


Figure 5-17 SEM & EDX analysis of sewage sludge AC R3 (at x1000 magnification).

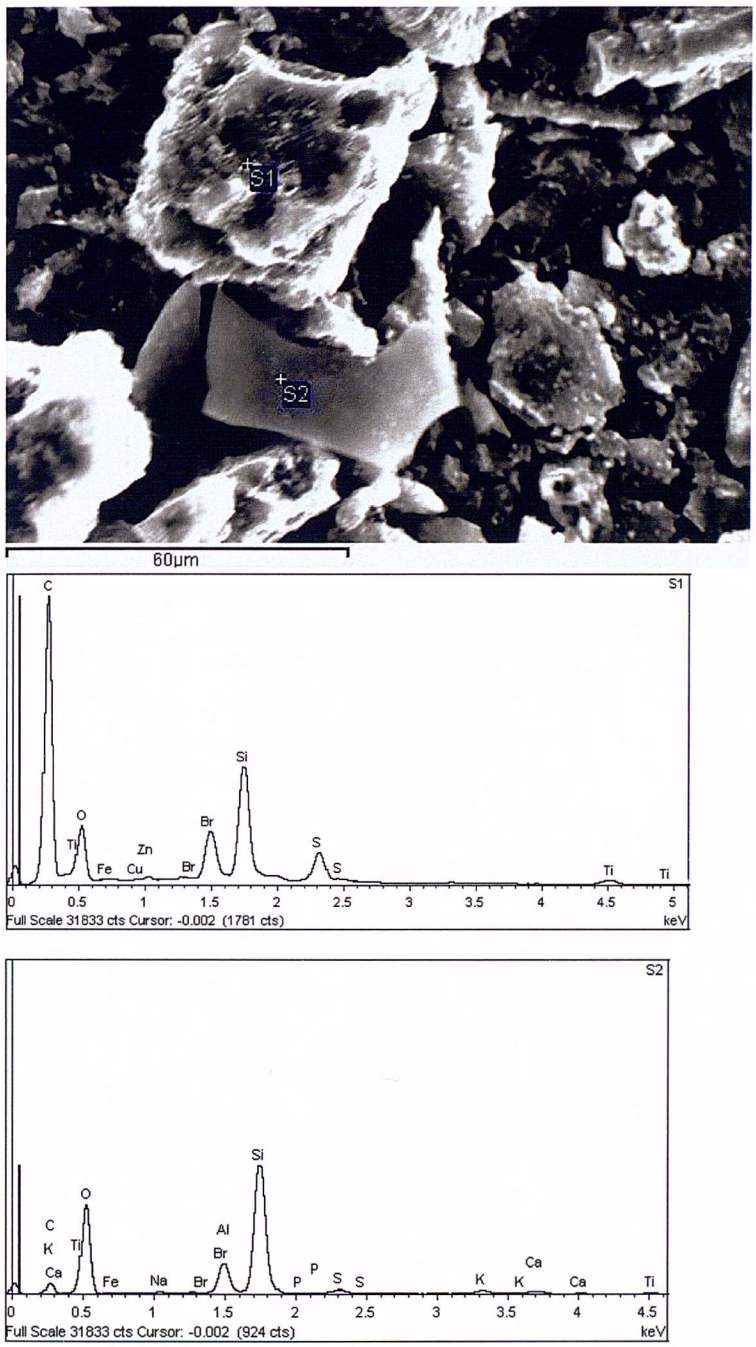


Figure 5-18 SEM & EDX analysis of sewage sludge AC R3 (at x1000 magnification).

5.5. Conclusions from sorbent characterisation

The sorbents that were evaluated for mercury capture during this study have been characterised using a number of analytical techniques. The bromide impregnated activated carbon produced from sewage sludge was found to be similar to commercially available Norit Darco Hg™ in regard to surface area and micropore volume; both these

PACs had significantly larger micropore surface area than all the other sorbents tested. When compared to the other sorbents evaluated in this study, charcoal and active carbon produced from scrap tyre rubber had a much greater proportion of macropores. In the case of scrap tyre rubber charcoal and bromide impregnated carbon, macropores made a substantial contribution towards the total surface area. However, high partial pressures are needed for an adsorbate to be captured on macropores. It is therefore unlikely that the high surface area of the macropores in these sorbents will play a major role in capturing mercury. When compared to $ZnBr_2$ activation, steam activation seemed to produce a more porous sorbent from scrap tyre rubber. The coal fly ash samples analysed during this study had much smaller BET surface areas and micropore surface areas than the other sorbents that were tested. This suggests that coal fly ash will show the least capacity for mercury capture of the sorbents tested in the current study. It has also been observed that the micropore surface area of the fly ashes can be correlated to their LOI content. Consequently, fly ashes with larger LOI content may have more capacity for capturing mercury.

The ash and elemental analysis of the bromide impregnated PACs indicated that their bromine concentrations were only a few percent greater that the sorbents which did not have bromide impregnation. A majority of the bromine which was added prior to the activation of scrap tyre rubber charcoal and DEMAD sewage sludge must, therefore, have been removed either during the thermal treatment or during the post-activation acid wash treatment processes. Analysis of the sorbents produced from scrap tyre rubber showed that the charcoal and PACs from steam activation contained a proportion of the sulphur that was initially present in the scrap tyre rubber. However, subsequent acid washing of the bromide impregnated PAC produced from the same raw material was seen to remove a significant fraction of the sulphur retained by the unwashed carbon. The acid washing procedure also decreased the amount of ash in the sorbents. Thus washed sorbent had a larger percentage of carbon than the "un-washed" sorbent made from the same raw material.

XRD and SEM, coupled with EDX, analysis confirmed some of the results from the elemental analysis of the sorbents (including the presence of bromine and sulphur). The different samples that were studied were found to have mainly amorphous phases and thus few crystalline phases which could be detected by the XRD analyser. Fly ash F was

found to contain CaO, which is thought to inhibit the mercury oxidation reaction with HCl. Although some of the fly ash samples used in this study contained magnetite, other researchers have suggested that it is a different form of iron oxide (maghemite) which actively catalyses mercury oxidation.[4] Since unburnt carbon is present in fly ash in concentrations much greater than either calcium oxide or iron oxide, it is believed that the LOI is the most important fly ash component for mercury oxidation.

The results from elemental analysis, coupled with XRD analysis, indicate that tyre pyrolysis charcoal contains a larger fraction of amorphous sulphur than the steam activated carbons. Since this sulphur may be able to react with mercury in the gas stream, the pyrolysis charcoal could prove to be a more effective sorbent for mercury capture than the steam activated carbon made from the same scrap tyre rubber.

SEM coupled with EDX analysis of fly ashes showed that the inorganic species in the ash had agglomerated into spherical particles, while the particles with larger dimensions were mainly unburnt carbon. This analysis also showed that wurtzite in scrap tyre rubber charcoal and steam activated carbon seemed to have separated from the carbon particles.

6. Experimental procedures

This chapter describes the experimental procedures which were used to test the sorbents evaluated in the present study. The two methods by which mercury adsorbed onto the samples was quantified are introduced first. This is followed by a section which details the scheme employed during the present study to evaluate the efficiency of sorbents for their capture of mercury. In this section, the newly designed reactor that was used is discussed along with an evaluation of its efficacy and consistency. An account of the different experiments that were conducted is then given. The last section of this chapter describes the leaching tests performed to determine the stability of the mercury captured on the sorbents.

6.1. Analytical techniques for mercury quantification

During this study, two different analytical techniques have been used to quantify mercury in the sorbent samples. While a majority of the samples were analysed by using the LECO AMA 254 mercury analyser, the PSA 10.025 Millenniun Merlin System was used to evaluate the bromide impregnated sorbents and to quantify the leachability of mercury captured by the sorbents.

6.1.1. LECO AMA 254 Mercury Analyser

The amount of mercury that was retained on the sorbents that did not have any bromide impregnation was determined by using a LECO AMA 254 mercury analyser [supplied by LECO Instruments (UK) Limited, Stockport, UK].[68] In this unit, solid samples (typically 20 mg) were placed in a "nickel boat" and combusted over a catalyst in a pure oxygen flow. Mercury vapour released from the sample is captured on a gold amalgamator. After purging, the amalgamator is heated to ca. 900°C to liberate the trapped mercury, which is then quantified by atomic absorbance of light at the 254 nm wavelength. Mercury concentrations within the solid samples as low as 0.01 ppm can be measured to within 20% accuracy. During the present study, the "large nickel boat" and sample holder (LECO part numbers 874-001-181 and 874-001-180) were used to minimise any spillages

when the spent sorbent is transferred from the reactor to the nickel boat. This unit was also used to analyse the external amalgamator which functioned as a backup capture device, i.e. to retain the residual mercury in the gas stream that exit the sorbent test reactor (refer § 6.2.2). In this case, the holder which held the nickel boat in place was changed to a holder that was specific for the external amalgamator. In both of the above mentioned instances, the instrument was set at a drying time of 100 seconds, a decomposition time of 180 seconds, and a waiting time of 45 seconds.

During the initial experiments, a potassium iodide impregnated activated carbon tube was used as the backup capture device. This activated carbon was also analysed with the LECO AMA 254 analyser. Subsequent analysis runs however showed that this instrument was not suitable for samples with high halogen concentrations. The catalyst tube was saturated very quickly resulting in the instrument losing its sensitivity for quantifying the amount of mercury in each sample. The analyser therefore needed a complete overhaul. The mercury in the bromide impregnated activated carbons evaluated in this study were therefore measured by using the PSA 10.1025 Millennium Merlin system (refer § 6.1.2).

A more complete description of the LECO AMA 254 mercury analyser is given in Appendix -C.

6.1.2. PSA 10.025 Millennium Merlin System

Since the mercury contents of the bromide impregnated samples tested in this study could not be analysed by the LECO AMA 254 analyser (refer § 6.1.1), the amount of mercury in these samples was found by using the PSA 10.025 Millennium Merlin System at P S Analytical in Orpington, Kent, UK.[69] A brief description of the procedure developed by P S Analytical for mercury quantification by the continuous flow vapour generation-atomic fluorescence spectrometer (PSA 10.025) is given below. It involves an initial wet digestion of the samples before mercury is quantified by the instrument.

6.1.2.1. Aqua Regia digestion procedure

The solid samples were placed in digestion vessels that had been cleaned overnight by using a concentrated Aqua Regia solution made from Aristar® grade HCl and HNO_3 reagents in a volume ratio of 3:1. These samples were then digested for two hours at 140°C with the same concentrated Aqua Regia solution. For a sorbent sample mass of 20 mg and its Kaowool support (refer § 6.2.1), 5 mL of concentrated Aqua Regia was used. After the two hour digestion, the solution and the solids were poured into 50 mL sample bottles. Approximately 40 mL of deionised water was used to wash any remaining solid particles and Aqua Regia solution from the digestion vessel to the 50 mL sample bottles. These sample bottles were shaken and then filtered into separate 50 mL sample bottles by using Whatman® No1 filter paper (Grade 1, Cat. No. 1001 110). Deionised water was added to the filtered solution until the final volume was 50 mL. The resulting solution therefore had an Aqua Regia concentration of 10% (vol/vol). The concentration of mercury in each sample bottle was subsequently analysed by using the PSA 10.025 analyser.

6.1.2.2. Preparation of the reductant

A 2% mass/volume of tin(II) chloride and 10% vol/vol of Aristar® grade HCl solution is used as the reducing reagent for the PSA 10.025 analyser. This solution was prepared by first adding 100 mL of Aristar® grade HCl to a beaker that contained 20 g of tin(II) chloride granules. The solution was then boiled until all the tin(II) chloride was dissolved which took approximately 5 minutes. After the beaker had cooled its contents were poured to a 1 L volumetric flask containing ca. 500 mL of deionised water. The final solution was prepared by adding more deionised water until the liquid level in the volumetric flask reached the 1 L mark.

6.1.2.3. Preparation of reagent for calibration standards and for blank solution

A 10%(vol/vol) Aqua Regia reagent similar to the Aqua Regia concentration in the 50 mL sample bottles was used to make the standards for calibrating the PSA 10.025 analyser. Furthermore this solution was also used as the reagent blank during the mercury quantification. It was prepared by pouring 75 mL of Aristar® grade HCl into a 1 L volumetric flask containing ca. 500 mL of deionised water. After 25 mL of Aristar®

grade HNO_3 was added, deionised water was poured until the liquid level reached the 1 L mark. This procedure was repeated so that a 2 L solution of 10% Aqua Regia was available for preparing the calibration standards and for use as the reagent blank.

6.1.2.4. Preparation of the calibration standards

A 100 ppb Hg stock solution (in 10% HNO_3) was used to prepare the calibration standards by first making a 10 ppb Hg solution in 10% Aqua Regia. The amount of mercury retained on the brominated active carbon was quantified using the following calibration solutions made by diluting the 10 ppb Hg solution with 10% Aqua Regia reagent.

- 0.0 ppb Hg in 10 % Aqua Regia solution (used only the 10% Aqua Regia reagent)
- 0.5 ppb Hg in 10% Aqua Regia solution
- 1.0 ppb Hg in 10% Aqua Regia Solution
- 1.5 ppb Hg in 10% Aqua Regia solution
- 2.0 ppb Hg in 10% Aqua Regia solution

Since the leachates from the leaching experiments had significantly less mercury, a different calibration schedule was used for that part of the study and it is discussed in sub-section 6.2.3.

6.1.2.5. Mercury determination using the PSA 10.025 analyser

The mercury present in the bromide impregnated sorbents was determined by using a continuous flow vapour generation-atomic fluorescence spectrometer (PSA 10.025 Millennium Merlin system). It was utilised to generate and detect gaseous mercury.[69] A schematic diagram is shown in Figure 6-1. The liquid sample and the reductant are mixed at the sample valve and as a result the oxidised mercury in the sample is reduced to elemental mercury. Since elemental mercury is insoluble[18] it is carried with the argon carrier gas at the gas/liquid separator. This gas stream is dried before the mercury is detected via atomic fluorescence. The excitation was achieved using a low-pressure mercury vapour discharge lamp at a wavelength of 253.7 nm.[69] The resonance fluorescence was detected at the same wavelength by a photomultiplier tube located at right angles to the excitation source. The operating conditions of the instrument are listed

in Table 6-1. During the initial experiments, the samples were in a more concentrated 20% Aqua Regia solution and this resulted in poor mercury recoveries due to precipitation occurring at the gas/liquid separator. The PSA 10.025 analyser produced the best results if the samples were in a 10% Aqua Regia reagent and the oxidised mercury was reduced by a 2% mass/vol $SnCl_2$ in 10% vol/vol HCl reducing agent.

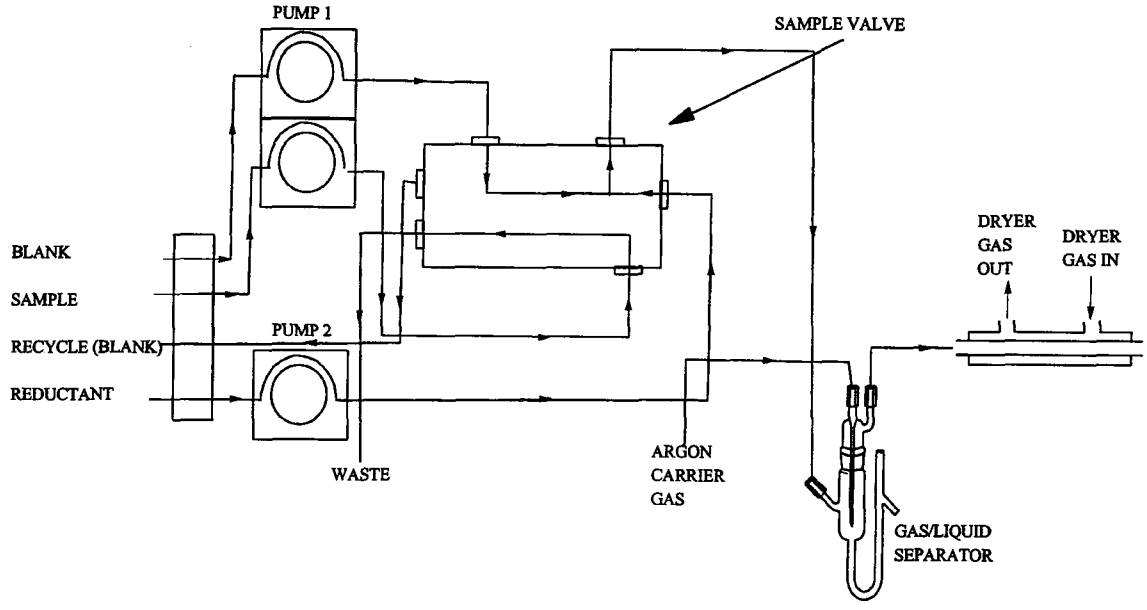


Figure 6-1 Schematic diagram of the continuous flow vapour generator (PSA 10.025).[69]

Table 6-1 Instrumental conditions for Millennium Merlin (PSA 10.025)

Reductant flow rate (mL/min)	4.5
Blank flow rate (mL/min)	9.0
Sample flow rate (mL/min)	9.0
Carrier gas flow rate (mL/min)	235
Dryer gas flow rate (mL/min)	2500
Blank concentration	10% vol/vol Aqua Regia
Reductant concentration	5% mass/vol SnCl2 in 10% vol/vol HCl
Delay period (s)	20
Analysis period (s)	40
Memory period (s)	60
Filter factor	32
Wavelength (nm)	253.7
Gain	100
Measurement mode	Height

6.2. Experimental scheme to test the sorbents at low temperatures

This section introduces the bench scale experimental system with a novel sorbent test reactor that was designed, constructed, commissioned and later used to evaluate the different sorbents tested during the current study. In order to obtain a better understanding on how each sorbent adsorbs mercury, the experiments were completed with different gaseous atmospheres and other process conditions (e.g. at varying test temperature, pre-treating the sorbents with acid gases, thermal desorption tests on spent sorbents etc.), which are also described in this section of Chapter 6.

6.2.1. Reactor for testing sorbents at low temperatures

The new reactor that was used to test the sorbents was based on the experience gained from a previous hot gas cleaning project.[53] The following factors were also considered when it was decided to make the reactor by using borosilicate glass.

- Stainless steel could not be used for any of the reactor's components since prior studies had reported poor mercury recoveries when gas streams containing mercury were in contact with stainless steel parts.[70, 71]
- As the main objective of the present study was to evaluate mercury adsorption by sorbents at temperatures close to the operating temperature of CS-ESPs (i.e. ca. 150°C), the reactor would be functioning below 300°C.[59] Consequently, unlike the unit used during the hot gas cleaning project, the sorbent test reactor for the present study did not need to be made from quartz as it would be operating at much lower temperatures.

Figure 6-2 has a schematic diagram of the new sorbent test reactor that was used to evaluate the sorbents during the present study. It was based around three concentric borosilicate glass tubes and was produced at Cambridge Glassblowing Limited (UK). Gas tight joints are maintained by keeping all connections at the lower end of the reactor, beneath the furnace, where the temperature was moderate and therefore minimised the effects of thermal expansion at the connections. Since the reactor was held only at its lower end, the upper portion of the unit was free to expand when it was heated, thereby limiting the possibility of any damage due to thermal stress on the borosilicate components of the unit.

During each sorbent test the simulated flue gas stream that enters the reactor was heated by an electric furnace as it flowed upwards along the annulus between the tubes of the unit. This heated gas flow was then reversed and passed downwards through the sorbent bed towards the reactor outlet. A 2 mm thick Kaowool felt disc located in the central annulus of the unit was used to support a fixed quantity of sorbent. Figure 6-3 and Figure 6-4 show the individual borosilicate components of the reactor and also how they fit together with the PTFE/rubber o-rings and clamps. The engineering drawings for each component of the reactor are given in Appendix -D. The 2 mm thick Kaowool support which held the sorbent samples in place is shown in Figure 6-5.

The purpose-built electric furnace for this system was based on the furnace Lachas[72] had used for his Hot Gas Cleanup Reactor. It consists of a 27 mm ID and 150 mm long high thermal conductivity alumina tube (25 Wm/K, supplied by Aegis Advanced Materials, Bewdley, UK). This tube is surrounded by a winding, approximately 7 m long, of 1.2 mm diameter Kanthal APM wire (supplied by Kanthal Limited, Stroke-on-Trent, UK) with an electrical resistance of 1.28 Ω/m at 20°C. The furnace therefore had a total electrical resistance of ca. 8.9 Ω. A 10 mm thick cement layer (supplied by Aegis Advanced Materials, Bewdley, UK) is used to electrically insulate the furnace. Thermal insulation is provided by a low thermal conductivity ceramic fibre blanket (Saffil Kaowool, 0.182 Wm/K at 1000°C in air; supplier Thermal Ceramics Limited, Wirral, UK) that was wrapped over the cement. This blanket was held in place by using a 40 mm wide and 3 mm thick wire-reinforced ceramic webbing tape (supplied by Warren Insulation Limited, Slough, UK). For safety reasons, the voltage into the furnace was limited by using a 100 V AC, 500 W transformer cum temperature controller with a 0 – 270 V Variac variable transformer (supplied by Zenith electrical Co. Limited, London). Since the Variac was used with a dial setting at 80 V, there was a 30 V electrical potential across the electric furnace. The thermal power dissipated from this furnace was therefore approximately 100W. A type-K nickel-chrome thermocouple fitted into the thermocouple well shown in Figure 6-2 measured the temperature of the sorbent bed and managed the furnace via the temperature controller.

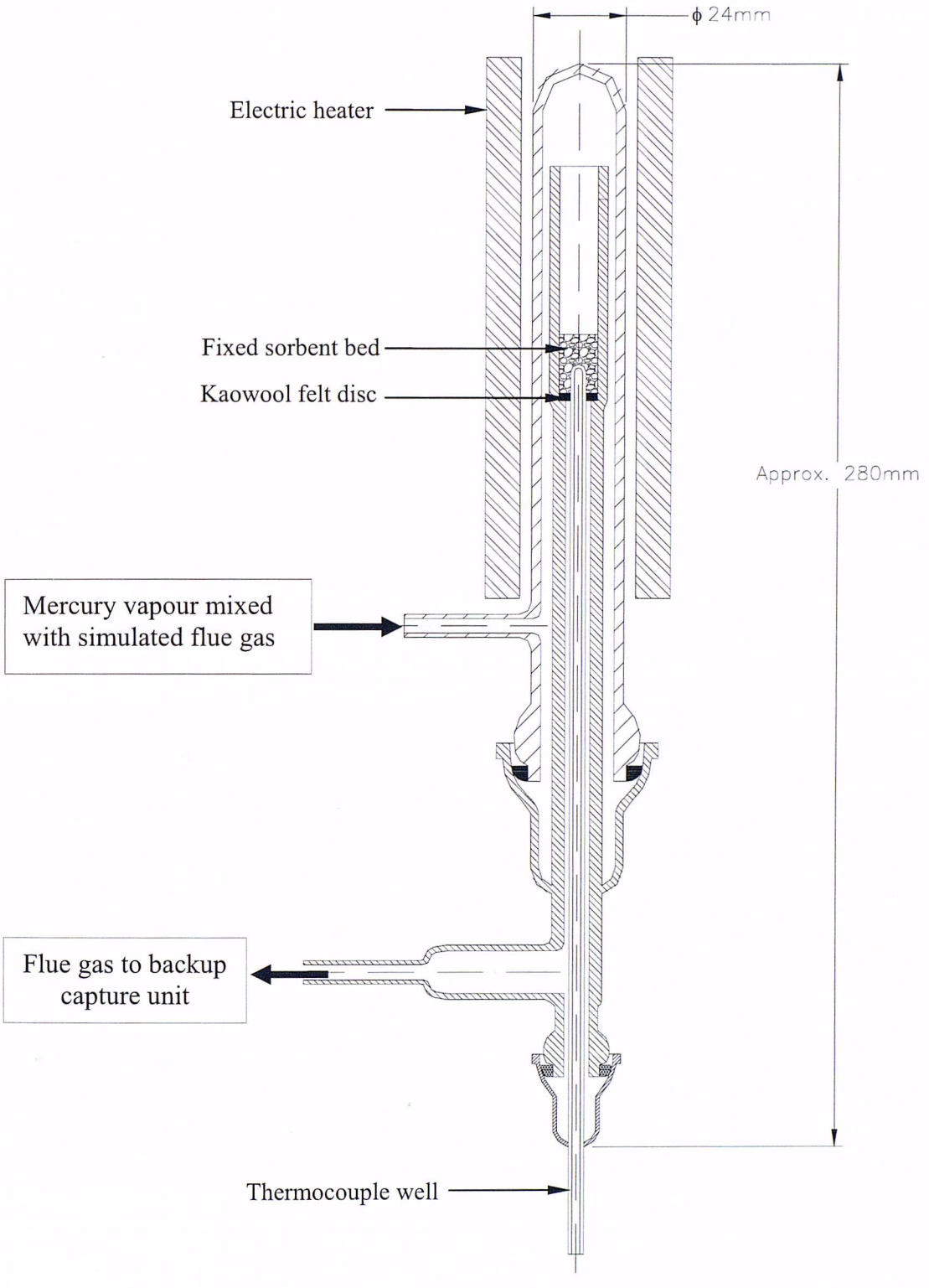


Figure 6-2 Sectional view of the low temperature sorbent test reactor

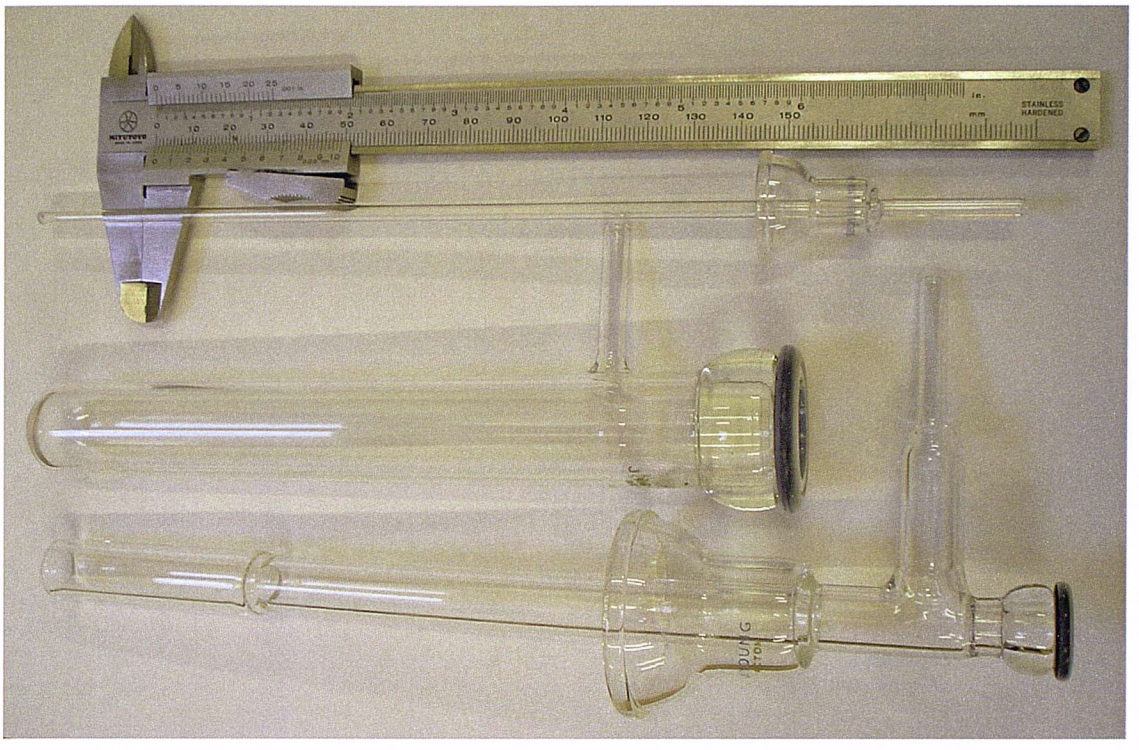


Figure 6-3 Individual borosilicate components of the low temperature sorbent test reactor

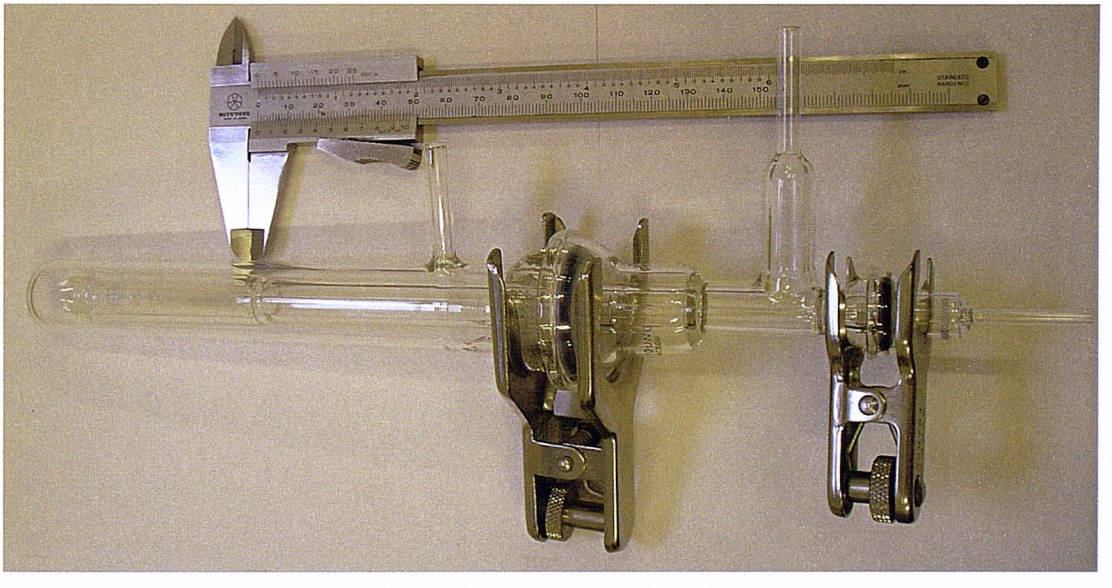


Figure 6-4 Low temperature sorbent test reactor with borosilicate components are assembled

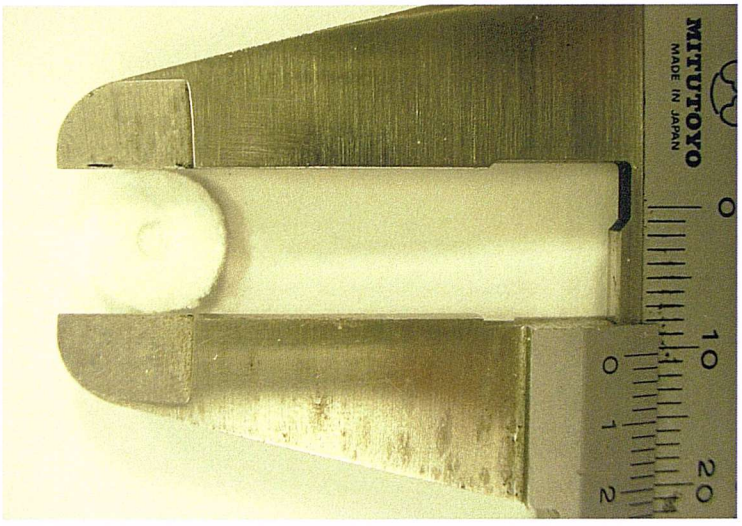


Figure 6-5 2mm thick Kaowool support used to hold the sorbent sample.

6.2.2. Experimental schemes to obtain information on mercury capture

A number of experimental schemes were employed to obtain information on the mechanism by which mercury may be captured on each of the sorbents evaluated in this study. In order to conduct a realistic investigation on the capture of mercury present in power plant flue gases, the efficiency of each sorbent was measured in different gas schemes based on the flue gas produced from the combustion of a Harworth coal, a typical UK bituminous coal.[54] Table 6-2 tabulates the constituents in the gas scheme, and the actual flow rates used in the experiments to represent the Haworth flue gas. When Harworth coal is used in a coal-fired power plant, it usually produces a flue gas with a mercury concentration of 29 ng/L (at normal temperature and pressure [NTP]). During each experiment, the total gas flow to the reactor was kept constant at 37 mL/min (measured at NTP) which results in a superficial gas velocity of 0.01 m/s through the reactor section, just above the sorbent bed. This velocity is similar to the air-to-cloth ratio for fabric filters installed in coal fired power plants.[73] When used in coal-fired power plants, the sorbent for mercury capture will most probably be injected into the flue gas duct after the air pre-heater and then be collected along with the fly ash using the particulate control system (either an ESP or a FF). Most UK coal-fired power plants are equipped with ESPs that operate at about 130°C whilst the typical operating temperature of cold-side ESPs in the USA is around 150°C.[59] In order to gain a better understanding of the mercury adsorption process, test temperatures between 100°C – 200°C have been used for the experiments. This temperature variation results in only a minor change to the

superficial velocity of the gas stream and is believed to have a negligible effect on the experimental results.

Table 6-2 Individual gas/vapour concentrations and flow rates for the more complete simulated flue gas schemes used during this study.

Constituent	concentration	Volume flow rate (mL/min at NTP)
N_2	75%	27.5
NO	490 ppmv	$1.8x10^{-2}$
NO_2	17 ppmv	$6.2x10^{-4}$
O_2	6%	2.1
CO_2	12%	4.5
SO_2	1799 ppmv	$6.6x10^{-2}$
HCl	200 ppmv	$7.3x10^{-3}$
H_2O	7%	2.5
Hg^0	3.5 ppbv	$1.3x10^{-7}$

A simplified schematic diagram of the bench-scale system that was used in the present study is illustrated in Figure 6-6. The use of stainless steel components was believed to have caused the observed poor mercury recoveries that were reported in previous studies.[70, 71] During the present study PTFE tubing with PFA and PVDF fittings (supplied by Polyflon Technology Limited, Staffordshire, UK) were therefore utilized to connect the mercury vapour generation unit to the sorbent test reactor and thereby minimise the risk of mercury losses during its transfer.

Previous studies generated the required Hg^0 vapour by using permeation tubes filled with pure Hg^0 liquid.[1, 74, 75] The mercury concentration during these earlier tests was controlled by placing the permeation tubes in a temperature controlled liquid bath of either oil or water.[1, 74, 75] However with the introduction of the U.S. Clean Air Mercury Rule a more robust system for generating mercury vapour was needed to ensure the integrity of mercury emission measurement systems installed at coal fired power plants. P S Analytical in Orpington, Kent, UK therefore developed suitable calibration source ("Cavkit" 10.534) which did not require such liquid baths to control the mercury output. The US National Institute of Standards and Technology (NIST) have recently used a PSA 10.534 for the generation of Hg^0 vapour mixtures in a flowing gas stream to establish a gaseous mercury standard.[76] As shown in Figure 6-6, mercury vapour for the experiments

completed during the present study was produced by using a similar PSA "Cavkit" 10.534 mercury generator.

This unit uses an oven arrangement to produce elemental mercury from a mercury-impregnated inert substrate. During each of the mercury capture tests the Cavkit was operated at an inlet nitrogen gas pressure of 16 psig and an oven temperature of 40°C. When the nitrogen gas entered the unit it was divided into two gas streams. The gas flow which was managed by mass flow controller – MFC1 passed through the oven and it was therefore saturated with mercury vapour. The gas flow through mass flow controller – MFC2 was used to dilute the mercury concentration of the exit gas stream to the level required for each experiment.

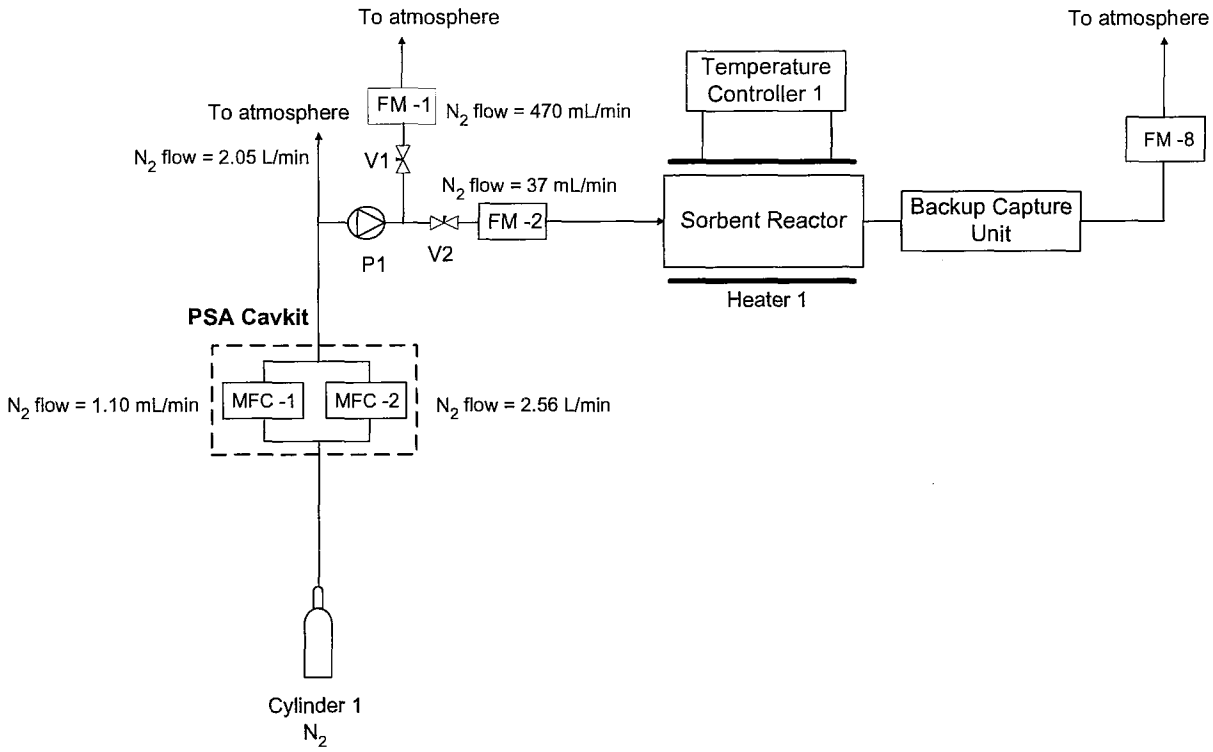


Figure 6-6 Bench scale system for testing sorbent's mercury capture efficiencies in a gas stream of Hg^0 vapour mixed with only N_2.

Since the Cavkit is designed to function without any backpressure at its outlet, the gas pressure at the exit of the unit was inadequate for balancing the pressure drop by the sorbent test system. Furthermore, this device is designed to produce mercury mixed in a nitrogen gas flow in the range of litres per minute, while the current mercury capture tests

need a gas flow in the millilitres per minute range. As shown in Figure 6-6 the Cavkit was therefore operated at a much larger nitrogen gas flow rate and with its exit at atmospheric pressure. The desired mercury vapour in nitrogen gas flow used for each test was obtained by taking a proportion of the gas leaving the Cavkit and pressurising it by using a Type N 86 KT.18 LABOPORT® PTFE lined diaphragm pump (supplied by KNF Neuberger UK Ltd, Oxon, UK). Since output of this pump exceeds the gas flow needed for each experiment, most of the gas had to be vented and only the amount required for each experiment was transferred to the reactor during the tests. In order to minimise the risk of loss of mercury during its transfer to the reactor, only variable area flow meters made from glass (i.e. with glass connectors) with PTFE control valves were used in the sorbent test rig (supplied by Dakota Instruments, Orangeburg, NY, USA).

A backup capture unit was used to retain any mercury which was not captured by the sorbent sample and so exited the reactor with the outlet gas stream. The mass balance for mercury was therefore calculated by analysing the total mercury content in the sorbent sample and the amount of mercury in the backup capture unit. These were also quantified by the LECO AMA 254 mercury analyser. An external gold amalgamator from LECO Instruments (UK) Limited (LECO part number 874-106-521) was used as this mercury backup capture unit. This external amalgamator was analysed for its mercury content by fitting an amalgamator holder (LECO part No. 874-106-700) to the LECO AMA 254 analyser. During the final part of this study, the effectiveness of the external amalgamator began to reduce, possibly due to the effect of acid gases in the more representative simulated flue gas stream. It was therefore substituted by a backup capture unit based on activated carbon (Figure 6-7). This unit consisted of a Quickfit® cone/flexible connector (cone size – 14/23; supplied by Fisher Scientific Limited, Leicestershire, UK) with approximately 200 mg of Norit Darco Hg™ held in place by 2mm thick Kaowool supports on either side of the bed. The LECO AMA 254 unit was unable to analyse large sample masses of activated carbon as it produced a "too high oxygen flow" error if such samples were used. The mercury in the Norit Darco Hg™ based backup capture unit was therefore quantified by dividing the activated carbon mass into three parts and individually evaluating each fraction with the LECO AMA 254 analyser.

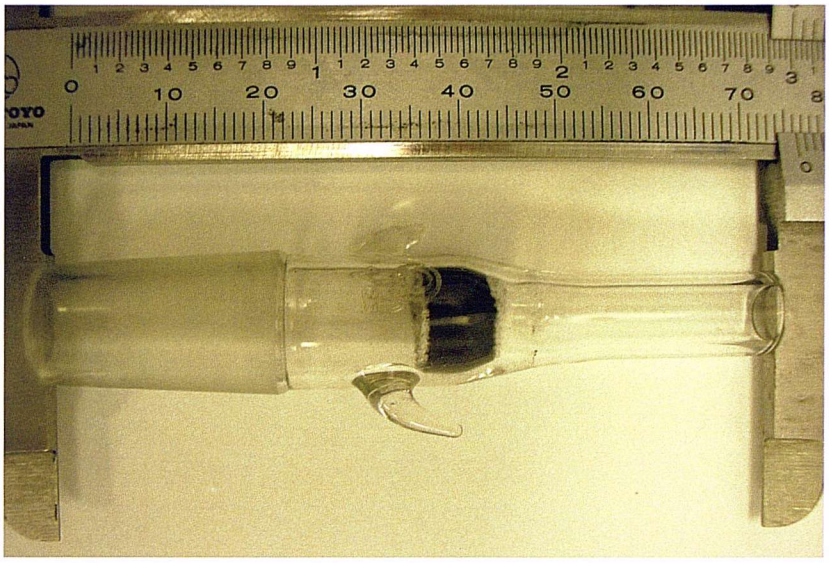


Figure 6-7 Norit Darco Hg™ based backup capture unit

During a typical experimental run, approximately 100 mg of sorbent was exposed to a simulated flue gas stream for a period of approximately 60 minutes. The above test conditions for the simulated flue gas flow, with an experimental time of 60 minutes, meant that approximately 64 ng of mercury flowed into the reactor during each test. The effect of transients that occurred during start-up, and at the end of each the test, had a minimal effect on overall experimental error given the long length of the test. Calibration of the Cavkit from PS Analytical was verified by testing the system for an hour with the external amalgamator connected directly to the simulated flue gas inlet. At the end of each calibration test, the Leco AMA 254 was used to quantify the mercury retained on the external amalgamator. The results proved that the system functioned within ± 10% of the required "set-point" for mercury concentration.

The mercury capture efficiency is deduced from the amount of mercury captured by both the sorbent and the backup capture unit. It is defined by the following formula.

$$Mercury\,capture\,efficiency = \frac{Hg\,captured\,by\,sorbent}{Total\,Hg\,to\,the\,reactor} \qquad \textbf{Equation 6-1}$$

In this particular case, "Hg captured by sorbent" is the difference between the total mass of mercury on the sorbent after the experiment less the initial mass of mercury already on the sorbent before the experiment. The "Total Hg to the reactor" is the sum of "Hg

captured by the sorbent" and the mass of mercury retained on the backup capture unit. If the external amalgamator was used, it was purged before each experimental run to eliminate any residual mercury. On the other hand, if Norit Darco Hg™ was used as the backup unit, then its initial mercury concentration was quantified by using the LECO AMA 254 analyser. The amount of mercury retained on this backup capture unit was calculated by subtracting the initial mass of mercury that may have been present in the activated carbon from the total mercury measured when the backup capture unit was analysed at the end to the experiment. The mercury mass balance for each experimental run was calculated by comparing the "Total Hg to the reactor" against the expected 64 ng of mercury that should have been present in the simulated flue gas stream.

The mercury capture efficiencies reported in Chapter 7 are from multiple tests with the fixed-bed reactor, which had a mass balance within ± 15% of the expected total mercury. More than 85% of the results reported are mean values calculated from two or more experimental runs at the same test conditions. The experiments that were repeated showed that the performance of each sorbent varied within a maximum standard deviation of 10% of the calculated mean values. Furthermore, on this basis, it was justifiable to use the other results acquired from single tests to obtain a better understanding of the performance of each sorbent.

In order to identify if the complete experimental system was suitable to evaluate the mercury capture efficiency of the sorbents, the coefficient of variability (defined by Equation 6.2) was calculated from results obtained from three different mercury adsorption tests schemes on selected sorbents. Table 6-3 has a tabulation of the results that were obtained, while the different gas schemes that were used during this study are described later in this sub-section 6.2.2. The coefficient of variability values listed in Table 6-3 show that the complete experimental system was very repeatable when a sorbent sample of ca. 100 mg was tested with gas scheme Exp. 1 and when a smaller sample mass of ca. 20 mg was tested with gas scheme Exp. 6. The performance of some sorbents was, however, very poor when they were evaluated with gas scheme Exp. 1 and with a sample mass of only ca. 20 mg (discussed later in sub-section 7.2). The outcomes from these experiments therefore have a coefficient of variability as large as 30%. These experimental results can still be used, however, since the maximum standard deviation of the results for each sorbent was only 4%. The complete experimental system can

therefore be considered to be suitable for evaluating the sorbent by using the different test conditions described in this sub-section 6.2.2.

$$Coefficient\ of\ variability = \frac{SD\ of\ experimental\ results}{Mean\ mercury\ capture\ efficiency} \qquad \textbf{Equation 6-2}$$

Table 6-3 Coefficient of variability of the results from three different experimental schemes

	Gas scheme Exp.1 with 20 mg sample	Gas scheme Exp.1 with 100 mg sample	Gas scheme Exp. 6 with 20 mg sample
Norit Darco Hg™	21%	8%	0.2%
Fly ash D	2%	1%	6%
Fly ash E	4%	2%	4%
Tyre char R1	17%	11%	0.3%
Tyre AC R1	30%	15%	0.1%
Tyre AC R2	10%	4%	0.1%

At the baseline test conditions [a gas flow of 37 mL/min (measured at NTP) with the reactor heated to 150°C], the pressure drop due to the Kaowool felt disc was approximately 30 mm of water column (1.2 inches water column). When the sorbent bed was added, this pressure drop (at the same test conditions) increased to approximately 65 mm water column (2.4 inches water column). During a full-scale sorbent injection test at a coal fired power plant in USA, the pressure drop across the bag house was found to range from 25 and 100 mm water column (2 and 4 inches water column).[77] The Kaowool felt disc can therefore be considered to cause a flow resistance similar to the fabric filter bags used in US coal-fired power plants, an important similarity in interpreting results here.

Previous studies have indicated that the presence of HCl, NO and NO_2 in the gas stream, either individually or in combination, enhance the capture of mercury.[4] Carey et al.[42] reported that the complete removal of water vapour from flue gas greatly increases the equilibrium sorption capacity of activated carbon for mercuric chloride. The sorbents in the current study were thus tested under the six different gaseous atmospheres which are listed in Table 6-4.

Table 6-4 The different gas schemes used in this study to evaluate the sorbents' mercury capture efficiencies

Gas scheme	Description
Exp. 1	A gas stream with Hg^0 vapour mixed only with N_2
Exp. 2	A gas stream with Hg^0 vapour mixed with N_2, NO and NO_2
Exp. 3	A gas stream with Hg^0 vapour mixed with N_2 and HCl
Exp. 4	A gas stream with Hg^0 vapour mixed with N_2, NO, NO_2, O_2, CO_2 and SO_2
Exp. 5	A gas stream with Hg^0 vapour mixed with N_2, NO, NO_2, O_2, CO_2, SO_2 and HCl
Exp. 6	A gas stream with Hg^0 vapour mixed with N_2, NO, NO_2, O_2, CO_2, SO_2, HCl and H_2O

The bench-scale set up for the most complete simulated flue gas scheme (i.e. Exp. 6) used in the present study is illustrated in Figure 6-8. Appendix E has the details of the combined flow meters/ flow controllers that managed the flow rates of each gas stream. The different gas cylinders that provided the constituents in the simulated flue gas streams were supplied by BOC, UK (now part of the Linde Group).

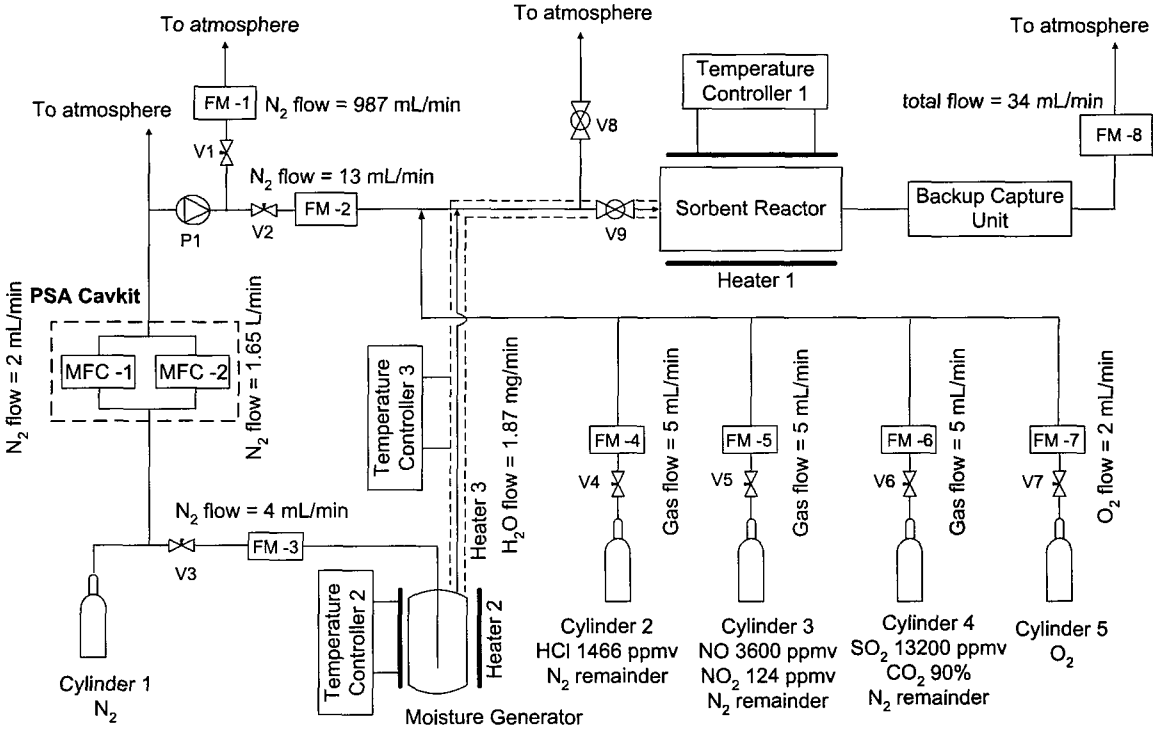


Figure 6-8 Experimental setup when the sorbents were tested with the most complete simulated flue gas stream – Exp. 6

The experimental protocol that was used to obtain information on mercury capture performance of the sorbents (incl. bromide impregnated PACs) and how this mercury may be adsorbed is illustrated in Figure 6-9. Thermal desorption and leaching tests on spent sorbents have also been included in this protocol. The next subsections in this chapter describe the individual experiments listed in Figure 6-9.

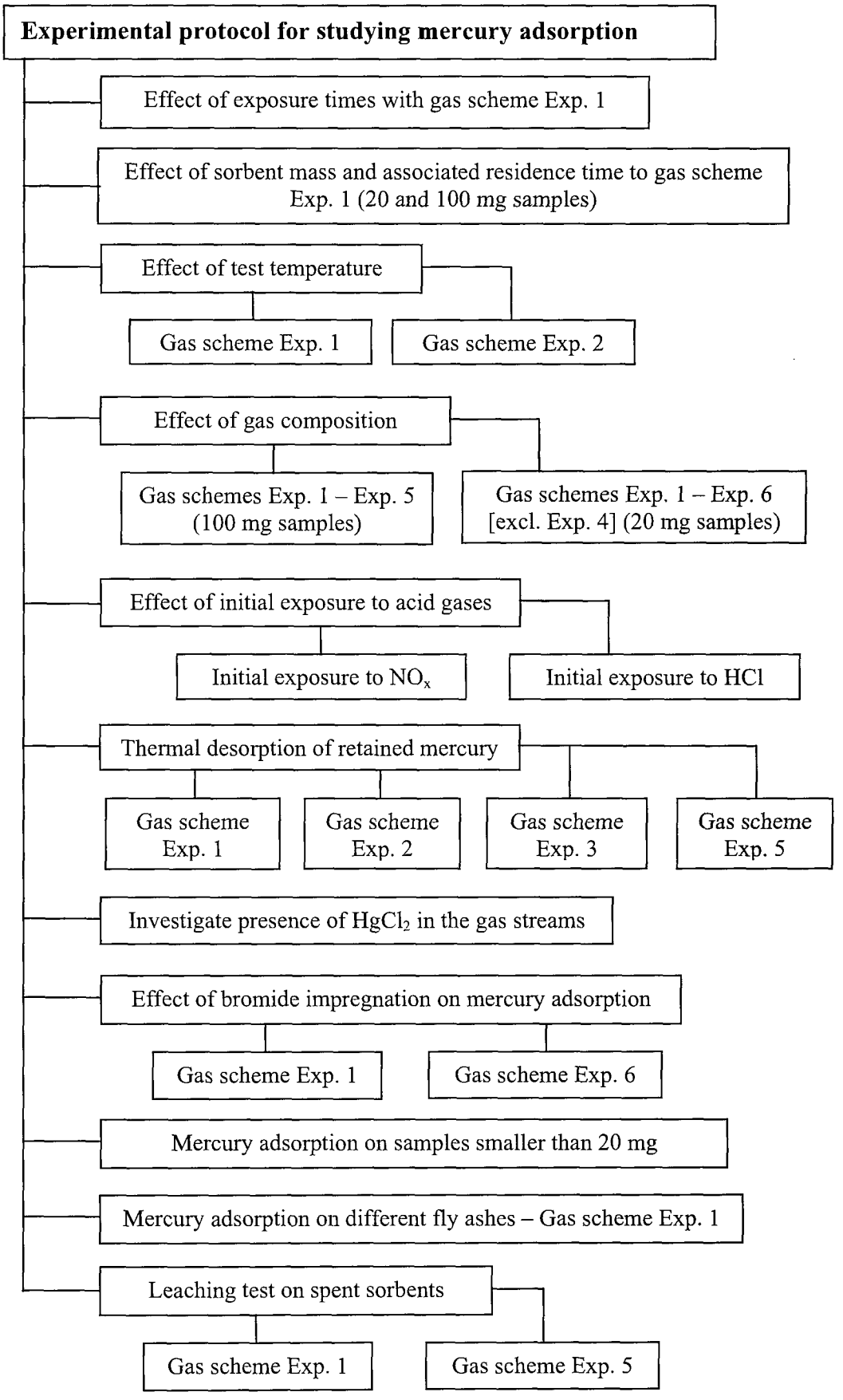


Figure 6-9 Experimental protocol used during the present study

6.2.2.1. Experimental setup used during tests with gas schemes Exp. 1 to Exp. 5

The setting for each flow controller used for gas schemes Exp. 1 to Exp. 5 are listed in Table 6-5, while Figure 6-8 illustrates which gases are controlled by each of the flow controllers. Only gas scheme Exp. 6 required all the flow controllers and gas cylinders to be connected to the reactor. When the other gas schemes were used in mercury capture experiments, the risk of gas leaks was minimised by disconnecting any gas lines that were not required.

Table 6-5 Flow controller setting used for the different gas conditions

Gas scheme	MFC-1	MFC-2	FM-1	FM-2	FM-3	FM-4	FM-5	FM-6	FM-7	FM-8
Exp. 1	1.10	2.56	470	37	-	-	-	-	-	37
Exp. 2	1.10	2.21	380	32	-	-	5	-	-	37
Exp. 3	1.10	2.21	470	32	-	5	-	-	-	37
Exp. 4	1.10	1.72	470	25	-	-	5	5	2	37
Exp. 5	1.59	2.00	470	20	-	5	5	5	2	37
Exp. 6	2.00	1.65	987	13	4	5	5	5	2	34

Note – All flow controller settings except MFC-2 are in mL/min. The flow setting for MFC-2 is in L/min

6.2.2.2. Experimental system used for tests with the most complete simulated flue gas scheme (Exp. 6).

The settings for the flow controllers which regulated the gas flows during the tests with gas scheme Exp. 6 are included in Table 6-5. Figure 6-8 and Figure 6-10 illustrates the system that was employed for these tests. The water vapour generation system that was used with this gas scheme was based on nitrogen gas bubbling though a column of heated deionised water and thereby carrying away the required quantity of water vapour. For this purpose, a borosilicate Dreschel bottle depicted in Figure 6-11 was manufactured by Cambridge Glassblowing Limited (UK) such that it allowed the input of nitrogen gas and also the measurement of the water/gas temperature. This bottle was filled with 0.9 mm diameter glass beads which introduced a tortuous route for the nitrogen gas bubbles and therefore increased the contact time between the gas bubbles and deionised water. The Dreschel bottle was heated in a similar manner as the sorbent reactor. In this case, a furnace with an electrical resistance of 5.3 Ω and a temperature controller with a 100 W

transformer were used. Appendix F has the single line diagram of the temperature controller. The required water vapour flow rate was obtained by heating the Dreschel bottle to 81°C and passing 4 mL/min of nitrogen gas through it.

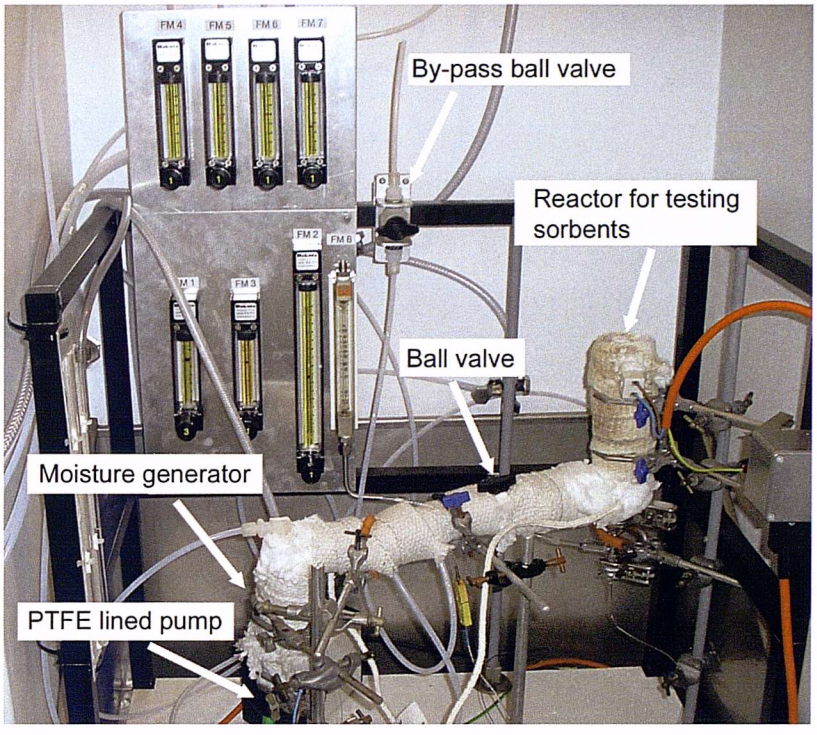


Figure 6-10 Bench-scale sorbent test system that was used with gas scheme Exp. 6

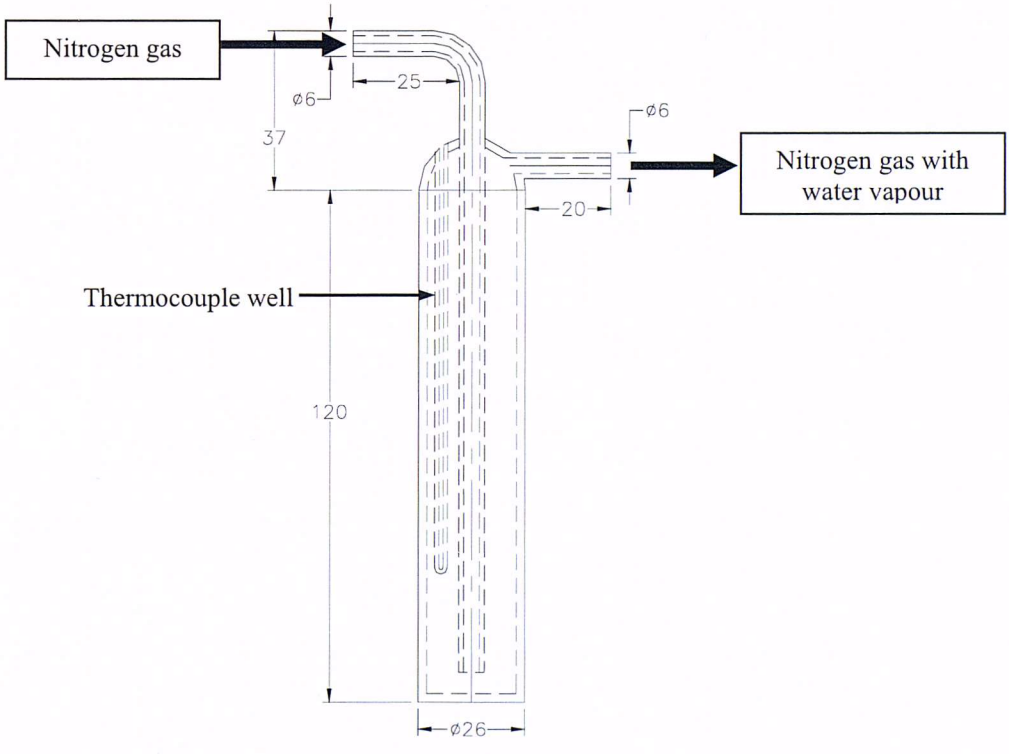


Figure 6-11 The Dreschel bottle that is used as a water vapour generator

Since the water vapour was produced at an elevated temperature, the PTFE tubing and PFA fittings though which the water vapour was transferred to the reactor were trace heated to 85°C, in order to minimise the possibility of it condensing before reaching the reactor. This heating was provided by using a 400 W, 4 ft long heating cord (Cat. No. HC503, supplied by Barnstead International/Electrothermal, Essex, UK). It was managed by a temperature controller with a 500 W, ±55 V transformer. Appendix F has a single line diagram for this temperature controller. A 2 mm thick Kaowool blanket (supplied by Warren Insulation Limited, Slough, UK) was inserted between the PTFE tubing and heating cord to ensure that there was no localised heating. The heating cord was externally insulated in the same way as the furnace for the sorbent reactor.

Until the sorbent test reactor and water vapour generator had reached their operating temperature, the PVDF ball valves V8 and V9 were used to by-pass the gas from water vapour generator and gas cylinders. After the required temperature was reached, the experiment was started and the managed gas flow entered the reactor when ball valve V9 was opened and ball valve V8 was closed.

6.2.2.3. Experimental procedure to test effect of initial exposure to NO_x or HCl

After evaluations in bench-scale tests, Pavlish et al.[29] suggested that an initial conditioning period is required for activated carbons to become effective mercury capture sorbents when exposed to simulated lignite flue gas with low chlorine content. Furthermore, tests completed during the present study indicated that when examined with gas scheme Exp. 1 some of the coal fly ashes were more effective than the un-brominated activated carbons (refer § 7.2). However, unlike the activated carbons, these coal fly ashes had been collected from coal-fired power plants where they had already been exposed to NO_x and HCl. During the present study, some selected sorbent were deliberately exposed to NO_x and HCl prior to mercury capture testing, in order to obtain more information on how mercury capture is affected by the presence of NO_x and HCl in the simulated flue gas stream. These experiments were conducted by passing either gas scheme Exp. 2 (for NO_x) or Exp. 3 (for HCl), in the absence of mercury, through a 100 mg sorbent bed for a period of 60 minutes (refer Figure 6-12). During this time, the sorbent bed was maintained at 150°C. After the initial exposure to either NOx or HCl, the

sorbent performance for mercury capture was then measured by using gas scheme, Exp. 1 with a test temperature of 150°C and a hold time of 60 minutes.

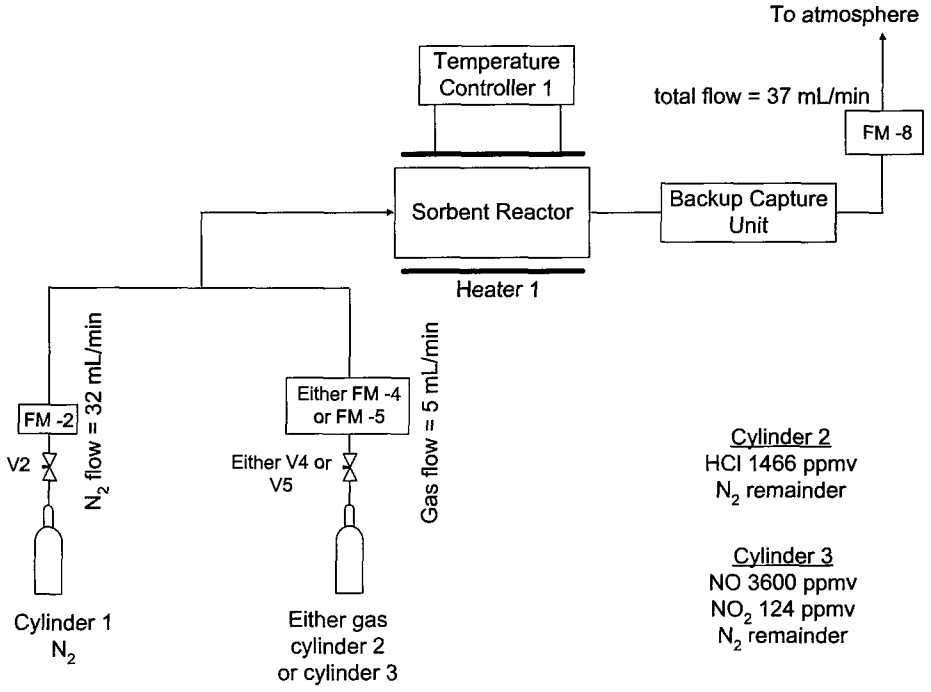


Figure 6-12 Experimental scheme to initially expose sorbents to NO_x and HCl gases.

6.2.2.4. Thermal desorption tests on spent sorbents

Li et al.[78] have investigated the thermal decomposition of model mercury compounds including $HgCl_2$, HgO, HgS and $HgSO_4$ and found that each of these compounds have a characteristic decomposition temperature and profile. During the present study, thermal decomposition tests were also completed in order to obtain more information on the mercury capture mechanism for some selected sorbents. The decomposition tests were done by first exposing 20 mg of sorbent to mercury in gas scheme Exp.1, Exp. 2, Exp. 3 or Exp. 5 for one hour at 150°C. The spent samples were later heated to 200°C at 5°C/min and held at this temperature for 60 minutes. A nitrogen sweep gas flow of 37 mL/min (measured at NTP) ensured that any mercury and other compounds released from the sorbent were removed from the reactor. Figure 6-13 illustrates the system that was used during the thermal decomposition stage of the tests.

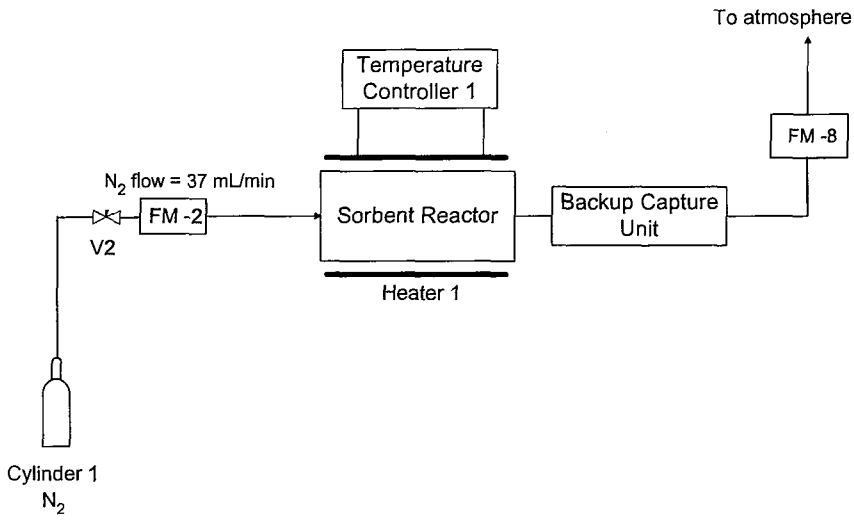


Figure 6-13 The experimental set-up used for the thermal decomposition test.

6.2.2.5. Test to determine if $HgCl_2$ is preset in the simulated flue gas streams

When compared to elemental mercury, oxidised mercury is less volatile and more chemically reactive.[28] Thus Hg^{2+} is more effectively captured in conventional APCDs.[28, 39] Bench-scale tests completed during the present study have also included HCl in the simulated flue gas stream. Mercury in the gas stream could have reacted with the HCl to form mercury chloride and this may have contributed to the sorbent effectiveness values reported in section 7.4. Thermodynamic equilibrium modelling completed during the present study indicated that if given adequate time at a temperature of 150°C, $HgCl_2$ would be the dominant mercury species in a gas stream simulating flue gases from the combustion of Harworth coal (refer § 3.2.2). From the time the simulated flue gas enters the reactor, it takes ca. 25 seconds for it to reach the sorbent bed. During this time, the gas is heated to the test temperature and this may favour gas phase reactions of mercury with other species in the gas stream. The present study therefore attempted to obtain information on the mercury chloride fraction present in gas schemes Exp. 3, Exp. 5 and Exp. 6 before these gases passed through the sorbent bed. This was done by using an anion resin from Dow Chemical Comp, USA called Dowex 1X8® (supplied by Fisher Scientific Limited, Leicestershire, UK).

Dowex 1X8® is a strongly basic anion resin and it has been used extensively in research to differentiate between mercuric chloride and elemental mercury.[79-81] This resin, with a

quaternary ammonium group as the fixed ion, is thermally stable up to a temperature of 150°C.[81] If used in its dried, non-conditioned form, adsorption rates of between 85 – 95% have been observed. However, Metzger and Braun[81] found that if the resin was subjected to hydrochloric acid conditioning treatment it had adsorption rates in excess of 98%. The treatment involves exposure to 5 M hydrochloric acid at a temperature of 90°C, followed by 14 hours drying at 130°C. The mercuric chloride reacts with the chloride in the resin by complexing to $[HgCl_3]^-$ or $[HgCl_4]_2^-$ and adsorption as an anion, according to the following formula[80]:

$$R-N^+(CH_3)_3Cl^- + HgCl_2 \rightarrow R-N^+(CH_3)_3HgCl_3^- \qquad \textbf{Equation 6-3}$$

Hocquel et al.[80] found that this resin does not react with other mercury species such as mercury oxide, mercury sulphide, mercurous chloride (Hg_2Cl_2) and metallic mercury.

The Dowex® 1X8 resin used in the present study was conditioned by using the hydrochloric acid treatment described by Metzger and Braun.[81] In order to obtain information on the concentration of mercurous chloride in the simulated flue gas stream, ca. 100 mg of the conditioned Dowex® 1X8 resin was placed on the Kaowool felt disc in the sorbent test reactor and exposed to the same experimental conditions as the sorbents. The resin was therefore heated to 150°C and either gas scheme Exp. 1, Exp. 3 or Exp. 5 was passed though the sample for 60 minutes. Any mercury that was not retained by the resin was captured on an activated carbon based backup unit (refer § 6.2.2). The mercury on the spent resin was quantified by first thermally decomposing the resin, using the same scheme that was employed for the thermal desorption tests on spent sorbents (refer § 6.2.2.4). Since Metzger and Braun[81] had indicated that Dowex® 1X8 was thermally stable up to 150°C, heating the resin to 300°C and keeping it at this temperature for one hour would have removed any mercury captured by the sample. Mercury released from the sample was collected by another activated carbon backup capture unit. The conditioned Dowex® 1X8 resin contained chlorine which may have been released when the sample was heated to 300°C. Some of this could have been retained on the activated carbon backup capture unit. Since the LECO AMA 254 was not suitable for evaluating samples with high halogen contents, the activated carbons which captured the mercury released from the Dowex® 1X8 resins were analysed using the PSA 10.025 Millennium

Merlin System at PS Analytical in Orpington, Kent, UK. These samples were thus analysed by following the procedure used to quantify mercury captured on the brominated sorbents (refer §6.1.2).

6.2.3. Leachability of mercury captured by the sorbents

If the sorbents examined in this study were to be used in a coal-fired power plant, they would most probably be collected along with the fly ash in the particulate control system. Currently the fly ash from coal-fired power plants is either sold for construction usage or disposed to landfills.[15, 16] Either way, the spent sorbent would be exposed to rain water over a long time-scale. It is known that Hg^0 is not soluble in water, whereas Hg^{2+} in ash is soluble.[18] The leachability of mercury captured by the test sorbents of the current project has been studied in order to ascertain the stability of the retained mercury.

The US-EPA toxicity characteristic leaching procedure (TCLP)[82] is often used to test the leachability of toxic elements in landfill.[17] This method is designed to simulate leaching in an unlined, sanitary landfill, based on a co-disposal scenario of 95% municipal waste and 5% industrial waste.[17] The tests have been conducted on 20 mg sorbent samples, after they had been exposed to either gas scheme Exp. 1 or Exp. 5. The contaminated sorbents have then been subjected to a modified form of a standard TCLP leaching method.[52] This micro-leaching scheme, which has been specifically adapted for smaller samples, was found to be accurate for masses in the 100 mg range.[52] The leaching tests completed during the present study were with sample masses of ca. 50 mg (sorbent mass of 20 mg and 30 mg of Kaowool support). As mentioned in the TCLP method, a solid to liquid ratio of 1:20 was used by adding 1 mL of 1M Aristar® grade glacial acetic acid (diluted with deionised water until the pH of the mixture was 2.88 ± 0.05) to a 50 mL conical PTFE container holding the solid sample. These vessels were then agitated for 18 hours. After this period of time, 4 mL of 10% dilute Aristar® grade nitric acid was added in order to have adequate liquid solution which could be separated from the solids. The samples were then centrifuged and later filtered using Whatman® No1 filter paper (Grade 1, Cat. No. 1001 110). Since the mercury concentration on the leachate was below the detection limit of the Leco AMA 254 analyser, the 5 mL leachate samples were analysed using the PSA 10.025 Millennium Merlin System at PS Analytical in Orpington, Kent, UK.[69] In this case, the mercury which needed to be quantified was already in

solution; Aqua Regia digestion was thus not necessary. The same analysis method described in sub-section 6.1.2.5 was also used to quantify the mercury in leachate samples, as it had already proved to give consistent results. Consequently 10% Aqua Regia solution was added to the 5 mL leachate samples until a 50 mL mixture was obtained. These leachates had very low mercury concentrations, therefore a more representative set of calibration standards were prepared in 10% Aqua Regia solution; these are listed below;

- 0 ppb Hg in 10 % Aqua Regia solution (used only the 10% Aqua Regia reagent)
- 0.05 ppb Hg in 10% Aqua Regia solution
- 0.10 ppb Hg in 10% Aqua Regia Solution
- 0.15 ppb Hg in 10% Aqua Regia solution
- 0.20 ppb Hg in 10% Aqua Regia solution

The results that were obtained for the different mercury sorption and leaching tests described in this Chapter 6 titled "Experimental procedures" are discussed in the next chapter – Chapter 7 titled "Mercury capture tests –Results and discussion".

7. Mercury capture tests – Results and discussion

This chapter discusses the results obtained when the sorbents were evaluated for their capability to capture mercury under different experimental schemes. Each of the schemes that were used has been described in the previous sub-section 6.2. Also included in Chapter 7 are the results that were obtained from the leaching tests done to study the stability of the mercury adsorbed on to the sorbents.

7.1. Mercury adsorption on selected sorbents in relation to different exposure times

Mercury capture efficiencies for 100 mg of Norit Darco Hg™, tyre char R1 and tyre AC R1 examined at different hold times while exposed to a gas stream of mercury vapour and pure nitrogen gas (gas scheme Exp. 1) at 150°C, are shown in Figure 7-1. The results for Norit Darco Hg™ and tyre char R1 suggest that they were more effective during the initial 30 to 45 minutes of exposure to the gas stream, after which the efficiency gradually decreased and stabilised at mercury capture efficiencies of 30- 45%. There may therefore have been a limited number of sites in these two sorbents which retain mercury more effectively and these were spent when the duration of the tests were more than 45 minutes. Since there was a considerable scatter in the results for tyre AC R1, it was not possible to determine if this sorbent was also more efficient at shorter hold times. Nevertheless the observation that the performance of all three sorbents had stabilised during the longer exposure experiments indicates that they had active sites which were capable of retaining mercury and that these sites were not fully exhausted, even after exceeding 120 minutes of exposure to the gas stream. This could be due to the fact that even after experiments which ran for 180 minutes, the total amount of mercury that entered the reactor was only 193 ng. Consequently, mercury loadings on the sorbents varied between approximately 1.0 and 0.5 ng/mg of sorbent, with the tyre AC R1 having the largest loading. After exposing Norit Darco Hg™ to the simulated flue gas for 180 minutes, the mercury loading was ca. 0.5 ng/mg of sample. This mercury loading is clearly negligible compared to the 2460 – 2590 ng/mg maximum capacity reported in literature.[4] The results from varying exposure time suggests that the mercury capture

performance of these three sorbents when examined with mercury vapour in a stream of pure nitrogen gas and a hold time of 60 minutes was not limited by their maximum capacity for element mercury.

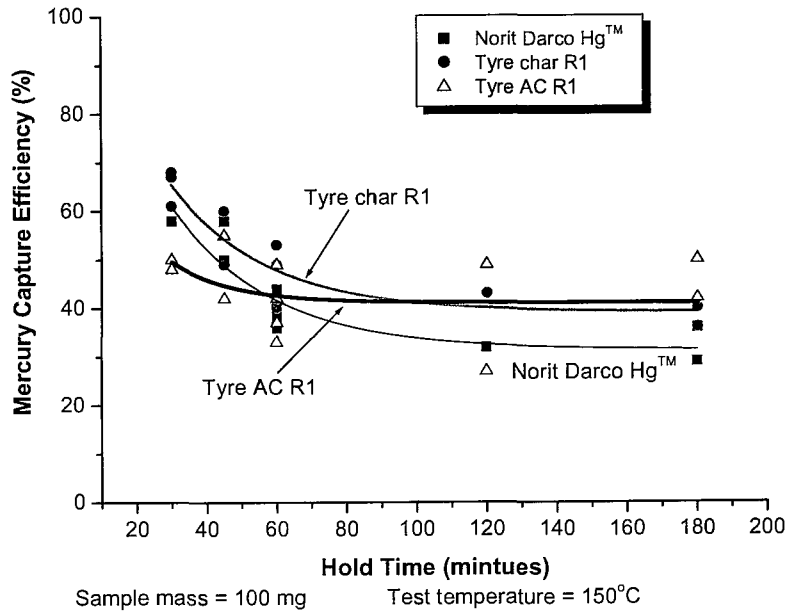


Figure 7-1 Mercury capture efficiencies at different hold times with a gas stream of only mercury vapour and nitrogen gas

7.2. Effect of varying the sorbent mass and the associated change in residence time

The effect of changing the residence time, i.e. the total time the gas stream was in contact with the sorbents, was evaluated during this study. This was accomplished by using two different sample masses. Mercury capture efficiencies of some selected sorbents examined with sample mass of 20 mg and 100 mg are shown in Figure 7-2. The design of the sorbent test reactor was such that the sorbent bed height was proportional to its sample mass. Consequently reducing the sample mass by a factor of five times caused a similar reduction in the residence time of the gas stream within the sorbent bed. Furthermore, as a gas stream of mercury vapour in pure nitrogen was used for the test, the results indicate each sorbent's effectiveness for capturing elemental mercury.

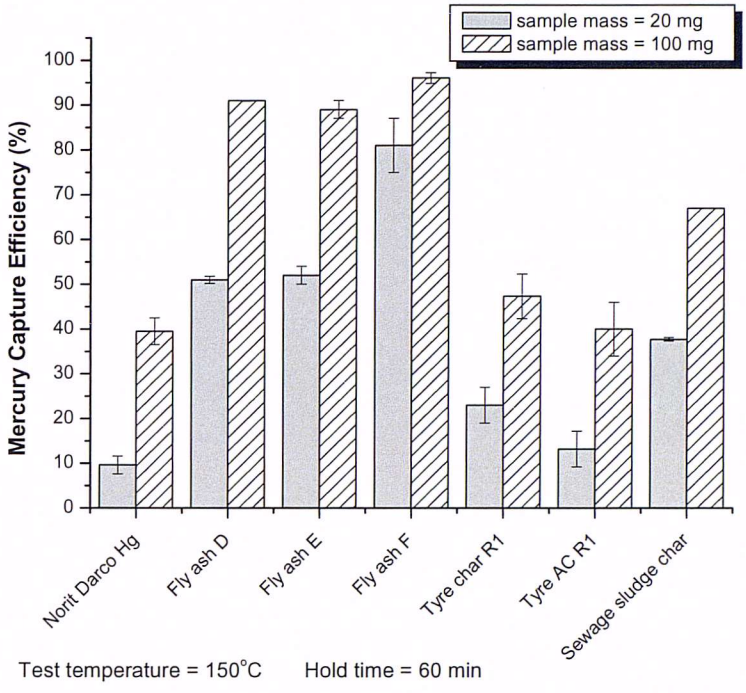


Figure 7-2 Mercury capture efficiencies when sorbent mass of 20 and 100 mg were used on tests with a gas scheme of only mercury vapour and nitrogen gas.

It was observed that the relative ranking of sorbent effectiveness did not change when the sample mass was reduced. The two coal fly ashes (fly ash D – F) were found to be the most efficient in both cases. However, except for fly ash F, the sorbent performance decreased significantly when the sample mass was lowered to 20 mg. In each tests, only about 64 ng of mercury entered the reactor, therefore at the end of each experiment the final mercury loading on the 20 mg sorbent samples were still considerably less than the maximum capacity of Norit Darco Hg mentioned in section 7.1. When the sample mass was reduced, the two fly ash D and E, and tyre char R1 captured 1.9 times and 2.2 times less mercury respectively. The sewage sludge char also showed a comparable reduction in its mercury capture efficiency ca. 1.8 times less. On the other hand the performance of Norit Darco Hg™ and tyre AC R1 reduced by similar ratios of about 3.5 times. When compared to the tyre pyrolysis charcoal and the coal fly ashes, the reduction in the mercury capture efficiency with the two activated carbons was closer to the reduction in the time during which the gas stream was in contact with the sorbent bed. This indicates the time during which the mercury vapour was in contact with the activated carbons had a more significant effect on the adsorption of elemental mercury. Furthermore these two activated carbons had similar efficiencies for capturing mercury. Thus the process by

which elemental mercury is adsorbed on the two activated carbons is comparable and may be different from the mercury capture mechanism on the fly ashes and charcoal from the pyrolysis of scrap tyre rubber and sewage sludge.

7.3. Effect of test temperature on sorbent performance

During the present study, tests have been completed at different temperatures to evaluate the effect of temperature on the performance of some selected sorbents. The dependency of sorbent performance on test temperature, when exposed to mercury vapour in pure nitrogen (i.e. gas scheme Exp. 1), is presented in Figure 7-3. A sorbent sample mass of 100 mg and an experimental time of 60 minutes was used for the test. The gas scheme Exp.1 indicates the sorbent performance for capturing elemental mercury since no oxidising species are present in the gas stream. At test temperatures above 150°C, fly ash samples D and F were found to be significantly superior to the other sorbents that were evaluated in this particular part of the study. It was also established that the sorbent's effectiveness for elemental mercury capture decreased with increasing test temperature for every sorbent tested. According to Rao and Leja[83] gas adsorption involves the loss of at least one degree of freedom for the adsorbing species. Since the adsorbing specie's entropy is decreased, the process of physical adsorption is always exothermic.[83] Furthermore, many previous studies have also shown that elemental mercury sorption on to activated carbon decreased with increasing temperature.[40, 84] These studies have therefore suggested that the adsorption process for mercury on activated carbon surfaces is exothermic, indicating that it is a typical physical adsorption mechanism.[40, 84] The results obtained from the present study also suggests that physical adsorption may be an initial step by which the different sorbents capture mercury when tested with a gas stream of mercury vapour mixed with pure nitrogen.

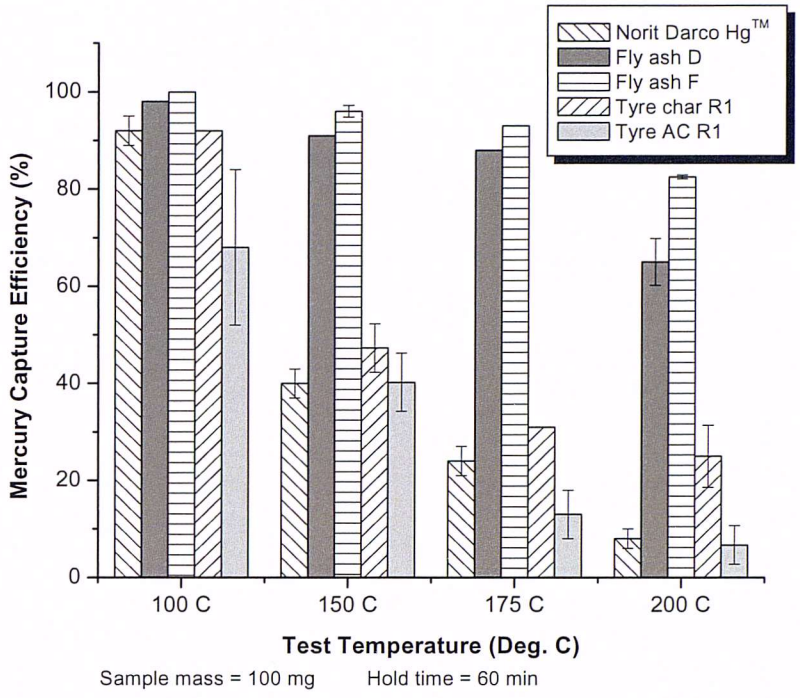


Figure 7-3 Mercury capture efficiencies at different test temperatures with a gas scheme of only mercury vapour and nitrogen gas (Exp. 1)

The effect of test temperature when NO and NO_2 was included in the gas stream is presented in Figure 7-4. The addition of NO_x seemed to significantly improve the performance of the activated carbons and the charcoal from pyrolysis of scrap tyre rubber. Dunham et al.[34] and Olson et al.[85] have suggested that Hg^0 may be catalytically oxidised on the surface of the sorbent in the presence of NO_2. Although there was only a marginal reduction in sorbent performance with increasing temperature, when tested with gas scheme Exp. 2, the results suggests that physical sorption may be an initial step in the mercury capture. Pavlish et al.[4] have also suggested an initial physical adsorption mechanism with mercury being finally bound to the sorbent by chemisorption.

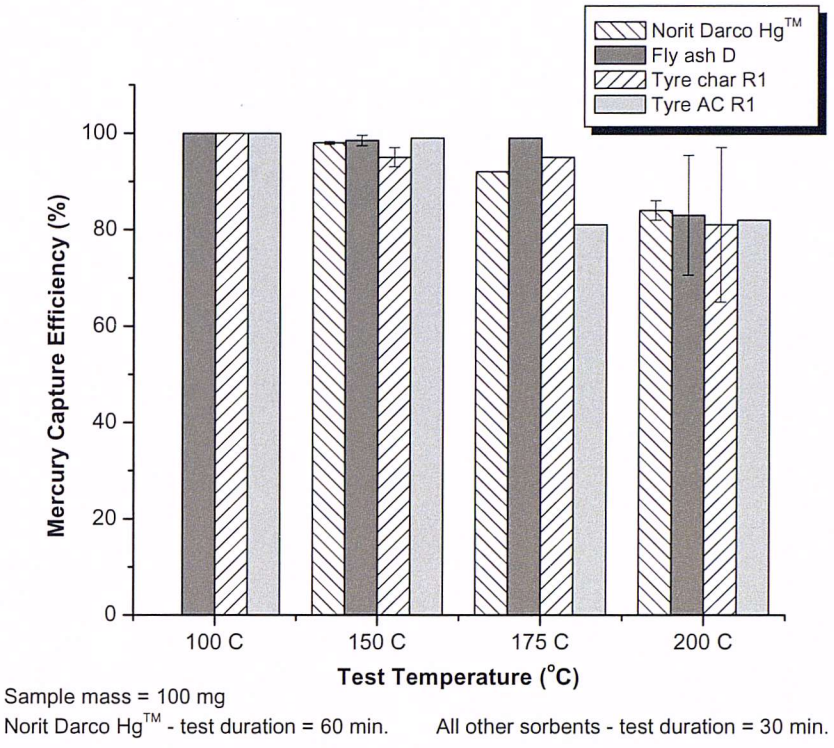


Figure 7-4 Mercury capture efficiencies at different test temperatures with gas stream of mercury vapour, nitrogen, nitrogen oxide and nitrogen dioxide gas (Exp. 2).

7.4. Effect of gas composition

Flue gas produced from the combustion of coals, including UK Harworth coal, usually contain HCl, NO and NO_2. Since previous studies have found that these constituents affect mercury capture on activated carbons,[4] some selected sorbents were evaluated in the present study using different gas compositions to identify the effect of flue gas constituents on mercury capture, for each sorbent. The initial experiments were completed with a sorbent sample mass of 100 mg. However, in order to accentuate the difference between sorbents more clearly, subsequent tests were conducted with a smaller sample mass of 20 mg.

7.4.1. Tests with a sample mass of 100 mg

Mercury capture efficiencies for four sorbents (100 mg sample mass) when exposed to five different gas mixtures, at a test temperature of 150°C and a hold time of 60 minutes

are shown in Figure 7-5. When exposed to a mercury vapour stream diluted in pure nitrogen, the efficiency of Norit Darco Hg™ and the sorbents from scrap tyre rubber was between ca. 40-50%. However, when the gas stream included NO and NO_2, the performance of these sorbents improved, with mercury retention in excess of 95%. Fly ash D captured practically all the mercury during this latter gas scheme and retained about 90% of mercury even under the conditions of Exp. 1.

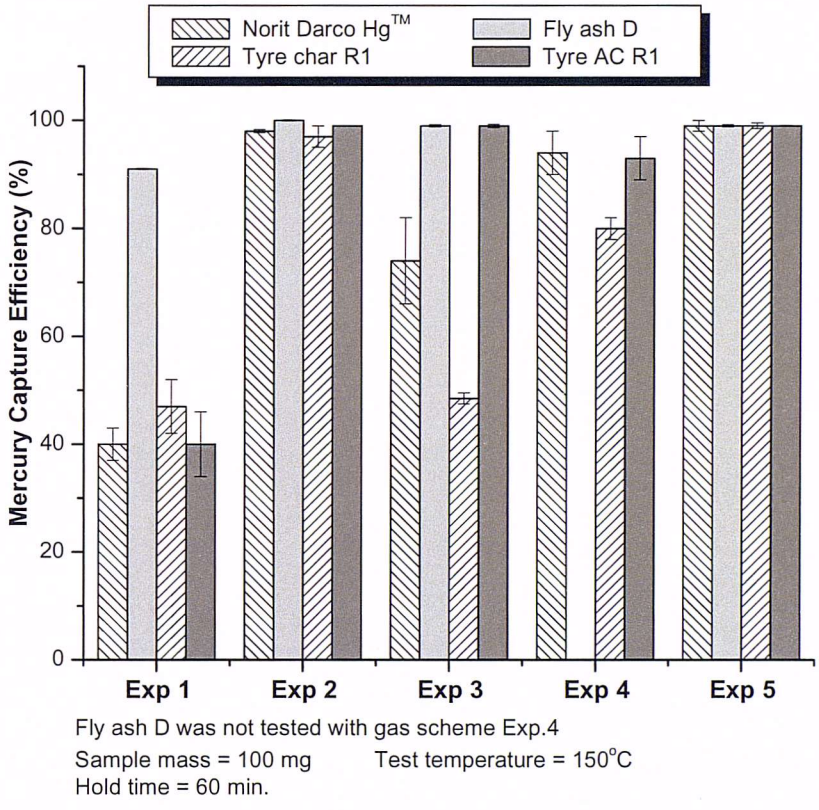


Figure 7-5 Mercury capture efficiencies of the sorbents when tested with gas schemes Exp. 1 to Exp. 5

As mentioned previously in sub-section 7.3 the improvement in sorbent performance when the gas scheme included NO_x could be due to the mercury capture method proposed by Dunham et al.[34] and Olson et al.[85] They suggested that in the presence of NO_2, elemental mercury is catalytically oxidised on the surface of the sorbent (refer § 2.2.2.2).

The introduction of chlorine into the gas stream (gas scheme Exp.3) improved the effectiveness of the activated carbons (Norit Darco Hg™ and PAC produced from steam activation of scrap tyre rubber) and fly ash D. The PAC from scrap tyre rubber and fly ash D had mercury capture efficiencies of ca. 99%. However the presence of HCl had no effect on the performance of tyre char R1 samples. These results suggest that Norit Darco Hg™ and PAC produced from steam activation of scrap tyre rubber are more capable of retaining mercury when the gas stream also includes HCl.

Miller et al.[41] found during mercury break-through tests the interaction between SO_2 and NO_2 impaired the capture of elemental mercury. SO_2 may react with the catalytic sites that would otherwise have aided the retention of mecury.[4] A similar outcome was therefore expected when the gas mix in Exp. 4 was used, as it contained a substantial concentration of SO_2. Tests with this gas scheme showed that the performance of tyre char R1 reduced by ca. 15% when compared to the results with gas scheme Exp. 2. However, only a marginal reduction was observed for the two activated carbons Norit Darco Hg™ and tyre AC R1. The observed high efficiency for the activated carbons may be because the current research investigated the capture efficiency for the activated carbons, rather than the break-through capacity of the sorbents. During each test only a limited amount of mercury entered the reactor, even with a hold time of 60 minutes. Thus only a relatively few sites were needed to retain all the mercury thus leaving others available to react with the SO_2.

When the more complete simulated flue gas mix, Exp. 5 was used, the sorbents retained almost all the mercury that entered the reactor. Compared to the results observed for Exp. 4, the inclusion of HCl in the gas stream may have caused the observed rise in the performance of the activated carbons for the tests with Exp. 5. The addition of HCl to the gas scheme consisting of N_2 and Hg^0 had shown no improvement in the performance of the tyre char R1 sample. However, this sorbent had a marked increase in its effectiveness when the gas scheme changed from Exp. 4 to Exp.5. The results therefore suggest that while HCl alone may not improve the effectiveness of tyre char R1, a combination of HCl with NO_x and SO_2 caused significant improvement to the mercury capture efficiency of this sorbent.

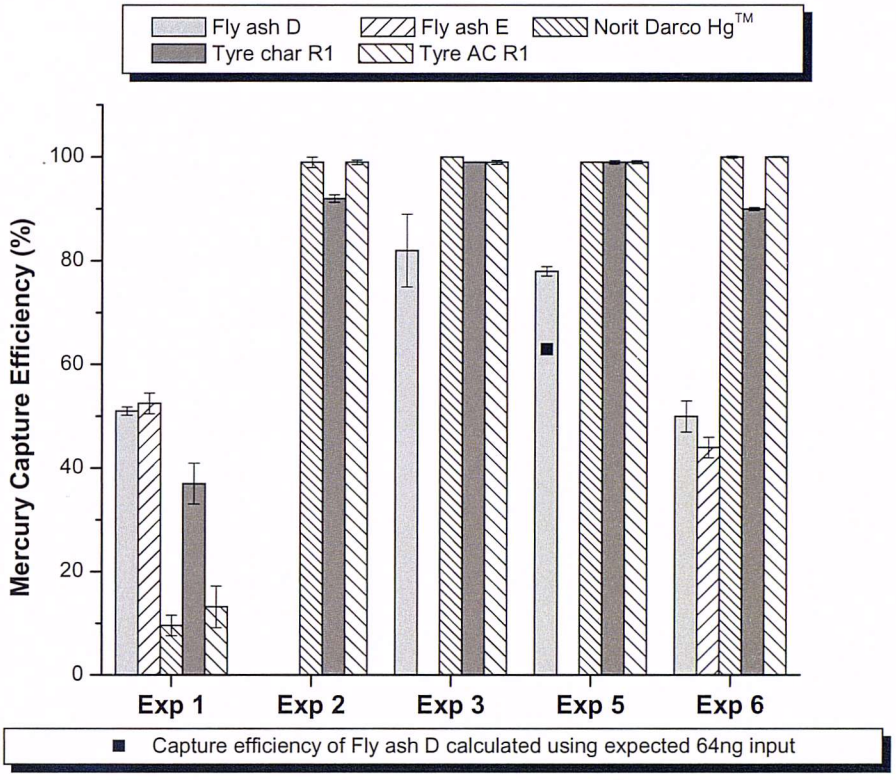
7.4.2. Tests with a sample mass of 20 mg

In order to observe the effect of the different gas compositions in greater detail, the sample mass of each sorbent was reduced from 100 mg to 20 mg. The effect of gas schemes Exp. 1, 2, 3, 5 and 6 on some selected sorbents is presented in Figure 7-6.

As with the 100 mg samples (refer § 7.4.1), tests with the smaller 20 mg sorbent bed showed that introduction of NO_x and HCl considerably improved the efficiency of Norit Darco Hg™ and the sorbents made from scrap tyre rubber. Consequently, even though the sample mass was only 20 mg, these sorbents were ca. 100% effective in capturing mercury. No significant reduction in mercury capture was observed when SO_2, and later water vapour, was also added to the simulated flue gas stream.

The introduction of HCl in gas scheme Exp. 3 seemed to improve the performance of fly ash D, although some of the mercury was still able to pass through the sample. Poor mercury mass balances were obtained when the fly ash samples were initial evaluated with gas scheme Exp. 6 which included water vapour. The water vapour that passed through the sorbent bed had condensed at the lower end of the reactor where the temperature was more moderate and close to ambient temperature. The condensed water vapour was collected with cotton buds and its mercury content was quantified by using the LECO AMA 254 mercury analyser. The mercury that was needed to complete the mass balance (ca. 24 – 34 ng) was found to be present in this condensed water vapour. The results therefore showed that when fly ashes D and E were tested a significant proportion of the 64 ng of mercury that entered the reactor had passed through the sorbent bed and condensed with the water vapour. Since only oxidised mercury is readily soluble in water,[19, 56, 81] the fact that mercury was found in the condensed water vapour suggests that the fly ash samples were not capable of adsorbing all the oxidised mercury in the gas stream used in this experiment. Lee et al.[67] noted that if NO_x is present in the gas stream, Al_2O_3 and SiO_2 in coal fly ash promote the oxidation of Hg^0. They suggested that the heterogeneous reaction of Hg^0 and NO_x may produce mercury nitrate monohydrate [$Hg(NO_3)_2 \cdot H_2O$].[67] This mercury compound is known to be adequately volatile and stable to exist in the gas phase under flue gas cleaning conditions. Since fly ash D and E contained Al_2O_3 and SiO_2 (refer § 5.3 and § 5.4), NO_x in gas scheme Exp. 6 could have reacted with mercury in the simulated flue gas to form mercury nitrate monohydrate. This

volatile oxidised mercury species could have then passed though the sorbent bed and as the temperature reduced, it may have condensed on the reactor's inner walls.



Fly ash D was not tested with gas scheme Exp. 2
Fly ash E was not tested with gas scheme Exp. 2, 3 & 5
Sample mass = 20 mg Test temperaure = 150°C
Hold time = 60 min.

Figure 7-6 Mercury capture efficiencies for the sorbents when tested with different gas schemes

Tests on fly ash D with gas scheme Exp. 5 also found that after passage through the sorbent bed some of the mercury condensed at the lower end of the reactor, which was cooler. Compared to the fly ash D results from the gas scheme Exp. 6 experiments, where this sorbent was only 50% effective, the tests with gas scheme Exp. 5 showed that this ash's mercury capture efficiency was as high as 78% for the latter gas scheme. However after each test, collecting all the mercury which had deposited on the walls of the lower part of the reactor during the experiments with gas scheme Exp. 5 proved difficult. It was not possible to account for 18% of the mercury that should have entered the reactor. Consequently, if empirical results from tests with reduced mercury mass balances are

used, the adoption of the definition of mercury capture efficiency used so far in this study (refer Equation 1, § 6.2.2) over estimates the sorbent performance. A "corrected" effectiveness of fly ash D, based on the amount of mercury that would have entered the reactor during the experiments with gas scheme Exp. 5, is also presented in Figure 7-6. If the mercury mass balance was accurate, then the outcome for the tests with this gas scheme should have been closer to gas scheme Exp. 6. However, as there would still be a 13% drop in the performance of fly ash D when water vapour is introduced it indicates that the presence of water vapour limits the effectiveness of this fly ash. Furthermore the "corrected" mercury capture efficiency for fly ash D suggests that, when compared to gas scheme Exp. 3, the fly ash D would be less efficient when tested with gas scheme Exp. 5. This could be due to the introduction of SO_2 which may be consuming the sites in the fly ash that would otherwise have captured mercury.

These tests thus illustrate that although the fly ash was able to oxidise the mercury, the 20 mg sample was unable to capture it all. This could be because the smaller mass of fly ash may have only a very limited number of sites capable of capturing oxidised mercury or due to the formation of a volatile form of oxidised mercury that avoids capture. The presence of SO_2 and water vapour in the gas stream may have used up some of these sites. Other studies have also found that while many fly ashes could oxidize elemental mercury, not all of them are able to capture the mercury.[47]

7.5. Effect of initial exposure to NO_x and HCl

Some selected sorbents which did not have bromide impregnation (Norit Darco Hg™, tyre char R1 and tyre AC R1) were initially exposed to NO_x and HCl in order to obtain more information on how mercury capture is affected by the presence of these species in the simulated flue gas stream. These experiments were conducted by passing either gas scheme Exp. 2 (for NO_x) or Exp. 3 (for HCl), but without any mercury present, through a 100 mg sorbent bed for a period of 60 minutes (refer § 6.2.2.3). During this time, the sorbent bed was maintained at 150°C. After the initial exposure to either NO_x or HCl, the sorbent performance was then measured using gas scheme Exp. 1, with a test temperature of 150°C and a hold time of 60 minutes. The results obtained for initial exposure to NO_x

are illustrated in Figure 7-7 while Figure 7-8 presents the outcomes from initial exposure to HCl. The empirical results from tests with gas scheme Exp. 1, Exp. 2 or Exp. 3 on sorbents with no pre-treatment have also been included in these figures. Direct comparison can therefore be made on the effect of initial exposure to NO_x or HCl.

Initial contact with NO_x does seem to improve the performance of all three sorbents significantly, with Norit Darco Hg™ capturing almost all the mercury that entered the reactor. The results thus suggest that mercury can be effectively captured by interactions with NO_x retained on the sorbents. The sorbents made from scrap tyre rubber had a mercury capture efficiency approaching ca. 80% when initially exposed to NO_x, however these sorbents captured almost all the mercury when tested with gas scheme Exp.2. The results illustrate that although there was a significant interaction between mercury and NO_x retained on the sorbent surface, there may also have been some gas phase interaction between mercury and NO_x during these experiments.

The initial exposure of sorbents to HCl was found to improve sorbent performance to varying degrees. When tested with gas scheme Exp. 1, the two activated carbons were ca.100% effective, while the charcoal from the pyrolysis of scrap tyre rubber was able to capture ca.70% of the mercury. Bench-scale fixed-bed test results reported in literature also indicated than the Hg^0 adsorption efficiency of carbon-based sorbents improved when they were initially conditioned by HCl in the simulated flue gas.[86] The results obtained during the present study further suggest that the tyre char R1 samples may have less active sites available for holding HCl. This may be the reason why tyre char R1 was less effective than the two activated carbons when they were studied using gas scheme Exp. 3.

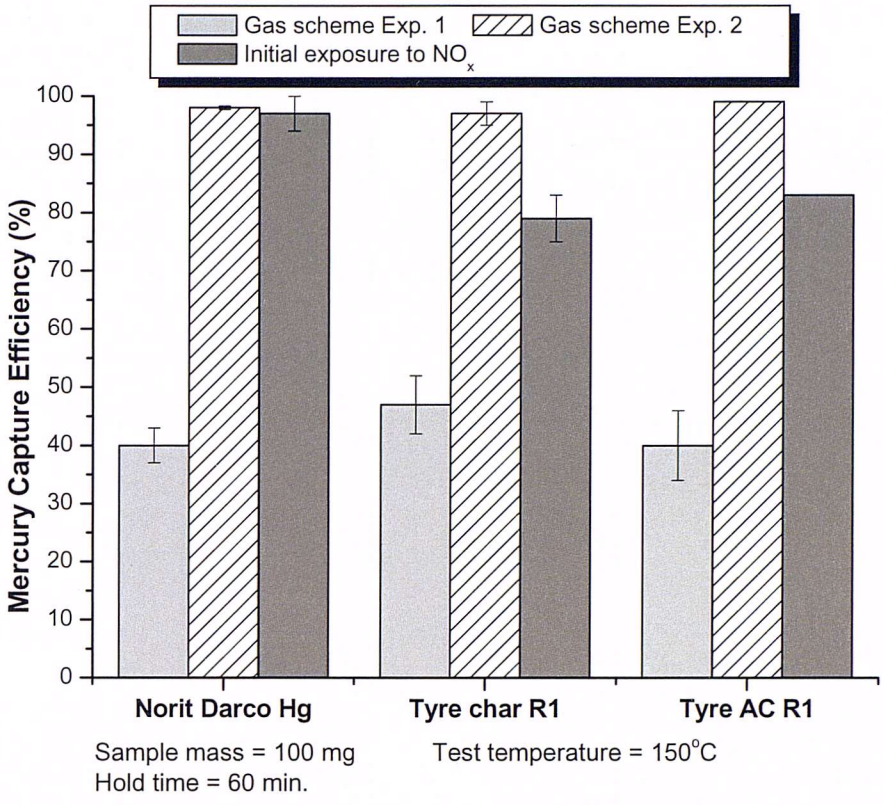


Figure 7-7 Comparing sorbent performance after initially being exposed to a gas stream with NO and NO_2.

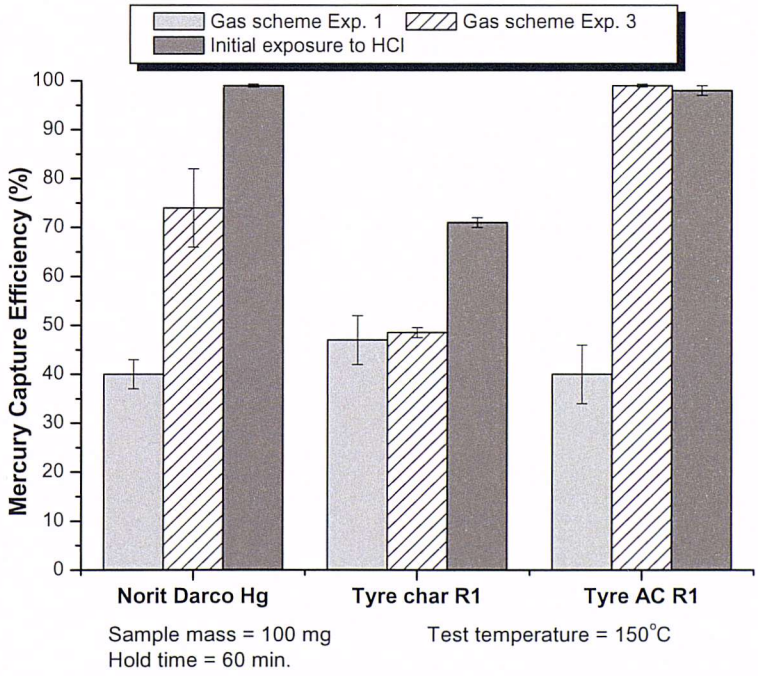


Figure 7-8 Comparing sorbent performance after initially being exposed to a gas stream with HCl.

The fact that initial exposure to either NO_x or HCl improved the effectiveness of both Norit Darco Hg™, and sorbents made from scrap tyre rubber, also explains why the coal fly ash samples, D and F, were very effective in capturing mercury when tested with gas scheme Exp. 1. These two ashes have already been in contact with the NO_2 and HCl in the coal-fired power plant flue gases from which they were recovered. Furthermore, the fly ashes D and F have high loss on ignition (LOI) values. LOI is a commonly used indicator for the carbon content in the fly ash and is a key parameter for mercury capture on fly ash.[33] Some of the NO_2 and HCl in the flue gas could have been adsorbed on the carbon in the fly ash particles and consequently contributed to the observed high mercury capture efficiencies of fly ashes D and F. Other studies have also shown that NO_2 and HCl improve mercury capture on coal fly ash collected from power plants.[32, 87]

7.6. Desorption of retained mercury

There are two principal forces involved with the interaction between gases and carbon surfaces: physical forces (primarily Van der Waals dispersion forces), and chemical forces (or "chemisorption") consisting of chemical bonds.[11] During the present study, desorption tests have been conducted in order to obtain more information on the mercury capture mechanism for some selected sorbents. The desorption tests were done using Norit Darco Hg™, tyre char R2 and tyre AC R1 samples that had first been exposed to mercury in either gas scheme Exp. 1, Exp. 2, Exp 3 or Exp. 5 for one hour at 150°C (refer § 6.2.2.4). During the desorption test, the sample was heated to 200°C at 5°C/min and held at this temperature for one hour. A nitrogen sweep gas flow of 37 mL/min (measured at NTP) ensured that any mercury, and other compounds, released from the sorbent were removed from the reactor. The results obtained are illustrated in Figure 7-9. Also included in this figure is the amount of mercury that was captured by each sorbent when exposed to the different gas schemes. Comparisons can therefore be made on the percentage of mercury that was released upon thermal heating, relative to the amount that each sorbent initially captured.

Even though Norit Darco Hg™ and tyre AC R1 captured less mercury than tyre char R2 when exposed to gas scheme Exp. 1, most of the mercury held by the two activated

carbons was desorbed at 200°C, while only ca. 22% of the mercury held by the char was removed. Thus tyre char R2 may be capturing mercury by both physisorption and chemisorption processes when exposed to gas scheme Exp.1, while physical adsorption seems to be the main mechanism for the two activated carbons. The chemisorption process that may be occurring on the tyre charcoal could be due to the larger concentration of organically-bound sulphur present in this sorbent as indicated by the XRD and SEM-EDX analysis (refer § 5.3 and § 5.4). Lehmann[11] also suggested that the sulphur in scrap tyre rubber may promote mercury adsorption.

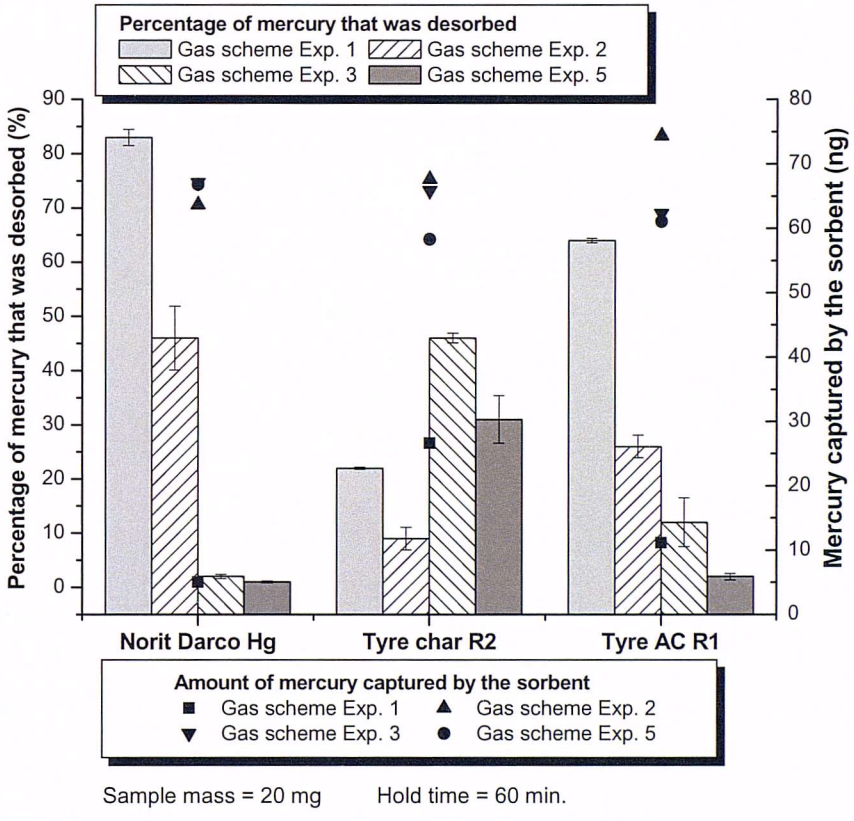


Figure 7-9 Results from mercury desorption tests with Norit Darco Hg, tyre char R2 and tyre AC R1

Although the addition of NO_2 to the gas stream had lead to increased capture of mercury, as illustrated in Figure 7-9, only a reduced proportion was desorbed from the sorbents. This suggests that the sorbents must be capturing mercury via a chemisorption mechanism. The fact that tyre char R2 also showed a smaller amount of mercury desorption suggests that the chemical sorption mechanism that includes NO_2 must be

occurring, in preference to some of the processes that took place when this sorbent was studied with gas scheme Exp. 1.

The level of mercury desorption from the activated carbons tested under gas scheme Exp. 3 (including HCl) also decreased. On the other hand, mercury desorption actually increased in the case of tyre char R2. The chemical adsorption process that occurs in the two activated carbons must therefore be similar, and result in a stronger bond than the forces holding mercury to the same sorbents during tests with gas scheme Exp. 2. However, the interaction between mercury in gas scheme Exp. 3 and the tyre char R2 must be via a different mechanism, which results in a weaker bond than the links formed with either of the activated carbons or between NO_x gases and the tyre char R2.

Desorption results for the activated carbons (Norit Darco Hg™ and tyre AC R1) that had been exposed to Exp.5 were similar to the outcomes from desorption tests on the spent activated carbon samples that had captured mercury from gas scheme Exp. 3. Since gas scheme Exp.3 had illustrated the effect of HCl on mercury adsorption it can be concluded from the desorption tests with Exp. 5, that Norit Darco Hg™ and tyre AC R1 captured mercury through an interaction between mercury and HCl, and this process may have dominated over the reactions with NO_x.

Desorption tests on spent tyre char R2 samples found that the samples which captured mercury from gas scheme Exp. 5 were marginally more stable thermally than the chars which had captured mercury from gas scheme Exp. 3. However the amount of mercury that was released from the first spent char samples was still significantly more than the quantity removed from the used samples that adsorbed the mercury present in gas scheme Exp. 2. The results obtained from the different desorption tests with tyre char R2 suggests therefore, that the mercury present in gas scheme Exp. 5 is adsorbed onto this sorbent via a number of separate mechanisms, with a larger fraction being between mercury and chlorine.

The thermal desorption tests with gas scheme Exp.5 suggest that interactions between HCl and Hg are the predominant mechanism for bonding mercury onto the three sorbents. However a recent study with mercury model compounds showed that $HgCl_2$ decomposes at ca.180°C.[78] Although the tyre char R2 did show an increase in the amount desorbed,

the activated carbons showed an opposite trend when HCl was included in the gas stream. Consequently, even though mercury had reacted with HCl, it may have not been captured by the activated carbons as $HgCl_2$, but as another oxidised species of mercury. Tyre char R2, on the other hand, could have captured a percentage of mercury as $HgCl_2$.

7.7. Studying the presence of $HgCl_2$ in the simulated flue gas streams

Experimental results from the present study indicated that the presence of HCl in the gas stream was beneficial for the mercury capture performance of some sorbents (refer § 7.4). Furthermore, tests completed during the present have also shown that if Norit Darco Hg™, tyre char R1 and tyre AC R1 were initially in contact with HCl, they would be more effective in capturing elemental mercury (refer § 7.5). Thermodynamic equilibrium modelling completed during this study suggested that if chlorine was present at the test temperatures used, $HgCl_2$ would be the most dominant mercury species in the gas stream (refer § 3.2.2). Tests using Dowex 1X8® which is a strongly basic anion resin, were thus undertaken to detect if $HgCl_2$ was present in three of the gas schemes. The experimental setup that was used is described in sub-section 6.2.2.5.

The results obtained from experiments with gas schemes Exp. 1, Exp. 3 and Exp. 4 are presented in Figure 7-10. According to Hocquel et al.[80], Dowex 1X8® reacts with mercuric chloride ($HgCl_2$) while being inert to other mercury species such as mercury oxide, mercury sulphide, mercurous chloride (Hg_2Cl_2) and metallic mercury. Of the three different gas schemes (Exp.1, Exp. 3 and Exp4) used, only gas scheme Exp.3 contained HCl. If $HgCl_2$ had been present in gas scheme Exp. 3, then it would have been possible to clearly differentiate the mercury capture efficiency of Dowex 1X8® with this gas scheme compared to the outcomes from gas schemes Exp.1 and Exp. 4. However, Figure 7-10 indicates that the Dowex 1X8® showed comparable mercury capture efficiencies for all three gas schemes, suggesting that $HgCl_2$ may not have formed when HCl was included in the gas stream.

It should however be noted that, as reported in Figure 7-10, the total amount of mercury measured at the end of each experiment was significantly less than the 64 ng expected to

have entered the sorbent test reactor. This may be due to a number of reasons including the thermal decomposition temperature of 300°C used to release the mercury retained by the Dowex 1X8® (refer § 6.2.2.5). The bond between mercury and the resin may have required a much higher temperature to release all the mercury. It could also be because some of the chemicals contained in the Dowex 1X8® resin may have been released during the decomposition stage of the tests and then adsorbed by the Norit Darco Hg™ based backup capture unit. The presence of these chemicals could have interfered with the mercury analysis that was subsequently completed on the Norit Darco Hg™ backup samples using the PSA 10.025 Millennium Merlin System (refer § 6.1.2).

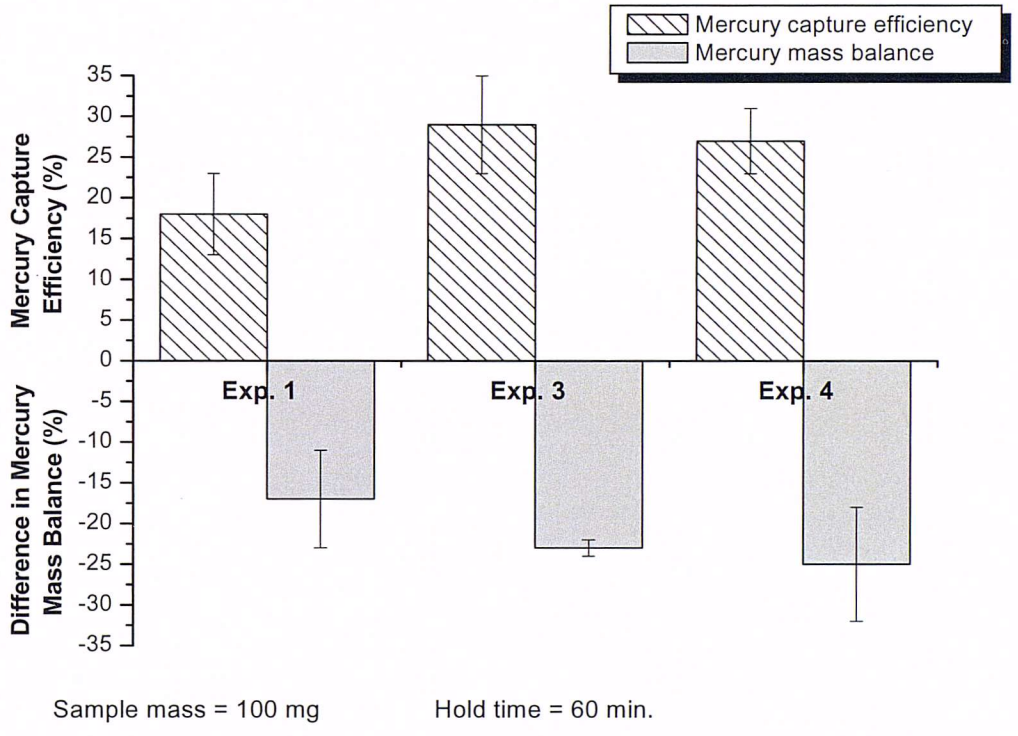


Figure 7-10 Experimental results obtained from the tests with Dowex 1X8®

The experimental setup used during the present study was such that, upon entering the sorbent test reactor, the gas stream took about 25 seconds to reach the sorbent bed. By then, the gas would have reached a maximum temperature close to the adsorption test temperature. This meant that the maximum gas temperature would most probably have been around 200°C. According to Ghorishi et al., oxidation of Hg^0 in the presence of hydrogen chloride (HCl) is slow, and proceeds at measurable rates only at temperatures

>700 °C, and HCl concentrations in the range of 100–200 ppm.[55] Although the HCl concentration in the present study was in the same range stated by Ghorishi et al. the gas streams would have experienced temperatures far less than 700°C. Consequently it would be very unlikely that any significant amount of homogeneous reactions occurred between Hg^0 and HCl within the short residence time available (25 seconds) before the gas reached the sorbent bed. Although it was not possible to have any conclusive empirical results, the outcome from this part of the study did not contradict the above suggestion on there being no $HgCl_2$ in the gas phase prior to the different gas streams coming into contact with the sorbent samples.

7.8. Bromide impregnated activated carbons

During full-scale field tests, sorbents with bromine present have shown improved mercury capture efficiency.[8, 50] Consequently, bromide impregnated activated carbons made from scrap tyre rubber and sewage sludge were evaluated in the present study. The results obtained from experiments under gas scheme Exp. 1, and Exp.6, are presented in Figure 7-11 and Figure 7-12, respectively. The effectiveness of the PAC and charcoal that had no bromide impregnation have also been included in these figures, so that they can be compared against the mercury capture efficiency of the bromide impregnated PACs.

Tests with gas scheme Exp.1 show that bromide significantly improves the mercury capture performance of the activated carbons from both scrap tyre rubber and sewage sludge. However, when the simulated flue gas mix, scheme Exp.6 is used, all the sorbents, except the fly ash samples, show mercury adsorption efficiencies approaching ca.100%. Commercially available, bromine impregnated activated carbons like B-PAC™ and Norit Darco Hg-LH™ were produced specifically for capturing mercury in flue gases generated from the combustion of coal with low halogen contents.[50] The results obtained from the present study confirm this, as the bromine impregnated sorbents appeared to be superior only when NO_2 and HCl are absent from the simulated flue gas stream.

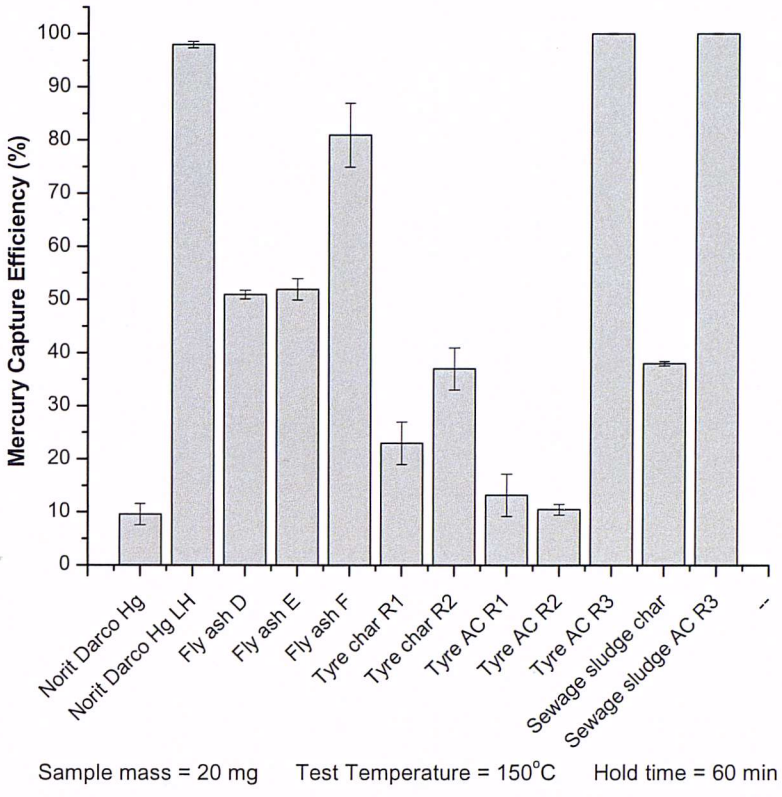


Figure 7-11 Comparing the effectiveness of bromide impregnated PAC against PAC with no bromide impregnation (Gas scheme Exp. 1)

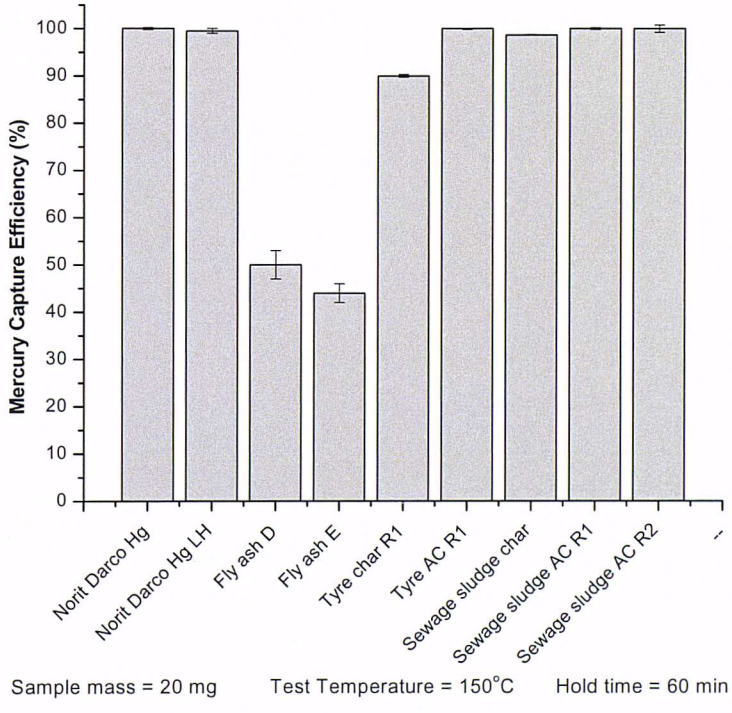


Figure 7-12 Comparing the effectiveness of bromide impregnated PAC against PAC with no bromide impregnation (Gas scheme Exp. 6)

Since the 20 mg bromide impregnated samples were virtually 100% effective when examined with gas scheme Exp.1, further tests were conducted with this gas scheme to find out if using a smaller sample mass would affect the sorbent performance. Thus experiments were carried out with 10 mg of Norit Darco Hg-LH™, 10 mg and then 5 mg of tyre AC R3. The outcomes from these tests are presented in Figure 7-13. This figure also includes mercury capture efficiencies of Norit Darco Hg™, tyre char R2 and tyre AC R1 evaluated with smaller sample mass of approximately 5 mg by using gas scheme Exp. 5. The experiments with the smaller sample mass of bromide impregnated sewage sludge activated carbons had very poor mercury mass balances; hence these results were not included in Figure 7-13.

Even with the reduced sample mass (hence reduced residence time) the bromide impregnated activated carbons were still able to capture all the mercury in the gas stream. Furthermore, the results also showed that although the sample mass of Norit Darco Hg™ and tyre AC R1 were reduced to ca. 5 mg, these sorbents were still able to capture more than 95% of the mercury that entered the sorbent test reactor with gas scheme Exp. 5. On the other hand, there was a significant reduction in the performance of tyre char R2 sample. Furthermore while this sorbent captured only 59% ± 5% of the mercury that entered the sorbent test reactor, the experiments with the reduced sample mass also had very low mercury mass balance values, i.e. at the end of each experimental run it was not possible to quantify 29% ± 1% of the expected total mercury. Approximately 26% of 64 ng of mercury that would have entered the sorbent test reactor was found to be on the cotton buds used to wipe the lower part of the reactor. Mercury in the gas stream had therefore passed though the sorbent bed and then deposited on the internal walls of the lower section which operates at cooler temperatures. The remaining mercury that was not measured may have collected on the internal surfaces of the reactor which were inaccessible to the cotton wipes. The performance of tyre char R2 samples may have been overestimated due to the method used to define mercury capture efficiency (refer Equation 1, § 6.2.2). Nevertheless, the observation that a considerable proportion of the mercury that passed though the sorbent bed had condensed on the lower section of the reactor, indicated that the sample was able to oxidise mercury. However, the tyre rubber charcoal sample was not capable of retaining all this oxidised mercury, possibly because it had only a limited number of sites capable of binding this form of mercury.

The results with the smaller sample masses suggested that bromide impregnated sorbents produced from scrap tyre rubber and Norit Darco Hg-LH™ were more than 20 times as effective as Norit Darco Hg™ for removing mercury under the conditions of gas scheme Exp. 1. Furthermore when gas scheme Exp. 5 which included NO_x and HCl were used the performance of Norit Darco Hg™ and steam activated carbon increased by as much as 20 times that of when these sorbents were evaluated with mercury vapour in pure nitrogen.

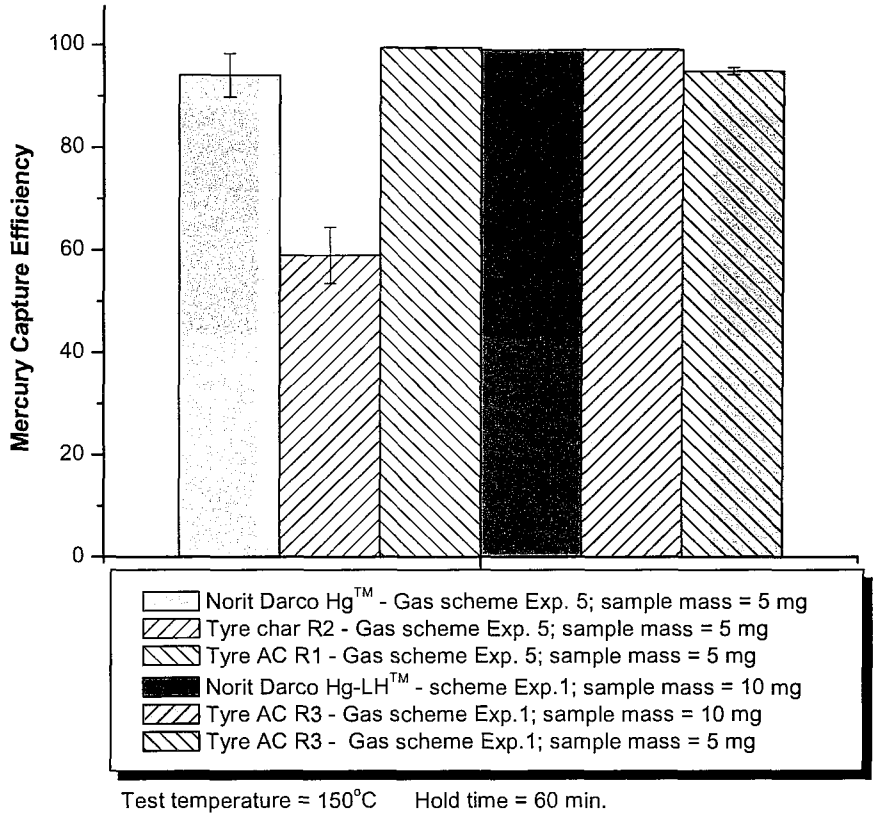


Figure 7-13 Mercury capture efficiencies of some selected sorbents when their mass was reduced to less than 20 mg.

7.9. A closer analysis of mercury capture by fly ash

Eight fly ash samples from three U.K. coal-fired power plants have been evaluated during the present study to obtain a better understanding of mercury capture by fly ashes. These ash samples were obtained from a DTI study (project number 408) that ran in parallel with the BCURA B73 project which funded the present research.[70] The effectiveness of the fly ashes when tested with a gas scheme of mercury vapour mixed with pure nitrogen

(gas scheme Exp. 1) are presented in Figure 7-14 and Figure 7-15. The results seem to suggest that both the initial mercury retained by the fly ashes in the power plant, and the subsequent mercury captured during the bench-scale tests, correlate well with the loss on ignition (LOI; a value used to approximate the level of carbon in ash).[26] Similar findings have also been made by other researchers.[26] Naik et al.[87] have suggested that the unburnt carbon component of LOI catalyzes Hg^0 oxidation and retains particulate-Hg, and is the most effective inherent sorbent for Hg in fly ash. A fair correlation between mercury capture efficiency and ash micropore surface area is also apparent in Figure 7-16.

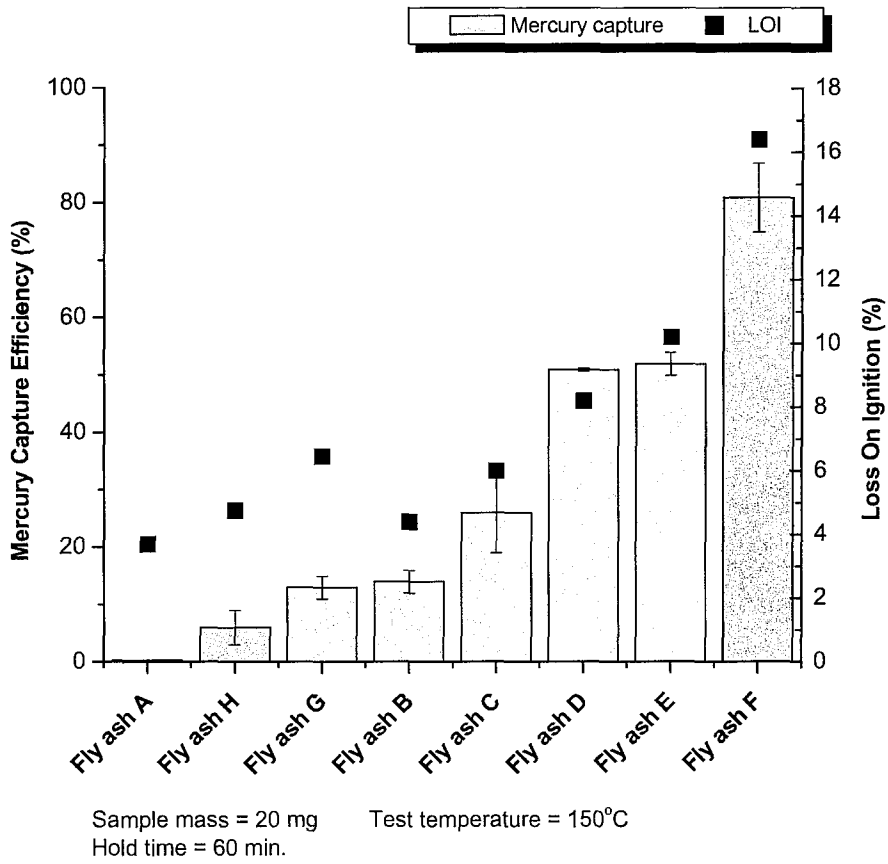


Figure 7-14 Mercury capture efficiencies of fly ashes (from coal-fired power plants in the UK) when tested with mercury vapour mixed with pure nitrogen gas.

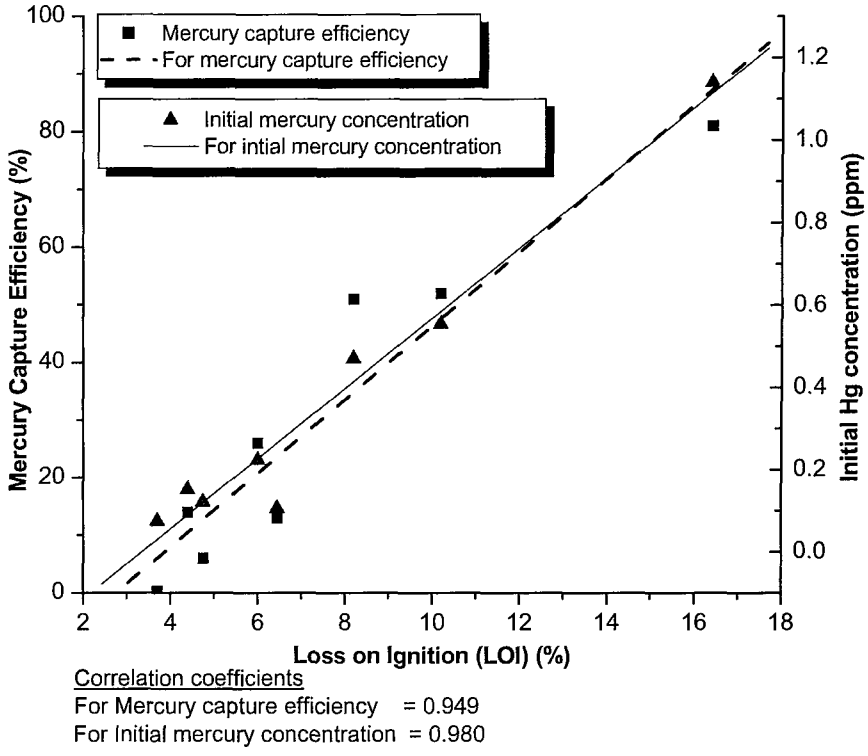


Figure 7-15 Mercury capture efficiency and initial mercury concentration versus LOI content in the fly ashes.

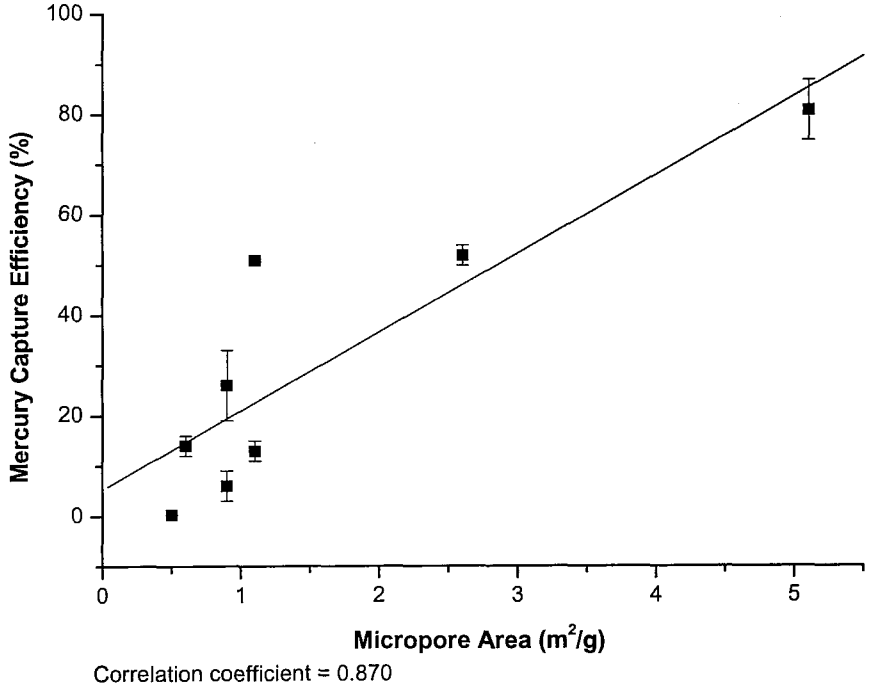


Figure 7-16 Mercury capture efficiency versus micropore surface area in the ash samples.

During this study, experiments have also been conducted to ascertain if there was any correlation between fly ash particle size and mercury capture efficiency. Figure 7-17 and Figure 7-18 present the initial mercury concentration on the different size fractions of fly ash D and F. The results obtained when 20 mg of the different size fractions of these two fly ashes were exposed to gas scheme Exp. 1, for one hour at 150°C, are illustrated in Figure 7-19 and Figure 7-20, respectively. It is apparent that the initial mercury concentration is practically the same for the each size fraction of fly ash D. Values are also the same for fly ash F, except where the particle size is larger than 106 μm, where a significantly lower initial mercury value is evident. The mercury capture tests show that fly ash D is marginally more effective as particle size is increased. On the other hand, the mercury capture efficiency of fly ash F seems independent of particle size. The majority of the fly ash particles in fly ash sample D and F are less than 38 μm in size (> 60% by mass). As a result the effectiveness of the two ashes might be expected to correspond most closely to the results obtained when the smaller sized particles were tested. Experimental results for sub-38 μm fly ash D did have mercury capture efficiencies close to that of the as-received fly ash D sample. However this was not the case for fly ash F. The results for fly ash F suggests that some of its larger particles play an enhanced role in capturing mercury, possibly because the larger particles may have higher carbon content.[88] The results of this set of experiments indicate factors other than fly ash particle size may be more correlated with mercury capture efficiency of fly ash. Similar observations regarding mercury capture efficiency and fly ash particles size have also be made during other studies.[59]

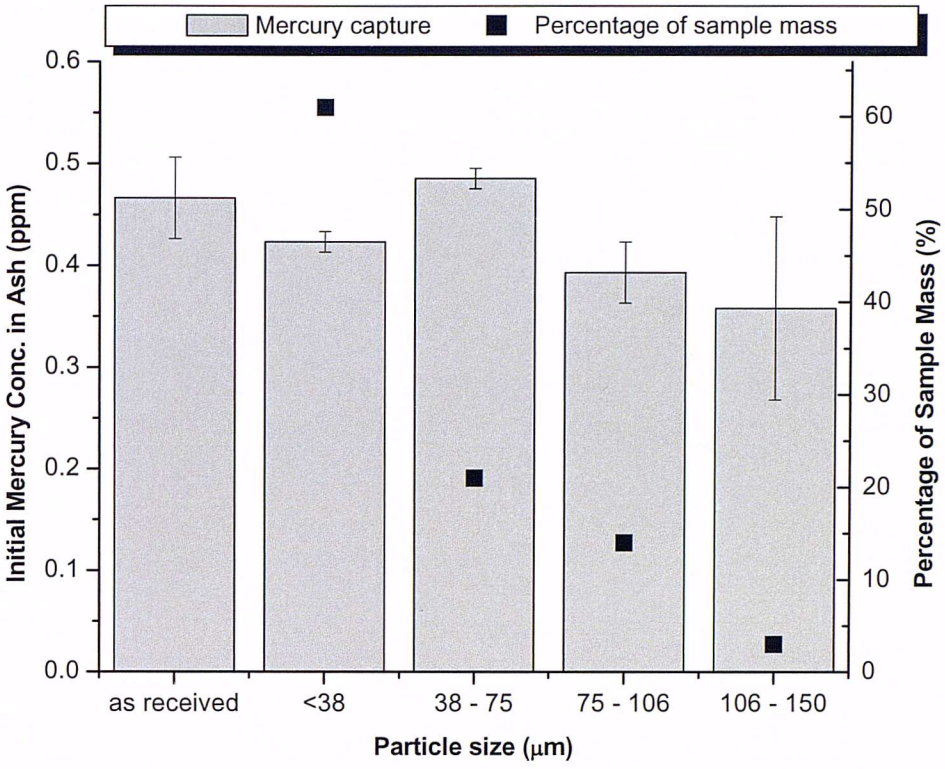


Figure 7-17 Initial mercury concentration on the different particle sizes in fly ash D

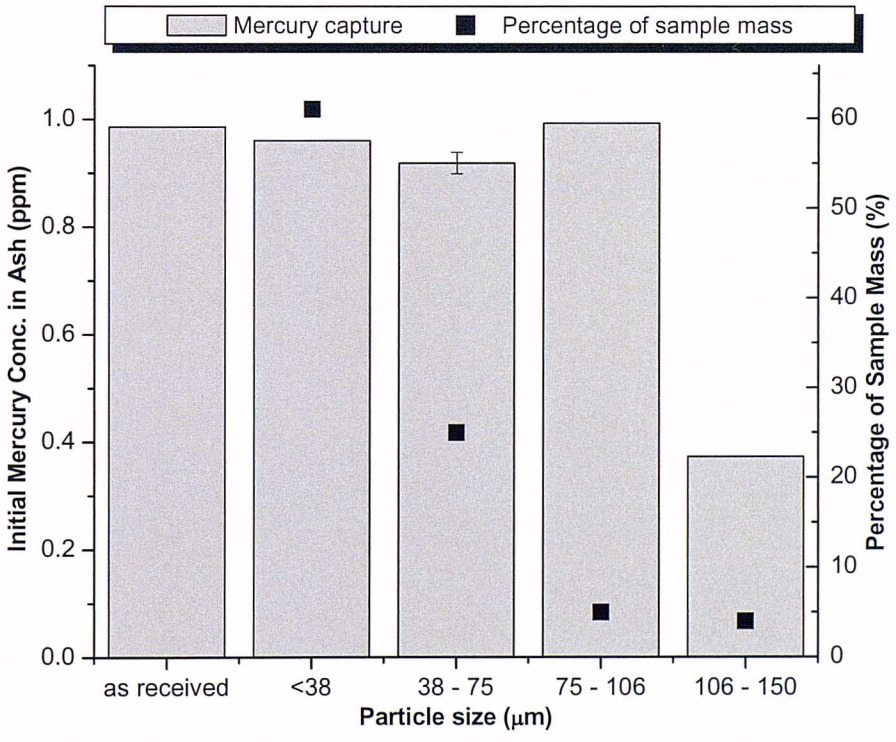


Figure 7-18 Initial mercury concentration on the different particle sizes of fly ash F.

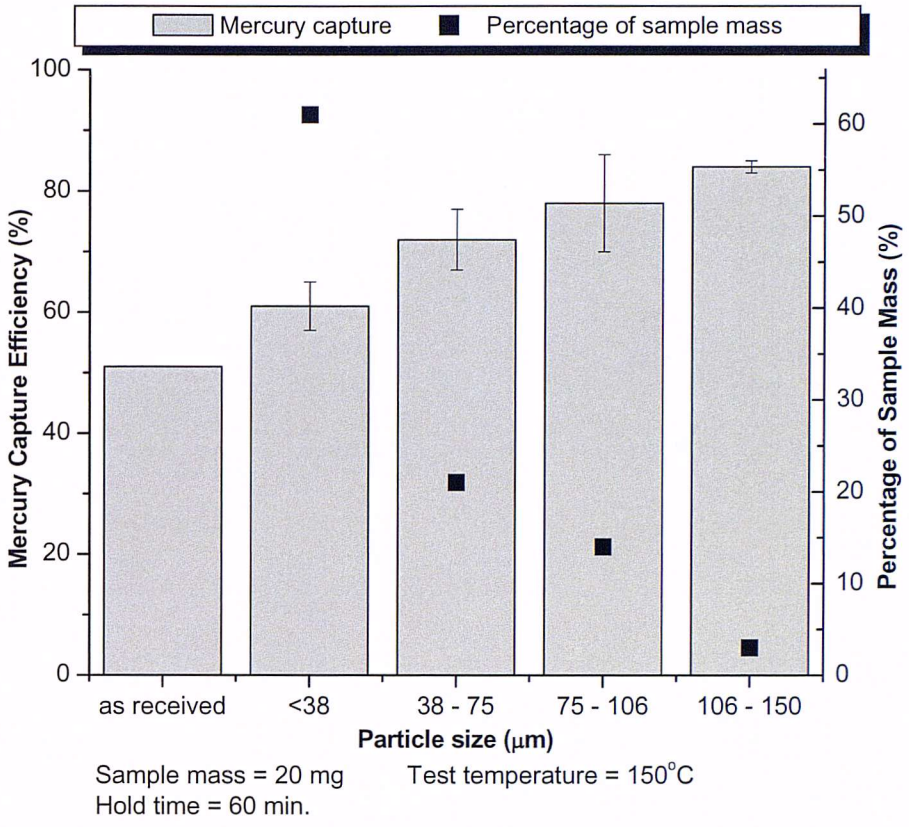


Figure 7-19 Mercury capture efficiencies of different particle sizes of fly ash D when tested with gas scheme Exp. 1.

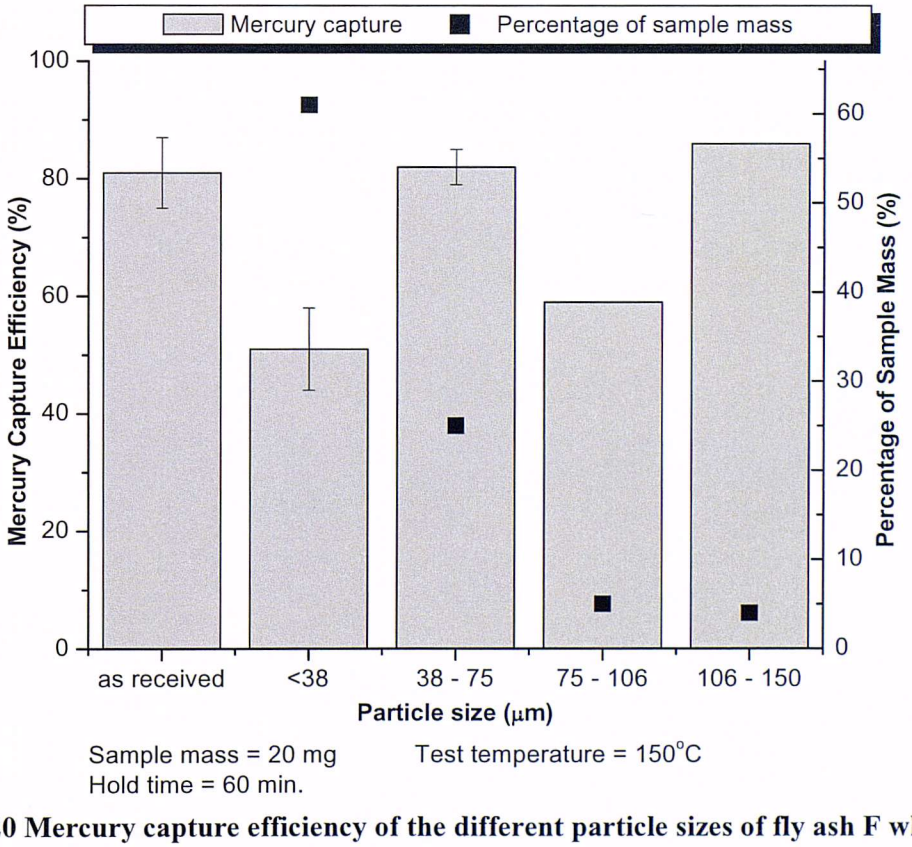


Figure 7-20 Mercury capture efficiency of the different particle sizes of fly ash F when tested with gas scheme Exp. 1.

The dominant market for the utilisation of coal fly ash is as a cement or concrete additive and it is the single largest use of coal combustion products.[88] Fly ash used as a partial replacement of Portland cement in the mix is beneficial to the properties of the concrete due to pozzolanic nature of the fly ash.[88] However, fly ash with high carbon contents have decreased marketability. The problem of unburned carbon in fly ash is associated with the use of special surfactants (known as air-entraining agents, or AEAs) which are added to concrete mixtures.[88] These AEAs impart freeze-thaw resistance to concrete by entraining air bubbles into the mixture. The AEAs can, however be adsorbed by unburned carbon in fly ash which is added to the concrete mixture, thus destroying freeze-thaw resistance. The adsorption of these organic AEAs from otherwise very polar concrete mixture is made possible by the presence of a relatively non-polar carbon phase in the mixture. Thus carbon in ash values above 1% can adversely affect the sale value of fly ash for cement replacement in concrete.[4] The British Standards impose an upper limit of 7% for category B fly ash when used in concrete.[89] Fly ash F had a very high efficiency for retaining mercury. However since its LOI content was ca. 16% it would be unsuitable for a coal-fired power plant to produce such fly ash as it cannot be sold for use in concrete. Furthermore such high LOI content in the fly ash would also have a detrimental effect on the electric power generation efficiency of the plant.

7.10. Leachability of mercury retained on the sorbents

Currently, the fly ash from coal-fired power plants is either sold for construction usage or disposed to landfills.[15, 16] If the sorbents examined in this study were to be used in a coal-fired power plant, they would most probably be collected along with the fly ash in the particulate control system. The spent sorbent would thus be exposed to rain water over a long time-scale. Although Hg^0 is not soluble in water, Hg^{2+} in ash is soluble in water.[18] The leachability of mercury captured by the sorbents evaluated during the present study was therefore investigated to ascertain the stability of the retained mercury. The modified TCLP tests that was used has been described in sub-section 6.2.3.

The results obtained from the TCLP leaching tests on selected bromide impregnated PACs and sorbents without any bromide impregnation are illustrated in Figure 7-21 and

Figure 7-22. Except for fly ash D and E the other the 20 mg spent sorbent samples that were used for the leaching test had captured almost all the mercury that had entered the reactor (refer § 7.4.2 § 7.8). Less than 3% of this captured mercury was however removed during the leaching tests.

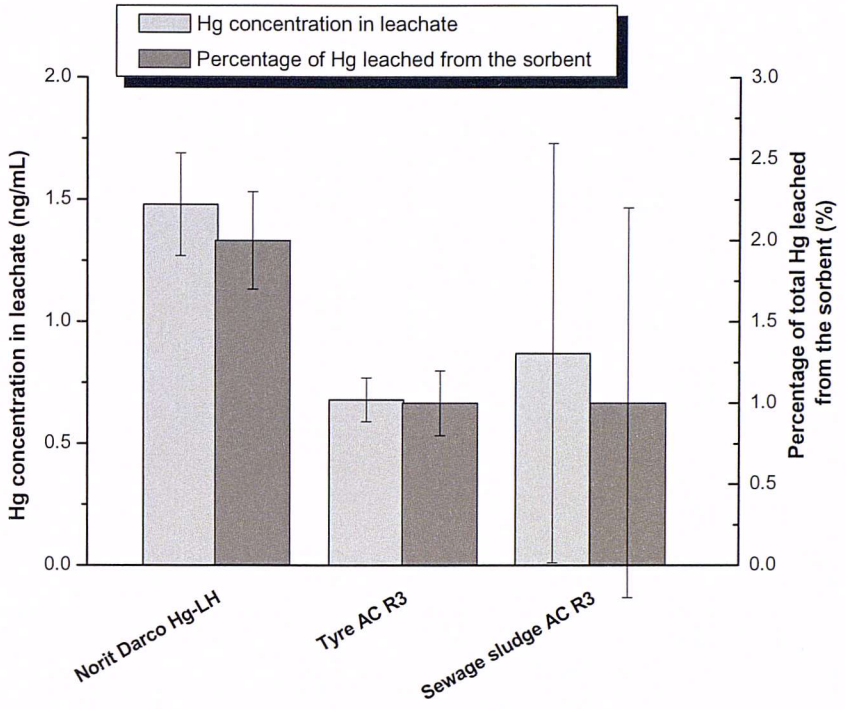


Figure 7-21 Mercury leaching results for bromide impregnated PACs that were exposed to gas scheme Exp. 1.

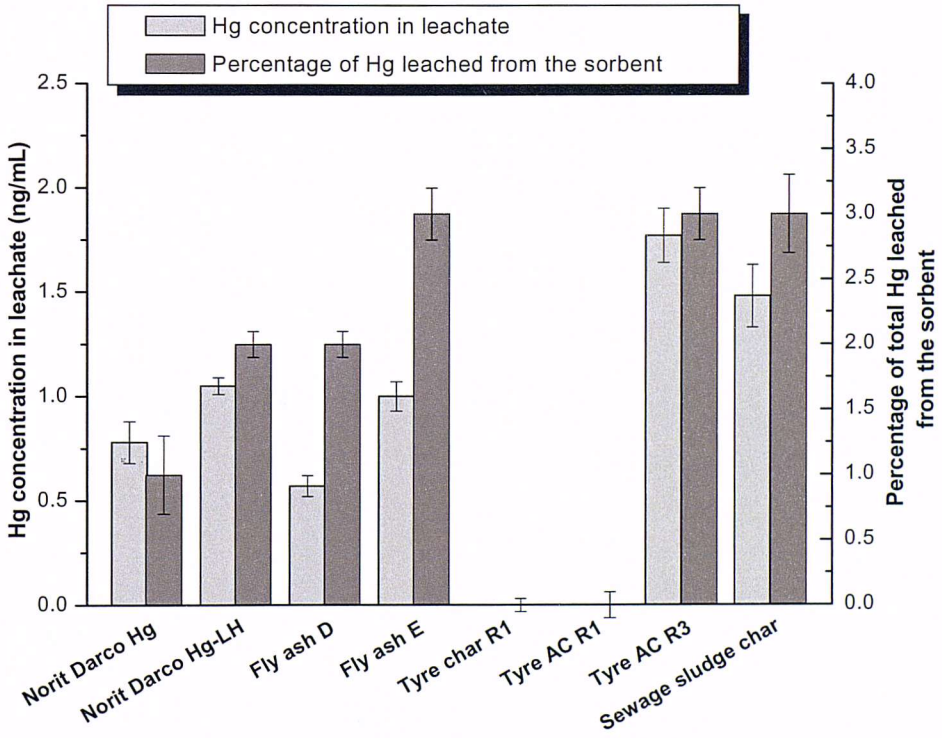


Figure 7-22 Mercury leaching results for selected sorbents that were exposed to gas scheme Exp. 5.

It was found that the maximum concentration of mercury in the leachates was approximately 1.8 ng/mL (ppb), while the overall "limit of quantification" (LOQ) was about 0.3 ng/mL (ppb).[90] The measurements for the mercury concentration have therefore been made close to the LOQ for the instrument. However except for sewage sludge AC R3, the results for all sorbents are consistent.

The current measurements (i.e. the maximum value of 1.8 ng/mL) are below the levels specified in the Safe Drinking Water Act of the US EPA which has recommend a maximum contaminant level for mercury of 2 ng/mL in drinking water.[19] Furthermore, the mercury concentration in the leachate from this study was less than a tenth of the Land Disposal Restrictions (LDR) 25 ng/mL TCLP limit for low mercury waste if disposed using technologies such as solidification and stabilisation.[19] It is thus safe to conclude that spent sorbents could be disposed to landfill, along with the fly ash (of which the sorbents will represent a very small mass fraction). Full-scale tests with Norit Darco Hg-LH™ have reported similar findings of low mercury concentrations in leachates from the spent carbon sorbent.[50]

7.11. Comparing sorbents made under the same process conditions

If any of the sorbents examined during this study are to be utilised in full-scale plants, they will need to be produced on a substantial scale and be of consistent quality in order to ensure reliable performance when in use. Accordingly an attempt has been made to test the reproducibility of manufacture for carbon sorbents produced from sewage sludge and scrap tyre rubber. A number of production runs using the same process conditions have been conducted during the present study, with encouraging results. Analysis based on the measurement of surface area, micropore volume and elemental composition suggests that it is possible to manufacture reproducible carbon sorbents (including bromide impregnated carbon) from both scrap tyre rubber and sewage sludge.

Figure 7-23 presents the mercury capture performance of different batches of sorbent when exposed to Exp.1 conditions, whilst Figure 7-24 presents data under Exp.5 and Exp.6 conditions. Although tyre char R2 was marginally more effective than tyre char R1 when examined with gas scheme Exp.1, both these sorbents did have similar high

mercury capture efficiencies went they were tested with gas scheme Exp. 5. Experiments with the most complete simulated flue gas scheme indicate reproducibility of performance for the steam activated carbon from scrap tyre rubber and bromide impregnated carbons from sewage sludge. The steam activated carbons made from tyre rubber had comparable mercury capture efficiencies under Exp.1 conditions when tested with a 20 mg bed. Considerable difference in the results was apparent however when these sorbents were evaluated using a 100 mg bed. Further investigation would be needed to explain this difference.

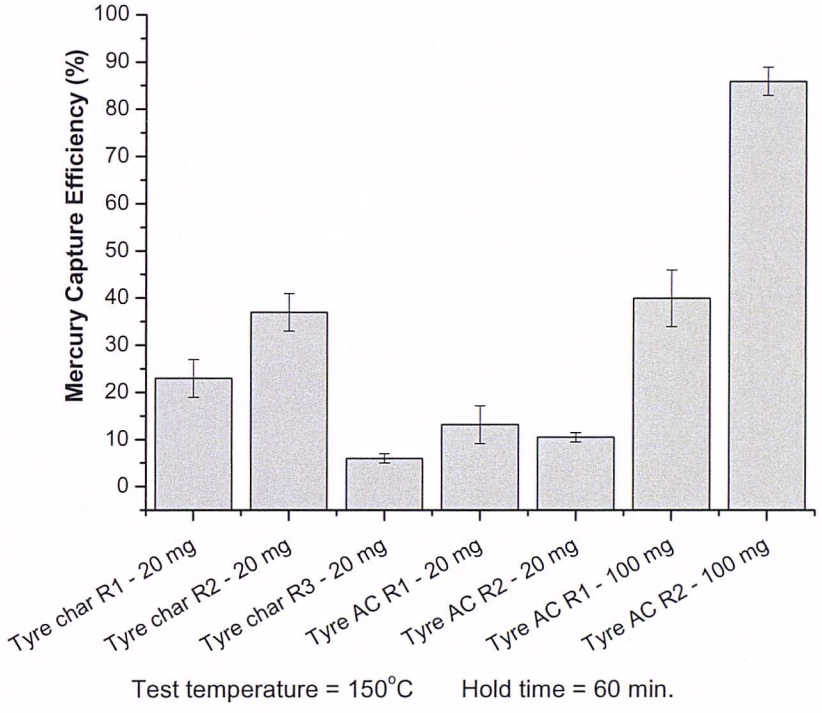


Figure 7-23 Mercury capture efficiencies of sorbents made from the same process conditions (Gas scheme Exp. 1).

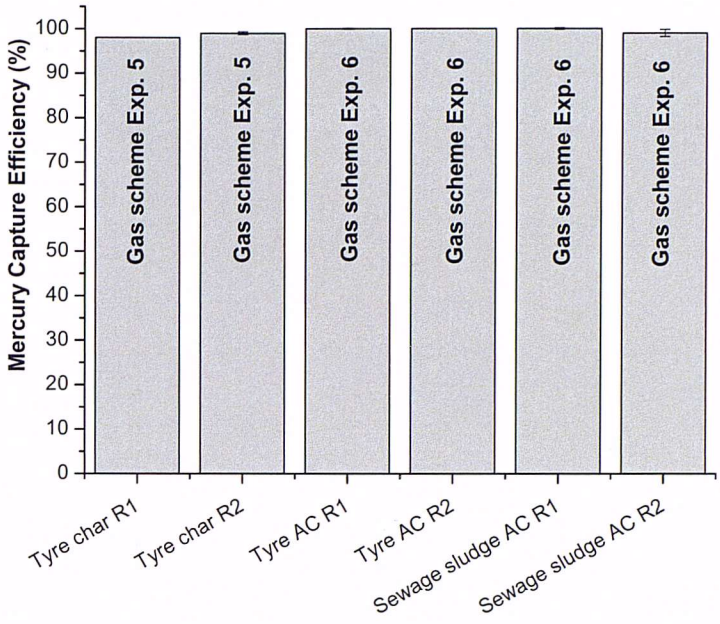


Figure 7-24 Mercury capture efficiencies of sorbents made from the same process conditions (Gas scheme Exp. 5 and Exp. 6).

Tyre char R3 and the two steam activated carbons were produced using the same heating procedure. Although the introduction of steam significantly improved the surface area and micro-porosity of the sorbents (refer § 5.1), Figure 7-23 does show that if a 20 mg sample mass is used, all three sorbents perform similarly when exposed to gas scheme Exp. 1 for a period of one hour. Since the mercury loadings on the sorbents would have been significantly less than their maximum capacities the larger surface area available on the steam activated carbons may have not been fully utilised.

7.12. Discussion on sorbent performance and stability of captured mercury

If the sorbents evaluated in the present study were used in a coal fired power plant to capture mercury in the flue gas, they would probably be injected into the flue gas stream after the air pre-heater and be collected along with the coal fly ash by an ESP or a FF. Miller et al.[41] summarised the following as being the critical steps necessary to accomplish effective mercury control:

1. Dispersion of the small sorbent particles and mixing with the flue gas must be adequate to ensure that all of the gas is effectively treated in the short residence time (typically a few seconds) between sorbent injection and particle collection systems like CS-ESPs.
2. Assuming the sorbent particles can be injected and dispersed adequately a second critical step is the mass transfer by diffusion of mercury from the bulk gas to the particle surface within the available residence time. The ideal case would be to achieve sufficient mass transfer in the duct and not depend on additional transfer within the collection device.
3. Once the mercury molecules reach the surface of a sorbent particle, they will not be trapped unless sorption can occur at a rate equal to the rate of mass transfer by diffusion to the particle surface. Analysis by Rostam-Abadi et al.[59] concluded that only a very small surface area would be theoretically required to trap the mercury. The implication is that reactive surface sites are much more important that the amount of surface area.
4. Assuming the sorbent has sufficient capacity and reactivity to trap the mercury that reaches the sorbent particles, the final critical step is long-term stability of the adsorbed mercury.

The next subsections of this chapter discusses how the results from the present study were used to obtain a better understanding of the mechanisms by which mercury is captured on each sorbent.

7.12.1. Transfer of mercury from the gas stream to the sorbent surface and into the particle's pores

The main objective of this study was to identify sorbents produced from waste material that are capable of adsorbing the mercury present in coal-fired power plant flue gases, and to gain a better understanding of how the mercury is captured. It is very difficult to use a bench-scale experimental set-up to completely replicate the mercury capture system that would be used in a coal-fired power plant. For example the present study used a fixed sorbent bed to evaluate potential sorbents while in a coal-fired power plant the sorbents would be injected into the flue gas duct. In the latter instance, mercury would therefore be

captured while the sorbent particles travel with the gas stream to the APCD. Since a fixed sorbent bed was used for the bench-scale experiments, this study did not produce information on how each sorbent may disperse when injected into the flue gas duct in a coal fired power plant. Although no direct information was obtained on mercury diffusion from the bulk gas onto the surface of sorbent particles, the results from the bench-scale tests can be used to gain an indication on the mechanisms that may be most critical for mercury capture by the sorbents.

Each mercury adsorption test was carried out with the mercury containing gas stream having a superficial velocity of approximately 0.01 m/s (refer § 6.2.2). The residence time of the gas stream as it passed through the fixed sorbent bed depended on the type of sorbent being used and the sorbent sample mass. Since the PACs and the charcoal samples had similar densities, for a given sample mass, the residence time of the gas stream in the bed was comparable for all these sorbents. Coal fly ash samples on the other hand were more dense. So, for the same sample mass, the sorbent bed height would be less than the bed height for the PACs and charcoal samples. Consequently, the residence time of the gas stream, as it flowed though the sorbent bed, would be smaller when coal fly ashes were tested with the same sample mass as the PACs and charcoal samples. The sorbent bed height and resulting residence times for some selected sorbents and sample masses are listed in Table 7-1.

Table 7-1 Sorbent bed height and gas stream residence time for different sample masses

	5 mg sample	20 mg sample	100 mg sample
	Bed height / Residence time		
Norit Darco Hg™	0.2 mm / 0.01 s	0.9 mm / 0.04 s	4.6 mm / 0.2 s
Tyre char R1	0.3 mm / 0.01 s	1.1 mm / 0.04 s	5.5 mm / 0.2 s
Tyre AC R1	0.3 mm / 0.01 s	1.2 mm / 0.04 s	6.2 mm / 0.2 s
Fly ash D	Not analysed	0.5 mm / 0.02 s	2.4 mm / 0.1 s
Fly ash F	Not analysed	0.5 mm / 0.01 s	2.4 mm / 0.1 s

Since only a minute concentration of NO_x and HCl (i.e. ppmv concentrations) were used in the different gas schemes, the addition of these acidic gases should not have significantly affected the diffusivity of mercury from the bulk gas into the pores within the sorbent particles. Test results for mercury capture on PACs and charcoal without

bromine impregnation showed that there was a considerable improvement in mercury capture efficiency when a gas atmosphere containing NO_x or HCl was used, in comparison to gas scheme Exp. 1. The outcome from these experiments indicated that the mass transfer of mercury from the gas stream to the sorbent particle, and then subsequently into the internal pores of the particles, was not the limiting factor for mercury capture on the sorbents when evaluated with the latter gas scheme.

Furthermore, if capture of mercury on these sorbents was controlled by mass transfer then when the residence time of the gas stream was reduced with a smaller sample size, there should also have been a reduction in sorbent performance. This is because the mercury in the gas stream would have not reached the sorbent pores in the reduced time available and therefore would not have been fully adsorbed by the sorbent. Tests with acid gases on reduced sample mass of Norit Darco Hg™ and tyre AC R1 did not show any decline in performance. Although a significant drop in sorbent performance was found when a smaller sample mass of 5 mg of tyre char R2 was examined with gas scheme Exp. 5, the majority of the mercury that avoided capture seemed to be in an oxidised form. Since homogeneous gas phase mercury oxidation is unlikely during the limited time available with the bench scale rig used in the present study (refer § 7.7), elemental mercury in the gas stream was probably oxidised on the sorbent surface. Most of the mercury in the gas stream thus managed to diffuse into the sorbent surface, even within the 0.01 s residence time available, when 5 mg of sorbent was examined. The results suggest that under the test conditions used for this study the film mass transfer of mercury and intra-particle mass transfer of mercury occurred at sufficient rates. This allows almost all the mercury to reach the pores within the sorbent particle. Mass transfer mechanisms are thus unlikely to be the factor that limits mercury capture on some of the sorbents evaluated.

The present study was completed by using a fixed sorbent bed which is more analogous with mercury capture on the filter cake of FFs. However ESPs are the preferred method of collecting fly ashes at coal-fired power plants in the U.S.A. and in the U.K.[4] Mercury capture would therefore take place during the 2 -2.5 s "in-flight" period while the sorbent particles travel to the CS-ESPs.[8, 91] Mass transfer analysis completed by Chen et al.[92] on the carbon injection process showed that the mass transfer from the bulk gas to the external surface of the carbon particles plays the dominant role in determining the carbon/mercury ratio of the injection process. In contrast they also found that intra-

particle diffusion was not important.[92] If film mass transfer is the limiting factor for "in-flight" mercury capture, then the amount of sorbent that needs to be injected can be significantly reduced by decreasing the sorbent particle size.[93]

7.12.2. Mercury capture by physical adsorption and by active sites on the sorbents

Bench-scale tests on the larger 100 mg sample mass of Norit Darco Hg™, steam activated carbon and charcoal produced from scrap tyre rubber showed that the effectiveness of these sorbents, when examined with a gas stream of mercury vapour in nitrogen, was not limited by their maximum capacity for mercury. However, with this gas stream (gas scheme Exp. 1), the sorbents had much reduced efficiencies for capturing Hg^0 when compared to the gas stream that included acid gases. Thermal desorption studies showed that during experiments with gas scheme Exp. 1, mercury was captured on the PACs via a physical adsorption mechanism. Although some chemisorption seemed to have occurred on the tyre rubber charcoal samples, this sorbent also captured a proportion of Hg^0 via physical adsorption. Experiments with reduced residence time showed that the effectiveness of these PACs' decreased if tested with gas scheme Exp. 1. Although the reduction in performance of tyre rubber charcoal was not to the same extent as the drop in effectiveness of the PACs, this charcoal did show reduced mercury capture efficiency with smaller sample masses. These results thus indicate that if physical adsorption is the final mechanism by which the sorbents retain mercury, then the complete process may require more contact time between the gas stream and the sorbent than provided in the current series of experiments.

Under gas scheme Exp. 1 test conditions, the charcoal produced from DEMAD sewage sludge was significantly more effective than the PACs without bromide impregnation (refer § 7.2). Although this charcoal captured less mercury as the sample mass reduced, the drop in the sorbent performance was less than the reduction in the sample mass. The present study illustrated that the presence of chlorine in sorbents without bromide impregnation improves the mercury adsorption efficiency (refer § 7.5). Sewage sludge charcoal has marginally more chlorine than Norit Darco Hg™ and the sorbents made from scrap tyre rubber (refer § 5.2). Although sewage sludge charcoal has sulphur in concentrations less than that in Norit Darco Hg™, and charcoal and steam activated

carbon made from scrap tyre rubber, the sulphur in the sewage sludge charcoal does not seem be in a crystalline phase. This sulphur may therefore be available to react with Hg^0. Hence the high mercury capture efficiency of DEMAD sewage sludge when studied with gas scheme Exp. 1, may thus be due to mercury being chemisorbed by active sites associated with chlorine or sulphur on this sorbent.

The experiments completed during the present study have shown that the presence of NO_x and HCl in the gas stream improves the performance of the PACs and charcoal sorbents that have no bromide impregnation (refer § 7.4). Furthermore if the sorbents had been pre-conditioned by either one of these acid gases, their capability for adsorbing elemental mercury was found to increase in a similar manner (refer § 7.5). The outcomes from these tests thus indicate that NO_x and HCl probably create active sites on the sorbents that facilitated the capture of elemental mercury. The thermal desorption tests results with the more complete gas schemes have shown that the mercury is mainly captured on Norit Darco Hg™, and on steam activated carbon from scrap tyre rubber, by its reactions with HCl, rather than with NO_x (refer § 7.6). However, mercury capture on the scrap tyre rubber seems have happened by a different mechanism. This may be because the sulphur content of the charcoal samples may be in excess of that required for reacting with the elemental mercury present in the gas streams. The thermal desorption results for the scrap tyre rubber pyrolysis samples, tested with gas scheme Exp. 5, suggest that the captured mercury was less stable thermally than the mercury retained on Norit Darco Hg™ or tyre AC R1 samples. Furthermore, the mercury retained on the charcoal sample from this gas scheme may have been captured by reactions with active sites that were created by reactions with NO_x, HCl or sulphur. Test results with the smaller 5 mg sample mass of scrap tyre rubber charcoal evaluated with gas scheme Exp. 5, showed that this sorbent was not as effective as Norit Darco Hg™, or the steam activated carbon prepared from scrap tyre rubber. Most of the mercury that was not captured on the charcoal sample was believed to be oxidised mercury which had formed by reacting with the sorbent. The results therefore suggested that, although charcoal from the pyrolysis of scrap tyre rubber had adequate sites that were capable of oxidising mercury with gas scheme Exp. 5, it had limited sites which could actually capture this form of mercury. The fact that charcoal made from scrap tyre rubber had a smaller micropore surface area than the activated carbons may be the reason why it has fewer sites capable of retaining oxidised mercury.

Tests on the fly ash samples indicated that the LOI was probably one of the most critical factors affecting mercury adsorption. All the fly ash samples evaluated during the current study would have been exposed to the acid gases present in coal combustion flue gas. Tests with mercury vapour mixed in pure nitrogen (gas scheme Exp. 1) showed that most fly ashes performed better than Norit Darco Hg™, probably because they already contained active sites for mercury capture due to the pre-conditioning with NO_x and HCl. Fly ash A and fly ash H, which have LOI values of less than 5%, were less effective than Norit Darco Hg™ when evaluated with gas scheme Exp .1. These two fly ash samples had probably not been able to adsorb sufficient NO_x and HCl from the coal combustion flue gas stream because they had less carbon particles than the other fly ash samples. When the fly ashes with 8 – 10% LOI content were evaluated using the more complete simulated flue gas scheme, they were found to be less effective than the carbon-based sorbents tested in the present study. The results indicated that the fly ash samples were capable of oxidising most of the mercury that was not captured. The inability of the fly ashes to retain oxidised mercury may be due to there being only limited numbers of active sites on the ash samples. This could be related to the coal fly ash samples having a significantly smaller micropore surface area than the activated carbons evaluated in the present study. Although high LOI content improved the mercury capture efficiency of the fly ash samples, as discussed in sub-section 7.9, high carbon in ash values are undesirable as they will adversely affect the saleability of the fly ash and reduce the electric power generation efficiency of the coal-fired power plant.

The bromide impregnated PACs evaluated during this study have shown that even with reduced sample mass and thus residence times as small as ca. 0.01 seconds, these sorbents were ca. 100% effective in capturing the elemental mercury from pure nitrogen. The bromide impregnated sorbents thus had adequate active sites that were capable of oxidising the Hg^0 and retaining it. These sorbents may therefore be more suitable for extracting mercury from flue gases that have lower NO_x and HCl concentrations.

The experiments completed during the present study have indicated that when sorbents are evaluated with a more complete simulated flue gas stream, the mercury in the gas stream is captured by a chemical adsorption process and hence it is oxidised mercury that is finally bound onto the sorbent. The bromine impregnated sorbents evaluated during this study were specifically prepared so that they would have enhanced mercury capture

via reactions between elemental mercury and the bromine in the sorbents. However, Hg^{2+} mercury species like mercuric chloride and methyl-mercuric chloride are soluble in water[18, 19] (refer Table 1-2). If the mercury captured on the sorbents was in this particular form of oxidised mercury, then it should have leached out during the TCLP leaching tests on selected spent sorbents. However, very little mercury was found to have leached from these samples. Unlike the reactive alkali and alkaline earth metals, mercury can form covalent bonds with organic radicals.[19] The results from the leaching tests suggest that either mercury was bound to the sorbents by a Hg^{2+} bond that was not leachable with the TCLP leaching tests or, that it may have been captured by forming a different species of oxidized mercury.

7.12.3. Long term stability of the adsorbed mercury

If sorbents are used in coal fired power plants the spent sorbents would probably be disposed via the systems currently employed for the disposal of coal fly ash. Utilisation of coal fly ash as a cement or concrete additive is the dominant market for the ash and the single largest use of coal combustion products.[88] The results from the thermal desorption tests on spent Norit Darco Hg™ and spent steam activated carbon produced from scrap tyre rubber indicated that less 2% of the captured mercury was released from these sorbents when they were heated to 200°C for 60 minutes. The mercury adsorbed by these two sorbents can therefore be considered as being thermally stable over the temperature range that it may be exposed to when used with fly ash as a cement filler.

Since Hg^{2+} is soluble in water[18], tests were completed during the present study to obtain information on the long term stability of captured mercury when exposed to rain water. The leaching procedure used was based on a modified TCLP leaching method that was designed to simulate leaching in an unlined, sanitary landfill, based on a co-disposal scenario of 95% municipal waste and 5% industrial waste.[17] Fly ash E, the sewage sludge charcoal and the bromide impregnated PAC made from scrap tyre rubber showed the largest percentage of captured mercury being released, amongst the spent sorbents. However, this maximum loss was still only 3% of the captured mercury. The mercury concentration in the leachates from these studies was always found to be less than a tenth of the Land Disposal Restrictions (LDR) 25 ng/mL TCLP limit for low mercury waste, if disposed using technologies such as solidification and stabilisation.[19] Furthermore, the

mercury concentration in the leachates was always found to be within limits of Safe Drinking Water Act established by the U.S. EPA.[19]

It can therefore be concluded, from the thermal desorption and leaching tests that the mercury captured on spent sorbents evaluated using the more complete simulated flue gas stream, is very stable. The spent sorbents may consequently be disposed of using the same practice currently employed for the disposal of coal-fly ash.

8. Selecting alternative sorbents for capturing mercury

Chapter 7 discussed the results that were obtained from the mercury adsorption tests and the leaching experiments completed during the course of the present study. A number of sorbents produced from waste material were matched against the mercury capture efficiencies of Norit Darco Hg™ and Norit Darco Hg-LH™. Chapter 8 examines the sorbents that would be the most suitable substitutes for these commercially available PACs and suggests methods for their large scale production.

8.1. Comparing the laboratory-scale results against full-scale tests

Tests on coal-fired utility plants have shown that, depending on the type of coal being combusted and APCD employed, Norit Darco Hg™ is able to capture between 60% - 90% of the mercury in the flue gas stream.[8] However, in the current study when the most complete simulated flue gas scheme (Exp. 6) was applied during 60 minutes to Norit Darco Hg™, this sorbent retained almost all of the mercury present in the gas stream. There are probably several reasons why bench-scale results differ somewhat from full-scale tests at coal-fired utility plants.

Sorbent injection tests at power plants equipped with ESPs have shown that mercury sorption occurs mainly during the "in-flight" period as the flue gas flows to the ESP. This suggests poor contact between gas-borne mercury and the sorbent powder once it has become attached to the ESP electrodes since most of the gas by-passes the electrode wires.[91] In contrast when sorbents are injected to plants equipped with fabric filters, mercury capture occurs both during the "in-flight" period and also within the filter cake, due to the excellent gas-solid contact across the dust cake on the filter.[4] The bench scale tests completed during the present study used a fixed sorbent bed to evaluate mercury capture from different gas schemes. The results obtained would thus be more representative of plants equipped with FFs. Fabric filters in coal-fired power plants are cleaned at frequencies that are related to the pressure drop across the bag house and filter-bag life; e.g. filters in the bag house at E.C. Gaston Electric Generating Plant in Alabama, USA have a cleaning frequency of 1.5 pulses/bag/hour.[91] Consequently, a filter cake of

coal fly ash and sorbent particles would gradually build up on the filter over a period of 40 minutes before the bag is cleaned. The sorbents used for capturing mercury would thus have remained in contact with the flue gas for a maximum of 40 minutes. Furthermore FFs in the large-scale tests had filter cakes that were 0.8 mm – 1.6 mm thick prior to cleaning.[94] In the current study, the sorbents were evaluated for a simulated flue gas exposure time of 60 minutes which is probably close to the maximum time between the cleaning pluses for the filter bags in the first row of a fabric filter. When the most complete simulated flue gas scheme (Exp. 6) was applied the sorbent sample mass was 20 mg, therefore the sorbent bed height varied between 0.5 – 1.2 mm (refer Table 7-1), this being comparable to the thickness of the filter cakes in FFs.

However the tests completed during the current study were done with a sorbent bed that had only sorbent particles. Miller et al.[41] suggested that typical dust loadings in coal-fired power plants are between 5 – 10 g/Nm^3. During a full-scale test at a U.S. coal fired power plant (Stanton Plant Unit 10), combusting lignite and equipped with a SDA and FF system, injection of Norit Darco Hg™ at 6 lb/MMacf resulted in a mercury capture efficiency of 75%.[6] Assuming that the fabric filter functions at 150°C (the typical operating temperature for such APCDs[8]) then the sorbent concentration in the flue gas was calculated to be 0.14 g/Nm^3. The Norit Darco Hg™ injection was therefore between 1.4 – 3% of the fly ash loading in the flue gas stream. The filter cakes that formed during the full-scale test at the Stanton plant unit 10 would have mainly consisted of coal fly ash with a very thin layer of activated carbon particles. The fact that a fixed bed made-up of only sorbent particles was used in the present study could be one of the reasons why the bench scale experiments had better results for mercury capture than full-scale tests at coal-fired power plants equipped with FFs.

Holmes et al.[95] have suggested that if SO_3 is present, even in ppm concentrations, it may bind to the basic sites on the sorbent and thus restrict the adsorption of mercury. SO_3 enters the flue gas via one of three pathways.[96] Generally a small fraction (a few percent) of sulphur in coal is converted to SO_3 in coal-fired combustion devices such as electric utility boilers.[96, 97] SO_3 can also form from the oxidation of SO_2 across selective catalytic reduction (SCR) catalysts that have been installed for NO_x control.[96] In addition, neat SO_3, or SO_3-producing additives, are widely used to improve the performance of electrostatic precipitators in coal-fired power plants.[17, 95] Depending on the type of coal

being used, and system in place for flue gas conditioning, the SO_3 concentration in the flue gas can be as much as ca. 50 ppm.[96, 98] This is in orders of magnitude larger than the typical mercury concentration which is in the parts per billion (ppb) range.[96]

The presence of SO_3 in the flue gas was suspected to have caused the poor mercury capture observed during pilot scale tests at the Center for Air Toxic Metals® (CATM®), University of North Dakota Energy & Environmental Research Center (EERC).[99] The carbon/mercury/flue gas interaction model developed by Dunham et al.[99] predicted that SO_2 and NO_2 interact at the carbon surface to form S^{6+}, as sulphuric acid or bisulphate, which then binds strongly to the basic sites on the carbon and also displaces the captured mercury. However, in flue gas containing high SO_3, the S^{6+} can accumulate via an alternative route, that is, adsorption and hydration to sulphuric acid and to bisulphate. Therefore, the presence of SO_3 may result in the quick consumption of the basic sites and subsequent displacement of any captured mercury.[99]

Presto et al.[96] have also published similar findings. They have postulated that mercury binding on the surface of activated carbon can be described by two generalised types of sites: stable sites with a high binding energy and catalytic sites with low binding energy. When a sample of activated carbon is exposed to mercury, the sites with high binding energy are occupied first and are responsible for mercury capture by the sorbent.[96] The abundance of sites with high binding energy determine the mercury capacity of the sorbent.[96] The mercury-site bond is strong, and the mercury is not re-released without a change to the process conditions such as heating.[96] The sites with lower binding energy do not retain mercury; they allow mercury to easily adsorb and desorb.[96] These sites serve to catalyze the formation of Hg^{2+}.[96] Presto et al.[96] noted that mercury which was later desorbed from the sorbent may have been in the form of Hg^{2+}. Since SO_3 and mercury compete for the same binding sites on the carbon surface, SO_3 preferentially binds to the sites with higher binding energy to form surface-bound S^{6+} species.[96] The presence of S^{6+} species reduces the mercury capacity of the sorbent.[96] As the high binding energy sites become filled, SO_3 begins to react with the lower binding energy sites. Thus, as the S^{6+} content increases the extent of catalytic mercury oxidation across the sorbent bed decreases.

Gas scheme Exp. 6, the most complete simulated flue gas schemes used during the present study contained SO_2 and water vapour. However the 20 mg carbon based sorbents were still able to capture almost all the mercury that entered the reactor (refer § 7.4.2). Due to safety reasons it was not possible to include SO_3 in the simulated flue gas mix used in the current study. The absence of SO_3 in the simulated flue gas scheme could be another reason why the mercury capture efficiencies measured in the present study differed from those of full-scale PAC tests.

The main objective of the present study was to use a bench scale system to compare the mercury capture efficiency of sorbents produced from waste material against the mercury capture efficiencies of commercial PACs, namely Norit Darco Hg™ and Norit Darco Hg-LH™. This objective was successfully completed and the results obtained have been discussed in Chapter 7. Furthermore, while brominated PACs were found to be more effective during full-scale mercury capture tests, the current bench-scale fixed-bed experiments with mercury vapour in nitrogen had a similar finding, with the bromine impregnated sorbents being more effective than the un-impregnated sorbents.

8.2. Alternative sorbents for Norit Darco Hg™ and Norit Darco Hg-LH™

This study has compared sorbents produced from waste material (scrap tyre rubber and sewage sludge) against commercially available sorbents made from lignite coal (Norit Darco Hg™ and Norit Darco Hg-LH™). A significant proportion of scrap tyre rubber and sewage sludge in the U.K. used to be incinerated or used as landfill (refer § 1.1.1and § 1.1.2). However from 2006 the new EU Landfill Directive has banned the latter practice with whole and shredded tyres.[10] New environmental legislations in Europe are also limiting the methods for the disposal of sewage sludge.[9] Producing sorbents for capturing mercury in flue gases by using these waste material will provide a method of reducing the volume of waste and, at the same time, produce a usable by-product.[9]

8.2.1. Substitute sorbent for Norit Darco Hg™

When evaluated with the experimental schemes used in the present study, the charcoal and activated carbons without bromide impregnation produced from the waste materials were found have a similar performance to Norit Darco Hg™. Tests with gas stream Exp. 6, the most complete simulated flue gas stream used in the present study, showed that Norit Darco Hg™ and both stream activated carbon produced from scrap tyre rubber and sewage sludge charcoal were able to capture almost all the mercury that entered the reactor (refer Figure 7-12). With this same gas stream, scrap tyre rubber charcoal had a mercury capture efficiency approaching 90%. To further differentiate the performance of each sorbent, additional tests have also been completed using reduced sample masses. Results with a 5 mg sample mass showed that Norit Darco Hg™ and steam activated carbon from scrap tyre rubber still had mercury capture efficiencies close to 95% when studied with gas scheme Exp. 5 (refer Figure 7-13). The effectiveness of scrap tyre rubber charcoal, on the other hand reduced to only 60%. The reduced efficiency of this sorbent may be due to less active sites for capturing mercury which could be related to its smaller micropore surface area, relative to the two PACs. When compared to the production of charcoal from scrap tyre rubber, manufacturing steam activated carbon from the same raw material is more costly. However as the latter sorbent was significantly more effective in capturing mercury when evaluated with the smaller samples, steam activated carbon made from scrap tyre rubber is recommended as a substitute for Norit Darco Hg™, in preference to tyre rubber charcoal.

Since mercury is found in waste and wastewater discharges from modern society, mercury removed during wastewater treatment ends up in the sludge residuals.[100] Many large municipalities throughout the world incinerate dewatered sludge, and Hg control systems for off-gases are therefore becoming more common.[100] The dried DEMAD sewage sludge that was used to make the sewage sludge charcoal had an initial mercury concentration of 1.177 ± 0.043 ppm. However, the initial mercury concentration in charcoal that was produced was very small (0.017 ± 0.024 ppm) and close to the detection limit of the mercury analyser. It was thus clear that most of the mercury originally present in the DEMAD sewage sludge was removed during the pyrolysis process that was employed to make sewage sludge charcoal. The production of 1 tonne of sewage sludge charcoal would thus result in the release of ca. 2.5 g of mercury. The

necessary installation of mercury capture on the pyrolysis plant would thus add significantly to the production cost.

Scrap tyre rubber contains a mercury concentration of 0.325 ± 0.212 ppm. Most of this mercury was also released during the heating process used to make the sorbents from scrap tyre rubber. However, production of 1 tonne of steam activated carbon from scrap tyre rubber would result in the release of ca. 1 g of mercury.

Feeley III et al.[6] and Landreth et al.[50] have published Norit Darco Hg™ injection rates and mercury capture efficiencies achieved during full-scale tests completed at U.S. coal-fired power plants (refer Table 8-1). The carbon/mercury ratios achieved during each test are shown in Table 8-1. The values for the mercury loading on Norit Darco Hg™ were calculated by assuming that the injection rates were measured at 150°C which is the typical operating temperature of CS-ESPs and FFs.[8] Each tonne of Norit Darco Hg™ used in the full-scale tests would therefore have captured between ca. 40 - 70 g of mercury.

Table 8-1 Mercury capture efficiencies and carbon/mercury ratios achieved during full-scale tests with Norit Darco Hg™ at U.S. coal-fired utility plants

	Injection rate	Hg capture efficiency	Carbon/mercury ratio
Pleasant Prairie plant[a]	11.3 lb/MMacf	66%	24,240
Meramec plant[b]	5 lb/MMacf	74%	19,132
Stanton plant unit 1[c]	3 lb/MMacf	50%	14,089
Stanton plant unit 10[d]	6 lb/MMacf	75%	18,785

a – Pleasant Prairie plant test with sub-bituminous coal & CS-ESP APCD [6]
b – Meramec plant with PRB sub-bituminous coal & CS-ESP APCD [6]
c – Stanton plant unit 1 with PRB sub-bituminous coal & CS-ESP APCD[50]
d – Stanton plant unit 10 with lignite & SDA/FF APCD [6]

Scrap tyre rubber steam activated carbon and DEMAD sewage sludge charcoal had similar mercury capture efficiencies to Norit Darco Hg™, when evaluated with gas scheme Exp. 6. Thus these sorbents may be equally effective in adsorbing mercury if tested in a coal-fired power plant. If steam activated carbon can be used at similar carbon/mercury ratio to Norit Darco Hg™ (refer Table 8-1) then, the amount of mercury released during the production of the carbon from scrap tyre rubber would equate to only 1.4 - 2.5% of the mercury captured during the power plant injection. DEMAD sewage

sludge, on the other hand contains a much larger initial concentration of mercury hence if it were used at the carbon/mercury ratios listed in Table 8-1 for Norit Darco Hg™, am amount of mercury equivalent to 3.6 – 6.2% of the potentially captured mercury would be released during its manufacture. These numbers illustrate that the mercury emissions during the production of sorbents from these waste material is very small compared to the amount of mercury each sorbent may capture if used in a coal-fired power plant. However, producing steam activated carbon from scrap tyre rubber would clearly produce less mercury emission during manufacture than starting from sewage sludge.

An additional factor is water content, since approximately 67% of DEMAD sewage sludge is water which had to be removed by drying before pyrolysis to make sewage sludge charcoal. If the charcoal made from sewage sludge is to be used in a large scale for capturing mercury in coal-fired power plants, then the water contained in the DEMAD sewage sludge needs to be removed before the solid residue is pyrolysed. A drying facility is thus required at the sorbent producing plant. Alternatively as it is more viable to transport dried sewage sludge, the waste water treatment plant would need to have a drying facility. The scrap tyre rubber used to make the sorbents evaluated during the present study on the other hand contained only 1% moisture. No drying step was therefore needed when the charcoal and steam activated carbon were produced from this tyre rubber. Since drying processes consume significant energy there would be an additional cost for production of charcoal from DEMAD sewage sludge. This is another reason why sorbent produced from scrap tyre rubber can be recommended as the preferred substitute for Norit Darco Hg™.

When 20 mg sorbent samples were evaluated with gas scheme Exp.1, fly ash D – F were found to be significantly more effective than the steam activated carbon made from scrap tyre rubber (refer § 7.2). With this experimental scheme fly ash F was able to retain as much as 81% of the mercury that entered the reactor. However since this fly ash has a very high LOI content (16%) it cannot be sold as a cement replacement additive (refer § 7.9). Furthermore, such a high LOI value is indicative of a less than optimum power generation efficiency due to incomplete combustion of carbon. When 20 mg samples of fly ash D and E were evaluated with gas scheme Exp. 6 they only captured 44 - 50% of the mercury in the gas stream (refer § 7.4.2). Steam activated carbon made from scrap tyre rubber, on the other hand captured all the mercury that entered the reactor. Since coal

fired power plants always have flue gases containing acid gases, steam activated carbon produced from scrap tyre rubber can be recommended as a suitable substitute for Norit Darco Hg™ in preference to coal fly ashes.

During the current study sorbents produced from scrap tyre rubber and DEMAD sewage sludge, and fly ashes from U.K. coal-fired power plants, have been compared against Norit Darco Hg™ for capturing mercury in different gas environments. The stability of the mercury adsorbed by the sorbents have also been evaluated by thermal desorption and leaching tests. The results obtained from these experiments indicated that steam activated carbon made from scrap tyre rubber would be the most suitable sorbent to substitute commercially available Norit Darco Hg™.

8.2.2. Substitute sorbent for Norit Darco Hg-LH™

Norit Darco Hg-LH™ is a brominated PAC marketed by Norit Americas Inc. specifically for capturing mercury present in coal-fired power plants combusting low halogen coals.[51] During the present study mercury capture efficiencies of bromide impregnated carbons made from scrap tyre rubber and DEMAD sewage sludge have been compared against the effectiveness of Norit Darco Hg-LH™. In order to observe the effect of bromine in the sorbents, they have been evaluated with a gas stream consisting only of mercury vapour in pure nitrogen. When 20 mg sorbent samples were tested with this gas stream, the bromide impregnated sorbents were 100% effective, while the non-impregnated sorbents showed much reduced mercury capture efficiencies. Norit Darco Hg-LH™ and bromide impregnated activated carbon made from DEMAD sewage sludge were also evaluated with gas scheme Exp. 6, which was closer to the flue gas composition in coal-fired power plants combusting U.K. Harworth coal. Tests with this gas scheme, and 20 mg samples, showed that both sorbents had ca. 100% mercury capture efficiency. It was also found that hardly any mercury captured by bromide impregnated sorbents exposed to either gas scheme Exp. 1 or Exp. 5 would leach out. The results therefore suggest that bromide impregnated activated carbon made from scrap tyre rubber or sewage sludge would be suitable substitutes for Norit Darco Hg-LH™.

In order to acquire information on which waste material should be used to produce the bromide impregnated sorbent that may substitute Norit Darco Hg-LH™, smaller sample

masses of the bromide impregnated PACs have been evaluated with mercury vapour in pure nitrogen. The reduced sample mass of 10 mg of Norit Darco Hg-LH™ or bromide impregnated activated carbon made from scrap tyre rubber was found to still be 100% effective in adsorbing mercury. However, experiments with 10 mg of bromide impregnated sewage sludge activated carbon produced a poor mercury mass balance and so the results were not used for direct comparison. The bromide impregnated PAC made from scrap tyre rubber was also evaluated with an even smaller sample mass of 5 mg and yet was still able to capture 95% of the mercury entering the reactor. The results indicate that bromide impregnated PAC made from scrap tyre rubber is extremely effective in adsorbing mercury present in the gas stream.

As described in subsection 8.2.1, DEMAD sewage sludge initially contains a substantial amount of water. The bromide impregnated activated carbon made from sewage sludge evaluated during the present study was produced by first mixing the DEMAD sewage sludge with a $ZnBr_2$ solution and then drying this mixture overnight in an oven (refer § 4.7). If this sorbent is to be produced in a large scale then the DEMAD sewage sludge would most probably be transported from waste water treatment facilities to the sorbent manufacturing plant without any drying. Although wet DEMAD sewage sludge contains a substantial amount of water it would probably cost less to transport the sewage sludge in its wet form than to have a second drying process. However, in this case the activated carbon yield for producing bromide impregnated carbon from wet DEMAD sewage sludge would only be ca. 11% while making bromide impregnated sorbents from scrap tyre rubber has a yield of ca. 26%. Furthermore, as mentioned in subsection 8.2.1, using sewage sludge would result in more mercury being released during the production of sorbents from DEMAD sewage sludge, than compared to making bromide impregnated PACs from scrap tyre rubber.

After considering the above facts, scrap tyre rubber was recommended as the more suitable raw material for producing the bromide impregnated PAC that may function as an alternative sorbent for commercially available Norit Darco Hg-LH™.

8.2.3. Proposed large scale manufacturing process for making the sorbents

Steam activation of coal is one of the most common means by which activated carbon is produced in the U.S.A.[60] It is the process that Norit Americas Inc. use to produce activated carbon from coal[60] and therefore would most probably be the method used to make Norit Darco Hg™. Koplan et al[60] have published the following stages as being the main processes used to manufacture steam activated carbon from coal.

- The raw material (i.e. coal) is first crushed and then fed to one or more rotary kilns for the carbonisation step, where it is heated in the absence of oxygen to ca. 400°C. During this step, the water and volatile organic compounds are vaporized and removed from the kiln in the exhaust gases.[60] The charred material is removed from the kiln after approximately six hours and is ready for the activation step.

- In steam activation, the carbonised material is transferred to a rotary kiln or multiple hearth kiln. A rotary kiln consists of a long cylindrical combustion chamber that is slightly tilted from the horizontal. The material to be burnt is added to the elevated end of the kiln. The tilt and rotation of the combustion chamber move the material out to the opposite end. Residence time is controlled by the feed and rotation rates.

  A multiple hearth kiln consists of a vertical column with grates at various heights in the column. Solid materials are fed into the top of the kiln and arms attached to a rotating centre shaft push the material to the lower grates. Steam and/or air are fed into the bottom of the kiln. The residence time of the solid material in the kiln is determined by the rotation rate of the centre shaft and by the feed rate, which controls the bed height on each grate.

  Variables such as the pore size and surface area are controlled by the temperature inside the activation kiln and residence time of the material.

- After the activated carbon is removed from kiln, it is milled and screened to final size and packaged for sale.

The above steps are similar to the process that was used to make the steam activated carbons from scrap tyre rubber evaluated in the present study (refer § 4.4). Dalai et al.[101] in their study produced steam activated carbons from Bienfait lignite (obtained from Bienait Coal Company Limited, Beinfait, Saskatchewan, Canada) with an average dry basis yield of approximately 30%. This is a comparable to the product yield to that obtained during the present study when steam activated carbon was made from scrap tyre rubber. Since Norit Darco Hg™ is also made from lignite[51] production of steam activated carbon from scrap tyre rubber may be possible by direct substitution of the raw material adopting only minor process changes as needed.

In the U.S.A., chemical activation is mainly used to produce wood based activated carbons.[60] According to Koplan et al[60], chemical activation of saw dust is done by first mixing the raw material with an activating agent. The material is then fed to a rotary kiln within which both the carbonisation process and the activation process occur.[60] The activating agent dehydrates the carbonaceous material and this influences pyrolysis process and inhibits the formation of tar.[11] Often a post-activation acid wash is done next, to remove minerals and ash and thus produce a purer product.[60] The washed material is later dried, milled and screened to final particle size, and packaged for sale.

When compared to the above chemical activation process for saw dust, more stages would be needed to produce bromide impregnated activated carbon from scrap tyre rubber. Although Norit Americas Inc. has not released any information pertaining to the manufacturing process for Norit Darco Hg-LH ™, the results obtained for its micropore surface area and volume (refer § 5.1) suggests that it may have been first carbonised before being impregnated with bromine. Consequently, the production of Norit Darco Hg-LH™ may also involve more stages than what was described by Koplan et al[60] for chemical activation of saw dust.

The proposed method for large scale production of bromide impregnated activated carbon from scrap tyre rubber follows the same steps that were used in the present study to make tyre AC R3 (refer § 4.5). The scrap tyre rubber therefore needs to be reduced to a size suitable for pyrolysis in a rotary kiln. This pyrolysis step was necessary because unlike saw dust; scrap tyre rubber would not mix adequately with the activation agent. The tyre

charcoal produced from the pyrolysis kiln, on the other hand would have sufficient porosity to mix with the $ZnBr_2$ solution. The next stages are the drying of tyre charcoal/$ZnBr_2$ slurry and the crushing of the solid which is produced so that it can be fed to an activation kiln. The $ZnBr_2$ impregnated activated carbon produced from this kiln would later be cleaned by using a post-activation HBr acid wash followed by a drying step. The final product would be obtained with a milling/screening stage to produce activated carbons with the required particle size.

Section 2.1 of this thesis suggested that coal-fired power plants would have made the most significant contribution to the 2.34 tonnes of mercury that was emitted during 2005 by the UK "public electricity and heat production" sector.[25] If it is assumed that all this mercury was from coal-fired power plants and that each tonne of PAC without bromine impregnation adsorbs ca. 40 – 70 g of mercury (refer § 8.2.1), then ca. 35,000 – 61,000 tonnes of PAC would be needed to capture the 2.34 tonnes of mercury that was emitted. Since around 70% of the 450,000 tonnes of scrap tyre rubber annually disposed in the UK are mainly recycled or used as fuel for cement kilns (refer § 1.1.1), it is therefore possible to produce ca. 40,500 tonnes of PAC from the remaining 30% of scrap tyre rubber that is not fully utilised.[10] The results thus suggest the potential to meet more than 67% of mercury sorbent requirement by producing PACs from this remaining portion of scrap tyre rubber.

This chapter described why it was difficult to compare the results from bench-scale mercury capture tests completed during the present study against the findings from full-scale sorbent injection tests at U.S. coal-fired power plants. Chapter 8 also includes the process by which the most suitable sorbents produced from different waste materials were selected as useful alternatives for commercially available Norit Darco Hg™ and Norit Darco Hg-LH™. The final section of this chapter proposed possible methods to manufacture the sorbents on a large scale.

9. Summary, conclusions and recommendations for future work

9.1. Summary

1. Coal-fired power plants are the largest anthropogenic source of mercury emissions. Canada and U.S.A. have therefore recently introduced mercury abatement legislations that are specific for these facilities. At the present time, injection of powdered activated carbon looks like being the most promising technology for the control of mercury emissions in the near term. However, these carbons are expensive and add to the unit cost of generated power. The current project aimed to determine mercury capture efficiencies of sorbents made from waste materials, compared to the effectiveness of commercial active carbons. With the new E.U. legislations limiting the methods available for disposing of waste materials, using these wastes to manufacture sorbents provides a cost-effective disposal solution whilst producing a re-usable by product.

2. During the present study, a novel bench-scale fixed-bed reactor system has been designed, fabricated and commissioned for evaluating mercury capture efficiencies of different sorbents samples. The system was used with a number of gas environments and the mercury adsorption tests were carried out at temperatures similar to those of cold-side electrostatic precipitators (CS-ESPs) and fabric filters (FFs) installed in coal-fired power plants. The superficial gas velocity used for experiments was similar to the air-to-cloth ratio for FFs. The mercury concentration in the different gas steams that were employed were comparable to that for flue gas produced when U.K. Harworth coal is combusted. The most complete simulated flue gas used in the present study contained N_2, NO, NO_2, HCl, SO_2, CO_2, O_2, H_2O in addition to the trace amount of mercury vapour.

3. A thermodynamic equilibrium study has been completed on the speciation of mercury when present in various gas environments, by using the MTDATA software and the SGTE database. This modelling was completed to obtain a better understanding of the heterogeneous mercury reactions that may occur with the different species in coal-fired power plant flue gases.

4. An attempt was made to acquire empirical information on the possibility of $HgCl_2$ forming via homogeneous mercury reactions within the sorbent test reactor.

5. Charcoal and activated carbon prepared from waste material (scrap tyre rubber and DEMAD sewage sludge) were produced on lab-scale. The presence of bromine in sorbents is known to improve their mercury capture efficiency; therefore bromide impregnated activated carbons were also made from scrap tyre rubber and DEMAD sewage sludge.

6. Mercury capture efficiencies of charcoal and activated carbons produced from two types of waste material have been evaluated against commercial PACs by using selected gas atmospheres. Fly ashes from three U.K. coal-fired power plants have been tested for the possibility of reusing the fly ash to capture more mercury. The effectiveness of bromine impregnation on mercury adsorption was also assessed during this study.

7. Some selected sorbents have been analysed for their elemental composition, surface area and volume of their micro/meso/macro-pores and their crystalline phases. SEM coupled with EDX analysis was also completed on a few chosen samples.

8. The thermal stability and leachability of the captured mercury was evaluated by testing some selected spent sorbents. The intention of this part of the study was to obtain more information on how mercury is captured by each sorbent and to acquire data on the long term stability of the captured mercury.

9. During the present study, possible alternative sorbents to Norit Darco Hg™ and Norit Darco Hg-LH™ were established by evaluating the different coal fly ashes and

sorbents produced from waste material. The methods for large-scale production of these alternative sorbents were also discussed.

9.2. Conclusions

9.2.1. Experimental scheme used during the study

1. The mercury capture tests completed during the present study showed that the bench scale system, including the novel sorbent test reactor was suitable for assessing mercury adsorption on the samples that were evaluated through this investigation. Experiments completed on 20 mg sorbent samples using the most complete simulated flue gas stream had coefficient of variability values less than 6%. Furthermore, tests on 100 mg sorbent samples evaluated with a gas scheme of mercury vapour in pure nitrogen had coefficient of variability values approaching a maximum of 15%. Although larger coefficient of variability values were calculated when 20 mg sorbent sample masses were tested with the latter gas scheme, the maximum standard deviation of these results for each sorbent sample was only 4%.The bench scale system was also successfully modified for thermal desorption tests on spent sorbents.

2. The suitability of the PSA Cavkit as an accurate mercury generator and the LECO AMA 254 mercury analyser for subsequent mercury analysis of the backup capture unit was proved when it was found that the system could generate a mercury concentration within ± 10% of the required set point. Mercury capture results reported in this thesis are from those experiments that achieved mercury mass balance values within ± 15% the expected total mercury.

3. The LECO AMA 254 mercury analyser was able to accurately quantify the mercury content in the sorbents that did not have any bromide impregnation. However this unit was not suitable for sorbents with high bromine concentrations and therefore the P S Analytical method of Aqua Regia digestion coupled with analysis using a PSA 10.025 Millennium Merlin system was employed for these samples. A good mass balance of within ± 15% was obtained when the latter method was used to quantify mercury

present in spent Norit Darco Hg-LH™ and spent bromide impregnated PAC made from scrap tyre rubber. The analysis of mercury captured by bromide impregnated sewage sludge PAC however proved to be sometimes inconsistent.

9.2.2. Thermodynamic equilibrium modelling

1. The MTDATA thermodynamic equilibrium modelling completed during the present study showed that mercury would mainly react with chlorine in the flue gas. When the flue gas temperature reduced to ca. 400°C, the mercury compounds in flue gas generated from combustion of lignite were predicted to differ from those produced by bituminous coal combustion. If the thermodynamic equilibrium conditions are still maintained while the flue gas cools to the operating temperature of CS-ESPs (ca. 150°C), then the flue gases from lignite and bituminous coals were expected to contain one mercury species only – gaseous $HgCl_2$.

2. Kinetic and mass transfer limitations are not considered in the MTDATA thermodynamic equilibrium models, while the actual residence time for reactions with mercury in the coal fired power plant flue gas are in the order of seconds. The results obtained from the MTDATA models should therefore be considered only as an indication of the mercury species that could form at thermodynamic equilibrium conditions.

9.2.3. Sorbents evaluated during this study

1. The lab-scale procedures used during the present study proved effective in producing charcoal and activated carbons (including bromide impregnated PACs) from scrap tyre rubber and DEMAD sewage sludge.

2. When compared to the other sorbents evaluated during the present study Norit Darco Hg™ and the bromide impregnated PAC made from DEMAD sewage sludge had the largest BET surface area and micro-porosity. The fly ash from U.K. coal-fired power plants had very small micropore surfaces and they were correlated to the LOI content of the fly ash. The addition of steam during the production of steam activated carbon from scrap tyre rubber produced a 20 fold increase in micropore surface area. Using

$ZnBr_2$ activation agent to produce the bromide impregnated sewage sludge PAC increased the micropore surface area by ca. 15 times. In contrast, the $ZnBr_2$ activation agent increased the micropore surface area of bromide impregnated scrap tyre rubber PAC by only ca. 2 times.

3. XRD analysis of Norit Darco Hg™, some selected sorbents produced from scrap tyre rubber and sewage sludge, and coal-fly ashes indicated that they contained mainly amorphous phases. The main crystalline phases in Norit Darco Hg™ were quartz and calcite. Mullite, quartz and magnetite were the main crystalline phases found in the coal fly ashes.

4. The bromide impregnated PACs made from waste material was produced by initially mixing $ZnBr_2$ with a similar mass of scrap tyre rubber or sewage sludge (on a dry basis). The fact that these bromide impregnated PACs contained only between 1 - 2% bromine indicated that most of the bromine was removed during the activation or post-activation process employed to make these sorbents. Nevertheless the concentration of bromine in scrap tyre rubber and sewage sludge bromide impregnated PACs was still similar to that of Norit Darco Hg-LH™.

5. Sulphur and ZnO are utilised in production of tyre rubber. The heating process employed to make the sorbents from scrap tyre rubber was found to remove approximately 50% of the sulphur initially present in the raw material and also promote the conversion of ZnO into ZnS. However XRD analysis indicated that tyre rubber charcoal still had some ZnO present while the steam activated carbon from scrap tyre rubber may have a larger concentration ZnS. The results suggested that tyre rubber charcoal could have a larger concentration of sulphur still organically bound to the carbon matrix of this sorbent and therefore be available to react with mercury in the gas stream.

6. The post-activation acid washing procedure removed a significant amount of the mineral matter in the sorbents produced from scrap tyre rubber and sewage sludge. XRD analysis of the bromide impregnated PAC made from scrap tyre rubber thus did not show any ZnS or ZnO present in this sorbent. XRD analysis also showed that acid washing of bromide impregnated PAC made from DEMAD sewage sludge had

removed the calcite that was present. However the quartz found in unwashed sewage sludge charcoal was also found in the bromide impregnated sewage sludge PAC.

7. SEM coupled with EDX analysis of the fly ashes showed that the inorganic species in the fly ash had agglomerated into spherical globules. This analysis also showed that the smaller particles in the fly ashes were mainly inorganic while the larger particles were predominantly unburnt carbon.

9.2.4. Mercury capture by the sorbents

1. Tests with mercury vapour in pure nitrogen have shown that bromide-impregnated PACs produced from scrap tyre rubber and sewage sludge are the most effective sorbents and that their performances were similar to that of Norit Darco Hg-LH™. When evaluated with this gas environment, these sorbents were capable of capturing all the mercury introduced into the reactor, using just 5% of mass of Norit Darco Hg™ which had adsorbed only 40%.of the mercury. These bromide impregnated sorbents thus appear suitable for capturing mercury in flue gases from the combustion of low halogen content coals.

2. Tests with the different gas schemes have shown that the presence of both NO_2 and HCl does significantly improve the performance of the pyrolysis chars and PACs without bromide impregnation. These sorbents had mercury capture efficiencies approaching 100% when exposed to the most complete simulated flue gas scheme, which included N_2, NO, NO_2, HCl, SO_2, O_2, CO_2, and water vapour. Although some of the coal fly ashes performed respectably when exposed to mercury vapour in a pure nitrogen stream, the tests with the most complete simulated flue gas scheme showed that their effectiveness was significantly less than the charcoal and PACs without bromide impregnation. This could be due to the smaller micropore surface area in the coal fly ashes.

3. The performance of Norit Darco Hg™, charcoal and steam activated carbon made from scrap tyre rubber improved if initially exposed to NO_2 or HCl. The fact that the fly ash samples had already been exposed to these gases at the coal-fired power plant, may explain why some fly ash samples were more effective than the sorbents without

bromide impregnation when they were evaluated with a gas stream of mercury vapour in pure nitrogen.

4. Dowex 1X8® was used to quantify the amount of $HgCl_2$ in the simulated flue gas before the gas passed through the fixed sorbent bed. The results obtained from experiments with three different gas atmospheres (one of which contained HCl and mercury in the gas stream) did not provide any conclusive evidence to the presence of $HgCl_2$ in the gas stream. Although oxidation of Hg^0 to $HgCl_2$ is thermodynamically favoured at the temperatures that were used to test mercury adsorption, it is also known that the oxidation reaction is very slow at these lower temperatures. The conversion of Hg^0 to $HgCl_2$ in the gas phase would have been very small and therefore resulting in a negligible amount of $HgCl_2$ in the simulated flue gas atmosphere before the sorbent bed.

5. The outcomes from the experiments with different gas atmospheres, sorbents and sample masses were used to acquire qualitative information on mass transfer of mercury from the gas stream to the pores in the sorbent particles of the fixed sorbent bed. The results indicated that mass transfer limitations did not cause the observed lower mercury capture efficiencies when the sorbents without bromide impregnation were tested with a gas stream of mercury vapour in pure nitrogen.

6. Thermal desorption tests suggest that the mercury captured by Norit Darco Hg™, and steam-activated carbon produced from scrap tyre rubber, when exposed to a gas stream of mercury vapour in pure nitrogen, is mainly physically adsorbed. On the other hand, chemical adsorption may also have been involved in mercury capture by the scrap tyre rubber charcoal, possibly via reactions with sulphur in this sorbent. When the gas scheme included NO_2, all three sorbents showed a marked reduction in the amount of mercury desorbed, suggesting a degree of chemisorption. However, Norit Darco Hg™ and steam-activated carbon from scrap tyre rubber which had been exposed to HCl-containing gas showed the lowest mercury desorption loss. The presence of HCl thus resulted in the strongest bond between mercury and these sorbents. Conversely, in the case of pyrolysis char derived from scrap tyre rubber, a significant desorption loss was apparent after exposure to HCl, implying weaker attraction forces between this sorbent and mercury in the presence of HCl. Tests with

the most complete simulated flue gas scheme suggest that HCl does play a predominant role in the capture of mercury by the Norit Darco Hg™, tyre charcoal and tyre steam activated carbon. These desorption tests also showed that in addition to mercury-chlorine reactions, tyre charcoal exposed to the most complete simulated flue gas could have captured mercury via reactions with sulphur in the charcoal and NO_x adsorbed by this sorbent.

7. Experiments with fly ash samples showed that mercury capture could be correlated to LOI and also to the micropore volume of the ash. However, a LOI in excess of 17% is necessary to bring fly ash up to the level of effectiveness of the bromide impregnated activated carbons (based on tests with mercury in nitrogen only). Such a high LOI value is unacceptable, both on the grounds of loss of combustion efficiency and also of reduction in the value of the ash. Fly ashes from most coal-fired utility plants are sold for construction usage and the price is sensitive to carbon content of the ash. Values above 1% can adversely affect the sale value of fly ash for cement replacement in concrete and the British Standards impose an upper limit of 7% for category B fly ash for use in concrete.

8. TCLP leaching tests conducted on sorbents, after mercury adsorption experiments, have shown very little evidence of mercury leaching; with the mercury concentration of leachates actually being below the safe limit for drinking water recommended by the US EPA. These observations suggest that spent sorbent could be disposed to landfills along with the fly ash.

9. When the sample mass of Norit Darco Hg™ and scrap tyre rubber steam activated carbon was reduced to 5 mg the samples were still able to capture more than 95% of the mercury in a simulated flue gas stream that included NO_x, HCl and SO_2. Although the 5 mg scrap tyre rubber charcoal samples were able to oxidise most of the mercury present in the same gas stream, the samples captured only 60% of the mercury. This reduced sorbent performance may be due to tyre charcoal having less active sites and possibly related to its smaller micropore surface area when compared to that of Norit Darco Hg™ and scrap tyre rubber steam activated carbon.

10. When the sorbents were evaluated in an atmosphere of mercury vapour in pure nitrogen, sewage sludge charcoal was more effective in capturing mercury than both Norit Darco Hg™ and non bromide impregnated sorbents made from scrap tyre rubber. This could be due to the larger concentration of chlorine and amorphous sulphur in sewage sludge charcoal. However since DEMAD sewage sludge initially contains more mercury than scrap tyre rubber, producing sorbents from sewage sludge will thus result in more mercury being released to during the manufacturing process than when starting up with scrap tyre rubber.

11. The main objective of this study has been to compare sorbents produced from waste materials against the performance of two commercially available activated carbons, Norit Darco Hg™ and Norit Darco Hg-LH™. The tests have shown that steam-activated carbons produced from scrap tyre rubber are the most suitable substitute for Norit Darco Hg™. Furthermore, the bromide impregnated activated carbons also made from scrap tyre rubber is recommended as an alternative to Norit Darco Hg-LH™. However, since the sorbents have been tested in a packed bed configuration, using a simulated flue gas stream, it has not been possible to obtain direct correlation between the results of the current project and data from tests on U.S. coal-fired power plants. As the new EU Landfill Directive has banned land-filling of both whole and shredded tyres, using scrap tyre rubber to produce sorbents for capturing mercury in coal-fired power plant flue gases may provide an environmentally friendly and cost-effective disposal solution for this waste material, whilst producing a re-usable by product.

9.3. Recommendations for future work

9.3.1. Formulating models to predict the effectiveness of activated carbons injected into coal combustion flue gases

During the present study, MTDATA thermodynamic equilibrium modelling was completed to investigate homogeneous mercury reactions that may occur in coal combustion flue gases (refer. Chapter 3). However, due to the following limitations this modelling software was not suitable for predicting the mercury adsorption on activated carbons that are injected into coal-fired power plant flue gas streams.

- MTDATA is a thermodynamic equilibrium modelling software, it therefore does not consider kinetic and mass transfer limitations that may occur during the mercury capture process.
- The Substance Database that was used by MTDATA to calculate the equilibrium compositions contains data for only a limited number of mercury species. It did not have information on the oxidised mercury species that may form when mercury reacts with NO_x.
- This software is not able to predict the heterogeneous reactions that occur between mercury and the active sites on the activated carbon.

Any future study to investigate predicting mercury capture performance by activated carbons should therefore be done with an alternative model. However, formulating a suitable model to accurately determine the partitioning of mercury as measured at coal fired power plants has proved to be very difficult.[102] At present the most promising model is one produced by Niksa Energy Associates, Belmont, CA, USA.[87, 102] It was formulated by using experimentally measured reaction rate constants when available, but most of the values were estimated or taken from estimates found in the literature.[102] Unlike many of the previous models, it includes a new three-step heterogeneous mechanism for mercury oxidation on the surface of unburnt carbon particles.[102] The heterogeneous mechanism included chlorination of unburnt carbon by HCl (step 1) with subsequent recombination of Cl atoms (step 2) and partial oxidation of Hg into HgCl on the chlorinated site (step 3).[102] The subsequent oxidation of desorbed HgCl by Cl_2 into $HgCl_2$ was assumed to be homogeneous and instantaneous.[102] The evaluation of this model showed that a heterogeneous reaction mechanism was necessary to explain Hg oxidation under utility

boiler exhaust conditions.[102] Although the Naik et al.[87] have suggested that this scheme is able to accurately predict mercury capture by activated carbons injected into coal fired power plants the model still needs further improvement. For example the reaction mechanism that was used is not suitable for bromide impregnated activated carbons and it does not consider mercury reacting with NO_x. Furthermore this model does not look into the surface chemistry of mercury adsorption by the activated carbons; it is therefore unable to suggest how the mercury is ultimately bound onto the sorbent. Consequently there is still much research needed to obtain a more complete model that is able to predict the mercury adsorption capability of activated carbons (incl. impregnated PACs) and to indicate the mercury species that is finally retained on the sorbent.

9.3.2. Inclusion of SO_3 in the simulate flue gas stream

Coal-fired utility boilers typically emit some SO_3, its concentration depending on many factors including the type of coal being burnt, the oxidation of SO_2 across selective catalytic reduction catalysts, and the addition of neat SO_3 or SO_3-producing additives employed to improve the performance of ESPs (refer § 8.1). Laboratory, pilot and full-scale tests have suggested that the presence of SO_3 may cause a reduction in the mercury capture ability of sorbents like PACs.[95, 96, 99] It is also believed to have caused reduction in performance of bromine impregnated PACs. According to a study in the U.S.A., B-PAC™ was evaluated at Progress Energy's Lee Station Unit 1 which is equipped with CS-ESPs.[50] Tests with 100% bituminous coal showed that SO_3 injection greatly reduced the mercury reduction performance of B-PAC™.[50] Holmes et al.[95] and Presto et al.[96] have suggested that SO_3 preferentially binds to the basic sites in the sorbents which would otherwise have captured mercury present in the gas stream.

Gas scheme Exp. 6 was the most complete simulated flue gas stream used in the present study. Unfortunately, SO_3 vapour is corrosive to eyes, skin, mucous membranes and respiratory tract[103], so it could not be included in gas scheme Exp 6 for safety reasons. Sub-section 8.1 discussed why the absence of SO_3 in the gas streams used in the present study may account for the observed difference in results compared to those obtained during full-scale mercury adsorption tests.

A key recommendation is that SO_3 be included in the gas, provided that proper safety precautions can be maintained. Such experiments would be able to determine whether the bromide impregnated sorbents evaluated in the present study could retain their high mercury capture performance, in the presence of SO_3 in the gas stream.

9.3.3. Entrained flow reactor

Electrostatic precipitators are the principal particulate matter control system employed in coal-fired power plants in U.K. and U.S.A. [4] If sorbent injection is used in these plants, then the main, effective contact between sorbent and flue gas is limited to the "in-flight" period as the sorbent is carried in the gas flow to the ESP. This results in a contact time of about 2 -2.5 seconds.[8, 91] In the present study, the simulated flue gas passed through a fixed bed of sorbent for a period of 1 hour, thereby providing a more effective interaction between the sorbent and the gas stream. This may be why the measured effectiveness of Norit Darco Hg™ was observed to be higher than that found in full-scale tests (refer § 8.1). It is thus suggested that subsequent studies should be done with a system that is more comparable to the configuration of UK power plants, i.e. using an entrained flow reactor where residence times are similar. Activated carbon injection tests using the entrained flow reactor at the National Risk Management Research Laboratory at Air Pollution Prevention and Control Division of the U.S. EPA produced results which correlated well with full-scale field test.[65] Furthermore, the Electric Power Research Institute Inc. (EPRI) have a Multi-Pollutant Control Test (PoCT) system which has been used to test sorbents for mercury capture by using a module that simulates in-flight removal upstream of an ESP.[44] The level of Hg removal from tests with this system was found to be consistent with the results from full-scale tests.[44]

9.3.4. Foam index tests on fly ash/sorbent mixtures

There is an increasing demand for concrete based construction and a growing acceptance of fly ash as an economically viable construction material.[104] According to the American Coal Ash Association, production of fly ash in the United States in 2004 totalled 70.8 million tons and 20% of this total was used as a partial replacement for cement in the manufacture of ready mix concrete.[104]

Sub-section 7.9 discussed why the use of air-entraining agents (AEA) added to concrete mixtures have limited the use of fly ashes with high LOI contents as cement replacement additives. When PACs are injected into the flue gas ducts for capturing mercury they will be collected with the coal fly ash by the particulate matter control devices. Therefore the sorbents will be mixed with the coal fly ash. If this fly ash and PAC mix is used for cement replacement, then the highly-adsorbent carbon sorbents will adsorb the air-entraining admixtures that are added to concrete and thus reduce the AEA's effectiveness for air entrainment and stabilization.[104] Unfortunately, the majority of concrete in the U.S. is air-entrained, with organic AEA chemicals added to the mix to provide the proper amount of fine air bubbles, usually 4 to 6 vol%, specified for the concrete.[104]

The full-scale Norit Darco Hg™ injection tests recently completed at the U.S. Pleasant Prairie plant can be used to illustrate the extent of the problem. Norit Darco Hg™ was injected into the ductwork at rates of from 1 - 10 lbs/MMacf.[104] It was discovered that this PAC badly contaminated the fly ash for concrete purposes.[104] In fact the sorbent effects were so harsh that no fly ash could be sold from the ESP that was used for over a month after the testing stopped due to residual PAC in the system.[104]

This plant produces nearly 200,000 tons of fly ash annually, all of which is currently sold into the ready mix concrete industry.[104] Based on U.S. national averages (US $10/ton) the annual revenue generated from ash sales is US $2 million.[104] If the ash becomes contaminated through traditional PAC injection for mercury control, not only would the revenue be lost, but an additional expense of $1.1 million would be incurred for landfill and disposal expense.[104]

The Foam Index tests is a rapid, industrially accepted method for gauging the degree to which the air content of a concrete will be affected by a fly ash (i.e. its carbon content).[104] This test is done by mixing fly ash and a representative amount of sorbent in a jar, into which distilled water is later added and the jar placed in a shaker.[104] Drops of an AEA solution, (e.g. Darex II®) are sequentially pipetted into the jar and the jar is re-shaken and examined.[104] This is repeated until a stable foam forms on the surface.[104] The Foam Index (FI) value is the quantity of AEA surfactant required to saturate the adsorbing carbon.[104] Dividing the FI by the mass of carbon or PAC in the sample yields the Specific Foam Index (SFI).[104] Lower values are better and increasing the foam index is bad not only

because more AEA is required but, more importantly because it introduces dramatic variability into the concrete-making process.[104]

It is therefore recommended that the sorbents examined during the present study are also evaluated by using the Foam Index tests before they are used in full-scale mercury adsorption studies. As suggested by Lockert et al.[104] each sorbent would need to be mixed with an appropriate quantity of fly ash so that a representative mixture can be reviewed. The results obtained may indicate if the sorbents can be used in a coal-fired power plant by directly injecting the sorbent to the flue gas duct and capturing it with the fly ash particles by using an ESP or FF, or if an alternative method is needed to capture mercury in the flue gas. One proposed option is to have sorbent injection after the APCD that captures fly ash and therefore use a second particulate matter control system to collect sorbent particles (e.g. Toxecon™ design).[16, 104] In this case, the coal fly ash will not be contaminated by the sorbent particles and the fly ash can therefore still be sold for use as a cement replacement additive.

References

1. Ghorishi, S. B.; Sedman, C. B., Low conentration mercury sorption mechanisms and control by calcium-based sorbents: application in coal-fired processes. *J. Air & Waste Manage. Assoc.* **1998,** 48, 1191-1198.

2. Mercury - Basic Information. U.S. Environmental Protection Agency: http://www.epa.gov/mercury/about.htm (Accessed 02 November 2007).

3. Cao, Y.; Duan, Y.; Kellie, S.; Li, L.; Xu, W.; T., R. J.; W., P., Impact of coal chlorine on mercury speciation and emission from a 100-MW utility boiler with cold-side electrostatic precipitators and low-NOx burners. *Energy & Fuels* **2005,** 19, 842-854.

4. Pavlish, J. H.; Sondreal, A. E.; Mann, M. D.; Olson, E. S.; C., G. K.; Laudal, D. L.; Benson, S. A., Status review of mercury control options for coal-fired power plants. *Fuel Processing Technology* **2003,** 82, 89-165.

5. Baek, J.-I.; Lee, S.-H.; L.; Lee, J. K. In *Tests on vapour-phase mercury removal by chemically modified heavy-oil fly ashes in fixed bed and entrained flow reactor*, 22nd Annual International Pittsburgh Coal Conference, Pittsburgh, PA, 15-18 September, 2005.

6. Feeley III, T. J.; Brickett, L. A.; O'Palko, A.; Murphy, J. T. *Field testing of mercury control technologies for coal-fired power plants*; National Energy Technology Laboratory, U.S. Department of Energy: 2005.

7. Carey, T. R.; Hargrove, O. W.; Richardson, C. F.; Chang, R.; Meserole, F. B. In *Factors affecting mercury control in utility flue gas using sorbent injection*, 90th Annual Meeting & Exhibition of the Air & Waste Management Association, 1997.

8. Nelson, S.; Landreth, R.; Zhou, Q.; Miller, J. In *Accumulated Power-Plant Mercury-Removal Experience with Brominated PAC Injection*, Combined Power Plant Air Pollutant Control Mega Symposium, 30 Aug. - 2 Sept., 2004.

9. Rio, S.; Le Coq, L.; Faur, C.; Le Cloirec, P., Production of porous carbonaceous adsorbent from physical activation of sewage sludge: application to wastewater treatment. *Water Science & Technology* **2006,** 53, (3), 237 - 244.

10. Landfill directive - A driefing paper. UK Department for environment food and rural affairs (DEFRA): http://www.defra.gov.uk/environment/waste/topics/landfill-dir/pdf/landfilldir.pdf (Accessed 21 November 2007).

11. Lehmann, C. M. B. Activated carbon adsorbents from waste tires for air quality applications. Master's thesis, University of Illinois at Urbana-Champaign, Urbana, Illinois, 1998.

12. Hsi, H.-C.; Rood, M.; Rostam-Abadi, M.; Chen, S.; Chang, R., Effect of sulphur impregnation temperature on the properties and mercury adsorption capacities of activated carbon fibres (acfs). *Environ. Sci. & Technol.* **2001,** 35, 2785 - 2791.

13. Gee, I. L. Production and application of activated carbons derived from waste materials. PhD thesis, Imperial College, University of London, 1997.

14. Ros, A.; Lillo-Rodenas, M. A.; Fuente, E.; Montes-Moran, M. A.; Martin, M. J.; Linares-Solano, A., High surface area materials prepared from sewage sludge-based precursors. *Chemosphere* **2006,** 65, 132 – 140.

15. Yudovich, Y. E.; Ketris, M. P., Mercury in coal: a review Part 2. Coal use and environmental problems. *International Journal of Coal Geology* **2005,** 62, 135–165.

16. Muggli, D.; Bustard, C. J.; Campbell, T.; Schlager, R.; O'Palko, A.; Chang, R.; Roberts, R.; Kolbus, M.; Rees, M. In *Toxecon II™ and high-temperature reagents or sorbents for low-cost mercury removal*, Power Plant Air Pollutant Control "Mega" Symposium, Baltimore, MD, 28 - 31 August, 2006.

17. Senior, C.; Bustard, C. J.; Baldrey, K.; Starns, T.; Durham, M. In *Characterization of fly ash from full-scale demonstration of sorbent injection for mercury control on coal-fired power plants*, International Technical Conference on Coal Utilization & Fuel Systems, Clearwater, FL, 10 - 13 March, 2003.

18. Mukherjee, A. B.; Zevenhoven, R., Mercury in coal ash and its fate in the Indian subcontinent: A synoptic review. *Science of the Total Environment* **2006,** 368, 384 - 392.

19. *Treatment technologies for mercury in soil, waste, and water*; EPA-542-R-07-003; U.S. Environmental Protection Agency: 2007.

20. Reed, G. P.; Ergudenler, A.; Grace, J. R.; Watkinson, A. P.; Herod, A. A.; Dugwell, D. R.; Kandiyoti, R., Control of gasifer mercury emissions in a hot gas filter: the effect of temperature. *Fuel* **2001,** 80, 623-634.

21. Zevenhoven, R.; Kilpinen, P. Control of pollutants in flue gases and fuel gases. http://users.tkk.fi/~rzevenho/gasbook (Accessed 23 October 2007).

22. Clean Air Mercury Rule. U.S. Environmental Protection Agency: http://www.epa.gov/air/mercuryrule/basic.htm (Accessed 23 October 2007).

23. Canada-wide standards for mercury emissions form coal-fired electric power generation plants. Canadian Council of Ministers for the Environment: http://www.ccme.ca/assets/pdf/hg_epg_cws_w_annex.pdf (Accessed 24 October 2007).

24. Peirce, M.; Jones, H.; Passant, N. R.; Holland, M. *Cost curves for the abatement of heavy metal, PAH and dioxin emissions*; AEAT/R/ENV/0159 Issue 1; Department for Environment, Food & Rural Affairs, the National Assembly for Wales, the Scottish Executive and the Department of the Environment in Northern Ireland: 2002.

25. Wagner, A.; Dore, C. Emissions Summary section of the NAEI. UK National Atmospheric Emissions Inventory: http://www.naei.org.uk/emissions/emissions.php (Accessed 17 October 2007).

26. Sloss, L. L. *Mercury - emissions and control*; CCC/58, ISBN 92-9029-371-3; International Energy Agency Coal Research - The Clean Coal Centre: 2002.

27. Goodarzi, F., Speciation and mass-balance of mercury from pulverized coal fired power plants burning western Canadian subbituminous coals. *Journal of Environmental Monitoring* **2004,** 6, (10), 792 - 798.

28. Galbreath, K. C.; Zygarlicke, C. J., Mercury transformations in coal combustion flue gas. *Fuel Processing Technology* **2000,** 65 - 66, 289 - 310.

29. Pavlish, J. H.; Holmes, M. J.; Benson, S. A.; Crocker, C. R.; Galbreath, K. C., Application of sorbents for mercury control for utilities burning lignite coal. *Fuel Processing Technology* **2004,** 85, 563 - 576.

30. Miller, B. Hazardous emissions from co-combustion of coal, biomass and waste. PhD thesis, Imperial College London, University of London, London, 2001.

31. Frandsen, F.; Dam-Johansen, K.; Rasmussen, P., Trace elements from combustion and gasification of coal—An equilibrium approach. *Progress in Energy and Combustion Science* **1994,** 20, (2), 115 - 138.

32. Hutson, N.; Singer, C.; Richardson, C.; Karwowski, J. In *Practical applications from observations of mercury oxidation and binding mechanisms*, Combined Power Plant Air Pollutant Control Mega Symposium, Washington, DC., 30 Aug. - 2 Sept., 2004.

33. Hassett, D. J.; Eylands, K. E., Mercury capture on coal combustion fly ash. *Fuel* **1999,** 78, 243 - 248.

34. Dunham, G. E.; Olson, E. S.; Miller, S. J. In *Impact of flue gas constituents on carbon sorbents*, Air Quality II - International Conference on Mercury, Trace Elements and Particulate Matter, McLean, VA, 19 - 21 September, 2000.

35. Crocker, C.; Olson, E.; Benson, S.; Laumb, J.; Mackenzie, J.; Mibeck, B. *Investigation of mercury and carbon-based sorbents reaction mechanisms*; Center for Air Toxic Metals - University of North Dakota Energy & Environmental Research Center: 2006.

36. Laumb, J. D.; Benson, S. A.; Olson, E. A., X-ray photoelectron spectroscopy analysis of mercury sorbent surface chemistry. *Fuel Processing Technology* **2004,** 85, 577 – 585.

37. Standards of performance for new and existing stationary sources: electric utility steam generating units. Environmental Protection Agency (EPA): http://www.epa.gov/air/mercuryrule/pdfs/camr_final_preamble.pdf (Accessed 24 October 2007).

38. McCarthy, J. E. *Mercury emissions from electric power plants: states are setting stricter limits*; RL33535; Congressional Research Service: 2007.

39. Zeng, H.; Jin, F.; Guo, J., Removal of elemental mercury from coal combustion flue gas by chloride-impregnated activated carbon. *Fuel* **2004,** 83, 143 – 146.

40. Krishnan, S. V.; Gullett, B. K.; Jorewlczt, W., Sorption of elemental mercury by activated carbons. *Environ. Scl. Technol* **1994,** 28, (8), 1506 - 1512.

41. Miller, S. J.; Dunham, G. E.; Olson, E. S.; Brown, T. D., Flue gas effects on a carbon-based sorbent. *Fuel Process. Technol.* **2000,** 65-66, 343-364.

42. Carey, T. R.; Hargrove, O. W.; Richardson, C. F.; Chang, R.; Meserole, F. B., Factors affecting mercury control in utility flue gas using activated carbon. *J. Air & Waste Manage. Assoc.* **1998,** 48, 1166 - 1174.

43. Stuart, J. L. Development of an experimental system to study mercury uptake by activated carbons under simulated flue gas conditions. Master's thesis, University of Pittsburgh, 2002.

44. Sjostrom, S.; Ebner, T.; Ley, T.; Slye, R.; Richardson, C.; Machalek, T.; Richardson, M.; R., C., Assessing sorbents for mercury control in coal-combustion flue gas. *J. Air & Waste Manage. Assoc.* **2002,** 52, 902 - 911.

45. Miguel, G. S.; Flower, G. D.; Sollars, C. J., Pyrolysis of tyre rubber: Porosity and adsorption characteristics of pyrolytic chars. *Ind. Eng. Chem. Res.* **1998,** 37, 2430-2435.

46. Vassilev, S. V.; Vassileva, C. G., Methods for characterization of composition of fly ashes from coal-fired power stations: A critical overview. *Energy & Fuels* **2005,** 19, (3), 1084 - 1098.

47. Dunham, G. E.; DeWall, R. A.; Senior, C. L., Fixed-bed studies of the interactions between mercury and coal combustion fly ash. *Fuel Process. Technol.* **2003,** 82, 197-213.

48. Dunham, G. E.; DeWall, R. A.; Senior, C. L. In *Fixed-bed studies of the interactions between mercury and coal combustion fly ashes*, EPRI-EPA-DOE-AWMA Mega Symposium and Mercury Conference, Chicago, IL, 20 - 23 August, 2001.

49. Miller, S. J. *Bench-scale tests to evaluate mercury fly ash interactions*; FY99-XXXI-87; Energy & Environmental Research Center, Univ. of North Dakota: 2001.

50. Landreth, R. R.; Nelson Jr, S.; Liu, X.; Tang, Z.; Miller, J. E.; Hoeflich, P. C.; Moore, G.; Brickett, L. A. In *New full-scale results from B-PAC control trials*, Power Plant Air Pollutant Control "Mega" Symposium, Baltimore, MD, 28 - 31 August, 2006.

51. Norit activated carbons for mercury removal from power plant flue gas. Norit Americas Inc.: http://www.norit-americas.com/pdf/Mercury_Removal_Power_Plants_rev4.pdf (Accessed 23 October 2007).

52. George, A., Dugwell, D.R. and Kandiyoti, R., The development of a miniaturised technique for measuring the leachability of toxic trace elements from coal-biomass co-combustion ash residues. *Energy & Fuels* **2007,** 21, 728 - 734.

53. Reed, G. P. Control of trace elements in gasification. PhD thesis, Imperial College, University of London, 2000.

54. Wigley, F.; Williamson, J. *Coal mineral transformations - effects on boiler ash behaviour*; Report no. COAL R278 DTI/Pub URN 05/659; DTI / Imperial College London: 2005.

55. Ghorishi, S. B.; Lee, C. W.; Jozewicz, W. S.; Kilgroe, J. D., Effects of fly ash transition metal content and flue gas HCl/SO_2 ratio on mercury speciation in waste combustion. *Environmental Engineering Science* **2005,** 22, (2), 221 - 231.

56. Gibb, W.; Quick, W.; Salisbury, M. *Technology status review - monitoring and control of trace elements*; COAL R249 DTI/Pub URN 03/1582; Department of Trade & Industry: 2003.

57. Niksa, S.; Bour, D. P.; Burnett, T. A.; Handagama, N. B. Mercury Monitoring - Use predictive techniques to guide your mercury compliance strategy. POWER Magazine: http://www.powermag.com/powerweb/archive_article.asp?a=60-SR_MM2&y=2007&m=august (Accessed 22 November 2007).

58. Miguel, G. S. Activated carbon produced by pyrolysis and physical activation of waste tyres. PhD thesis, Imperial College, University of London, 1999.

59. Rostam-Abadi, M.; Lu, Y.; Funk, C. In *Properties of unburned carbons form three coal-fired power plants and their relationships to mercury capture*, Air Quality V - International Conference on Mercury, Trace Elements, Trace Elements and Particulate Matter, 18-21 September, 2005.

60. Koplan, S.; Okun, D. T.; Hillman, J. A.; Lane, C. R.; Pearson, D. R.; Aranoff, S. L.; Rogowsky, R. A.; McClure, J.; Comly, N.; Stone, P.; Trost, S.; Yost, C.; Fishberg, D.; Driscoll, K. *Certain activated carbon from china - Investigation No. 731-TA-1103 (Preliminary)*; Publication 3852; United States International Trade Commission: Washington, DC, 2006.

61. Pollard, S. J. T. Low-cost adsorbents from industrial wastes. PhD thesis, Imperial College, University of London, 1990.

62. Bansal, R. C.; Goyal, M., *Activated carbon adsorption*. 1st ed.; CRC Press, Taylor & Francis Group: Boca Raton, FL, 2005.

63. Dean, J. A., *Lange's Handbook of Chemistry*. 13th Edition ed.; McGraw-Hill Company: 1985.

64. Green, D. W., *Perry's chemical engineers' handbook*. 7th ed.; McGraw-Hill Inc.: New York, 1998.

65. Ghorishi, S. B.; Keeney, R. M.; Serre, S. D.; Gullett, B. K.; Jozewicz, W. S., Development of a Cl-impregnated activated carbon for entrained-flow capture of elemental mercury. *Environ. Sci. Technol.* **2002,** 36, 4454 - 4459.

66. Ghorishi, S. B.; Lee, C. W.; Kilgroe, J. D. In *Mercury speciation in combustion systems: studies with simulated flue gases and model fly ashes*, Air and Waste Management Association 92nd Annual Meeting and Exhibition, St. Louis, MO, 20 - 24 June, 1999.

67. Lee, C. W.; Kilgroe, J. D.; Ghorishi, S. B. In *Speciation of mercury in the presence of coal and waste combustion fly ashes*, Air and Waste Management Association 93rd Annual Meeting and Exhibition, Salt Lake City, UT, 18 - 22 June, 2000.

68. Richaud, R.; Lachas, H.; Collot, A.; Mannerings, A. G.; Herod, A. A.; Dugwell, D. R.; Kandiyoti, R., Trace mercury concentrations in coals and coal-derived materials determined by Atomic Absorption Spectro-photometry. *Fuel* **1998,** 77, 359-368.

69. Rahman, L.; Corns, W. T.; Bryce, D. W.; Stockwell, P. B., Determination of mercury, selenium, bismuth, arsenic and antimony in human hair by microwave digestion atomic fluorescence spectrometry. *Talanta* **2000,** 52, (5), 833 - 843.

70. Fitzgerald, F. D.; Thomson, C.; McGhie, C.; Dexter, M. A.; Corns, W. T.; Stockwell, P. B.; Dugwell, D. R.; Kandiyoti, R.; George, A.; Seneviratne, H. R.; Quick, W. J.; Weatherstone, S.; Curtis, S. *Towards zero emissions of NO_x and mercury from coal-fired power plant*; DTI/Pub URN 06/***; UK Department of Trade and Industry (DTI): 2007.

71. Norton, G.; Eckels, D.; Criswell, C. In *Continuous mercury and chloride Monitors for coal gasifiers*, Advanced Coal-Fired Power Systems '96 Review Meeting, Morgantown, West Virginia, 16 - 18 July, 1996.

72. Lachas, H. Trace element partitioning and emission control during coal gasification. PhD thesis, Imperial College London, University of London, 1999.

73. Scheck, R. W.; Mora, R. R.; Belba, V. H.; Horney, F. A. *Economics of fabric filters and electrostatic precipitators - 1984. Final report*; EPRI-CS-4083; Stearns Catalytic Corp., Denver, CO (USA): 1985.

74. Meyer, D. E.; Sikdar, S. K.; Hutson, N. D.; Bhattacharyya, D., Examination of sulfur-functionalized, copper-doped iron nanoparticles for vapor-phase mercury capture in entrained-flow and fixed-bed systems. *Energy & Fuels* **2007,** 21, 2688 - 2697.

75. Vidic, R. D. *Development of novel activated carbon-based adsorbents for control of mercury emissions from coal-fired power plants*; DE-FG22-96PC96212; Department of Civil and Environmental Engineering, University of Pittsburgh: 17 March, 1997.

76. Mitchell, G. D.; Dorko, W. D. *Mercury in nitrogen gas research gas mixture*; EPA Reference : DW13939860-01-0; National Institute of Standards and Technology: 2004.

77. Sjostrom, S.; Ebner, T.; Slye, R.; Chang, R.; Strohfus, M.; Pelerine, J.; Smokey, S. In *Full-scale evaluation of mercury control at Great River Energy's Stanton generating*

station using injected sorbents and a spray dryer/baghouse, Air Quality III Conference, Arlington, VA, 10 - 12 September, 2002.

78. Li, J.; Yuan, Y.; Perry, R.; Maroto-Valer, M. M.; Quick, W. In *Mercury speciation and retention in fly ash*, International Conference on Coal Science and Technology, Nottingham, UK, 28 - 31 August, 2007.

79. Fahlke, J.; Bursik, A., Impact of the state-of-the-art of flue gas cleaning on mercury species emissions from coal-fired steam generators. *Water, Air, and Soil Pollution* **1995,** 80, 209 - 215.

80. Hocquel, M.; Unterberger, S.; Hein, K. R. G., Influence of temperature and HCl concentration on mercury speciation in the presence of calcium oxide (CaO). *Chem. Eng. Technol.* **2001,** 24, (12), 1267 - 1272.

81. Metzger, M.; Braun, H., In-situ mercury speciation in flue gas by liquid and solid sorption systems. *Chemosphere* **1987,** 16, 821 - 832.

82. *Toxicity characteristic leaching procedure*; SW-846 Ch.8.4.; US Environmental Protection Agency (EPA): Issued: 07/01/1992.

83. Rao, S. R.; Leja, J., *Surface chemistry of froth flotation*. Second ed.; Springer: 2004.

84. Padak, B.; Brunetti, M.; Lewis, A.; Wilcox, J., Mercury binding on activated carbon. *Environmental Progress* **2006,** 25, (4), 319 - 326.

85. Olson, E. S.; Sharma, R. K.; Miller, S. J.; Dunham, G. E. In *Identification of the breakthrough oxidized mercury species from sorbents in flue gas*, Specialty Conference on Mercury in the Environment, 15-17 September, 1999.

86. Pavlish, J. H.; Holmes, M. J.; Benson, S. A.; Crocker, C. R. *Mercury control technologies for uitlities burning lignite coal*; Energy & Environmental Research Center, University of North Dakota - prepared for National Energy Technology Laboratory, U. S. Department of Energy: 2002.

87. Naik, C. V.; Krishnakumar, B.; Niksa, S. In *Predicting Hg emissions rates from utility gas cleaning systems*, International Conference on Coal Science and Technology, Nottingham, UK, 28 - 31 August, 2007.

88. Kulaots, I.; Hurt, R. H.; Suuberg, E. M., Size distribution of unburned carbon in coal fly ash and its implications. *Fuel* **2004,** 83, 223 - 230.

89. *Fly ash for concrete — Part 1: definition, specifications and conformity criteria*; BS EN 450-1:2005; ISBN 0 580 45506 8; British Standards: 2005.

90. Jarvis, K. E.; Gray, A. L., *Handbook of inductively coupled plasma mass spectromerty*. 3rd ed.; Blackie Academic & Professional: Glasgow, 1995.

91. Bustard, C. J.; Durham, M.; Lindsey, C.; Starns, T.; Martin, C.; Schlager, R.; Sjostrom, S.; Renninger, S.; McMahon, T.; Monroe, L.; Goodman, J. M.; R., M. In

Results of activated carbon injection for mercury control upstream of a COHPAC fabric filter, Mega Meeting: Power Plant Air Pollution Control Symposium, Washington D.C., 19-22 May, 2003.

92. Chen, S.; Rostam-Abadi, M.; Hsi, H.-C.; Rood, M.; Richardson, C. F.; Chang, R. *Preparation and evaluation of novel activated carbons from Illinois coal for mercury removal*; 97-1/1.4A-4; Illinois Clean Coal Institute: 1999.

93. Chen, S.; Rostam-Abadi, M., Mercury Removal from combustion flue gas by activated carbon injection: Mass transfer effects. *ACS Division of Fuel Chemistry* **1996,** 41, (1), 442 - 446.

94. Bustard, C. J.; Durham, M.; Lindsey, C.; Starns, T.; Bladrey, K.; Martin, C.; Sjostrom, S.; Slye, R.; Renninger, S.; Monroe, L. In *Full-scale evaluation of mercury control with sorbent injection and COHPAC at Alabama Power E.C. Gaston*, EPRI-EPA-DOE-AWMA Mega Symposium and Mercury Conference, Chicago, IL, 20 - 23 August, 2001.

95. Holmes, M.; Dunham, G.; Edwin, O.; Mibeck, B.; Zhaung, Y.; Pavlish, J. *Development of mercury control technologies*; Center for Air Toxic Metals - University of North Dakota Energy & Environmental Research Center: 2004.

96. Presto, A. A.; Granite, E. J.; Karash, A., Further investigation of the impact of sulfur oxides on mercury capture by activated carbon. *Ind. Eng. Chem. Res.* **2007,** 46, 8273 - 8276.

97. Srivastava, R. K.; Miller, C. A.; Erickson, C.; Jambhekar, R., Emissions of sulfur trioxide from coal-fired power plants. *J. Air & Waste Manage. Assoc.* **2004,** 54, 750 - 762.

98. Olson, E. S.; Crocker, C. R.; Sun, J.; Brandt, K. H.; Dunham, G. E.; Pavlish, J. H. In *The interactions of SO_2 and SO_3 on a carbon sorbent and their impact on mercury capture*, Power Plant Air Pollutant Control "Mega" Symposium, Baltimore, MD, 28 - 31 August, 2006.

99. Dunham, G. E.; Hill-Brandt, K. L.; Olson, E. S.; Pavlish, J. H. In *The effect of SO_3 on Mercury Capture by activated carbons sorbents*, Clearwater Coal Conference, Clearwater, Fl, 21 - 26 May, 2006.

100. Balogh, S. J.; Nollet, Y. H., Mercury mass balance at a wastewater treatment plant employing sludge incineration with offgas mercury control. *Science of The Total Environment* **2008,** 389, (1), 125 - 131.

101. Dalai, A. K.; Zaman, J.; Hall, E. S.; Tollefson, E. L., Preparation of activated carbon from Canadian coals using a fixed-bed reactor and a spouted bed-kiln system. *Fuel* **1996,** 75, 227 - 237.

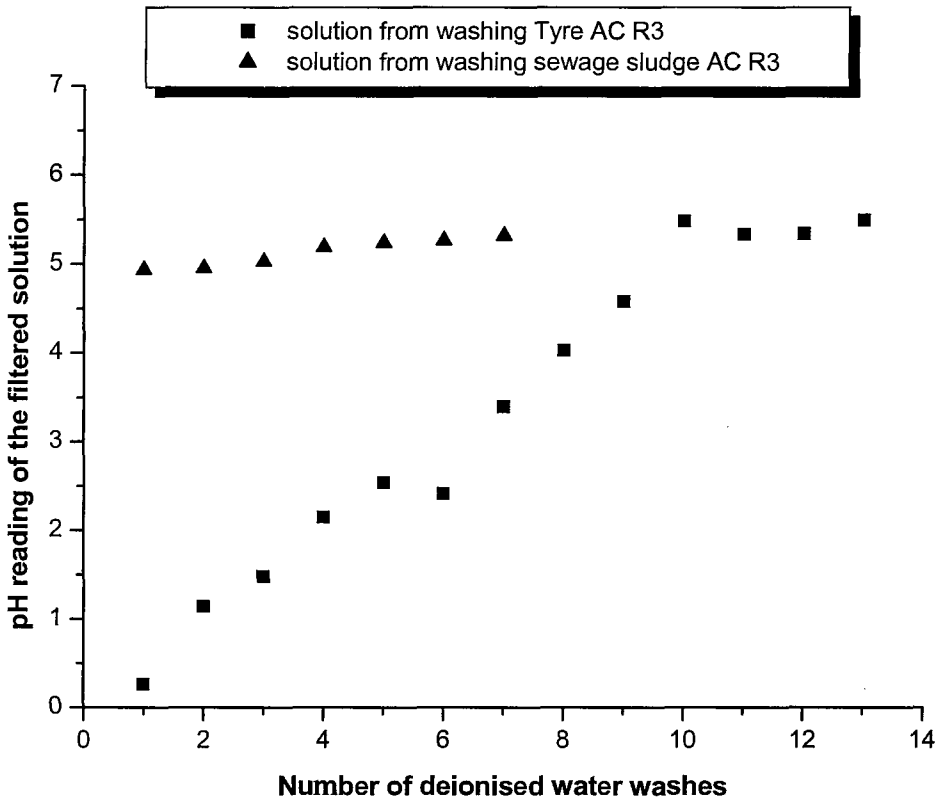
102. Hutson, N. D., Mercury capture on fly ash and sorbents: the effects of coal properties and combustion conditions. *Water, Air, & Soil Pollution: Focus* **2008,** 8, 323 - 331.

103. Instructions for handling glass bottles of sulfur trioxide, stabilized - Technical Information Bulletin AL-141. Sigma Aldrich: http://www.sigmaaldrich.com/aldrich/bulletin/al_techbull_al141.pdf (Accessed 11 June 2007).

104. Lockert, C. A.; Zhou, Q.; Zhang, Y.; S., N. J. In *Further progress toward concrete-friendly™ mercury sorbents*, Air Quality V - International Conference on Mercury, Trace Elements, SO_3 and Particulate Matter, Arlington, VA, 18 - 21 September, 2005.

Appendix -A

pH readings of the filtered solutions after washing Tyre AC R3 or sewage sludge AC R3 with deionised water for 5 minutes.



Appendix -B

The analysis methods used by TES Bretby (UK) to analyse the sorbents evaluated during this study [obtained from TES Bretby (UK)].

Method	Parameter	Principle of method
Documented In-House Methods based on BS 1016 Part 1:1973 and BS1017 Part 1:1989	6 mesh Moisture %	A known mass of sample is heated in a stream of nitrogen at a temperature of 105°C to 110°C for a minimum of 3 hours. The moisture content is determined from the loss in mass.
Documented In-House Method based on BS 1016 Part 104 Section 104.1:1991	Moisture %	A known mass of sample is heated in a stream of nitrogen at a temperature of 105°C to 110°C for 2.5 hours. The moisture content is determined from the loss in mass
Documented In-House Method based on BS 1016 Part 104 Section 104.4:1991	Ash %	A known mass of the sample is heated in air to 815°C +/- 10 in 60 minutes and is kept at this temperature for a minimum of an additional 90 mins. The ash content is determined from the mass of residue remaining after incineration
Documented In-House Methods by instrumental analysis using Leco SC 132 and SC 432 analysers	Sulphur %	A known mass of sample is incinerated at 1350°C in an oxygen- enriched atmosphere. The sulphur in the sample is converted to sulphur dioxide and is measured by an infrared cell. The measured quantity is converted into a percentage
Documented In-House Method by Exeter CE440 Elemental Analyser	Carbon % Hydrogen % Nitrogen %	A known mass of coal is burnt in oxygen. The combustion gases are passed over suitable reagents to assure complete oxidation and removal of undesirable by-products such as sulphur, phosphorus and halogen gases. The oxides of nitrogen are converted to molecular nitrogen and residual oxygen is removed in the reduction tube. The concentrations of carbon dioxide, water vapour and nitrogen gas are measured by thermal conductivity cells. The instrument uses the concentration of these gases together with the sample weight to give a direct readout of the percentages of carbon, hydrogen and nitrogen.
Documented In-House Method based on method described in Analyst:November 1990, Vol 115 using Wavelength Dispersive XRF	Chlorine %	A sample is presented to the X Ray tube operating at 40kV, 5mA via the robotised sample arm. X Ray Fluorescence of the elements chlorine and silicon in the sample are measured via fixed monochromators. The X Rays counts are converted to concentrations from calibration and equation for chlorine and silicon respectively.

Appendix -C

LECO AMA 254 Mercury Analyser – Theory of operation (information obtained from Leco Instruments (UK) limited in Stockport)

The Leco AMA 254 Advanced Mercury Analyser is an Atomic Adsorption Spectrometer that is specifically designed to determine total mercury content in various solids and liquids - without sample pre-treatment or sample pre-concentration. Designed with a front-end combustion tube that is ideal for the decomposition of difficult matrices like coal, combustion residues, soils, and fish. The instrument's operation may be separated into three phases during any given analysis; Decomposition, Collection, and Detection.

The first stage of an analysis is known as Decomposition phase. During this phase, a sample container with a nominal amount of the matrix is placed inside a pre-packed combustion tube. This combustion tube-heated to ~750°C through an external coil - provides the necessary thermal decomposition of the sample into a gaseous form. The evolved gases are then transported (via an oxygen carrier gas) to the other side of the combustion tube. This portion of the tube, pre-packed with specific catalytic compounds, represents the area in the instrument where all impurities (i.e. ash, moisture, halogens and minerals) are removed from the evolved gas.

Following decomposition, the cleaned, evolved gas is transported to the amalgamator for the Collection phase of the system. The amalgamator, a small glass tube containing gold-plated ceramics, collects all the mercury in the vapour. With a strong affinity for mercury and a significantly lower temperature than the decomposition phase, the amalgamator is capable of trapping all the mercury for subsequent detection. When all the mercury is has been collected from the evolved gases, the amalgamator is heated to ~900°C - essentially releasing all the mercury vapour to the detection system.

The released mercury vapour is transported to the final phase of the analysis - Detection phase. During the Detection phase, all the vapour passes through two sections of an apparatus known as a cuvette. The cuvette is positioned in the path length of a standard

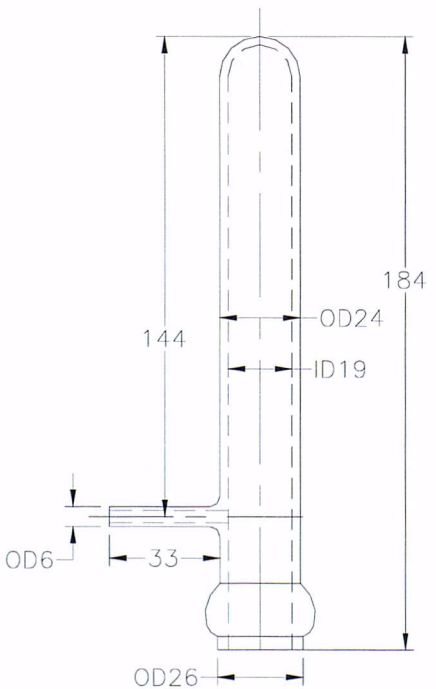
Atomic Adsorption Spectrometer. The Spectrometer uses an element-specific lamp that emits at a wavelength of 253.7 nm, and a silicon UV detector for mercury quantification.

AMA 254 Advanced Mercury Analyser Specification Sheet

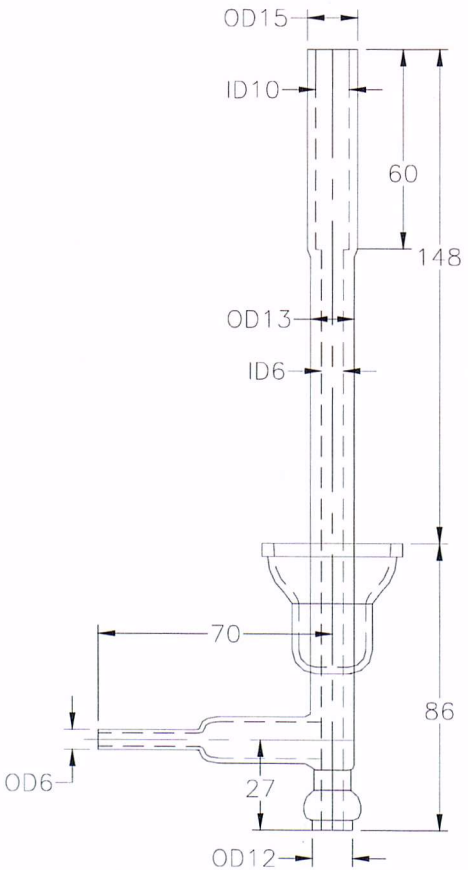
Instrument range @ 100 mg:	Mercury: 5 ppb to 5 ppm
Precision:	Mercury: 2.5 ppb or ≤ 5% RDS, whichever is greater
Readability:	1 ppb
Analysis time:	5 minutes
Nominal sample size:	Solids: 100 mg
	Liquids: 100 µL
Gas required:	Carrier: Oxygen, 99.5%, 30 psi, 160 to 180 mL/min

Appendix -D

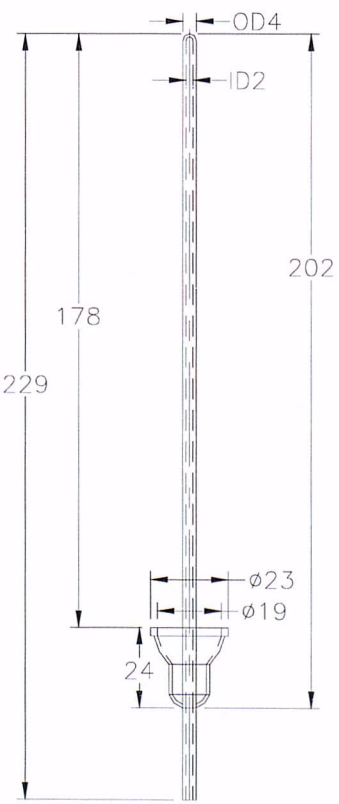
Details of the sorbent test reactor's components



Outer body



Main body –
Sorbent sample holder



Thermocouple well

Appendix -E

Details of the flow meters FM-1 to FM-8 supplied by Dakota Instruments Inc. Orangeburg, NY, USA

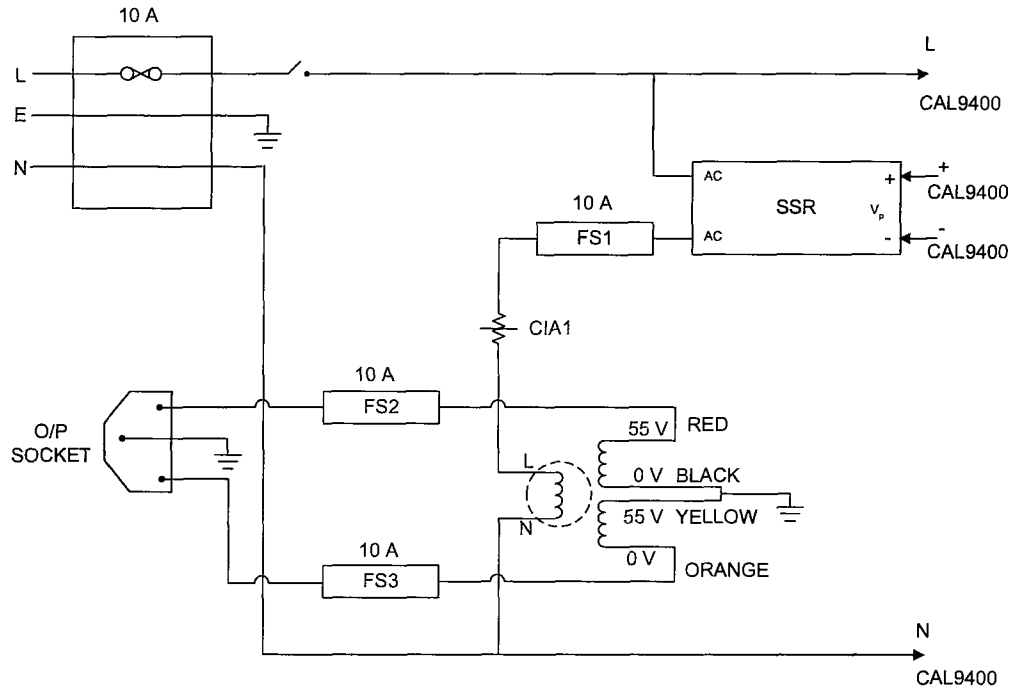
Flow meter	Model number	Tube number	Float
FM-1	6AT3221M6-GHN	023-92-N	Glass
FM-2	6AT3205M1-GHN	032-41-N	Glass
FM-3	6AT3201M6-GHN	042-08-N	Glass
FM-4	6AT3231M6-GHN	042-07-N	Sapphire
FM-5	6AT3231M6-GHN	042-07-N	Sapphire
FM-6	6AT3231M6-GHN	042-07-N	Sapphire
FM-7	6AT3232M6-GHN	042-07-N	Glass

Each of the above flow meters had OD 10mm glass nipple connections at the inlet and outlet, and PTFE precision metering valves (MFV™) for controlling the flow.

Flow meter FM-8 was a GAP variable area flow meter with tube number CID 388PC.

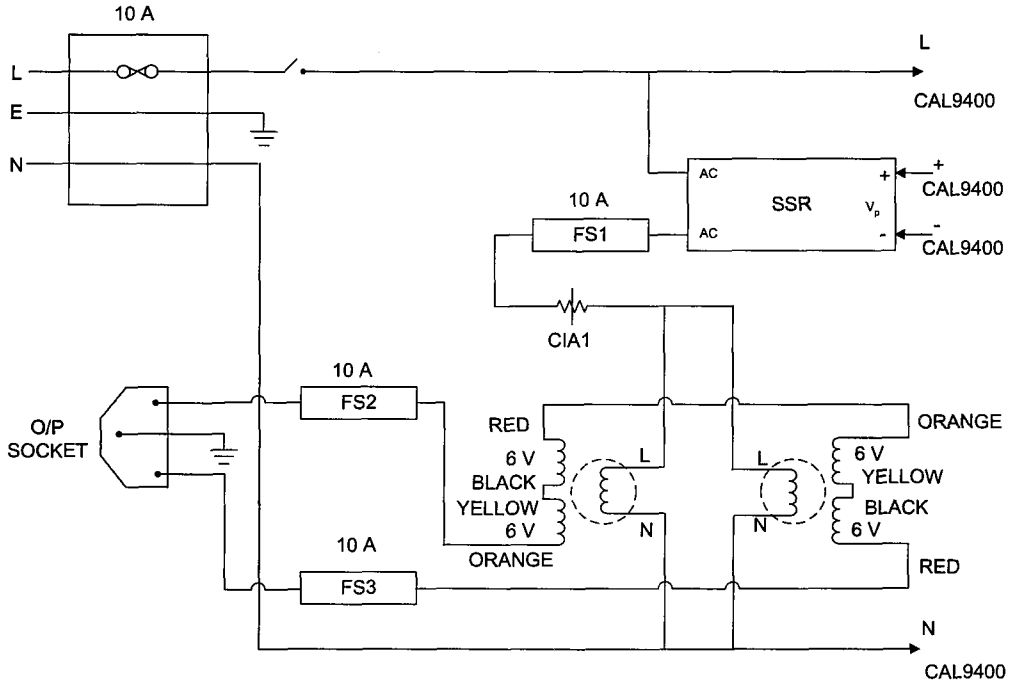
Appendix -F

Single line diagram of Temperature Controller 1



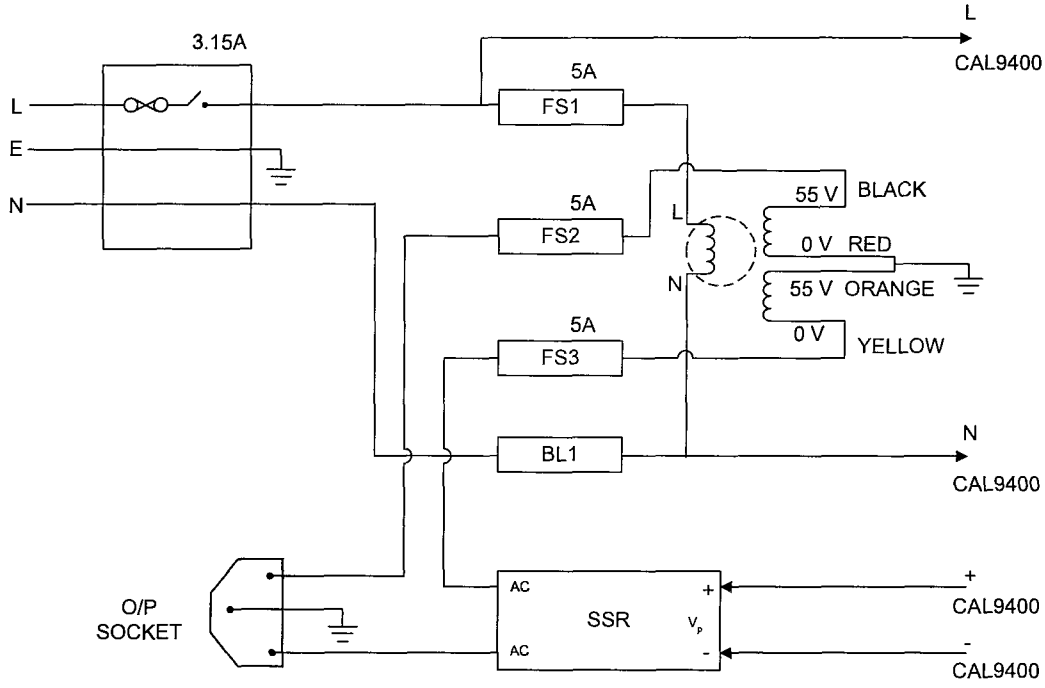
CIA1 - Current inrush attenuator (RS # 210-752 5R 6A)

Single line diagram of Temperature Controller 2



CIA1 - Current inrush attenuator (RS # 210-752 5R 6A)

Single line diagram of Temperature Controller 3



Appendix -G

Table G-1 Mercury capture efficiencies at different hold times with a gas stream of only Hg^0 vapour and nitrogen gas

Norit Darco Hg™ (Test temperature = 150°C)

Hold time (min.)	Test date	Sorbent mass (mg)	Total Hg in sorbent (ng)	Initial Hg conc. on sorbent (ppm)	Hg captured by sorbent (ng)	Hg in backup (ng)	Hg into the reactor (ng)	Hg capture efficiency	Hg mass balance diff.	Mean efficiency	SD
30	29/05/07	100.3	20.2	0.0040	19.82	14.4	34.3	58%	6%	58%	-
45	06/06/07	98.0	25.7	0.0011	25.64	18.4	44.0	58%	-9%	54%	4%
	08/07/07	100.0	21.9	0.0015	21.73	22.1	43.8	50%	-9%		
60	04/04/07	99.9	29.9	0.0082	29.05	36.9	65.9	44%	2%	40%	3%
	12/04/07	100.0	21.1	0.0011	20.96	37.7	58.6	36%	-9%		
	12/04/07	99.9	24.1	0.0011	24.03	38.4	62.4	38%	-3%		
	17/05/07	99.7	28.3	0.0064	27.71	41.9	69.6	40%	8%		
120	01/06/07	99.7	33.6	0.0015	33.43	71.7	105.1	32%	-18%	32%	-
180	03/06/07	100.1	46.7	0.0013	46.55	113.4	160.0	29%	-17%	32%	3%
	20/07/07	100.3	54.8	0.0037	54.46	98.9	153.3	36%	-21%		

Table G-1 Mercury capture efficiencies at different hold times with a gas stream of only Hg^0 vapour and nitrogen gas (continued)

Tyre char R1 (Test temperature = 150°C)

Hold time (min.)	Test date	Sorbent mass (mg)	Total Hg in sorbent (ng)	Initial Hg conc. on sorbent (ppm)	Hg captured by sorbent (ng)	Hg in backup (ng)	Hg into the reactor (ng)	Hg capture efficiency	Hg mass balance diff.	Mean efficiency	SD
30	29/05/07	100.3	31.5	0.1055	20.9	10.0	30.9	68%	-4%	66%	3%
	07/06/07	100.9	26.0	0.0729	18.7	11.7	30.4	61%	-6%		
	10/06/07	100.5	25.3	0 .0729	18.0	8.7	26.7	67%	-17%		
45	06/06/07	100.5	31.0	0.0701	23.9	24.6	48.5	49%	1%	54%	6%
	07/06/07	100.2	34.8	0.0729	27.5	18.1	45.6	60%	-6%		
60	20/04/07	99.5	36.1	0.0935	26.8	28.3	55.1	49%	-14%	47%	5%
	02/05/07	100.5	31.3	0.0837	22.9	33.8	56.7	40%	-12%		
	02/05/07	90.0	42.0	0.0837	34.4	30.3	64.7	53%	1%		
120	30/05/07	99.9	63.9	0.1026	53.65	72.2	125.9	43%	-2%	43%	-
180	02/06/07	100.5	78.7	0.0955	69.1	101.9	171.0	40%	-11%	38%	2%
	19/07/07	100.0	73.2	0.0799	65.2	115.4	180.6	36%	-6%		

Table G-1 Mercury capture efficiencies at different hold times with a gas stream of only Hg^0 vapour and nitrogen gas (continued)

Tyre AC R1 (Test temperature = 150°C)

Hold time (min.)	Test date	Sorbent mass (mg)	Total Hg in sorbent (ng)	Initial Hg conc. on sorbent (ppm)	Hg captured by sorbent [ng]	Hg in backup [ng]	Hg into the reactor [ng]	Hg capture efficiency	Hg mass balance diff.	Mean efficiency	SD
30	30/05/07	99.2	27.9	0.1017	17.9	18.1	36.0	50%	12%	49%	1%
	04/07/07	100.4	20.9	0.0525	15.6	17.0	32.6	48%	1%		
45	05/07/07	100.2	31.0	0.0471	26.3	21.3	47.6	55%	-1%	49%	7%
	08/07/07	99.5	24.5	0.0263	21.9	30.1	52.0	42%	8%		%
60	01/03/07	99.8	35.6	0.0775	27.8	37.9	65.7	42%	2%	40%	6%
	13/04/07	99.7	30.1	0.0856	21.6	36.7	58.3	37%	-10%		
	13/04/07	100.1	29.2	0.0856	20.6	42.6	63.2	33%	-2%		
	05/07/07	99.7	38.5	0.0471	33.8	35.0	68.8	49%	7%		
120	01/06/07	100.2	38.6	0.0099	28.6	76.5	105.1	27%	-18%	38%	11%
	13/10/07	100.2	83.0	0.0493	78.1	80.3	158.4	49%	23%		
180	21/07/07	100.2	75.8	0.0605	69.7	98.2	168.0	42%	-13%	46%	4%
	06/10/07	100.3	107.9	0.0513	102.7	104.3	207.0	50%	7%		

Table G-2 Mercury capture efficiencies for different sorbent sample masses when evaluated using a gas stream of only Hg^0 vapour and nitrogen gas

Norit Darco Hg™ (Test temperature = 150°C, hold time = 60 minutes)

Approx. sample mass (mg)	Test date	Sorbent mass (mg)	Total Hg in sorbent (ng)	Initial Hg conc. on sorbent (ppm)	Hg captured by sorbent (ng)	Hg in backup (ng)	Hg into the reactor (ng)	Hg capture efficiency	Hg mass balance diff	Mean efficiency	SD
20	15/03/07	19.8	6.9	0.0053	6.8	59.8	66.6	10%	3%	10%	2%
	16/03/07	19.8	8.3	0.0047	8.2	57.2	65.4	13%	2%		
	16/03/07	20.3	7.0	0.0047	6.9	55.0	61.8	11%	-4%	49%	7%
	21/08/07	20.0	4.5	0.0009	4.4	67.2	71.70	6%	11%		%
	21/08/07	20.4	5.6	0.0009	5.6	62.7	68.3	8%	6%		
10	Refer Table G-1 for Norit Darco Hg™ results with 100 mg sample mass										

Fly ash D (Test temperature = 150°C, hold time = 60 minutes)

Approx. sample mass (mg)	Test date	Sorbent mass (mg)	Total Hg in sorbent (ng)	Initial Hg conc. on sorbent (ppm)	Hg captured by sorbent (ng)	Hg in backup (ng)	Hg into the reactor (ng)	Hg capture efficiency	Hg mass balance diff	Mean efficiency	SD
20	08/03/07	20.2	40.8	0.4225	32.3	31.2	63.5	51%	-1%	51%	0.8%
	24/08/07	20.3	45.8	0.5151	35.3	35.0	70.3	50%	9%		
100	18/05/07	100.1	107.9	0.4979	58.0	5.6	63.6	91%	-1%	91%	0.1%
	18/05/07	99.0	108.7	0.4979	59.4	5.9	65.3	91%	1%		

Table G-2 Mercury capture efficiencies for different sorbent sample masses when evaluated using a gas stream of only Hg^0 vapour and nitrogen gas (continued)

Fly ash E (Test temperature = 150°C, hold time = 60 minutes)

Approx. sample mass (mg)	Test date	Sorbent mass (mg)	Total Hg in sorbent (ng)	Initial Hg conc. on sorbent (ppm)	Hg captured by sorbent (ng)	Hg in backup (ng)	Hg into the reactor (ng)	Hg capture efficiency	Hg mass balance diff	Mean efficiency	SD
20	12/03/07	20.4	42.7	0.5306	31.9	31.2	63.2	51%	-2%	53%	2%
	15/08/07	20.6	52.4	0.6624	38.8	33.3	72.1	54%	12%		
100	22/03/07	100.5	110.0	0.5107	58.7	9.1	67.8	87%	5%	89%	2%
	22/03/07	100.5	117.0	0.5107	65.6	6.1	71.7	91%	11%		

Fly ash F (Test temperature = 150°C, hold time = 60 minutes)

Approx. sample mass (mg)	Test date	Sorbent mass (mg)	Total Hg in sorbent (ng)	Initial Hg conc. on sorbent (ppm)	Hg captured by sorbent (ng)	Hg in backup (ng)	Hg into the reactor (ng)	Hg capture efficiency	Hg mass balance diff	Mean efficiency	SD
20	15/08/07	19.9	78.8	0.9855	59.2	9.0	68.1	87%	6%	81%	6%
	15/08/07	19.1	72.0	0.9855	53.2	18.4	71.6	74%	11%		
100	19/08/07	99.5	166.6	1.1589	51.2	1.4	52.7	97%	-18%	91%	0.1%
	20/08/07	100.5	167.5	1.1215	54.8	2.9	57.7	95%	-10%		

Table G-2 Mercury capture efficiencies for different sorbent sample masses when evaluated using a gas stream of only Hg^0 vapour and nitrogen gas (continued)

Tyre char R1 (Test temperature = 150°C, hold time = 60 minutes)

Approx. sample mass (mg)	Test date	Sorbent mass (mg)	Total Hg in sorbent (ng)	Initial Hg conc. on sorbent (ppm)	Hg captured by sorbent (ng)	Hg in backup (ng)	Hg into the reactor (ng)	Hg capture efficiency	Hg mass balance diff	Mean efficiency	SD
20	03/05/07	20.3	11.3	0.0614	10.0	45.7	55.8	18%	-13%	53%	2%
	04/05/07	20.5	15.0	0.0781	13.4	43.0	56.3	24%	-12%		
	17/08/07	20.4	20.7	0.1035	18.6	49.4	68.1	27%	-1%		
100	Refer Table G-1 for tyre char R1 results with 100 mg sample mass										

Tyre char R2 (Test temperature = 150°C, hold time = 60 minutes)

Approx. sample mass (mg)	Test date	Sorbent mass (mg)	Total Hg in sorbent (ng)	Initial Hg conc. on sorbent (ppm)	Hg captured by sorbent (ng)	Hg in backup (ng)	Hg into the reactor (ng)	Hg capture efficiency	Hg mass balance diff	Mean efficiency	SD
20	26/08/07	19.8	30.7	0.0097	30.46	41.4	71.9	42%	12%	37%	4%
	26/08/07	20.0	24.7	0.0097	24.5	50.2	74.7	33%	16%		
	31/08/07	20.7	25.2	0.0132	24.9	43.8	68.8	36%	7%		

Tyre char R3 (Test temperature = 150°C, hold time = 60 minutes)

Approx. sample mass (mg)	Test date	Sorbent mass (mg)	Total Hg in sorbent (ng)	Initial Hg conc. on sorbent (ppm)	Hg captured by sorbent (ng)	Hg in backup (ng)	Hg into the reactor (ng)	Hg capture efficiency	Hg mass balance diff	Mean efficiency	SD
20	03/04/07	20.1	4.0	0.0363	3.2	48.1	51.4	6%	-20%	6%	1%
	03/04/07	20.0	3.6	0.0363	2.9	51.9	54.7	5%	-15%		

Table G-2 Mercury capture efficiencies for different sorbent sample masses when evaluated using a gas stream of only Hg^0 vapour and nitrogen gas (continued)

Tyre AC R1 (Test temperature = 150°C, hold time = 60 minutes)

Approx. sample mass (mg)	Test date	Sorbent mass (mg)	Total Hg in sorbent (ng)	Initial Hg conc. on sorbent (ppm)	Hg captured by sorbent (ng)	Hg in backup (ng)	Hg into the reactor (ng)	Hg capture efficiency	Hg mass balance diff	Mean efficiency	SD
20	17/03/07	20.3	9.5	0.0834	7.8	49.0	56.8	14%	-12%	13.2%	4%
	17/03/07	20.3	7.3	0.0834	5.6	56.0	61.6	9%	-4%		
	21/08/07	20.2	9.4	0.0381	8.6	63.8	72.4	12%	12%		
	08/09/07	20.4	14.9	0.0633	13.6	51.5	65.1	21%	1%		
100	Refer Table G-1 for tyre AC R1 results with 100 mg sample mass										

Tyre AC R2 (Test temperature = 150°C, hold time = 60 minutes)

Approx. sample mass (mg)	Test date	Sorbent mass (mg)	Total Hg in sorbent (ng)	Initial Hg conc. on sorbent (ppm)	Hg captured by sorbent (ng)	Hg in backup (ng)	Hg into the reactor (ng)	Hg capture efficiency	Hg mass balance diff	Mean efficiency	SD
20	26/02/07	20.5	7.4	0.0634	6.2	49.2	55.4	11%	-14%	10%	1%
	26/02/07	19.8	7.1	0.0634	5.9	55.8	61.6	10%	-4%		
100	30/06/07	100.3	67.2	0.0756	59.6	7.0	66.6	89%	3%	86%	3%
	01/07/07	100.5	58.5	0.0768	50.7	9.6	60.3	84%	-6%		
	31/08/07	99.8	64.4	0.0542	58.9	12.0	70.9	83%	10%		

Table G-2 Mercury capture efficiencies for different sorbent sample masses when evaluated using a gas stream of only Hg^0 vapour and nitrogen gas (continued)

Sewage sludge char (Test temperature = 150°C, hold time = 60 minutes)

Approx. sample mass (mg)	Test date	Sorbent mass (mg)	Total Hg in sorbent (ng)	Initial Hg conc. on sorbent (ppm)	Hg captured by sorbent (ng)	Hg in backup (ng)	Hg into the reactor (ng)	Hg capture efficiency	Hg mass balance diff	Mean efficiency	SD
20	23/02/07	20.4	24.0	0.0082	23.9	40.1	63.9	37%	-1%	53%	2%
	23/02/07	20.4	25.3	0.0082	25.1	40.9	66.0	38%	3%		
100	23/03/07	100.4	49.1	0.0072	48.4	23.8	72.2	67%	12	67%	-

Table G-3 Mercury capture efficiencies at different temperatures when evaluated using a gas stream of only Hg^0 vapour and nitrogen gas

Norit Darco Hg™ (hold time = 60 minutes, approx. sample mass = 100mg)

Test Temp. (°C)	Test date	Sorbent mass (mg)	Total Hg in sorbent (ng)	Initial Hg conc. on sorbent (ppm)	Hg captured by sorbent (ng)	Hg in backup (ng)	Hg into the reactor (ng)	Hg capture efficiency	Hg mass balance diff	Mean efficiency	SD
100	23/05/07	99.8	54.2	0.0056	53.7	2.8	56.5	95%	-12%	91.5%	3%
	23/05/07	100.4	52.5	0.0056	52.0	6.9	58.8	88%	-9%		
150	Refer Table G-1 for Norit Darco Hg™ results at 150°C										
175	24/05/07	100.0	14.5	0.0069	13.8	41.8	55.6	25%	-14%	24%	3%
	25/05/07	100.2	17.7	0.0065	17.0	45.2	62.3	27%	-3%		
	25/05/07	100.5	13.7	0.0065	13.0	50.0	63.1	21%	-2%		
200	27/07/07	100.4	6.7	0.0013	6.6	56.7	63.3	10%	-2%	8%	2%
	27/07/07	100.8	4.3	0.0013	4.1	60.3	64.4	6%	-2%		

Fly ash D (hold time = 60 minutes, approx. sample mass = 100mg)

Test Temp. (°C)	Test date	Sorbent mass (mg)	Total Hg in sorbent (ng)	Initial Hg conc. on sorbent (ppm)	Hg captured by sorbent (ng)	Hg in backup (ng)	Hg into the reactor (ng)	Hg capture efficiency	Hg mass balance diff	Mean efficiency	SD
100	24/07/07	99.8	109.7	0.4475	65.1	1.6	66.7	98%	4%	98%	-
150	Refer Table G-2 for fly ash D results at 150°C										
175	22/07/07	99.9	95.9	0.4515	50.8	7.1	57.9	88%	-10%	88%	-
200	22/07/07	99.9	87.6	0.4515	42.5	27.9	70.5	60%	9%	65%	4.8%
	06/08/07	99.8	94.3	0.4747	47.0	20.2	67.1	70%	4%		

Table G-3 Mercury capture efficiencies at different temperatures when evaluated using a gas stream of only Hg^0 vapour and nitrogen gas (continued)

Fly ash F (hold time = 60 minutes, approx. sample mass = 100mg)

Test Temp. (°C)	Test date	Sorbent mass (mg)	Total Hg in sorbent (ng)	Initial Hg conc. on sorbent (ppm)	Hg captured by sorbent (ng)	Hg in backup (ng)	Hg into the reactor (ng)	Hg capture efficiency	Hg mass balance diff	Mean efficiency	SD
100	20/08/07	99.8	163.7	1.1215	51.76	0.2	52.0	100%	-19%	100%	-
150	Refer Table G-2 for fly ash F results at 150°C										
175	20/08/07	99.5	165.0	1.1215	53.4	4.0	57.5	93%	-11%	93%	-
200	19/08/07	99.5	159.4	1.1589	44.1	8.9	53.0	83%	-18%	82%	0.4%
	19/08/07	100.1	170.0	1.1589	54.0	11.5	65.5	82%	2%		

Tyre char R1 (hold time = 60 minutes, approx. sample mass = 100mg)

Test Temp. (°C)	Test date	Sorbent mass (mg)	Total Hg in sorbent (ng)	Initial Hg conc. on sorbent (ppm)	Hg captured by sorbent (ng)	Hg in backup (ng)	Hg into the reactor (ng)	Hg capture efficiency	Hg mass balance diff	Mean efficiency	SD
100	27/05/07	100.1	76.1	0.1136	64.7	5.4	70.1	92%	9%	92%	-
150	Refer Table G-1 for tyre char R1 results at 150°C										
175	28/05/07	99.5	32.3	0.1114	21.3	47.4	68.7	31%	7%	31%	0.02%
	28/05/07	100.2	30.4	0.1114	19.2	42.8	62.1	31%	-4%		
200	20/07/07	100.2	27.6	0.0799	19.6	42.8	62.4	31%	-3%		
	21/07/07	100.0	22.0	0.1112	10.9	47.8	58.7	19%	-9%	19%	-

Table G-3 Mercury capture efficiencies at different temperatures when evaluated using a gas stream of only Hg^0 vapour and nitrogen gas (continued)

Tyre AC R1 (hold time = 60 minutes, approx. sample mass = 100mg)

Test Temp. (°C)	Test date	Sorbent mass (mg)	Total Hg in sorbent (ng)	Initial Hg conc. on sorbent (ppm)	Hg captured by sorbent (ng)	Hg in backup (ng)	Hg into the reactor (ng)	Hg capture efficiency	Hg mass balance difference	Mean efficiency	SD
100	20/05/07	99.8	45.8	0.1213	33.7	34.8	68.5	49%	6%	68%	16%
	20/05/07	100.0	55.0	0.1213	42.9	20.9	63.8	67%	-1%		
	21/05/07	100.0	68.6	0.1228	56.3	8.0	64.4	88%	0%		
150	Refer Table G-1 for tyre AC R1 results at 150°C										
175	19/05/07	100.0	18.0	0.1222	5.83	67.3	73.1	8%	14%	13%	5%
	07/09/07	100.9	18.5	0.0646	11.99	53.7	65.7	18%	-3%		
200	21/07/07	100.3	8.0	0.0605	1.9	62.2	64.1	3%	0%	6.7%	4%
	19/08/07	99.8	6.8	0.0317	3.6	68.1	71.7	5%	11%		
	24/08/07	100.5	12.5	0.0355	8.90	66.6	75.6	12%	17%		

Table G-4 Mercury capture efficiencies at different temperatures when evaluated using a gas stream of NO, NO_2,Hg^0 vapour and nitrogen gas

Norit Darco Hg™ (hold time = 60 minutes, approx. sample mass = 100mg)

Test Temp. (°C)	Test date	Sorbent mass (mg)	Total Hg in sorbent (ng)	Initial Hg conc. on sorbent (ppm)	Hg captured by sorbent (ng)	Hg in backup (ng)	Hg into the reactor (ng)	Hg capture efficiency	Hg mass balance difference	Mean efficiency	SD
150	27/07/07	100.2	60.2	0.0013	60.0	1.1	61.1	98%	-5%	98%	0.3%
	06/08/07	99.6	56.7	0.0016	56.5	1.4	58.0	98%	-10%		
175	06/08/07	100.2	59.7	0.0016	59.6	5.3	64.8	92%	1%	92%	-
200	16/05/06	99.3	57.2	0.0078	56.4	12.3	68.7	82%	7%	84%	2%
	22/05/06	99.6	49.0	0.0042	48.6	8.1	56.7	86%	-12%		

Fly ash D (hold time = 30 minutes, approx. sample mass = 100mg)

Test Temp. (°C)	Test date	Sorbent mass (mg)	Total Hg in sorbent (ng)	Initial Hg conc. on sorbent (ppm)	Hg captured by sorbent (ng)	Hg in backup (ng)	Hg into the reactor (ng)	Hg capture efficiency	Hg mass balance difference	Mean efficiency	SD
100	08/06/06	99.9	68.6	0.3985	28.78	0.1	28.9	100%	-10%	100%	-
150	07/08/07	99.8	82.9	0.4747	35.5	0.9	36.5	97%	13%	97%	-
175	02/06/07	100.0	77.6	0.4202	35.6	0.3	35.9	99%	11%	99%	-
200	02/06/06	100.5	66.5	0.4202	24.3	10.1	34.3	71%	3%	83%	12.4%
	06/08/07	100.5	81.4	0.4678	34.42	1.6	36.0	95%	12%		

Table G-4 Mercury capture efficiencies at different temperatures when evaluated using a gas stream of NO, NO_2,Hg^0 vapour and nitrogen gas (continued)

Tyre char R1 (hold time = 30 minutes, approx. sample mass = 100mg)

Test Temp. (°C)	Test date	Sorbent mass (mg)	Total Hg in sorbent (ng)	Initial Hg conc. on sorbent (ppm)	Hg captured by sorbent (ng)	Hg in backup (ng)	Hg into the reactor (ng)	Hg capture efficiency	Hg mass balance difference	Mean efficiency	SD
100	01/06/06	99.9	41.2	0.0598	35.3	0.1	35.4	100%	10%	100%	-
150	31/05/06	100.1	42.2	0.0615	36.1	1.2	37.2	97%	16%	95%	2%
	01/06/06	100.0	40.6	0.0598	34.6	2.7	37.3	93%	16%		
175	26/05/06	99.3	39.1	0.0699	32.1	1.8	33.9	95%	5%	95	-
200	26/05/06	100.5	29.0	0.0699	22.0	11.8	33.8	65%	3%	81%	16%
	04/08/07	99.3	44.1	0.0733	36.8	1.1	37.9	97%	16%		

Tyre AC R1 (hold time = 30 minutes, approx. sample mass = 100mg)

Test Temp. (°C)	Test date	Sorbent mass (mg)	Total Hg in sorbent (ng)	Initial Hg conc. on sorbent (ppm)	Hg captured by sorbent (ng)	Hg in backup (ng)	Hg into the reactor (ng)	Hg capture efficiency	Hg mass balance difference	Mean efficiency	SD
100	12/06/06	100.3	34.0	0.0102	33.0	0.1	33.1	100%	3%	100%	0.03%
	14/06/06	100.4	27.9	0.0102	26.9	0.1	27.0	100%	-16%		
150	30/05/06	100.1	29.4	0.0126	28.1	0.3	28.4	99%	-12%	99%	-
175	28/05/06	100.0	29.4	0.0117	28.2	6.7	34.9	81%	8%	81%	-
200	26/05/06	100.0	29.4	0.0117	28.2	6.4	34.6	82%	6%	82%	-

Table G-5 Mercury capture efficiencies of sorbents when tested with gas schemes Exp. 1 to Exp. 5

Norit Darco Hg™ (hold time = 60 minutes, approx. sample mass = 100mg, test temperature = 150°C)

Gas scheme	Test date	Sorbent mass (mg)	Total Hg in sorbent (ng)	Initial Hg conc. on sorbent (ppm)	Hg captured by sorbent (ng)	Hg in backup (ng)	Hg into the reactor (ng)	Hg capture efficiency	Hg mass balance difference	Mean efficiency	SD
Exp. 1	Refer Table G-1 for Norit Darco Hg™ results with gas scheme Exp. 1										
Exp. 2	Refer Table G-4 for Norit Darco Hg™ results with gas scheme Exp. 2										
Exp. 3	18/06/07	99.7	45.3	0.0065	44.6	23.3	67.9	66%	6%	74%	8%
	19/06/07	100.5	55.5	0.0060	54.9	11.7	66.5	82%	3%		
Exp. 4	14/06/07	100.4	65.9	0.0065	65.3	7.3	72.6	90%	13%	94%	4%
	01.07/07	100.3	55.7	0.0040	55.3	0.8	56.1	99%	-13%		
Exp. 5	07/8/06	100.8	68.6	0.0022	68.4	0.0	68.4	100%	6%	99%	1%
	10/08/06	100.2	61.5	0.0022	61.3	0.9	62.2	99%	-3%		

Fly ash D (hold time = 60 minutes, approx. sample mass = 100mg, test temperature = 150°C)

Gas scheme	Test date	Sorbent mass (mg)	Total Hg in sorbent (ng)	Initial Hg conc. on sorbent (ppm)	Hg captured by sorbent (ng)	Hg in backup (ng)	Hg into the reactor (ng)	Hg capture efficiency	Hg mass balance difference	Mean efficiency	SD
Exp. 1	Refer Table G-2 for fly ash D results with gas scheme Exp. 1										
Exp. 2	27/07/07	99.5	107.3	0.3906	68.4	0.1	68.5	100%	6%	100%	0.1%
	27/07/07	99.4	109.2	0.3906	70.41	0.3	70.7	100%	10%		
Exp. 3	03/10/07	100.3	114.8	0.4967	65.0	0.5	65.5	99%	2%	99%	0.02%
	03/10/07	99.6	113.9	0.4967	64.4	0.5	64.9	99%	1%		
Exp. 4	Fly ash D was not analysed with gas scheme Exp. 4										
Exp. 5	14/08/06	100.7	101.7	0.4137	60.0	0.4	60.4	99%	-6%	99%	0.2%
	28/07/07	100.4	115.7	0.4317	72.4	0.3	72.6	100%	13%		

Table G-5 Mercury capture efficiencies of sorbents when tested with gas schemes Exp. 1 to Exp. 5 (continued)

Tyre char R1 (hold time = 60 minutes, approx. sample mass = 100mg, test temperature = 150°C)

Gas scheme	Test date	Sorbent mass (mg)	Total Hg in sorbent (ng)	Initial Hg conc. on sorbent (ppm)	Hg captured by sorbent (ng)	Hg in backup (ng)	Hg into the reactor (ng)	Hg capture efficiency	Hg mass balance difference	Mean efficiency	SD
Exp. 1	Refer Table G-1 for tyre char R1 results with gas scheme Exp. 1										
Exp. 2	16/07/07	99.5	59.7	0.0804	51.7	2.8	54.5	95%	-15%	97%	2%
	03/08/07	100.4	76.2	0.0733	68.8	0.6	69.4	99%	8*		
	04/08/07	99.7	80.9	0.0733	73.6	1.5	75.0	98%	17%		
Exp. 3	19/06/07	100.7	50.6	0.1405	36.4	37.3	73.7	49%	14%	49%	1%
	26/06/07	100.3	49.9	0.1345	36.4	40.1	76.5	48%	19%		
Exp. 4	14/06/07	100.7	72.1	0.1405	58.0	16.6	74.6	78%	16%	80%	2%
	26/06/07	100.0	69.1	0.1345	55.7	12.6	68.3	82%	6%		
Exp. 5	11/08/06	99.3	78.2	0.1136	66.9	0.2	67.2	100%	4%	99%	0.5%
	30/06/07	99.8	75.4	0.1244	63.0	0.8	63.8	99%	-1%		

Table G-5 Mercury capture efficiencies of sorbents when tested with gas schemes Exp. 1 to Exp. 5 (continued)

Tyre AC R1 (hold time = 60 minutes, approx. sample mass = 100mg, test temperature = 150°C)

Gas scheme	Test date	Sorbent mass (mg)	Total Hg in sorbent (ng)	Initial Hg conc. on sorbent (ppm)	Hg captured by sorbent (ng)	Hg in backup (ng)	Hg into the reactor (ng)	Hg capture efficiency	Hg mass balance difference	Mean efficiency	SD
Exp. 1	Refer Table G-1 for tyre AC R1 results with gas scheme Exp. 1										
Exp. 2	01/08/07	100.5	65.0	0.0383	61.2	0.4	61.5	99%	-4%	99%	0.04%
	01/08/07	99.2	80.5	0.0383	76.6	0.4	77.0	99%	16%		
Exp. 3	30/07/07	99.5	58.2	0.0490	53.3	0.1	53.4	100%	-17%	99%	0.3%
	30/06/07	100.2	73.8	0.0291	70.9	0.6	71.5	99%	11%		
Exp. 4	06/07/07	99.4	53.5	0.0319	50.3	6.3	56.6	89%	-12%	93%	4%
	06/07/07	99.1	56.9	0.0319	53.8	1.7	55.4	97%	-14%		
Exp. 5	14/08/06	99.7	75.6	0.0453	71.1	0.4	71.4	100%	11%	99%	0.1%
	28/07/07	100.7	62.9	0.0533	57.5	0.3	57.8	99%	-10%		
	28/07/07	99.8	65.3	0.0533	59.9	0.4	60.3	99%	-6%		

Table G-6 Mercury capture efficiencies when 20 mg sorbents samples were tested with different gas schemes

Fly ash D (hold time = 60 minutes, test temperature = 150°C)

Gas scheme	Test date	Sorbent mass (mg)	Total Hg in sorbent (ng)	Initial Hg conc. on sorbent (ppm)	Hg captured by sorbent (ng)	Hg in backup (ng)	Hg into the reactor (ng)	Hg capture efficiency	Hg mass balance difference	Mean efficiency	SD
Exp. 1	Refer Table G-2 for Fly ash D results with gas scheme Exp. 1										
Exp. 2	Fly ash D was not analysed with gas scheme Exp. 2										
Exp. 3	03/10/07	20.3	71.9	0.4967	61.8	7.5	69.3	89%	8%	82%	7%
	03/10/07	20.2	57.8	0.4967	47.7	15.7	63.4	75%	-1%		
Exp. 5	13/10/07	20.0	49.7	0.4779	40.2	11.4	51.5	78%	-20%	77%	0.9%
	13/10/07	20.0	50.7	0.4779	41.1	12.9	54.0	76%	-16%		
Exp. 6	24/01/07	19.7	37.9	0.4149	29.8	25.8	55.5	54%	-14%	50%	3%
	30/01/07	20.5	35.3	0.4526	26.0	28.7	54.7	47%	-15%		
	01/02/07	20.3	40.6	0.4254	32.0	31.9	63.9	50%	-1%		
	01/02/07	20.3	37.2	0.4254	28.6	31.7	60.3	47%	-6%		

Fly ash E (hold time = 60 minutes, test temperature = 150°C)

Gas scheme	Test date	Sorbent mass (mg)	Total Hg in sorbent (ng)	Initial Hg conc. on sorbent (ppm)	Hg captured by sorbent (ng)	Hg in backup (ng)	Hg into the reactor (ng)	Hg capture efficiency	Hg mass balance difference	Mean efficiency	SD
Exp. 1	Refer Table G-2 for Fly ash E results with gas scheme Exp. 1										
Exp. 2	Fly ash E was not analysed with gas scheme Exp. 2										
Exp. 3	Fly ash E was not analysed with gas scheme Exp. 3										
Exp. 5	Fly ash E was not analysed with gas scheme Exp. 5										
Exp. 6	31/01/07	20.4	41.1	0.4871	31.2	36.6	67.7	46%	5%	44%	2%
	31/01/07	20.5	38.4	0.4871	28.4	39.6	67.9	42%	6%		

Table G-6 Mercury capture efficiencies when 20 mg sorbents samples were tested with different gas schemes (continued)

Norit Darco Hg™ (hold time = 60 minutes, test temperature = 150°C)

Gas scheme	Test date	Sorbent mass (mg)	Total Hg in sorbent (ng)	Initial Hg conc. on sorbent (ppm)	Hg captured by sorbent (ng)	Hg in backup (ng)	Hg into the reactor (ng)	Hg capture efficiency	Hg mass balance difference	Mean efficiency	SD
Exp. 1	Refer Table G-2 for Norit Darco Hg™ results with gas scheme Exp. 1										
Exp. 2	20/09/07	19.8	55.4	0.0036	55.3	0.2	55.5	100%	-14%	99%	1%
	23/09/07	20.4	72.1	0.0034	72.1	1.5	73.6	98%	14%		
Exp. 3	23/09/07	20.3	56.8	0.0034	56.7	0.2	56.9	100%	-12%	99%	0.3%
	20/10/07	21.5	77.5	0.0027	77.4	0.7	78.1	99%	21%		
Exp. 5	14/09/07	20.4	68.9	0.0072	68.7	0.8	69.5	99%	8%	99%	0.05%
	14/09/07	20.1	65.1	0.0072	65.0	0.7	65.6	99%	2%		
Exp. 6	18/01/07	19.8	73.1	0.0040	73.1	0.4	73.5	99%	14%	100%	0.22%
	19/01/07	20.2	62.4	0.0051	62.3	0.0	62.3	100%	-3%		

Tyre char R1 (hold time = 60 minutes, test temperature = 150°C)

Gas scheme	Test date	Sorbent mass (mg)	Total Hg in sorbent (ng)	Initial Hg conc. on sorbent (ppm)	Hg captured by sorbent (ng)	Hg in backup (ng)	Hg into the reactor (ng)	Hg capture efficiency	Hg mass balance difference	Mean efficiency	SD
Exp. 1	Refer Table G-2 for tyre char R1 results with gas scheme Exp. 1										
Exp. 2	07/08/07	20.5	66.7	0.0089	67.6	5.1	72.6	93%	13%	92%	0.7%
	21/09/07	19.6	68.1	0.0210	67.7	6.2	74.0	92%	15%		
Exp. 3	07/10/07	20.5	63.2	0.0163	62.9	0.4	63.2	99%	-2%	96%	3%
	20/10/07	19.8	69.1	0.0108	68.9	4.8	73.7	94%	14%		
Exp. 5	12/09/07	19.4	62.1	0.0617	60.9	1.0	61.9	98%	-4%	99%	0.05%
Exp. 6	29/01/07	20.0	61.8	0.1004	59.8	6.5	66.2	90%	3%	90%	0.3%
	29/01/07	20.6	68.1	0.1004	66.0	6.7	72.8	91%	13%		

Table G-6 Mercury capture efficiencies when 20 mg sorbents samples were tested with different gas schemes (continued)

Tyre char R2 (hold time = 60 minutes, test temperature = 150°C)

Gas scheme	Test date	Sorbent mass (mg)	Total Hg in sorbent (ng)	Initial Hg conc. on sorbent (ppm)	Hg captured by sorbent (ng)	Hg in backup (ng)	Hg into the reactor (ng)	Hg capture efficiency	Hg mass balance difference	Mean efficiency	SD
Exp. 1	Refer Table G-2 for tyre char R2 results with gas scheme Exp. 1										
Exp. 5	18/09/07	20.7	60.7	0.0437	59.8	0.7	60.5	99%	-6%	99%	0.3%
	20/09/07	20.3	57.7	0.0239	57.2	1.0	58.2	98%	-10%		

Tyre AC R1 (hold time = 60 minutes, test temperature = 150°C)

Gas scheme	Test date	Sorbent mass (mg)	Total Hg in sorbent (ng)	Initial Hg conc. on sorbent (ppm)	Hg captured by sorbent (ng)	Hg in backup (ng)	Hg into the reactor (ng)	Hg capture efficiency	Hg mass balance difference	Mean efficiency	SD
Exp. 1	Refer Table G-2 for tyre AC R1 results with gas scheme Exp. 1										
Exp. 2	02/08/07	19.6	70.9	0.0384	70.2	0.5	70.6	99%	6%	99%	0.4%
	23/09/07	20.3	79.8	0.0583	78.6	1.2	79.8	98%	20%		
Exp. 3	07/10/07	20.4	69.5	0.0494	68.5	0.9	69.4	99%	8%	99%	0.4%
	07/10/07	20.6	57.1	0.0494	56.0	0.3	56.4	99%	-12%		
Exp. 5	16/09/07	20.1	57.4	0.0657	56.1	0.3	56.4	99%	-12%	99%	0.3%
	17/09/07	20.0	67.3	0.0635	66.0	0.8	66.9	99%	4%		
Exp. 6	22/01/07	20.0	61.9	0.0572	60.8	0.1	60.9	100%	-5%	100%	-

Table G-7 Mercury capture efficiencies when 100 mg sorbents samples were initially exposed to NO_x or HCl and then tested a gas stream of mercury vapour in pure nitrogen gas

Norit Darco Hg™ (hold time = 60 minutes, test temperature = 150°C)

Initial exposure	Test date	Sorbent mass (mg)	Total Hg in sorbent (ng)	Initial Hg conc. on sorbent (ppm)	Hg captured by sorbent (ng)	Hg in backup (ng)	Hg into the reactor (ng)	Hg capture efficiency	Hg mass balance difference	Mean efficiency	SD
NO_x	01/09/07	100.1	63.7	0.0015	63.5	0.1	63.6	100%	-1%	97%	3%
	01/09/07	100.5	62.9	0.0015	62.8	4.5	67.3	93%	5%		
HCl	24/07/07	100.6	62.9	0.0013	62.7	0.4	63.1	99%	-2%	99%	0.3%
	25/07/07	99.8	54.3	0.0019	54.1	0.6	54.7	99%	-15%		

Tyre char R1 (hold time = 60 minutes, test temperature = 150°C)

Initial exposure	Test date	Sorbent mass (mg)	Total Hg in sorbent (ng)	Initial Hg conc. on sorbent (ppm)	Hg captured by sorbent (ng)	Hg in backup (ng)	Hg into the reactor (ng)	Hg capture efficiency	Hg mass balance difference	Mean efficiency	SD
NO_x	03/08/07	99.5	66.3	0.0717	59.1	11.9	71.0	83%	10%	79%	4%
	03/08/07	99.7	58.1	0.0717	50.98	16.5	67.5	76%	5%		
HCl	25/07/07	100.6	58.2	0.1220	46.0	19.5	65.5	70%	2%	71%	1%
	25/07/07	99.2	56.4	0.1220	44.3	16.6	60.8	73%	-5%		

Table G-7 Mercury capture efficiencies when 100 mg sorbents samples were initially exposed to NO_x or HCl and then tested a gas stream of mercury vapour in pure nitrogen gas (continued)

Tyre AC R1 (hold time = 60 minutes, test temperature = 150°C)

Initial exposure	Test date	Sorbent mass (mg)	Total Hg in sorbent (ng)	Initial Hg conc. on sorbent (ppm)	Hg captured by sorbent (ng)	Hg in backup (ng)	Hg into the reactor (ng)	Hg capture efficiency	Hg mass balance difference	Mean efficiency	SD
NO_x	02/08/07	99.6	62.0	0.0381	58.2	12.2	70.5	83%	9%	83%	-
HCl	26/07/07	99.5	72.5	0.0538	67.2	1.7	68.9	97%	7%	98%	1%
	26/07/07	99.7	72.1	0.0538	66.7	0.4	67.1	99%	4%		

Table G-8 Thermal desorption test results on 20 mg samples of spent sorbents

Norit Darco Hg™ (hold time = 60 minutes)

Adsorption gas scheme	Test date	Sorbent mass (mg)	Hg remaining on the sorbent (ng)	Hg in backup (ng)	Total Hg captured by sorbent (ng)	Hg desorbed	Mean Hg desorbed	SD	Average Hg captured by the sorbent (ng)
Exp. 1	21/08/07	20.0	0.8	3.6	4.5	81%	83%	1.5%	5.0
	21/08/07	20.4	0.9	4.7	5.6	84%			
Exp. 2	20/09/07	19.8	26.5	28.8	55.4	52%	46%	6%	63.7
	23/09/07	20.4	43.1	29.1	72.2	40%			
Exp. 3	23/09/07	20.3	56.2	0.6	56.8	1%	2%	0.4%	67.1
	20/10/07	21.5	75.4	1.5	77.5	2%			
Exp. 5	14/09/07	20.4	68.5	0.4	68.9	1%	1%	0.2%	66.8
	14/09/07	20.1	64.5	0.6	65.1	1%			

Tyre char R2 (hold time = 60 minutes)

Adsorption gas scheme	Test date	Sorbent mass (mg)	Hg remaining on the sorbent (ng)	Hg in backup (ng)	Total Hg captured by sorbent (ng)	Hg desorbed	Mean Hg desorbed	SD	Average Hg captured by the sorbent (ng)
Exp. 1	26/08/07	19.8	24.1	6.6	30.7	21%	22%	0.2%	26.6
	21/08/07	20.4	0.9	4.7	5.6	84%			
Exp. 2	07/08/07	20.5	67.7	5.1	72.8	7%	9%	2.1%	67.6
	21/09/07	19.6	60.5	7.7	68.1	11%			
Exp. 3	07/10/07	20.5	33.4	29.8	63.2	47%	46%	0.9%	65.9
	20/10/07	19.8	37.7	31.3	69.1	45%			
Exp. 5	18/09/07	20.7	39.2	21.5	60.7	35%	31%	4.42%	58.3
	20/09/07	20.3	42.3	15.4	57.7	27%			

Table G-8 Thermal desorption test results on 20 mg samples of spent sorbents (continued)

Tyre AC R1

Adsorption gas scheme	Test date	Sorbent mass (mg)	Hg remaining on the sorbent (ng)	Hg in backup (ng)	Total Hg captured by sorbent (ng)	Hg desorbed	Mean Hg desorbed	SD	Average Hg captured by the sorbent (ng)
Exp. 1	21/08/07	20.2	3.3	6.1	9.4	65%	65%	0.4%	11.1
	08/09/07	20.4	5.3	9.6	14.9	64%			
Exp. 2	02/08/07	19.6	50.9	20.0	70.9	28%	26%	2.1%	74.4
	23/09/07	20.3	60.6	19.1	79.8	24%			
Exp. 3	07/10/07	20.4	58.3	11.2	69.5	16%	12%	4.5%	62.3
	07/10/07	20.6	53.0	4.1	57.1	7%			
Exp. 5	16/09/07	20.1	55.8	0.8	56.5	1%	1%	0.6%	61.1
	17/09/07	20.0	63.5	1.6	65.3	2%			

Table G-9 Mercury capture efficiencies when 100 mg Dowex 1X8® was evaluated with different gas schemes

Hold time = 60 minutes, test temperature = 150°C

Gas scheme used	Test date	Sorbent mass (mg)	Total Hg in sorbent (ng)	Initial Hg conc. on sorbent (ppm)	Hg captured by sorbent (ng)	Hg in backup (ng)	Hg into the reactor (ng)	Hg capture efficiency	Hg mass balance difference	Mean efficiency	SD
Exp. 1	13/07/07	98.4	11.9	0.0448	7.4	49.7	57.2	13%	-11%	18%	5%
	14/07/07	104.3	15.9	0.0448	11.2	38.8	50.1	22%	-22%		
Exp. 3	14/07/07	99.6	21.7	0.0448	17.3	32.1	49.4	35%	-23%	29%	6%
	14/07/07	104.3	15.9	0.0448	11.2	38.8	50.1	22%	-22%		
Exp. 4	15/07/07	98.0	20.5	0.0448	16.2	36.5	52.7	31%	-18%	27%	4%
	16/07/07	100.5	14.6	0.0448	10.1	34.0	44.1	23%	-31%		

Table G-10 Mercury capture efficiencies when bromide impregnated sorbents samples were tested with a gas scheme Exp. 1

Norit Darco Hg-LH™ (hold time = 60 minutes, test temperature = 150°C)

Approx. sample mass (mg)	Test date	Sorbent mass (mg)	Total Hg in sorbent (ng)	Initial Hg conc. on sorbent (ppm)	Hg captured by sorbent (ng)	Hg in backup (ng)	Hg into the reactor (ng)	Hg capture efficiency	Hg mass balance difference	Mean efficiency	SD
10	18/08/07	9.9	62.4	0.0050	62.35	0.6	62.9	99%	-2%	99%	-
20	02/03/07	19.6	59.9	0	59.9	1.3	61.2	98%	-5%	98%	-

Tyre AC R3 (hold time = 60 minutes, test temperature = 150°C)

Approx. sample mass (mg)	Test date	Sorbent mass (mg)	Total Hg in sorbent (ng)	Initial Hg conc. on sorbent (ppm)	Hg captured by sorbent (ng)	Hg in backup (ng)	Hg into the reactor (ng)	Hg capture efficiency	Hg mass balance difference	Mean efficiency	SD
5	05/09/07	5.1	60.5	0.0568	60.2	2.7	62.9	92%	-4%	95%	0.7%
	07/09/07	5.2	66.0	0.0568	65.7	3.9	69.6	94%	6%		
10	05/08/07	10.5	63.4	0.0568	62.8	0.6	63.4	99%	-2%	99%	0.1%
	20/08/07	10.0	68.6	0.0568	68.0	0.5	68.5	99%	5%		
20	02/08/07	20.1	58.0	0.0568	56.9	0.2	57.1	100%	-11%	100%	0.1%
	04/08/07	19.5	67.3	0.0568	66.2	0.1	66.3	100%	1%		

Sewage sludge AC R3 (hold time = 60 minutes, test temperature = 150°C)

Approx. sample mass (mg)	Test date	Sorbent mass (mg)	Total Hg in sorbent (ng)	Initial Hg conc. on sorbent (ppm)	Hg captured by sorbent (ng)	Hg in backup (ng)	Hg into the reactor (ng)	Hg capture efficiency	Hg mass balance difference	Mean efficiency	SD
20	24/08/07	19.9	61.9	0.0778	60.4	0.2	60.6	100%	-6%	100%	0.1%
	26/08/07	20.2	60.2	0.0778	58.6	0.3	58.9	99%	-10%		

Table G-11 Mercury capture efficiencies when bromide impregnated sorbents samples were tested with a gas scheme Exp. 6

Norit Darco Hg-LH™ (hold time = 60 minutes, test temperature = 150°C)

Test date	Sorbent mass (mg)	Total Hg in sorbent (ng)	Initial Hg conc. on sorbent (ppm)	Hg captured by sorbent (ng)	Hg in backup (ng)	Hg into the reactor (ng)	Hg capture efficiency	Hg mass balance difference	Mean efficiency	SD
02/02/07	20.3	74.6	0	74.6	0.2	74.8	100%	16%	99%	0.5%
02/02/07	20.4	68.4	0	68.4	0.9	69.3	99%	8%		

Sewage sludge AC R1 (hold time = 60 minutes, test temperature = 150°C)

Test date	Sorbent mass (mg)	Total Hg in sorbent (ng)	Initial Hg conc. on sorbent (ppm)	Hg captured by sorbent (ng)	Hg in backup (ng)	Hg into the reactor (ng)	Hg capture efficiency	Hg mass balance difference	Mean efficiency	SD
05/02/07	20.1	78.3	0.0179	77.9	0.3	78.2	100%	21%	100%	0.2%
05/03/07	20.5	68.6	0.0179	68.2	0.4	68.7	99%	7%		

Sewage sludge AC R2 (hold time = 60 minutes, test temperature = 150°C)

Test date	Sorbent mass (mg)	Total Hg in sorbent (ng)	Initial Hg conc. on sorbent (ppm)	Hg captured by sorbent (ng)	Hg in backup (ng)	Hg into the reactor (ng)	Hg capture efficiency	Hg mass balance difference	Mean efficiency	SD
06/02/07	20.3	78.1	0.0220	77.65	1.8	79.4	98%	23%	99%	0.8%
06/02/07	19.9	88.7	0.0220	88.3	0.5	88.8	99%	33%		

Table G-12 Mercury capture efficiencies when 5 mg sample of sorbents without bromide impregnated sorbents were tested with a gas scheme Exp. 5

Norit Darco Hg™ (hold time = 60 minutes, test temperature = 150°C)

Test date	Sorbent mass (mg)	Total Hg in sorbent (ng)	Initial Hg conc. on sorbent (ppm)	Hg captured by sorbent (ng)	Hg in backup (ng)	Hg into the reactor (ng)	Hg capture efficiency	Hg mass balance difference	Mean efficiency	SD
21/10/07	4.7	59.5	0.0018	59.5	6.7	66.2	90%	3%	94%	4.2%
21/10/07	4.9	62.5	0.0018	62.5	1.1	63.6	99%	-1%		

Tyre char R2 (hold time = 60 minutes, test temperature = 150°C)

Test date	Sorbent mass (mg)	Total Hg in sorbent (ng)	Initial Hg conc. on sorbent (ppm)	Hg captured by sorbent (ng)	Hg in backup (ng)	Hg into the reactor (ng)	Hg capture efficiency	Hg mass balance difference	Mean efficiency	SD
27/09/07	5.3	24.2	0.0089	24.2	20.8	44.9	54%	-30%	59%	5.5%
21/10/07	4.8	29.8	0.0089	29.8	16.2	46.0	65%	-29%		

Tyre AC R1 (hold time = 60 minutes, test temperature = 150°C)

Test date	Sorbent mass (mg)	Total Hg in sorbent (ng)	Initial Hg conc. on sorbent (ppm)	Hg captured by sorbent (ng)	Hg in backup (ng)	Hg into the reactor (ng)	Hg capture efficiency	Hg mass balance difference	Mean efficiency	SD
21/10/07	5.5	58.4	0.0393	58.2	0.4	58.6	99%	-9%	99%	0.2%
21/10/07	5.1	61.6	0.0393	61.4	0.2	61.6	100%	-4%		

Table G-13 Mercury capture efficiencies of 20 mg coal fly ash samples when were tested with a gas stream of mercury vapour in pure nitrogen gas

Fly ash A (hold time = 60 minutes, test temperature = 150°C)

Test date	Sorbent mass (mg)	Total Hg in sorbent (ng)	Initial Hg conc. on sorbent (ppm)	Hg captured by sorbent (ng)	Hg in backup (ng)	Hg into the reactor (ng)	Hg capture efficiency	Hg mass balance difference	Mean efficiency	SD	LOI
22/08/07	20.0	1.7	0.0750	0.2	67.3	67.5	0.3%	5%	0.3%	0.03%	3.7%
21/10/07	19.4	1.7	0.0750	0.2	71.9	72.1	0.3%	12%			

Fly ash B (hold time = 60 minutes, test temperature = 150°C)

Test date	Sorbent mass (mg)	Total Hg in sorbent (ng)	Initial Hg conc. on sorbent (ppm)	Hg captured by sorbent (ng)	Hg in backup (ng)	Hg into the reactor (ng)	Hg capture efficiency	Hg mass balance difference	Mean efficiency	SD	LOI
22/08/07	20.2	13.4	0.1497	10.4	56.9	67.3	15%	5%	14%	2%	4.4%
24/08/07	20.3	12.0	0.1553	8.8	64.7	73.5	12%	14%			

Fly ash C (hold time = 60 minutes, test temperature = 150°C)

Test date	Sorbent mass (mg)	Total Hg in sorbent (ng)	Initial Hg conc. on sorbent (ppm)	Hg captured by sorbent (ng)	Hg in backup (ng)	Hg into the reactor (ng)	Hg capture efficiency	Hg mass balance difference	Mean efficiency	SD	LOI
24/08/07	19.6	28.1	0.2255	23.7	46.9	70.7	34%	10%	25%	8%	6.0%
24/08/07	19.5	16.7	0.2255	12.3	62.1	74.4	16%	16%			
24/08/07	20.3	26.1	0.2255	21.5	54.8	76.3	28%	18%			

Table G-13 Mercury capture efficiencies of 20 mg coal fly ash samples when were tested with a gas stream of mercury vapour in pure nitrogen gas (continued)

Fly ash D (hold time = 60 minutes, test temperature = 150°C)

Test date	Sorbent mass (mg)	Total Hg in sorbent (ng)	Initial Hg conc. on sorbent (ppm)	Hg captured by sorbent (ng)	Hg in backup (ng)	Hg into the reactor (ng)	Hg capture efficiency	Hg mass balance difference	Mean efficiency	SD	LOI
08/03/07	20.2	40.8	0.4225	32.3	31.2	63.5	51%	-1%	51%	0.8%	8.2
24/08/07	20.3	45.8	0.5151	35.3	35.0	70.3	50%	9%			

Fly ash E (hold time = 60 minutes, test temperature = 150°C)

Test date	Sorbent mass (mg)	Total Hg in sorbent (ng)	Initial Hg conc. on sorbent (ppm)	Hg captured by sorbent (ng)	Hg in backup (ng)	Hg into the reactor (ng)	Hg capture efficiency	Hg mass balance difference	Mean efficiency	SD	LOI
12/03/07	20.4	42.7	0.5306	31.9	31.2	63.2	51%	-2%	53%	2%	10.2
15/08/07	20.6	52.4	0.6624	38.8	33.3	72.1	54%	12%			

Fly ash F (hold time = 60 minutes, test temperature = 150°C)

Test date	Sorbent mass (mg)	Total Hg in sorbent (ng)	Initial Hg conc. on sorbent (ppm)	Hg captured by sorbent (ng)	Hg in backup (ng)	Hg into the reactor (ng)	Hg capture efficiency	Hg mass balance difference	Mean efficiency	SD	LOI
15/08/07	19.9	78.8	0.9855	59.2	9.0	68.1	87%	6%	81%	6%	16.4
15/08/07	19.1	72.0	0.9855	53.3	18.4	71.6	74%	11%			

Table G-13 Mercury capture efficiencies of 20 mg coal fly ash samples when were tested with a gas stream of mercury vapour in pure nitrogen gas (continued)

Fly ash G (hold time = 60 minutes, test temperature = 150°C)

Test date	Sorbent mass (mg)	Total Hg in sorbent (ng)	Initial Hg conc. on sorbent (ppm)	Hg captured by sorbent (ng)	Hg in backup (ng)	Hg into the reactor (ng)	Hg capture efficiency	Hg mass balance difference	Mean efficiency	SD	LOI
22/08/07	20.5	9.9	0.1061	7.72	58.8	66.5	12%	3%	13%	2%	6.4
22/08/07	20.4	13.2	0.1061	11.01	62.1	73.1	15%	14%			

Fly ash H (hold time = 60 minutes, test temperature = 150°C)

Test date	Sorbent mass (mg)	Total Hg in sorbent (ng)	Initial Hg conc. on sorbent (ppm)	Hg captured by sorbent (ng)	Hg in backup (ng)	Hg into the reactor (ng)	Hg capture efficiency	Hg mass balance difference	Mean efficiency	SD	LOI
20/08/07	19.8	7.9	0.1197	5.5	55.6	61.1	9%	-5%	6%	3%	4.8
22/08/07	19.8	5.2	0.1224	2.7	69.9	72.6	4%	13%			

Table G-14 Mercury capture efficiencies when different fly ash particle sizes were tested with a gas stream of mercury vapour in pure nitrogen gas

Fly ash D (hold time = 60 minutes, test temperature = 150°C)

Particle size (μm)	Test date	Sorbent mass (mg)	Total Hg in sorbent (ng)	Initial Hg conc. on sorbent (ppm)	Hg captured by sorbent (ng)	Hg in backup (ng)	Hg into the reactor (ng)	Hg capture efficiency	Hg mass balance difference	Mean efficiency	SD
<38	08/08/07	19.7	46.5	0.4113	38.4	28.4	66.8	57%	4%	61%	4%
	14/08/07	20.4	52.0	0.4358	43.1	23.5	66.6	65%	3%		
38 - 75	08/08/07	20.3	60.0	0.4793	50.3	15.0	65.3	77%	1%	72%	5%
	09/08/07	19.6	53.5	0.4924	43.9	22.6	66.4	66%	3%		
75 - 106	08/08/07	20.5	56.9	0.3653	49.5	21.6	71.0	70%	10%	78%	8%
	09/08/07	19.9	63.6	0.4216	55.3	9.1	64.4	86%			
106 - 150	07/08/07	19.9	67.3	0.2687	61.9	10.9	72.8	85%	13%	84%	1%
	09/08/07	19.9	69.6	0.4479	60.6	12.4	73.0	83%	13%		

Fly ash F (hold time = 60 minutes, test temperature = 150°C)

Particle size (μm)	Test date	Sorbent mass (mg)	Total Hg in sorbent (ng)	Initial Hg conc. on sorbent (ppm)	Hg captured by sorbent (ng)	Hg in backup (ng)	Hg into the reactor (ng)	Hg capture efficiency	Hg mass balance difference	Mean efficiency	SD
<38	14/08/07	20.3	51.1	0.9604	31.6	40.1	71.7	44%	11%	51%	7%
	14/08/07	19.5	60.6	0.9604	41.9	30.8	72.7	58%			
38 - 75	08/08/07	20.2	79.4	0.9387	60.4	16.8	77.2	78%	20%	82%	3%
	09/08/07	20.1	75.1	0.8987	57.0	10.2	67.2	85%	4%		
75 - 106	08/08/07	19.8	65.2	0.9927	45.5	31.3	76.9	59%	19%	59%	-
106 - 150	07/08/07	19.7	69.8	0.3725	62.4	10.3	72.7	86%	13%	86%	-

Table G-15 Results from mercury leaching experiments

Gas scheme	Sorbent	Hg conc. in acetic acid (ppb)	average Hg conc. (ppb)	SD (ppb)	mass of Hg in leachate (ng)	total Hg in 20mg sorbent [ng]	Percent of captured Hg that leached out	Average leached out	SD
Exp. 1	Norit Darco Hg-LH™	1.69 1.27	1.48	0.21	1.69 1.27	61.2	3% 2%	2%	0.3%
	Tyre AC R3	0.59 0.78	0.68	0.09	0.59 0.78	62.7	1% 1%	1%	0.2%
	Sewage sludge AC R3	0.01 1.72	0.87	0.86	0.01 1.72	73.5	0% 2%	1%	1.2%
Exp. 5	Norit Darco Hg™	0.88 0.68	0.78	0.10	0.88 0.68	67.0	1% 1%	1%	0.2%
	Norit Darco Hg-LH™	1.09 1.01	1.05	0.04	1.09 1.01	61.2	2% 2%	2%	0.1%
	Tyre char R1	-0.01 -0.06	-0.03	0.03	-0.01 -0.06	62.1	0% 0%	0%	0.05%
	Tyre AC R1	-0.09 -0.03	-0.06	0.03	-0.09 -0.03	62.4	0% 0%	0%	0.1%
	Tyre AC R3	1.63 1.90	1.77	0.13	1.63 1.90	62.7	3% 3%	3%	0.2%
	Sewage sludge char	1.33 1.63	1.48	0.15	1.33 1.63	58.1	2% 3%	3%	0.3%
	Fly ash D	0.62 0.52	0.57	0.05	0.62 0.52	37.8	2% 1%	2%	0.1%
	Fly ash E	0.93 1.08	1.00	0.07	0.93 1.08	39.7	2% 3%	3%	0.2%